Use of Electromagnetic Radiation (EMR) and Antimicrobial Peptides for Wound Healing Promotion

A thesis submitted in fulfilment of the requirements for the degree of Doctor of Philosophy

Jie Hu

Master of Biomedical Science

School of Electrical and Computer Engineering

College of Science Engineering and Health

RMIT University

October 2014

Use of electromagnetic radiation (EMR) and antimicrobial peptides for wound healing promotion

A thesis submitted in fulfilment of the requirements for the degree of Doctor of Philosophy

Jie Hu
(Master of Biomedical Science)

School of Electrical and Computer Engineering
College of Science Engineering and Health
RMIT University
Melbourne, Australia

October 2014

DECLARATION

I certify that except where due acknowledgement has been made the work is that of the author alone. The work has not been submitted previously, in whole or in part, to qualify for any other academic award. The content of the thesis is the result of work, which has been carried out since the official commencement date of the approved research program, and, any editorial work, paid or unpaid, carried out by a third party is acknowledged.

Jie Hu

October, 2014

ACKNOWLEDGEMENTS

I would gratefully thank my wife Yanan, daughter CoCo and son Jason for their incredible support during my studies in the past and present.

I would like to express my sincere thanks to my senior supervisor, Dr. Elena Pirogova, for her inspiring supervision, assistance and time that have made my study at RMIT very enjoyable and worthwhile during my PhD project. Her professional experience and extensive contacts have contributed greatly to my research work. This thesis would be impossible without my supervisor Dr Elena Pirogova's support and encouragement throughout the past four years.

I would like to thank Dr. Taghrid Istivan, my second supervisor, for her invaluable advices and recommendations, and also for providing me with the adequate training prior to commencing my experimental work in the Microbiology Lab, Department of Environmental Biology and Biotechnology, School of Applied Sciences, RMIT University, Bundoora Campus.

I would like to thank Dr. Vuk Vojisavljevic, my consultant during this PhD project, for his vital inputs during different phases of my research study.

Many thanks go to my colleagues in the Biomedical Engineering research group at School of Electrical and Computer Engineering, RMIT University City campus and in the Microbiology Lab, at RMIT University, Bundoora Campus for their support and friendship without whose company and affable presence, the atmosphere at University would have been monotonous and not conducive to pleasant research.

Special thanks go to Taher, Pantea and Ishti for sharing their scientific expertise and help. In particular, I would like to thank Mr. El Taher Elshaqmani, School of Applied Science, RMIT University, Bundoora campus for his invaluable friendship and patience in providing me with hands-on training pertaining to handling of live organisms and techniques required as a part of live cell counts.

I would like to thank Prof. Robert and Josephine Shanks for their kindly donated scholarship throughout the duration of this project. This study was supported by Robert and Josephine Shanks Scholarship and Australia Postgraduate Award (APA).

TABLE OF CONTENTS

Chapter 4

Methodology

Chapter 5

LIST OF FIGURES

LIST OF TABLES

LIST OF ABBREVIATIONS

AU Absorbance units

Azu Azurocidin protein

Azu-RRM synthetic bioactive peptide analogue of Azurocidin protein designed computationally by the Resonant Recognition Model

Azc-RRM synthetic non-active peptide analogue of Azurocidin protein designed computationally by the Resonant Recognition Model

CFU Colony forming unit

DFT Discrete Fourier Transform

DNA Deoxyribonucleic acid

EIIP Electron Ion Interaction Potential

EMF Electromagnetic field

EMR Electromagnetic radiation

FIR Far infra red

IFT Inverse Fourier Transformation

IR Infra Red

MHA Mueller-Hinton Agar

MHB Mueller-Hinton Broth

MIC Minimum inhibitory concentration

OD Optical density

RRM Resonant Recognition Model

RNA Ribonucleic acid

UV Ultra violet

VIS Visible Light

SUMMARY

Wounds are one of the most common reasons for patients of all ages requiring health care [1,2]. It is well known that neglected wounds may lead to installation of multiple disabilities with negative impact on patients' daily activities [3]. Delayed healing, infections and wound dehiscence can cause a transformation of acute wounds in chronic wounds, which from an economic point of view is important, due to increased cost of healthcare. Chronic wounds are estimated to affect 433,000 Australians and to cost the health system $2.6 billion a year [4]. In USA, the health care cost associated with wound management and treatment has reached $20 billion a year [5]. Wounds are a major therapeutic problem and burden on the healthcare system. This is due to the increase in aged population, and the rising incidence of obesity and diabetes all of which delay the healing of wounds and lead to the development of chronic wounds. These debilitating wounds cause significant morbidity and mortality and are an escalating burden to the health care system.

Developing new methodologies to improve wound healing is of significant importance and the use of low level light radiation with optimal parameters as a means to promote wound healing would lead to changes in clinical practice. Applications of light therapy can offer a possibility of more economical and effective non-invasive therapies for tissue healing, presently considered refractory to conventional treatments. Promoting

the rate of healing would reduce both the likelihood and effect of secondary complications. There is substantial evidence that the application of electromagnetic radiation (EMR) in visible (VIS) and infra-red (IR) light ranges can result in physiologically beneficial biological effects in soft tissue repair [6-9].

This project has two arms:

1. First study aims to investigate and experimentally evaluate the effects of applied electromagnetic radiation in the range of visible light on biological activity of Collagenase enzyme, a key molecule playing a central role in wound healing process.
2. In the second study, a novel bioactive peptide is computationally designed to mimic the activity of the native antimicrobial peptide Azurocidin. The antimicrobial properties of this novel peptide are experimentally evaluated on different types of bacteria.

In **Study 1**, the *collagenase enzyme* was selected as a model system for computational analysis and determination of its activation frequency. The activation frequency/wavelength range (450-460nm) of collagenase was computationally determined using RRM. To validate the computational predictions, collagenase protein samples were irradiated by monochromatic visible light in a frequency range predicted computationally by the RRM. The kinetics of the irradiated collagenase was measured

by continuous monitoring of the collagen (substrate of collagenase) absorption at 340 nm. The experimental findings are presented and discussed in Chapter 5.

In **Study 2**, the native antimicrobial peptide Azurocidin was selected as a model system for its computational analysis and *de novo* design of a synthetic peptide analogue. Using the RRM approach, the synthetic Azurocidin peptide analogue (Azu-RRM) was designed to mimic the anti-microbial activity of the selected native Azurocidin peptide. A control synthetic Azurocidin peptide (Azc-RRM) is also designed to lack anti-microbial activity. The anti-microbial activities of the designed synthetic peptide analogues Azu-RRM and Azc-RRM are experimentally evaluated on selected Gram-positive and Gram-negative bacteria. In addition, the experimental evaluation of the synthetic Azu-RRM and Azc-RRM analogues is conducted to compare their activities with the biological activity of the native Azurocidin protein. These experiments are performed using the selected Gram-positive bacterium *Staphylococcus aureus* (ATCC25923). The results are presented and discussed in Chapter 5.

The experimental findings obtained within **Studies 1 and 2** reveal that application of visible light irradiation and synthetic peptide therapy provide an evidence-based approach towards development of novel treatment modalities for wound healing.

Chapter1

Introduction

Wound healing is a complex and dynamic process of replacing devitalized and missing cellular structures and tissue layers. The wound-healing process consists of four highly integrated and overlapping phases: hemostasis, inflammation, proliferation, and tissue remodeling [10]. The events of each phase must occur in a precise and regulated manner. Interruptions, aberrancies, or prolongation in the process can lead to delayed wound healing or a formation of non-healing/chronic wound. Multiple factors can lead to impaired wound healing. In general terms, the factors that influence repair can be categorized into local and systemic. Local factors are those that directly influence the characteristics of the wound itself (such as oxygenation, infections etc), while systemic factors are the overall health or disease state of an individual that affect his or her ability to heal. Many of these factors are related, and the systemic factors act through the local effects affecting wound healing [11].

Up to date, the research on treating local factors for chronic wound healing is more focused on:

1. Stimulation of cell growth;

2. Wound bed preparation; and

3. Anti-infection treatment.

Wound bed preparation involves debridement and managing exudates [12]. Debridement is the process of removing necrotic tissue to diminish infection and promote healing. It is an essential component of any plan to prepare the chronic wound bed for healing [13]. There are several debridement methods applied in clinics, such as surgical debridement; enzymatic debridement; mechanical debridement; and autolytic debridement [14]. Enzymatic debridement may be used as the primary technique for debridement in certain cases, when a surgical debridement is not feasible owing the bleeding disorders or other complications [15]. In enzymatic debridement process, the collagenase shows more selectivity on denatured collagen in devitalized tissue. This selectivity is beneficial as it keeps the vital tissue and growth factors crucial to wound healing [16].

This research project is focused on *improvement of wound bed preparation* and *development of a novel anti-infection treatment for wound healing promotion*. In particular, this project comprises two major research studies:

- *Study 1:* The application of external electromagnetic radiation (EMR) of the computationally determined frequency that can modulate the biological activity of Collagenase enzyme (a key player in wound repair process) and thus, promote the process of enzymatic debridement for a better wound bed preparation that can lead to enhanced wound healing; and
- *Study 2:* Investigation of the antimicrobial activity of a novel computationally

designed synthetic peptide analogue that emulates the function of a native antimicrobial peptide Azurocidin. This study evaluates the antimicrobial efficacy of the novel anti-infection agent against the selected Gram-positive and Gram-negative bacteria in vitro.

There are studies showing that applied electromagnetic radiation (EMR) in the visible light range can effect protein and cellular activity [17-19]. It was also reported that the protein activity can be modified by the electromagnetic radiation within the specific frequency range which could be computationally predicted with using the Resonant Recognition Model (RRM) [20-22]. In *Study 1*, the selected model system, Collagenase enzyme, was computationally analyzed using the RRM approach. The activation frequency/wavelength range of Collagenase enzymes was computationally determined to be 450–460 nm. The Collagenase enzyme was irradiated by monochromatic visible light in a wavelength range of 400– 900nm (that includes the computationally predicted wavelengths). The kinetics of the irradiated Collagenase was monitored and compared with the kinetics of non-irradiated enzyme sample. The obtained results revealed that enzymatic activity of collagenase is modulated by exposures to visible light radiation with the maximum effect observed at the wavelengths determined computationally (456 nm), thus confirming that applied EMR can be used to produce the desired alterations in selected proteins. By modulating the biological activity of collagenase enzyme, it becomes possible to improve collagenase debridement and hence, enhance would bed preparation stage of wound healing process.

Presently, antibiotics are the common anti-infection drugs applied in clinic. However, the rising antibiotics' resistance is a major problem that limits current use of traditional antibiotics for treatment of various infections. Hence, there is a growing need to find alternative drugs that can eradicate the antibiotics resistance arising from their excessive applications [23]. Antimicrobial peptides (AMP) are found in virtually all life forms where they work as a first line of defense against invading pathogens. These AMP are one of the innate immunity actors which were conserved along evolution [24,25]. In recent years, one of the natural antimicrobial peptides "Azurocidin" has been found to have various antimicrobial, antiviral, and immunomodulatory properties [26-29]. Azurocidin is found in neutrophils. Neutrophils are the most abundant (40% to 75%) type of white blood cells in mammals and form an essential part of the innate immune system [30-32].

Study 2 is focused on development of a novel anti-infection agent. The antimicrobial activity of the synthetic bioactive peptide, computationally designed by the RRM, and mimicking the activity of Azurocidin protein is evaluated on the selected Gram-positive and Gram-negative bacteria. The antimicrobial activity of the synthetic peptide analogue, Azu-RRM, is compared to the native antimicrobial peptide Azurocidin (Azu) and evaluated against the Gram-positive bacterium *Staphylococcus aureus* (ATCC25923), the Gram-negative bacterium *E. coli* (ATCC25922) and the ampicillin resistant bacterium strain *Staphylococcus aureus*344. The experimental findings showed that novel Azu-RRM peptide affected the growth of both *Staphylococcus aureus* ATCC 25923, 344 and *E. coli* 25922. The activity of Azu-RRM peptide against *Staphylococcus*

aureus ATCC 25923, and penicillin resistant *Staphylococcus aureus* 344 and *E. coli* ATCC 25922 was shown to be *dose- and time-dependent*. The results clearly indicate that synthetic Azu-RRM shows a potent antimicrobial activity and can potentially present a new alternative therapeutic compound to control bacterial infections.

1.2 Aims of the research project

In essence, this project aims to test *two hypotheses* as shown in Figure 1:

1. *Electromagnetic radiation of the computationally determined frequency can modulate the enzymatic activity and thus, promote a wound healing process.*
2. *The computationally designed synthetic peptide can exhibit an antimicrobial activity and thus, promote wound healing process.*

1.3 Research Questions

- Is it possible to apply EMR of certain parameters that will induce biological effects on the selected protein activity?
- If there is a biological effect, can we modulate enzymatic activity using EMR with a specific frequency (increase or inhibit the enzymatic activity)?
- Can we design a synthetic peptide analogue which can emulate the native antimicrobial peptide?
- How the selected bacterium will respond to the treatment by the synthetic peptide analogue?

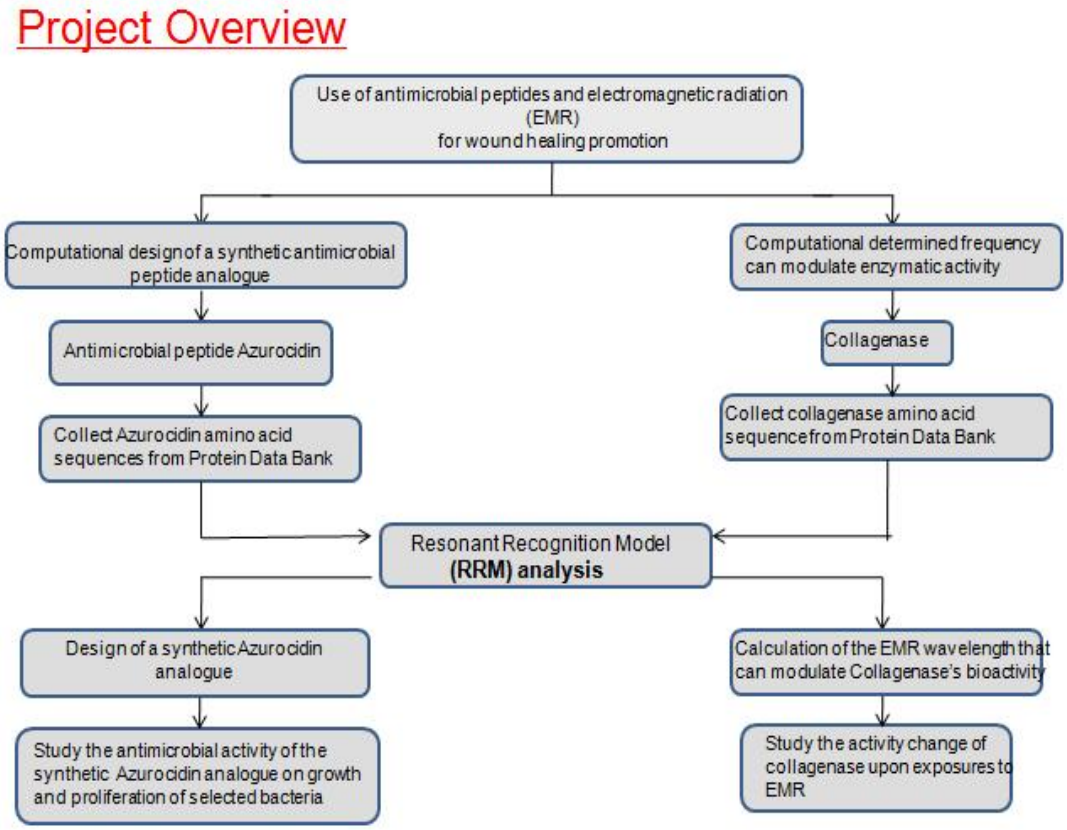

Figure 1.1. Flow chart of the project

1.4 Thesis Outline

This thesis contains seven chapters.

Chapter 1 presents a general introduction describing the overall aim and objectives of the project.

Chapter 2 presents a literature review of relevant published literature of interest for this project. It covers general aspects of wound healing, anti-infection, wound bed preparation, the effects of electromagnetic radiation on proteins and cells.

Chapter 3 presents the biological effects electromagnetic radiation and its therapeutic

applications

Chapter 4 presents the materials and methods used in this project. The concepts and possible applications of the Resonant Recognition Model (RRM) are also presented. The computational analysis of the selected protein examples (Collagenase enzyme and Azurocidin antimicrobial protein) carried out within the project is described.

Chapter 5 presents the experimental studies conducted in this project. One study is the experimental evaluation of the effects of applied electromagnetic radiation (EMR) in the visible light range on biological activity of Collagenase enzyme. The second study is the investigations of the antimicrobial activity of the synthetic, computationally designed Azurocidin peptide analogue on growth and proliferation of selected pathogenic bacteria.

Chapter 6 outlines the conclusion drawn from the experimental results of the project, and presents and discusses the findings in the light of the research questions set for this project.

Chapter 7 provides the recommendations for a further research.

Chapters of this thesis are concluded by a list of references used in the project.

Chapter2

Literature Review

2.1 Wound healing: Overview

Wound healing is an intricate process whereby the skin repairs itself after injury [33]. It's classically comprises hemostasis, inflammation, proliferation, and remodeling [34]. Chronic wounds do not follow the same orderly progression toward healing as acute wounds but are trapped in a phase of inflammation [35]. Chronic wound represents necrotic tissue, corrupt matrix, hypoxia, high bacterial burden and senescent cells within the wound bed. Up to date, the research on chronic wound healing is mostly focused on (i) stimulation of cell growth; (ii). anti-infection; and (iii) wound bed preparation [36-38].

Recent advances in molecular and cellular biology have greatly expanded general understanding on the biological process involved in wound healing and tissue regeneration. The interactive process of wound healing comprise of soluble mediators, blood cells, extracellular matrix and parenchymal cells. Four distinct phases of wound healing are discussed below in greater details.

2.1.1 Phases of wound healing

Hemostasis Phase:

Wound disrupts normal tissue integrity, leading to division of blood vessels and direct exposure of extracellular matrix (ECM) to platelets. This result in platelets to adhere to the site of injury, become activated, and aggregate. Under the influence of adenosine diphosphate (ADP) leaking from damaged tissues, the platelets aggregate and adhere to the exposed collagen. They also secrete factors, which interact with and stimulate the intrinsic clotting cascade through the production of thrombin, which in turn initiates the formation of fibrin from fibrinogen. The fibrin mesh strengthens the platelet aggregate into a stable hemostatic plug. Finally platelets also secrete cytokines such as platelet-derived growth factor (PDGF), which is recognized as one of the first factors secreted in initiating subsequent steps. Hemostasis occurs within minutes of the initial injury unless there are underlying clotting disorders [39,40].

Inflammation Phase:

During the inflammation phase, bacteria and cell debris are phagocytosed and removed from the wound by white blood cells. The inflammatory response causes the blood vessels to become leaky releasing plasma and polymorphonuclear leukocytes (PMNs, neutrophils) into the surrounding tissue. The neutrophils phagocytize debris and microorganisms and provide the first line of defense against infection. They are aided by local mast cells. As fibrin is broken down as part of this clean-up the degradation products attract the next cell involved. Macrophages are able to phagocytize bacteria and provide a second line of defense. They also secrete a variety of chemotactic and

growth factors such as fibroblast growth factor (FGF), epidermal growth factor (EGF), transforming growth factor beta (TGF) and interleukin-1 (IL-1) which appears to direct the next stage [41,42].

Proliferative Phase:

During this phase, the wound site is being cleared of debris. Fibroblasts and endothelial cells are infiltrating the healing wound. The fibroblasts grow and form a new, provisional extracellular matrix (ECM) by excreting collagen and fibronectin resulting in matrix synthesis, granulation tissue formation and remodeling. Endothelial cells participate in formation of new capillaries resulting in angiogenesis. Concurrently, re-epithelialization of the epidermis occurs, whereby epithelial cells proliferate and "crawl" atop the wound bed, covering the new tissue. In the final stage of epithelializtion, contracture occurs as the keratinocytes differentiate to form the protective outer layer or stratum corneum. All wounds undergo some degree of wound contraction and area of wound will be decreased. Myofibroblasts have been postulated as being major cell responsible for contraction. Typically this cell contains alpha smooth actin in thick bundles called stress fibers [43,44].

Remodeling Phase:

During remodeling, collagen is remodeled and realigned along tension lines. Collagen is broken down by matrix metallipoproteinases (MMPs) and net wound collagen is result of a balance between collagenolysis and collagen synthesis. There is a shift towards

collagen synthesis and eventually re-establishment of extracellular matrix composed of a relatively extracellular collagen rich scar. Scar remodelling continues for several months post injury, gradually resulting in a mature, avascular and acellular scar [45].

Wound healing classically comprises four phases mentioned above. It is critical to acknowledge that wound healing is not linear and often wounds can progress both forwards and backwards through these phases depending on intrinsic and extrinsic forces within a particular patient. This process is fragile and susceptible to interruption or failure that can cause the formation of non-healing chronic wounds. Among the factors that may contribute are diabetes, venous or arterial disease, infection, and metabolic deficiencies of old age [46].

2.1.2 Classification of wounds

(Classification is with respect to healing of wounds that can be classified as either acute or chronic).

Acute wound: they heal in a predictable manner and time frame. The process results in a well-healed wound with a few complications if any.

Chronic wound: wounds that have failed to proceed through the orderly process that produces satisfactory anatomic and functional integrity [47,48].

2.1.3 Chronic wound

Chronic wounds do not follow the same orderly progression toward healing as acute

wounds but are trapped in a phase of inflammation. Chronic wound represents necrotic tissue, corrupt matrix, hypoxia, high bacterial burden and senescent cells within the wound bed [35].

2.1.4 Features of chronic wounds [49]

Clinical

- Presence of necrotic and unhealthy tissue
- Lack of adequate blood supply
- Absence of healthy granulation tissue
- Lack of re-epithelization
- Recurrent wound breakdown due to superficial bridging

Molecular and biochemical changes

Elevated levels of:

- Inflammatory cytokines
- Collagenolytic activity – elevated levels of Matrix metalloproteinases (MMP-1, MMP-8, and MMP-13)
- Gelatinases – MMP-2,and MMP-9
- Stromelysins – MMP-3,MMP-10, and MMP-11
- Serine proteases

Diminished level of:

- Tissue inbitor of metalloproteinases (TIMPs)
- α1-protease inhibitor

- α2-macroglobulin

Significant degradation of:

- Fibronectin
- Vitronectin
- Tenascin

Cellular features

- Low mitotic activity
- Altered cellular phenotype
- Presence of senescent cells
- Decreased growth factor activity

Microbiology

- High levels of bacterial content
- Presence of more than one bacterial strain
- Presence of multi-drug resistant organisms
- Presence of biofilms

Long-term complications

- Sinus or fistula formation
- Involvement of the bone leading to osteomyelitis
- Contractures and deformity in surrounding joints

- Malignant change
- Systemic amyloidosis
- Calcification

2.1.5 Wound bed preparation

Wound bed preparation focuses on all of the critical components, including debridement, bacterial balance, and management of exudates and takes into account the overall health status of the patient and how this may impinge upon the wound healing process. It is the management of a wound to accelerate endogenous healing or to facilitate the effectiveness of other therapeutic measures [13,15].

It involves:

- An ongoing debridement phase
- Management of exudates
- Resolution of bacterial imbalance

2.1.6 Necrotic tissue and its accumulation in chronic wounds

Necrotic tissue is a dead tissue, which usually results from an inadequate local blood supply. Necrotic tissue contains dead cells and debris that are a consequence of the fragmentation of dying cells. Necrotic tissue changes color from red to brown or black/purple, as it becomes more dehydrated. Finally, the tissue goes from a black, dry, thick, and leathery structure known as eschar. This can be seen in a wide variety of wound types, including burns and all types of chronic wounds. In contrast, slough is a yellow fibrinous tissue that consists of fibrin, pus, and proteinaceous material .Slough can be found on the surface of a previously clean wound bed and it is thought to be associated with bacterial activity. The accumulation of necrotic tissue or slough in a chronic wound is of major clinical significant, because it is thought to promote bacterial colonization and prevent complete repair of the wound [50].

Recently, the term necrotic burden has been proposed as an all-encompassing term to describe necrotic tissue, excess exudates, and high levels of bacteria present within dead tissue. Due to the underlying pathogenic abnormalities in chronic wounds and the altered biochemical and cellular environment, necrotic tissue tends to continually accumulate [36]. However, it is not always feasible to fully remove the underlying pathogenic abnormality, making it even more essential to adequately prepare the wound bed. If the necrotic burden is allowed to accumulate in the chronic wound, it can prolong the inflammatory response, mechanically obstruct the process of wound contraction and impede re-epithelization [51].

2.1.7 Debridement

Debridement is the process of removing necrotic tissue to diminish infection and promote healing. It is an essential component of any plan to prepare the chronic wound bed for healing. Chronic wounds are likely to require ongoing maintenance debridement rather than a single intervention. The underlying pathogenic abnormalities in chronic wounds cause a continual build-up of necrotic tissue, and regular debridement is necessary to reduce the necrotic burden and achieve healthy granulation tissue [52,53].

There are several methods of debridement are applied in clinics, each with its own advantages and limitations. Those methods that are most efficient for removal of debris may, at the same time, be the most detrimental to fragile new growth, and more than one method may be appropriate [54]:

- Autolytic debridement
- Surgical and sharp debridement
- Enzymatic debridement
- Mechanical debridement

2.1.8 Enzymatic debridement

Enzymatic debridement may be used as the primary technique for debridement in certain cases, when a surgical debridement is not feasible owing the bleeding disorders or other complications. Autolytic debridement occurs through the action of endogenous

enzymes including elastase, collagenase, myeloperoxidase, acid hydrolase, and lysosomes. Enzymatic methods use topical application of exogenous enzymes to the wound surface where they work synergistically with endogenous enzymes to debride the surface. This method appears to be most useful in the removal of eschar from large wounds where surgical techniques cannot be used. Cross-hatching or scoring of the eschar may be necessary prior to application of the enzyme. Excess exudates may be produced with these agents, and local irritation to the surrounding skin or infection sometimes occurs [55,56].

Several agents are available, although not in all markets, including fibrinolysin, desoxyribonuclease (fibrinolysin/DNase), collagenase and papain/urea. Fibrinolysin/DNase breaks down fibrin, inactivates fibrinogen and several coagulation factors, and dilates blood vessels in the wound bed, all of which allow macrophages to enter the wound and degrade necrotic tissue. The products of fibrinolysin degradation are not resorbed and must be removed from the wound by irrigation. DNase cleaves nucleic acids, leading to liquefaction of exudates and decreased viscosity. Bacterial collagenase isolated from Clostridium histolyticum displays great specificity for the major collagen types in the skin (type I and type II collagen) and has been successfully used as an enzymatic debrider. It cleaves glycine in native collagen and digests collagen, but is not active against keratin, fat, or fibrin. The wound healing process is promoted by the digestion of native collagen bundles which bind nonviable tissue to the wound surface, and by the dissolution of collagen debris within the wound. Papain is a

proteolytic enzyme derived from the papaya fruit. It is inactive against collagen and digests necrotic tissue by liquefying fibrinous debris. Papain requires the presence of activators in order to function: urea is used as an activator and it also denatures nonviable protein matter, making it more susceptible to proteolysis [57,58].

Figure 2.1 shows the application of the enzymatic debriding agent for a 4-hour period. All burns in the Debrase group had evidence of the effective, complete debridement as indicated by a clean wound bed without any escher and the presence of a punctuate bleeding in the remaining wound bed. In contrast, there was no evidence of debridement or any changes in the control burns. Figure 2.2 shows the percentage of completely re-epithelialized burns was higher for Debrase than control burns at the 11th day.

Figure 2.1. Appearance of burns immediately after a 4-hour application of Debrase® (left) or control vehicle (right). Note the presence of punctate bleeding in Debrase-treated burns indicating viability of remaining wound surface [59]

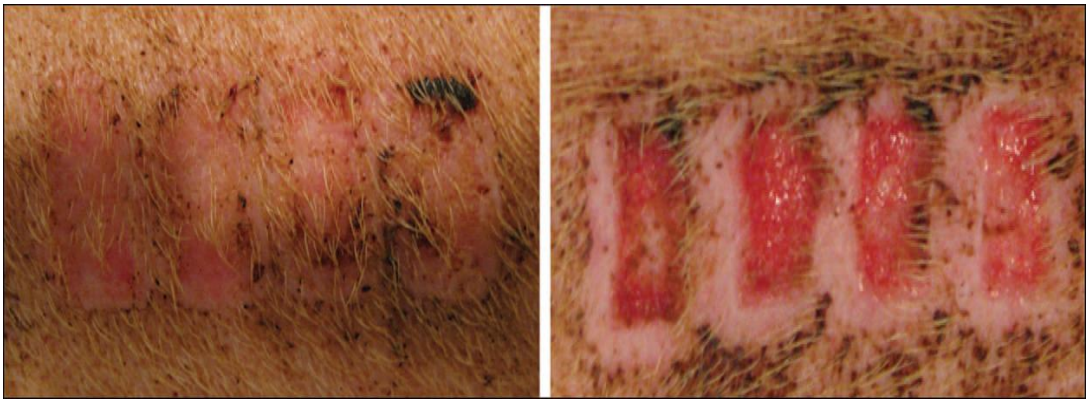

Figure 2.2. Comb burns at day 11 treated with Debrase® (left) and control vehicle (right). The debrided wounds are reepithelialized, whereas the control burns are moist and glistening indicating little reepithelialization [59]

2.1.9 Collagenase debridement

In the last 20 years, several enzymatic products for wound debridement have been developed [60]. The two most frequently used commercial products in this area are currently the combination of fibrinolysin and desoxyribonuclease (DNAse) and collagenase [61]. Several studies revealed that the product of collagenase ointment was significantly more effective in removing necrosis than other products. The speed of wound surface epithelialization was significantly enhanced by collagenase gel. It is important to note that the newly formed epithelium at the wound margins was not damaged at all by this enzymetic product. Moreover, collagenase shows more selectively on denatured collagen in devitalized tissue. This selectivity is beneficial as it keeps the vital tissue and growth factors crucial to wound healing. The comparative results are presented in Figure 2.3.

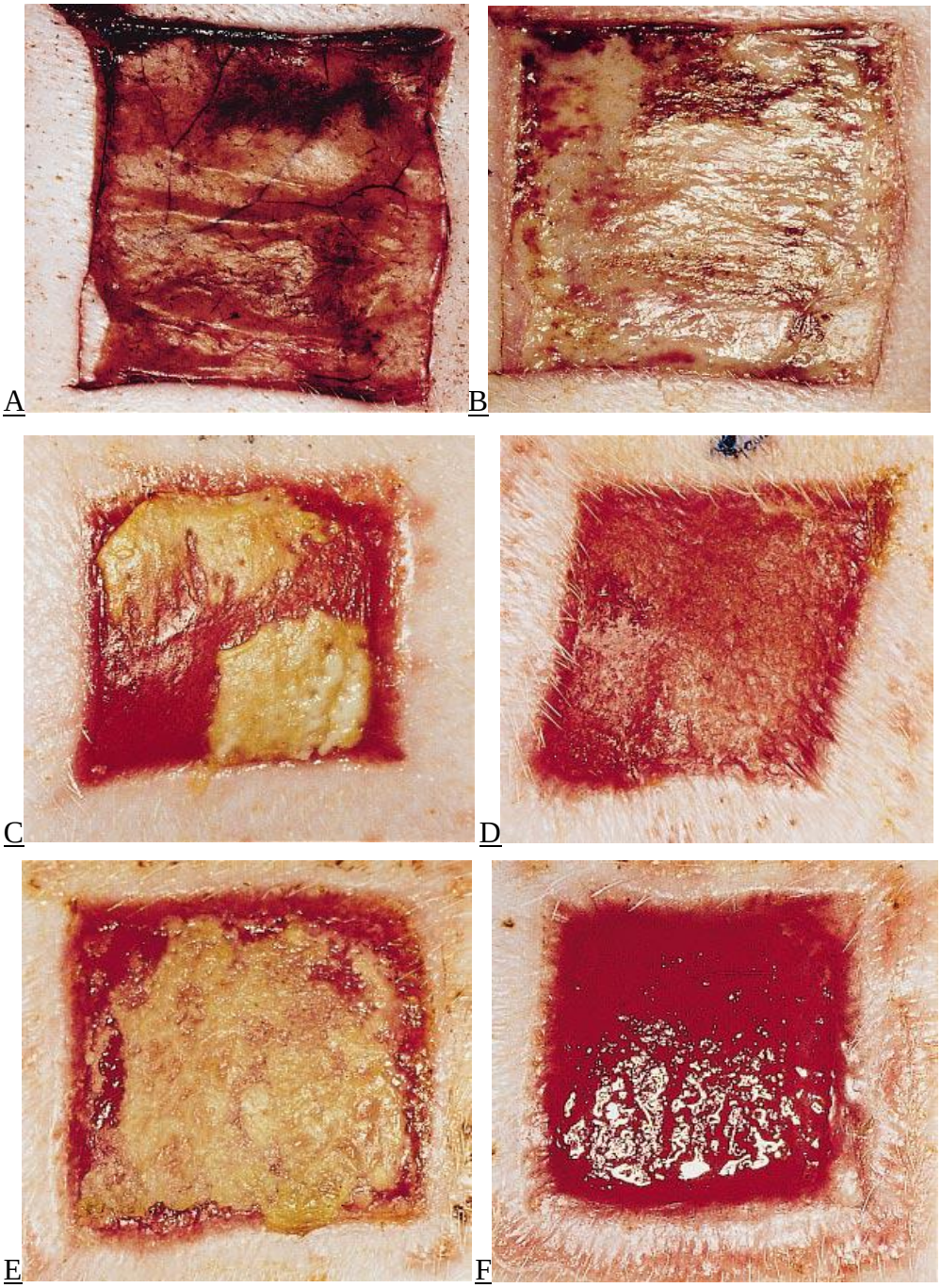

Fig. 2.3. (A) Appearance of a necrotic wound just before treatment, 2 days after excision of the epidermis and the major part of the dermis, followed by application of trichloroacetic acid; (B) The same wound after 2 days of treatment with collagenase gel (2 U/cm2). During treatment, the necrotic layer is becoming gradually thinner; (C) Artificial necrotic ulcer, treated with fibrinolysin/desoxyribonuclease oleogel for 1 week. The wound surface is still covered with necrotic tissue; (D) Identical necrotic ulcer treated with collagenase ointment for 1 week. The yellow necrotic material has been removed and red granulation tissue has become visible; (E) Necrotic ulcer, treated with placebo (gel only) for 1 week. The wound is still covered with necrotic tissue; (F) Identical necrotic ulcer treated with collagenase gel (2 U/cm2) for 1 week. The wound is entirely clean and epithelialization has started from the margins [62].

Currently, Collagenase Ointment (Healthpoint Biotherapeutics, Fort Worth, TX) is the only Food and Drug Administration (FDA)-approved biological enzymatic debridement agent in the United States. The enzyme used in this drug is a bacterially derived Collagenase from *Clostridium histolyticum* (C. collagenase) [15,63,64].

2.1.10 Collagen

Collagen is a major protein of the extracellular matrix and the most profuse protein in mammals, making up about 40% of the total. It makes up 75% of our skin [65]. Collagens are proteins that assemble into fibrous aggregates surrounding cells made up of three polypeptide chains with the characteristic repetitive amino acid sequence Gly-X-Y which wind together to form into a triple helix structure [66].

In its molecular structure, there is a high proportion (about 30%) of the simplest amino acid glycine which having virtually no side chain nestles well into the helix, and also an unusual amino acid proline - together with a modified version of it - hydroxyproline. This complex structure has been devised by nature to be invulnerable to the circulating enzymes and other materials in the body. Nature accomplished this purpose superbly which is why no other enzyme but a "collagenase" can break it into its component parts [66].

Collagen itself confers th7 the way the collagen fibres aggregate. Collagens have many other functions including cell adhesion and migration. Collagen acts as a scaffold for our bodies, controls cell shape, cell growth, differentiation, broken bones regeneration;

wound healing. When the body needs to build any new cellular structure as in the healing process, collagen or collagen fragments play a central role [68].

Common types of Collagen [67]

There are 28 different types of collagen so far identified with type I being by far the most abundant:

Type I– most widely occurring collagen found in skin, tendon, bone, cornea, lung, vasculature and is the component of scar tissue when a wound heals;

Type II- major component of cartilage;

Type III- Makes up elastic tissues such as embryonic skin, lungs, blood vessels;

Type IV- Non fibrillar collagen type IV- also known as basement membrane collagen; is found at tissue boundaries;

Type V- less abundant, found in the cornea;

Type VI- minor component in cartilage.

Procollagen

Collagen is expressed with N- and c-terminal peptidases which are cleaved before collagen fibrils can assemble.

Tropocollagen

Tropocollagen is the product when procollagen is removed which assembles into fibrils.

Subunits

Each polypeptide chain which makes up the triple helix can be the same or they can all be different. They may have different lengths or features

Collagen Synthesis

Stages:

1. Transcription
2. Translation into pre-pro-peptide
3. Pre-pro-peptide modification
4. Tropocollagen formation
5. Collagen fibril
6. Collagen fibre

The process of the collagen synthesis is shown in Figures 2.4 and Figure 2.5

Figure 2.4 indicates that genes encoding the collagen molecule must be turned on and transcribed firstly, then the mRNA transcript exits the nucleus and is translated by the ribosome into the signal sequence and pre-pro-peptide, the pre-pro-peptide is modified in the endoplasmic reticulum, and then the procollagen is modified by the addition of oligosaccharides and then packaged again into a secretory vesicle to be excreted into the extracellular matrix.

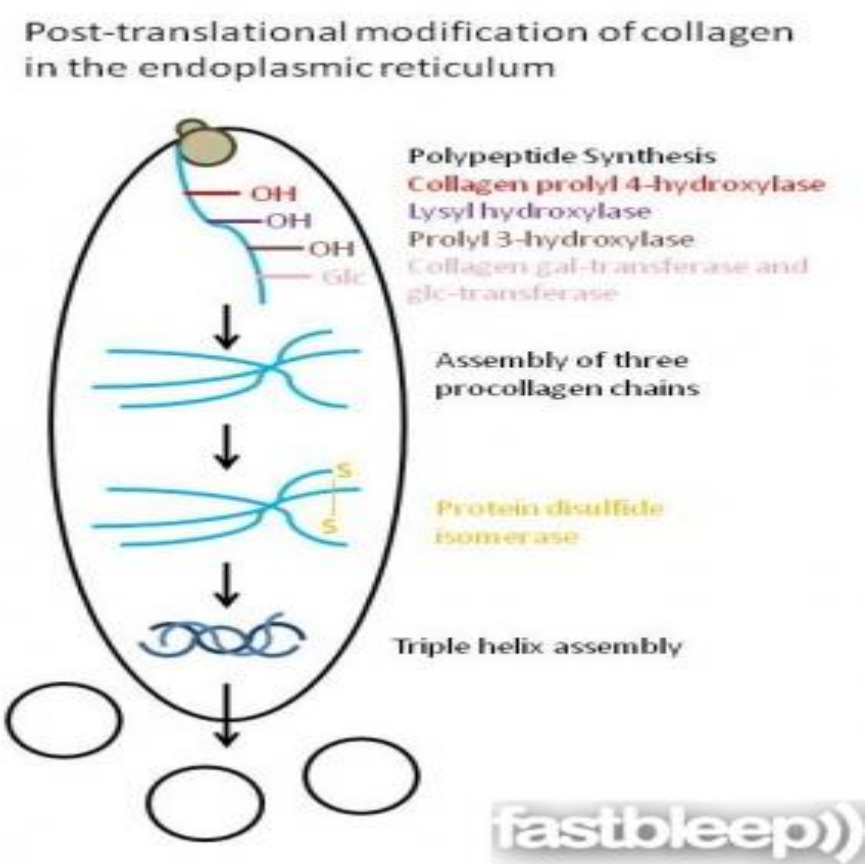

Figure 2.4. Pre-pro-peptide modification [67]

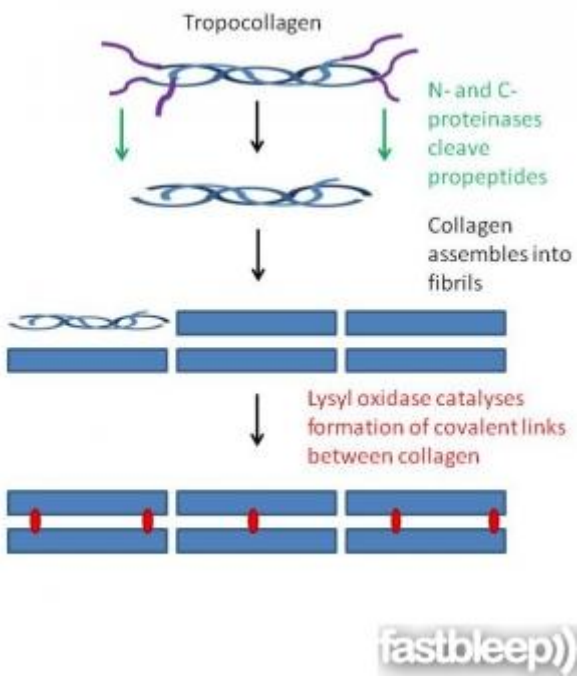

Figure 2.5. Collagen fibril formation [67]

Figure 2.5 indicates that collagen peptidases in the extracellular matrix cleave the terminal N- and C- propeptides and spontaneous assembly of the collagen molecules into tropocollagen triple helices occurs, then the enzyme lysyl oxidase is responsible for this step where hydroxyl groups on lysines and hydroxyl-lysines are converted into aldehyde groups which covalently bond between tropocollagen molecules to form a collagen fibril.

2.1.11 Collagenase

Collagenase is a highly specific proteinase and is the only enzyme that can specifically cleave the triple helix of the fibrillar collagens [69,70]. By nature, it is a water soluble proteinase that specially attacks and breaks down collagen into simple peptides and is most effective in a pH range of 6 to 8 [71].

Collagenases are members of the family of zinc-dependent enzymes known as the matrix metalloproteinases (MMPs). These enzymes have a similar domain structure: an N-terminal signal sequence to target for secretion, a pro-peptide domain to maintain latency, a catalytic domain containing the catalytic zinc, a linker region, and a C-terminal four-bladed propeller structure called the hemopexin domain. The MMPs are a family of approximately 27 Zn^{2+} ion-dependent endopeptidases acting at neutral pH which are involved in the proteolytic processing of several components of the extracellular matrix, such as collagens, proteoglycans and fibronectin. The extracellular matrix breakdown involved in a number of important biological processes such as cell

migration, angiogenesis and wound healing [69,74].

MMPs are usually classified into five main groups, namely:

1) Collagenases (i.e., MMP-1, MMP-8 and MMP-13),

which are able to preferentially cleave fibrillar collagen, recognizing the substrate through the haemopexin-like domain.

2) Gelatinases (i.e., MMP-2 and MMP-9), which are able to enzymatically process various substrates of the extracellular matrix (ECM), such as collagen I and collagen IV. Beside the haemopexin-like domain, these MMPs are characterized by the presence of an additional domain, called collagen binding domain (CBD) and located in their catalytic domain. CBD is made of three fibronectin II-like repeats and represents the preferential binding domain for fibrillar collagen I.

3) Stromelysins (i.e., MMP-3, MMP-10 and MMP-11),

which are able to hydrolyse collagen IV, but do not cleave fibrillar collagen I.

4) Matrilysins (i.e., MMP-7 and MMP-26), which lack the haemopexin-like domain and are able to process collagen IV but not collagen I.

5) Membrane-type (MT-MMPs) (i.e., MMP-14, MMP-15, MMP-16, MMP-17 and MMP-24), which contain at the C-terminal an additional domain, represented by an intermembrane region, completed by a short cytoplasmic tail. Only MMP-14 has been shown to be able to cleave fibrillar collagen I [72].

The collagenases (MMP-1, MMP-8 and MMP-13) are the only proteinases that

specifically cleave the collagen triple helix, and are important in a large number of physiological and pathological processes. Structures are known for the N-terminal 'catalytic' domain of collagenases MMPs 1, 8 and 13) are the only enzymes with significant activity against native triple-stranded collagen types I, II, III, VII and X, which they degrade by cleavage of a specific peptide bond in all three strands. The unique cleavage point is at bond 775-776 of mature triple-stranded collagen, producing fragments that are one-quarter and three-quarters the size of the whole collagen molecule.

The collagenase, matrix metalloproteinase 1 (MMP-1), plays a pivotal role in degradation of interstitial collagen types I, II, and III. The structure of full-length MMP-1 (Figure 2.6) presented here provides a model for the structures of the other MMPs, all of which are highly homologous. The structure of human MMP-1 comprises of the N-terminal catalytic domain, the linker region and the C-terminal hemopexin domain. The catalytic domain of one monomer contacts the hemopexin domain of the other monomer [73].

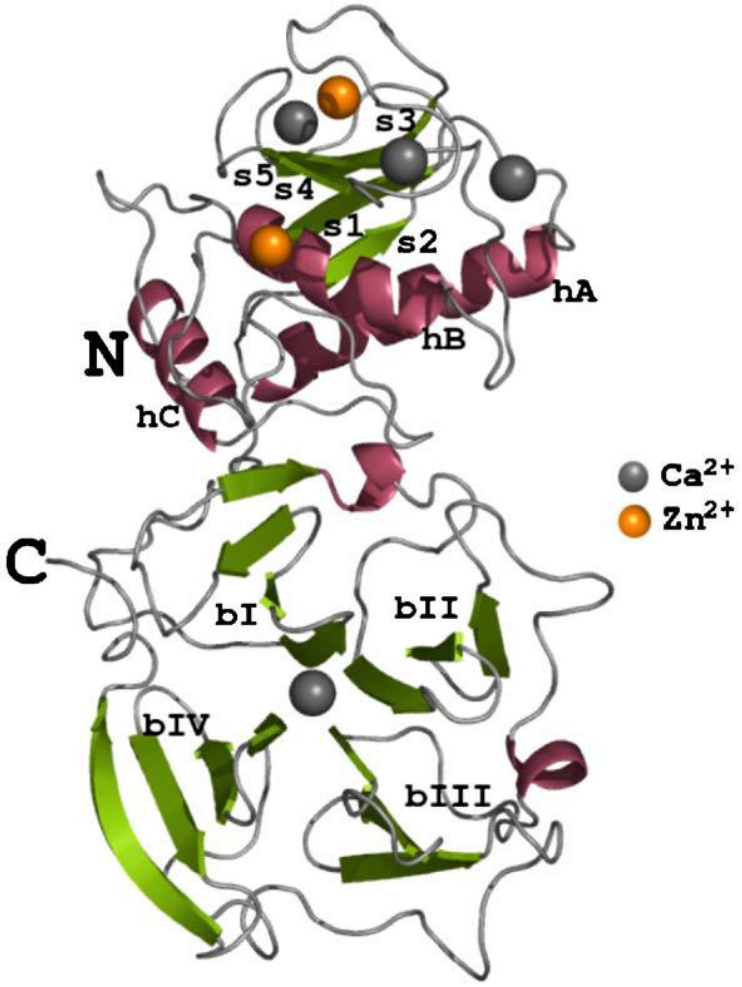

Figure 2.6. Ribbon representation of the three-dimensional structure of human MMP-1. Helices have been coloured pink and the strands shown in green. There are four calcium ions and two zinc ions found in the structure that have been colored grey and orange, respectively. The secondary structural elements have been annotated: helices (hA-hC), strands (s1–s5) of the catalytic domain and blades (bI–bIV) of the hemopexin domain [73]

2.1.12 Collagenase biological implications: specific importance to this research study

Collagen is the major structural protein of vertebrates. Collagenase is a highly specific proteinase and is the only enzyme that can specifically cleave the triple helix of the fibrillar collagens. Consequently an understanding of its mechanism of action is very important to the process of enzymatic debridement through the destruction of collagen.

Analysis of the enzymatic properties of collagenases, and of chimeras between them, demonstrates that features of the two folded domains (the N-terminal catalytic domain and the C-terminal haemopexin domain and the linker peptide that connects them are all essential for collagen binding and hydrolysis [75].

An investigation of type I collagen reaction to collagenase solution using real-time atomic force microscope revealed that the collagenase degrades the entire fibrillar structure down to shorter and thinner fragments. Collagenase cleaves glycine in helical regions of native collagen containing the sequence x-proline-yglycine-proline-z. In vitro study investigating the digestive ability of collagenase on human collagen types I, III, IV, V and VI showed that these enzymes displayed proteolytic power to digest all these types of human collagen present in necrotic tissue, except type IV [76].

There is considerable rationale for using Collagenase enzyme in wounds for the purpose of enhancing or accelerating re-epithelization [77]. Clinical trials of Collagenase reported rapid cleansing and enhanced removal of necrotic debris. A conducted study suggested that Collagenase ointment is more effective than placebo (inactivated ointment or petrolatum ointment) for debridement of necrotic tissue. *In vivo* and *in vitro* studies have shown that collagenase promotes the cellular responses to injury and wound healing [15].

Application of collagenase to a wound could help it heal faster. Collagenase is an

enzymatic debrider that specifically attack collagen in wound necrotic tissue which contains mostly the denatured collagens and cleans the wound of any dead tissue leaving the wound bed ready for healing [51]. One of the exogeneous enzymes used for wound debridement is collagenase which is extracted from Clostridium hystolyticum by fermentation. With a few exceptions, different commercial collagenases are all made from C. histolyticum, or is recombinant versions where, Escherichia coli expresses a gene cloned from C. histolyticum [15,78].

2.2 Wound-infections

2.2.1 Infection

If a microorganism either harms or lives at the expense of another organism, it is called a parasitic organism and the relationship is termed parasitism. Those organisms are capable of causing disease are called pathogens. Infection is the invasion of a host organism's bodily tissues by disease-causing organisms, their multiplication, and the reaction of host tissues to these organisms and the toxins they produce [79].

2.2.2 Pathogen

A pathogen is a biological agent that causes disease or illness to its host. The term is most often used for agents that disrupt the normal physiology of a multicellular animal or plant. However, pathogens can infect unicellular organisms from all of the biological kingdoms. There are several substrates and pathways whereby pathogens can invade a

host. The human body contains many natural defenses against some of common pathogens in the form of the human immune system and by some "helpful" bacteria present in the human body's normal flora. Some pathogens have been found to be responsible for massive amounts of casualties and have had numerous effects on afflicted groups. Today, while many medical advances have been made to safeguard against infection by pathogens, through the use of vaccination, antibiotics and fungicide, pathogens continue to threaten human life [80].

Pathogens include:

- Bacteria (example: bacterial meningitis or strep throat)
- Viruses (example: hepatitis A, hepatitis B, and hepatitis C)
- Fungi (example: athlete's foot)

2.2.3 Bacteria

Bacteria are a category of microorganisms of Prokaryotes. There are many different types of bacteria which may be classified according to differences in their shape and cell wall. Cocci (spherical shaped cells), bacilli (rods) and sprirochaetes (spirals) can be arranged singly; however cocci and bacilli can also be found in pairs, chains and irregular clusters. The growth and survival of all bacteria is dependent upon environmental factors, for example strict aerobes require oxygen whereas anaerobes are rapidly killed by oxygen. It is important to note, however, that both aerobes and anaerobes can survive in close proximity to each other and that some can survive in both conditions by growing aerobically and then switching to anaerobic metabolism in

the absence of oxygen; these are known as facultative anaerobes [81].

● Types of Bacteria According to Gram Staining

Since bacterial organisms are so minute, it is impossible to view the organisms without compound microscope. In order to visualize the cellular components and to differentiate bacteria from other microbial agents, staining techniques are used to categorize different bacteria.

Gram staining (or Gram's method) is a method of differentiating bacterial species into two large groups (gram-positive and gram-negative). The name comes from its inventor, Hans Christian Gram. Gram staining differentiates bacteria by the chemical and physical properties of their cell walls by detecting peptidoglycan, which is present in a thick layer in gram-positive bacteria [82].

On the basis of gram staining, bacteria with the thick peptidoglycan layer in the cell wall are purple which are classified as gram positive (such as Staphylococcus aureus) and bacteria without a thick peptidoglycan layer in cell-wall are red which are classified as gram negative (such as *Escherichia coli*). Species that fail to stain with the Gram reaction due to presence of large spores, such as Clostridia, require specialized stains [83]. From Figure 2.7 we can observe Gram positive (purple/blue colored cells) and Gram negative (pink/red colored cells) bacteria.

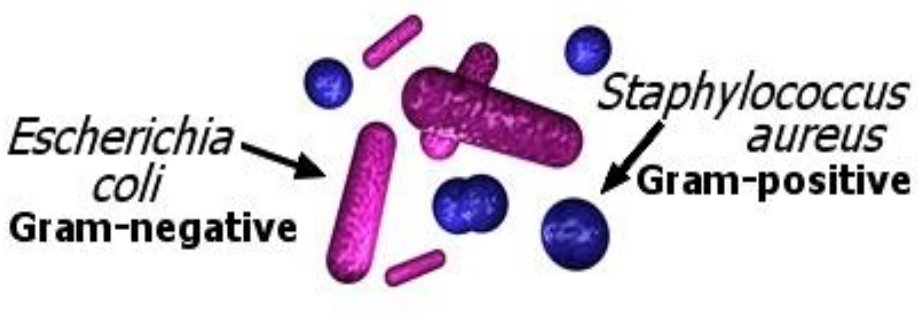

Figure 2.7. Gram staining primarily detects peptidoglycan, which is present in a thick layer in Gram positive bacteria
http://www.microbiologyinpictures.com/morphology%20of%20bacterial%20cells.html
(Gram positive: purple/blue colored cells
Gram negative: pink/red colored cells)

2.2.4 *Staphylococcus aureus*

Staphylococcal aureus bacterium, also called S. aureus is a spherical gram-positive bacteria based on their appearance under a microscope, which also means that the cell wall of this bacteria consists of a very thick peptidoglycan layer. It is also called golden staph. They may occur singly or grouped in pairs, short chains or grape-like clusters (Figure 2.8). They are usually facultative anaerobes, that is, they are capable of surviving at various levels of oxygenation, and are generally very hardy organisms. *Staphylococcus aureus* belongs to the family *Staphylococcaceae* [84].

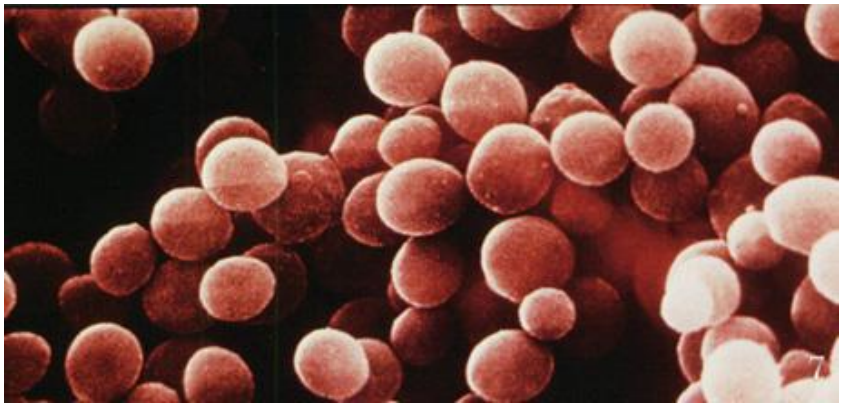

Figure2.8. Staphylococcus aureus Electron micrograph from

http://textbookofbacteriology.net/staph.html

S. aureus is a common bacterium that frequently colonizes the human skin and is present in the nose. In most situations, *S. aureus* is harmless. It can exist in this form without harming its host or causing symptoms. However, if there is a break in someone's skin from a wound or surgery, or if there is a suppression of a person's immune system, then the colonizing *S. aureus* can cause a range of mild to severe infections, which may lead to death in some cases. It affects all known mammalian species, including humans. Further due to its ability to affect a wide range of species, *S. aureus* can be readily transmitted from one species to another. This includes transmission between humans and animals [79].

***S. aureus* can cause:**

- Minor skin infections, such as pimples, impetigo etc.
- It may cause boils (furuncles), cellulitis folliculitis, carbuncles
- It is the cause of scalded skin syndrome and abscesses
- It may lead to lung infections or pneumonia
- Brain infections or meningitis
- Bone infections or osteomyelitis
- Heart infections or endocarditis
- Generalized life threatening blood infections or Toxic shock syndrome (TSS), bacteremia and septicaemia [79]

The growth and survival of *S. aureus* is dependent on a number of environmental factors such as the temperature range for growth of *S. aureus* is 7–48 ℃, with an

optimum of 37 ℃. It is resistant to freezing and survives well in temperature below -20 ℃, however, the viability is reduced at temperatures of -10 to 0 ℃; Growth of *S. aureus* occurs over the pH range of 4.0–10.0, with an optimum of 6–7; and it is a facultative anaerobe which can grow under both aerobic and anaerobic conditions. However, growth occurs at a much slower rate under anaerobic conditions [85].

Pathology

S. aureus is the most common cause of staphylococcal infections and is responsible for various diseases including: mild skin infections (impetigo, folliculitis, etc.), invasive diseases (wound infections, osteomyelitis, bacteremia with metastatic complications, etc.), and toxin mediated diseases (food poisoning, toxic shock syndrome or TSS, scaled skin syndrome, etc.). Infections are preceded by colonization. Common superficial infections include carbuncles, impetigo, cellulitis, folliculitis. Community-acquired infections include bacteremia, endocarditis, osteomylitis, pneumonia and wound infections are less common. *S. aureus* also causes economically important mastitis in cows, sheep and goats [85].

As a pathogen, it is important to understand the virulence mechanisms of *S. aureus* especially the Methicillin-resistant (Figure 2.9).

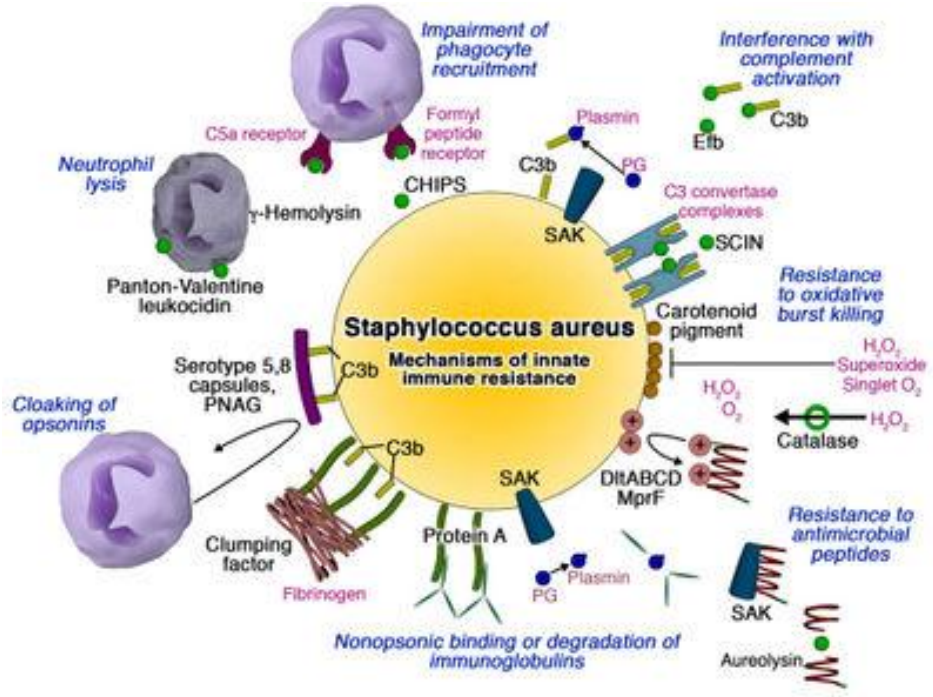

Figure 2.9. The pathogenic capacity of a given strain of S.aureus is the combined effect of extracellular factors, virulence factors together with invasive properties of the strain. "*Staphylococcus aureus* : Lab Diagnosis and Diseases"
http://medchrome.com/mbbs-exams/staphylococcus-aureus-lab-diagnosis-and-diseases/

Staphylococci are becoming increasingly resistant to many commonly used antibiotics including penicillins, macrolides such as erythromycin, tetracyclines and aminoglycosides. Penicillin resistance in *S. aureus* is due to production of an enzyme called beta-lactamase or penicillinase. Methicillin (meticillin) and flucloxacillin are lactamase-resistant penicillins so are the antibiotics of choice in most staphylococcal skin infections. Unfortunately there is now increasing methicillin resistance (MRSA). MRSA infection is caused by a strain of staph bacteria that's become resistant to the antibiotics commonly used to treat ordinary staph infections. This strain expressed a modified penicillin-binding protein encoded by mecA gene and is present in 4 forms of Staph. The MRSA, resistant to the antibiotic methicillin, was eventually isolated.

Consequently, vancomycin (the most powerful antibiotic in our arsenal) became the primary antibiotic used to combat staphylococcal infection. In 1997 a strain of *S. aureus* resistant to vancomycin was isolated, and people are once again exposed to the threat of untreatable staphylococcus infection [86].

MRSA strains are currently a major pathogen worldwide and a very significant health care problem. MRSA infections are associated with increased morbidity and mortality, in comparison with other *S. aureus* infections. Over the past decade, the changing pattern of resistance in *S. aureus* has underscored the need for new antimicrobial agents. Increasing population of "super germs" and antibiotic resistant pathogens has increased pressure on researchers to find alternative, more effective ways of fighting these "super germs" [87,88].

2.2.5 *Escherichia coli*

Cell Structure

E. coli is a Gram-negative rod-shaped bacteria, which possesses adhesive fimbriae and a cell wall that consists of an outer membrane containing lipopolysaccharides, a periplasmic space with only 1 to 2 layers of peptidoglycan, and an inner cytoplasmic membrane. Each bacterium measures approximately 0.5 μm in width by 2 μm in length (Figure 2.10). They can be commonly found in animal feces, lower intestines of mammals, and even on the edge of hot springs [89].

Some strains are piliated and capable of accepting and transferring plasmid to and from other bacteria. Such property enables *E. coli* under bad/stress conditions to survive. Even though it has extremely simple cell structure, with only one chromosomal DNA and a plasmid, it can perform complicated metabolism to maintain its cell growth and cell division. *E. coli* is a facultative anaerobe, which means it does not require oxygen, but grows better in the presence of oxygen. Optimal growth of *E. coli* occurs at 37 ℃ but some laboratory strains can multiply at temperatures of up to 49 ℃. They prefer to live at a higher temperature rather than the cooler temperatures. *E. coli* is a Gram-negative organism that cannot sporulate. Therefore, it is easy to eradicate by simple boiling or basic sterilization [90].

Figure 2.10, Ultrastructure of Gram-negative rod-shaped *Esherichia coli* cell http://ecdc.europa.eu/en/healthtopics/escherichia_coli/basic_facts/pages/basic_facts.aspx

Most *E. coli* strains are harmless, but some serotypes can cause serious food poisoning in their hosts. However, *E. coli* strains are able to produce a toxin that could cause severe infections in many mammals, such as humans, sheep, horses, dogs, etc. The one that only found in humans is called enteroaggregative *E. coli*. Urinary tract infection, for example, can be caused by ascending infections of urethra. Such infections can be

found in both adult male and female, and some infants can be infected as well. *E. coli* consists of a diverse group of bacteria. Pathogenic *E. coli* strains are categorized into several pathotypes. Six pathotypes are associated with diarrhea and collectively are referred to as diarrheagenic *E. coli* [91,92].

E. coli O157:H7 is one of the most infective strains that can cause food poisoning. It is an enterohemorrhagic strain and can lead to bloody diarrhea and kidney failure when one gets infected by contaminated ground beef, unpasteurized milk or contaminated water. The toxin that *E. coli* O157:H7 produces is called Shiga-like toxin which is a regulated toxin that catalytically inactivates the 60S ribosomal subunits of most eukaryotic cells, blocking mRNA translation and thus causing cell death. Some important symptoms are diarrhea that is acute and severe, either bloody or not bloody, stomach cramping, vomiting, loss of appetite, abdominal pain, and fever. *E. coli* O157:H7 is also notorious for causing serious and even life-threatening complications such as hemolytic-uremic syndrome. The O104:H4 strain is equally virulent. It is the strain behind the ongoing and deadly June 2011 *E. coli* outbreak in Europe [93,94].

Shiga toxin-producing *E. coli* (STEC) is a group of pathogenic *Escherichia coli* strains capable of producing Shiga toxins, with the potential to cause severe enteric and systemic disease in humans. Transmission of STEC infection mainly occurs through contaminated food or water and contact with animals. Person-to-person transmission is also possible among close contacts [95].

Some studies revealed *Escherichia coli* strains are resistant to many of the commonly used antibiotics such as ampicillin, and some research showed that 74% of them are resistant to two or more antibiotics. *E. coli* isolates recovered from raw poultry meat are highly resistant to antimicrobials and carry antimicrobial resistance genes that could be transferred to other microbes in the food chain, even important human pathogens. Nowadays, *E. coli* accounts for 17.3% of clinical infections requiring hospitalization and is the second most common source of infections behind *Staphylococcus aureus* (18.8%). Scientists have warned that *E. coli*, as a frequent cause of infection, is becoming resistant to antibiotics and the resistance problem could become as big as MRSA [96,97].

***E. coli* can cause:**

- Abdominal pain - typically, the first symptom is severe abdominal cramping that comes on suddenly.
- Diarrhea - a few hours after the sudden abdominal pain, the patient typically has watery diarrhea. A day later there may be bright red bloody stools, caused by sores in the intestines.
- Nausea
- Vomiting - note that many patients who become ill may not vomit
- Fever - note that many infected people may not have a fever
- Fatigue - diarrhea causes loss of fluids and electrolytes (dehydration),

making the patient feel sick and tired [98].

2.2.6 Wound infection

Wound infection presents the deposition and multiplication of microorganisms within a wound that cause an associated host reaction. When such wounds become infected, they are often colonized by multiple bacterial species. The most common pathogens are aerobic Gram-positive cocci such as: *S. aureus*, but complicated infections frequently involve Gram-negative bacilli like *E. coli* and anaerobic bacteria. These infections are often further characterized as being acute (present for days to at most a few weeks) or chronic (persisting for many weeks to months). Soft-tissue infections can be localized or focal (e.g. impetigo, abscess) or diffuse (e.g. cellulitis, fasciitis) [84].

2.2.7 Antimicrobial Treatment for Wound Infection

Antibiotics

An antibiotic is an antibacterial agent that either destroys or suppressing the growth or reproduction of bacteria. Antibiotics are commonly classified based on their mechanism of action, chemical structure, or spectrum of activity [99].

- **Bactericidal**

The antibiotics have activities to target the bacterial cell wall (penicillins and

cephalosporins) or the cell membrane (polymyxins), or interfere with essential bacterial enzymes (rifamycins, lipiarmycins, quinolones, and sulfonamides) to kill bacteria.

● **Bacteriostatic**

The antibiotics have activities to target bacteria protein synthesis (macrolides, lincosamides and tetracyclines) to inhibit the growth of a microorganism [100,101].

Antibacterial agents for the control of acute traumatic and chronic wounds [102,103]

1. Acute wounds

Since *S. aureus* is considered to be the most problematic pathogen associated with infected traumatic wounds, flucloxacillin and oxacillin are often the choice of treatment. If methicillin-resistant strains are involved, the glycopeptide antibiotics vancomycin and teicoplanin are alternatives.

2. Chronic wounds

The majority of chronic wounds are characterized by polymicrobial aerobic and anaerobic bacteria. The use of broad-spectrum antimicrobial agents is likely to be the most successful treatment in the management of clinically infected chronic wounds. However, the probability of a successful outcome in chronic wounds may be compromised by the presence of ischemic and necrotic tissue which may impair tissue distribution and therapeutic efficacy of the drug. Topical antibiotics are used as double antibiotic combinations to provide an appropriate spectrum of activity.

Complementary therapy

Wound bed debridement may assist antibiotic treatment by reducing the microbial load, and hence the opportunity for infection, and enabling better penetration of antibiotics to where they are needed.

Antiseptics

Antiseptics are chemical agents that are potentially toxic to both microbial cells and host cells. Therefore, their use is limited to topical application to wounds and intact skin. Commonly used topical antiseptic agents are iodine-releasing agents, chlorine-releasing solutions, hydrogen peroxide, chlorhexidine, silver-releasing agents [104].

Alternative antimicrobial therapy: specific importance to this research study

As the development of bacterial resistance to antibiotics continues, the need for identification and development of new antimicrobial agents become increasingly critical [105]. In recent years, widespread interest has focused on a class of naturally occurring peptides that protect a variety of animals from infection. These peptides are found in a variety of cell types and operate by attaching to microbial cells, perforating the cell wall, and inducing leakage of cell contents. Such pore-forming antimicrobial peptides are widespread throughout nature such as human neutrophils produce defensins, magainins have been isolated from the skin of the African clawed frog, and cecropins have a similar function in the giant silkworm moth [106].

2.2.8 Antimicrobial peptides (AMP)

Background

The discovery of antibiotics has definitely been the major achievement in the treatment of infectious agents and it is one of the most important medical developments of the twentieth century. Up to date, the antibiotics are the common anti-infection drugs applied in clinic, but the rising antibiotics resistance making the currently applied standard anti-infection drugs losing effectiveness. The rise of resistant pathogens is posing increasing difficulties and the increasing severity of infections within hospital populations. Resistance to antibiotics is highly prevalent in bacterial isolates worldwide, particularly in developing countries as the excessive use of antibiotics which result the pathogenic bacteria diversified into resistant to the use of traditional antibiotics each year [107,108].

Although effective new types of antibiotics against multidrug-resistant Gram-positive bacteria such as methicillin-resistant *S. aureus* (MRSA) have been introduced or are in clinical trials, the situation regarding new treatment options for infections produced by multidrug-resistant Gram-negative pathogens such as *Acinetobacter baumannii*, *Pseudomonas aeruginosa*, *Klebsiella pneumoniae*, and *Stenotrophomonas maltophilia* is still less encouraging [109,110]. Due to increasing antibiotic resistance by pathogenic bacteria, it has become necessary to develop new antimicrobial molecules as

therapeutic agents to overcome this problem. Hence, there is an urgent need to find new types of alternative antimicrobial agents with activity against these microorganisms to eradicate the antibiotics resistance pathogens [111].

For the development of next-generation antibiotics, in recent decades, it has been found that a new class of antimicrobial agents called antimicrobial peptides (AMPs) and proteins also known as "natural antibiotics" which have shown to represent promising alternative drugs for overcoming the problems of antibiotic resistance [112].

AMPs represent a part of non-specific immune response and have been described as "evolutionary ancient weapons". Currently, they have received much more attention due to their rapid and broad-spectrum antibiotic effect, and apart from their direct bactericidal effect they also have immunomodulatory properties, such as stimulating immune cells and enhancing the inflammatory response. These types of peptides constitute an important part of the immune defense and most of them act by disrupting the bacterial membrane [113,114].

Diversity of AMPs

Thousands of AMPs have been discovered and isolated from organisms as diverse as plants, insects, amphibians, humans and even bacteria. Since many AMPs exert rapid bactericidal activity against a broad range of microbes, and as the probability of pathogens acquiring resistance is low, AMPs open new avenues for antibacterial drug

development, especially against multidrug-resistant strains. These natural antimicrobial peptides or the host defenses peptides are generally positively charged and comprised of less than 100 amino acid residues with amphipathic properties. These peptides are conserved during evolutionary process in response to their innate immunity and serve as a first line of defense system. These peptides have been identified in virtually all forms of life from bacteria and animals to plants [112,115].

The peptides have been classified into four groups on the basis of their structure [116]:

(i) α-helical

(ii) β-sheet

(iii) α-helical&β-sheet

(iv) Non-α&β families(AMPs rich in specific amino-acids)

In general, α-helical peptides are amphipathic, often with a bend around the central region disrupting an otherwise fairly perfect cylindrical structure. The β-sheet AMPs are usually formed by the presence of disulfide bonds with amphipathic patches scattered on the surface. The αβ-peptides consist of both α-helical and β-sheet structures, whereas non-αβ AMPs are free of α-helical and β-sheet structures, often unstructured, and rich in proline, arginine or histidine residues (Figure 2.11).

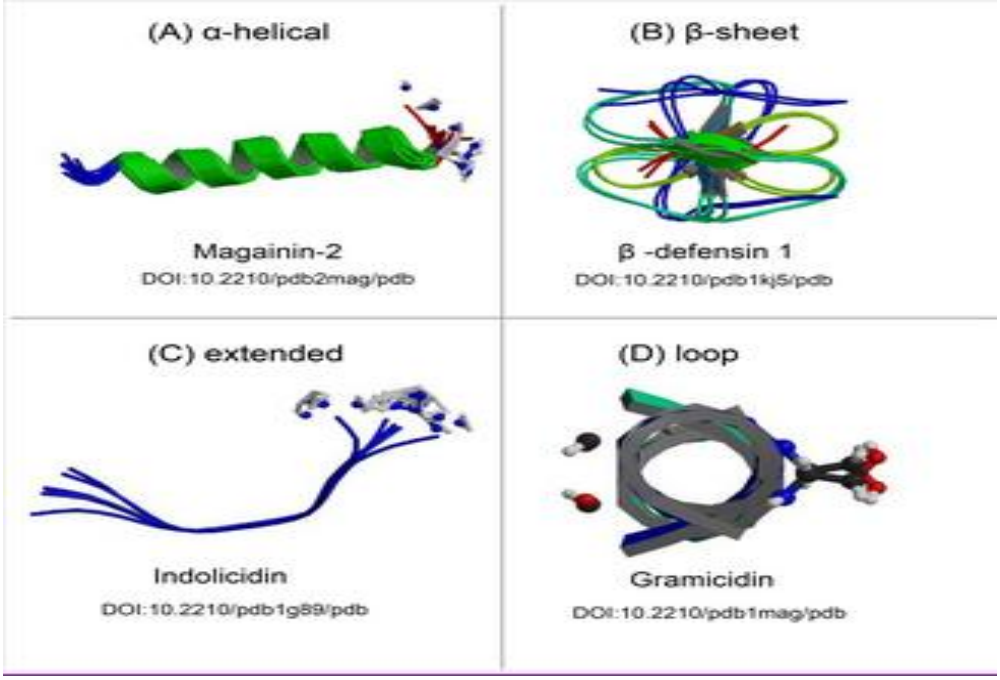

Figure 2.11. Structures of antimicrobial peptides
http://www.plospathogens.org/article/info%3Adoi%2F10.1371%2Fjournal.ppat.1001067

It has been found that AMPs possess approximately 50% hydrophobic residues and exhibit spatially separated hydrophobic and hydrophilic regions with amphipathic properties during interaction with biological membranes. In fact, the majority of AMPs present similar physicochemical properties with conventional antibiotics, including small molecular size and cationic and amphiphilic properties, that seem to be essential for activity. Their broad spectrum of action and the low number of observed phenomenon of resistance are advantages over conventional antibiotics, although their mode of action is not fully understood and not always studied yet [117].

The mechanism of antibacterial activity of peptides

Virtually every peptide sequence with a net positive charge and a few hydrophobic

residues will have antimicrobial activity. In general, the amphiphilic drugs often have targets that are associated with the cytoplasmic membrane, to which they bind and laterally diffuse within, until they come in contact with their target molecule. The fundamental function of the plasma membrane is to act as a barrier allowing cellular organisms to maintain a chemical gradient of ions and solutes, the loss of which inevitably leads to death [118,119].

The cationic and amphiphilic nature of antimicrobial peptides is associated with positive charge and amphiphilic activity. The mechanism of antimicrobial activity of AMPs is to interact with microbe membranes and disrupt them. Some of the peptides may form pores or holes in the membrane, others may change the membrane structure by poking into it in many places. But the bottom line is these peptides damage membranes and makes them more permeable. When a microbe's membrane is too permeable, it will die. One reason is that it can lose important metabolites and ions, and molecules from the environment that the microbe would rather keep out can come right in. The bactericidal activities of AMPs are dependent on their ability to permeabilize membranes by creating pores or disrupting the organization of the lipid bilayer. The initial steps of membrane attack are thought to include electrostatic and receptor-mediated interactions [106-120].

It has become increasingly clear that AMPs can also act through mechanisms involving interaction with membraneassociated protein targets or by penetration into the bacterial

cytoplasmand interacting with intracellular targets to reduce the activities of essential cellular processes including the synthesis of protein, DNA, RNA, and components of the bacterial cell envelope (Figure 2.12). Relying primarily on the physical membrane-lytic mechanisms, the AMPs kill bacteria with a low risk of triggering resistance [121,122].

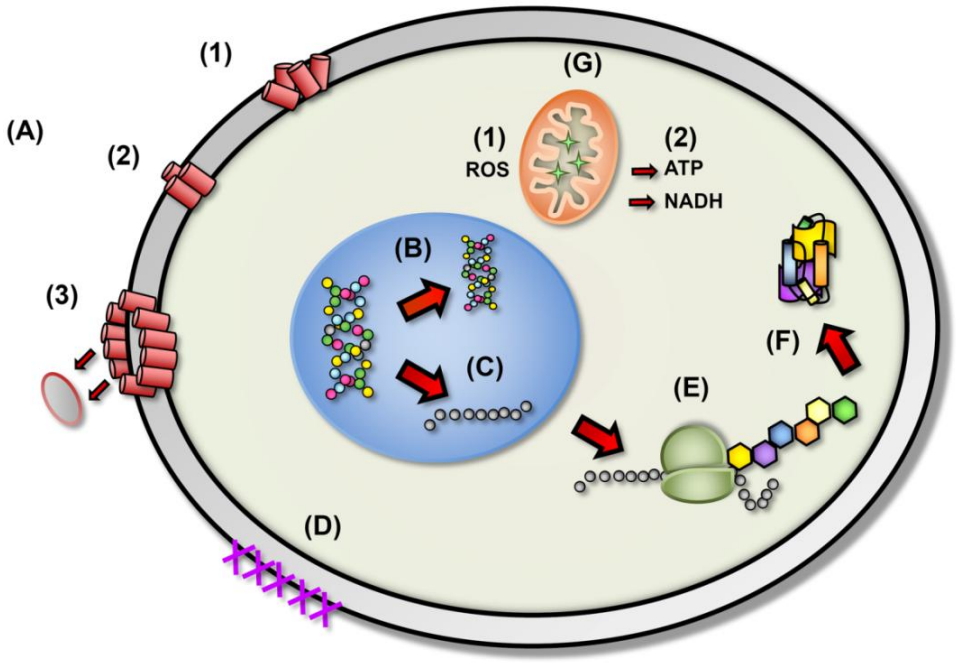

Figure 2.12. The proposed diverse mechanistic modes of action for antimicrobial peptides in microbial cells.
(A) Disruption of cell membrane integrity: (1) random insertion into the membrane, (2) alignment of hydrophobic sequences, and (3) removal of membrane sections and formation of pores. (B) Inhibition of DNA synthesis. (C) Blocking of RNA synthesis. (D) Inhibition of enzymes necessary for linking of cell wall structural proteins. (E) Inhibition of ribosomal function and protein synthesis. (F) Blocking of chaperone proteins necessary for proper folding of proteins. (G) Targeting of mitochondria: (1) inhibition of cellular respiration and induction of ROS formation and (2) disruption of mitochondrial cell membrane integrity and efflux of ATP and NADH.
http://www.plospathogens.org/article/info%3Adoi%2F10.1371%2Fjournal.ppat.1001067

Immunomodulation

In addition to these direct antimicrobial effects, AMPs recently have been found to interact specifically with several membrane-bound or intracellular receptors with a profound ability to modulate the host response by enhancing protective immunity and suppressing inflammation [123,124].

2.2.9 Neutrophils

Neutrophils are the most common type of mature white blood cell and are normally exist in the bloodstream. It is the most abundant (40% to 75%) type of white blood cells in mammals and forms an essential part of the innate immune system. Neutrophils are spherical shape when they unactivated and circulate in the bloodstream. Once activated, they change shape and become more amorphous or amoeba-like and can extend pseudopods as they hunt for antigens [32].

Neutrophils deal with defence against bacterial infection and other very small inflammatory processes and are usually the first responders of inflammatory cells to migrate towards the site of inflammation. They migrate through the blood vessels, then through interstitial tissue, following chemical signals such as Interleukin-8 (IL-8), C5a, fMLP and Leukotriene B4 in a process called chemotaxis. Neutrophils have an impressive range of toxic molecules that contribute to killing bacteria. Neutrophils capture and phagocytose bacteria and subsequently internalize them into

phagolysosomes, in which microbial killing takes place. The protein constituents of phagolysosomes include NADPH oxidase (which generates reactive oxygen species), myeloperoxidase, proteases (such as elastase and cathepsin G) and antimicrobial proteins (including defensins, azurocidin and actericidal/permeability increasing protein) [30,125].

2.2.10 Azurocidin

2.2.10.1 Biosynthesis and processing

According to phylogenetics and evolution studies, the azurocidin belongs to sixth class of serine proteases containing subfamily of proteinases of the immune defense system. This family also includes neutrophil elastase, proteinase 3, cathepsin G, chymase and granzymes. A cluster of genes for neutrophil elastase, proteinase 3 and azurocidin is located in the terminal region of the short arm of human chromosome 19. The neutrophil elastase, proteinase 3 and azurocidin genes are constitutively expressed in a cell-specific manner during the promyelocyte stage of neutrophil differentiation and, after processing. All these proteins are localized inside granular structures of different immune effect or cells and contribute to the destruction of ingested microorganisms [126].

Azurocidin is synthesized in the early stages of neutrophil maturation process as a precursor of 351 amino acids and processed to a glycosylated mature form of 222

amino acids, and stored in mature neutrophil azurofilic granules together with a set of glycosidases. It bears substantial similarities to serine proteases, especially neutrophil elastase (45% homology), but has no enzymatic activity. Azurocidin possesses some features that make it unique among the neutrophil granule proteins: It is the only neutrophil granule protein stored in two different compartments. As a result of its storage in secretory vesicles and primary granules, azurocidin is released at a very early stage of neutrophil extravasation as well as at a later stage when the neutrophil has reached the site of inflammation, thereby allowing it to target cells in the bloodstream, the endothelial lining, and the extravascular environment [127].

2.2.10.2 Structure of Azurocidin

Structurally, azurocidin is a member of the serine protease family that includes Cathepsin G, Neutrophil Elastase (NE), and Proteinase 3 (PR3). However, as a result of mutations in two of the three essential amino acids in the highly conserved catalytic triad seen in all serine proteases, azurocidin is devoid of protease activity. It is a single polypeptide glycoprotein synthesized as a 251 amino-acid precursor processed by removal of 26 amino-acid residues from the N-terminus and three residues from the C-terminus. Sequence analysis shows 45% homology to human neutrophil elastase, 42% homology to proteinase 3, and 32% homology to cathepsin G from human neutrophils [29].

Azurocidin is an Azurophil granule antibiotic protein, with monocyte chemotactic and antibacterial activity. It possesses antibacterial activity through its binding to

Gram-negative bacterial lipid A. As a modulator of endothelial permeability, Azurocidin acts as Neutrophils arriving first at sites of inflammation release Azurocidin which acts in a paracrine fashion on endothelial cells causing the development of intercellular gaps and allowing leukocyte extravasation. Azurocidin thus can be regarded as a reasonable therapeutic target for a variety of inflammatory disease conditions [128].

2.2.10.3 Antimicrobial Activity

The Azurocidin released extracellularly from neutrophil granules not only exerts antimicrobial activity to eliminate bacteria but also modulate immune response to direct monocytes and macrophages to the site of infection and activate their antimicrobial function [129-132].

Direct antimicrobial effects

Azurocidin exerts its antimicrobial activity by directly disrupting the microbial cell membrane, based on the combination of cationicity, amphipathicity and hydrophobicity appear to be unique to this antimicrobial peptides. The Azurocidin demonstrates direct antimicrobial activity through its binding capacity with lipopolysaccharide (LPS) and lipid A that was found on the surface of microbial cells, disrupting lipid bilayers through a variety of mechanisms and induce leakage of the bacterial membrane and to kill microorganisms [133-135]. The capacity of Azurocidin to kill bacteria within phagolysosomes may be regulated by the intraphagosomal

hydrogen ion concentration. It has been generally appreciated that the intraphagosomal hydrogen ion concentration in time extends over a broad range, eventually becoming quite acidic. Thus, it would be advantageous to the O_2-independent antimicrobial petides, such as Azurocidin, capable of bactericidal activity at various intraphagosomal hydrogen ion concentrations. Evidence presented shows the existence of Azurocidin that functions in vitro over a pH range similar to that of maturing phagolysosomes and is most active at or near pH 5.5. This pH is considered to be at or near the final pH of the mature phagolysosome. These results suggest that Azurocidin may contribute significantly to the capacity of polymorphonuclear granulocytes (PMN) to kill intraleukocytic bacteria by nonoxidative pro-cesses as the pH of the maturing phagolysosome declines after phagocytosis [128,136-138].

Modulation of immune response

Azurocidin has a broad spectrum of antimicrobial activity. In addition, it is also recognized as a multifunctional inflammatory mediator for its contracting effects on endothelial cells causing an increase of vascular permeability, capacity to bind endotoxin and ability to attract monocytes to inflammation sites. Monocytes and macrophages are multifunctional cells contributing to bacterial clearance by phagocytosis and killing of bacteria. Moreover, ingestion of bacteria by resident or newly recruited macrophages is an essential mechanism of host defense. Azurocidin, released from PMN secretory vesicles act as chemoattractant and activator for monocytes, T-cells, and K-cells and induces longevity and differentiation of monocytes

toward a macrophage phenotype.The consequence is enhancement of cytokine release and bacterial phagocytosis, allowing for a more efficient bacterial clearance [130,139].

CHAPTER 3

Electromagnetic Radiation: Biological Effects and Therapeutic Applications

---

3.1 Electromagnetic radiation

Non-ionizing radiation is the radiation that has enough energy to move atoms in a molecule around or cause them to vibrate, but not enough to remove electrons from atoms. Sound waves, visible light, and microwaves are referred to as "non-ionizing" radiation. Non-ionizing radiation has found many different applications in everyday life:

- Microwave radiation: telecommunication industry, microwave ovens (cooking and heating food), medical devices, and food technology.
- Infrared radiation: infrared lamps, toasters, security etc.
- Ultraviolet radiation: for microbial sterilization, photo-chemotherapy.
- Radio waves: broadcasting

Ionizing radiation has more energy than non-ionizing radiation; enough to cause chemical changes by breaking chemical bonds. This effect can cause damage to living tissue. Shorter wavelength ultraviolet radiation begins to have enough energy to break chemical bonds. X-ray and gamma ray radiation, which are at the upper end of

electromagnetic spectrum, have very high frequencies (in the range of 100 billion billion hertz) and very short wavelengths (1 million millionth of a metre). Radiation in this range has extremely high energy. It has enough energy to strip electrons from an atom or, in the case of very high-energy radiation, break up the nucleus of the atom. The process in which an electron is given enough energy to break away from an atom is called ionization. This process results in the formation of two charged particles or ions: the molecule with a net positive charge, and the free electron with a negative charge. Each ionization releases energy which is absorbed by material surrounding the ionized atom. Compared to other types of radiation that may be absorbed, ionizing radiation deposits a large amount of energy into a small area. In fact, the energy from one interaction with an atom is more than enough to disrupt the chemical bond between two carbon atoms. All ionizing radiation is capable, directly or indirectly, of removing electrons from most molecules.

The examples of utilizing ionizing radiation in everyday life:

- The main use of X-rays is in medicine (with a X-ray machine as a common application)

- Gamma radiation is often used to kill living organisms. Applications of this include sterilizing medical equipment, removing decay-causing bacteria from many foods or preventing fruit and vegetables from sprouting to maintain

freshness and flavor. Gamma rays are also used to treat some types of cancer, in the procedure called gamma-knife surgery [148].

Visible light

Of particular interest to this PhD project are biological effects of visible light radiation on proteins and cells. The visible spectrum is the portion of the electromagnetic spectrum that can be detected by human eye. The electromagnetic radiation in this range of wavelengths is called visible light (Figure 3.4). A typical human eye can respond to wavelengths from about 390 to 700 nm. In terms of frequency, this corresponds to a band in the vicinity of 430–790 THz (Table 3.1) [149].

The human eye is not capable of seeing radiation with wavelengths outside the visible spectrum. The visible colors from shortest to longest wavelength are: violet, blue, green, yellow, orange, and red. Ultraviolet radiation has a shorter wavelength than the visible violet light. Infrared radiation has a longer wavelength than visible red light. The white light is a mixture of the colors of the visible spectrum. Black is a total absence of light [150].

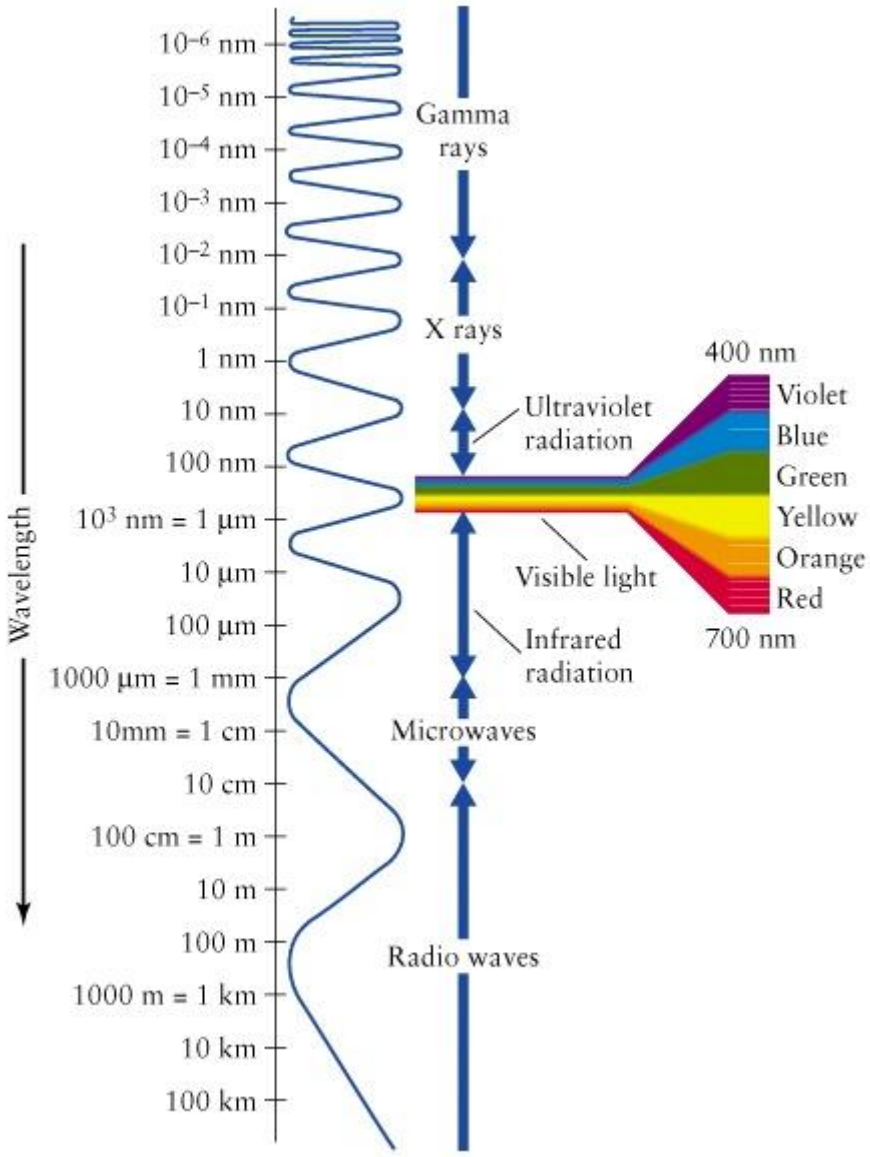

Figure 3.3 Wavelength image from Universe by Freedman and Kaufmann

Energy with wavelengths too short for humans to see

- Light with shorter wavelength than the violet light is called "Ultraviolet" light

Energy with wavelengths too long for humans to see

- Light with longer wavelength than red light is called "Infrared" light.

Table 3.1 Visible light wavelength and corresponding frequency [151]

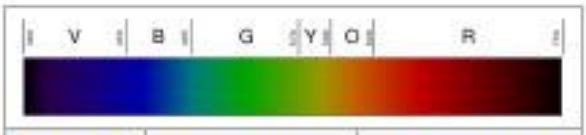

Color	Wavelength	Frequency
violet	380–450 nm	668–789 THz
blue	450–495 nm	606–668 THz
green	495–570 nm	526–606 THz
yellow	570–590 nm	508–526 THz
orange	590–620 nm	484–508 THz
red	620–750 nm	400–484 THz

3.2 Bioelectromagnetism

There has been increasing concern about the harmful effects of exposure to ambient electromagnetic fields. However, electromagnetic energy is not a general toxin but a specific modality for transferring information to and from biological systems. Thus, there is great potential for beneficial use of electromagnetic field in different biological and medical applications.

A human body produces its own very complex electrical activity. Wherever there is electrical activity, there is also a magnetic field. The natural internal electrical and magnetic fields of the body regulate all the body's processes and interact with one

another [152]. Groups of functional cells constitute higher organisms. There are narrow fluid channels between cells that take on special importance in signaling from cell to cell. These channels act as windows on the electrochemical world surrounding each cell. Hormones, antibodies, neurotransmitters and chemical cancer promoters, for example, move along them to reach binding sites on cell membrane receptors [153].

The cell is the smallest unit of living organisms. It is believed that the cell membrane is an important site of interaction for electromagnetic fields. There are free ions that can move across the cell membrane, such as K^+, Na^+, $Cl^-$and Ca^{2+}, on both sides of every cell membrane, but in different concentrations. These ions control the cell volume, help the signaling process, and create a strong electric field between both sides of the cell membrane. The cell membrane contains ion channel proteins, the opening of which can be regulated by the transmembrane voltage, mechanical stress (mechanically gated channels gated by ion pressure) of chemical signals. The basic mechanism proposed is the forced vibration of all the free ions on the outer surface of a cell membrane, caused by an oscillating electric field. It is showed that this vibration of electric charge is able to irregularly gate voltage-gated channels in the plasma membrane, and thus disrupt the cell's electrochemical balance and function [154,155].

Nothing in a living organism is static as there are movements of cells, tissues and organs. Thus in living tissue, it is mostly find alternating fields as well as a combination of EF and MF. Short-lived electrical events called action potentials occur

in several types of animal cells which are called excitable cells, a category of cell include neurons, muscle cells, and endocrine cells, as well as in some plant cells. These action potentials are used to facilitate inter-cellular communication and activate intracellular processes. The physiological phenomena of action potentials are possible because voltage-gated ion channels allow the resting potential caused by electrochemical gradient on either side of a cell membrane to resolve [156]. The EMF frequencies in human body are normally in the range of extremely low frequencies (ELF). This EMF includes the action potentials of nerves and heart tissue, skeletal muscle vibrations and frequencies elicited by rhythmic activities within other body tissues. The strength of human body's magnetic fields in relation to the strength of the Earth's magnetic field is shown in the table (Table 3.2) [152]. It can be seen that using the Earth's magnetic field as a comparison, the body's natural are incredibly tiny.

Table 3. 2 Strengths of endogenous magnetic fields versus Earth's field [152]

Signal source	**Femto Tesla**	**Gauss**	**Earth's field stronger by**
Skeletal Muscle	~50,000	0.0000005	1 million times
Heart	~500,000	0.000005	100,000 times
Physiologic "noise"	50,000-5,000,000	0.0000005-0.00000005	1–10 million times
Earth's field	50,000,000,000	0.5	

3.3 Biological effects of electromagnetic fields

Overview

During the past two decades, it has become increasingly interesting for the biological effects of electromagnetic fields exert a wide range of athermal effects to alternate the specific physiological process, when energetic patterns and "biotargets" are properly matched. The interaction of electromagnetic fields with biological systems involves exposures ranging from continuous waves to short pulses and field magnitudes that range from “weak” to “strong” [157]. Electromagnetic waves in the frequency range 3–300 GHz are often referred to as millimeter waves (MMWs) and are of interest because of health and safety concerns or diagnostic and therapeutic use [158].

Currently, the interaction of EMF with biological systems involves [159]:

1) **The passive effect** (detection of endogenous magnetic fields) is in use for diagnostic purposes. It is possible to get valuable information about the functioning of various organs by analysis of the magnetic fields which they emit.
2) **The active effect** of EMFs - its use for different therapeutic applications.

The most biological molecules take place in the cells and in organisms are likely made of elements from C, O, H, N and S. When biological objects are exposed to EMF, changes occur in the energy levels of uncoupled EMF sensitive electrons of molecules,

which are in the cells of living organisms that are exposed to EMF. These changes affect the ratios of chemical reactions and thus, noticeable different chemical changes do occur at different EMF intensities. Since biological molecules are highly heterogeneous in structures, when they are exposed to electrical fields, important changes occur in their properties. The current that passes through the biological system, causes the positively and negatively charged molecules in the environment to drift towards opposite directions. In this way, the structural ingredient order of the environment changes and there is an increase in the concentration of certain loaded ions in different parts of the cell [160].

3.3.1 Effects of low frequency EMF on cells

1) Membrane changes

The cell membrane is a biological membrane that separates the interior of all cells from the outside environment. The cell membrane is selectively permeable to ions and organic molecules and controls the movement of substances in and out of cells. It consists of the phospholipid bilayer with embedded proteins (Figure 3.5). Cell membranes are involved in a variety of cellular processes such as cell adhesion, ion conductivity and cell signaling and serve as the attachment surface for several extracellular structures, including the cell wall, glycocalyx, and intracellular cytoskeleton [161].

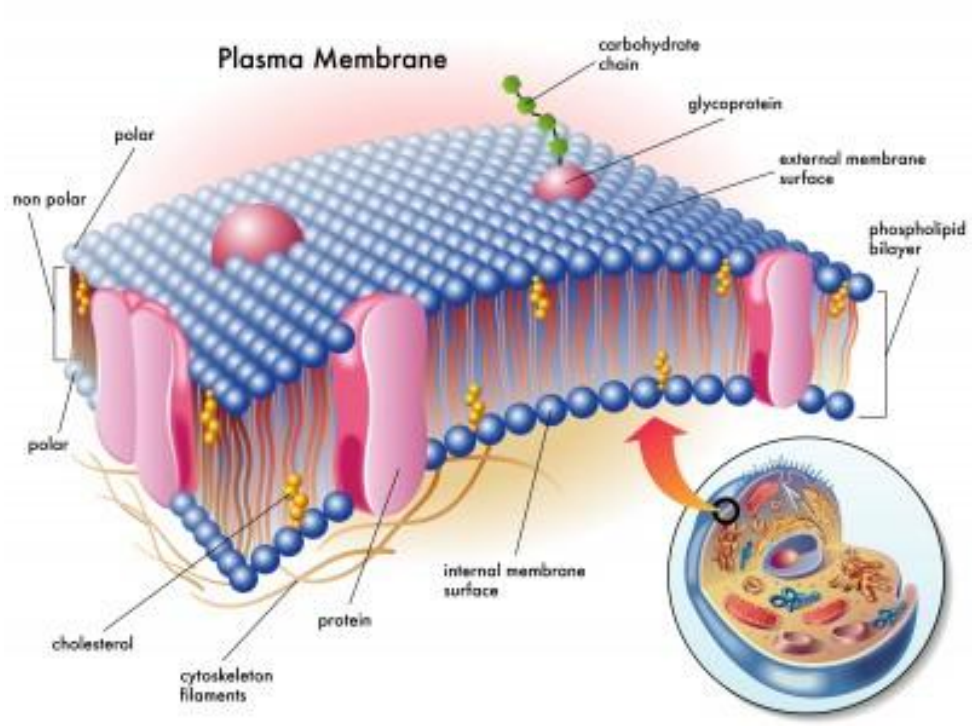

Figure 3.4 Cell membrane detailed diagram [162]

Cell membranes not only keep apart materials that not be allowed to mix, they also act as electrical insulators for the natural electric currents upon it. Natural electric currents are normally generated by molecular ion pumps in cell membranes. These are proteins that use metabolic energy to transport specific ions, usually one or two at a time, from one side of the membrane to the other. This, in turn, generates a voltage across the membrane (the membrane potential) and a chemical imbalance between the concentrations of ions on either side. Their combined effect gives an electrochemical gradient, which provides energy for other functions [163].

The main signs of radiation-induced membrane perturbation are the changes in the

organization and/or composition of the glycocalyx, manifested as alterations in the amount and/or distribution of the negatively charged membrane components (i.e. sialic acid), lectin-, and calcium-binding sites. It is well known that the exposition to ionizing radiation is followed by reversible decrease of surface negative charges in several cell types [164]. Electromagnetic field expositions (non-ionizing radiation) may also modify the amount of cell surface's negative charges. However, the magnitude of this effect is dependent on the type of the field applied. Changes of lectin-binding capacity of cell membranes following ionizing and non-ionizing radiation have been observed by many authors [165-167].

When the erythroleukemia series of K 562 cells were exposed to 2.5 mT EMF for 24 to 72 h, and the cellular surfaces of the control and experiment groups were compared afterwards using the electron microscopy, it was observed that cellular surfaces with many microvillus and bubble-like structures were created quickly in cells that were reproduced in result to direct EMF exposures [168].

2) Ionic effects

It was shown that Ca++ channel blockers, parathyroid hormone, and IGF-II, among others are affected by weak time-varying EMF [169].

●Calcium

It was found that low frequency (LF) EMF affects the concentrations of free intracellular Ca^{2+} concentrations when 50 Hz, 0.1 mT EMF was applied to Jurkat cells

[170]. In this study, the researchers passed the cells through Helmholtz coil for periods between 15 and 200 s. During this exposure, the intracellular Ca^{2+} level increased two to four-fold, from its normal values of 50 to 100 nM to the values of 200 to 400 nM. Similar studies were carried out on peripheral lymphocytes and the response of the intracellular Ca^{2+} concentrations was found to be the same. It was reported that 10% of the lymphocytes responded to magnetic field. On the other hand, it was observed that 85% of the Jurkat cells responded to EMF exposures, with an increase in the intracellular Ca^{2+} concentration.

Changes in calcium flux in lymphocytes exposed to electric and magnetic fields have also reported [171]. Experiments with rat thymocytes showed both an inhibition in uptake of Ca^{2+} due to magnetic field application, and a stimulation when the cells were simultaneously stimulated with a mitogen and an electric field [172].

●Sodium and potassium

As reported in study [173-175], the researchers observed an increase in the Rb^{+} transportation which is potassium analog. Despite the concentration gradient, there was no change in the ATP hydrolysis. In view of this result, it was suggested that Na^{+}-K^{+} ATPase enzyme increases the Rb^{+} transportation by using the energy coming from the applied EMF.

3) Nucleic acid and gene expression

DNA

The effects of EMF on DNA replication was also studied and it was determined that EMF at a level of 0.1 to 0.4 mT inhibits the DNA synthesis in Jurkat cells [176].

In another study, brain cells of the experimental rats were exposed to 0.01 mT of magnetic field at 60 Hz for 24 h by using applied electromagnetic field. It was observed that 24 h application of EMF increased the DNA single and double strand breaks in brain cells compared to that of the control [177].

●RNA

When 50 MHz radio frequency radiation with the low frequency modulation at 16 Hz was applied to Jurkat T-lenfoblast and Leydig TM3 cells, it was observed that 16 Hz frequency caused a high increase in the RNA synthesis rate of ets1 oncogenes [178].

Proteins

Along with the effects of EMF on RNA transcription, its effect on translation phase was also studied. A study [179] evaluated the changes in the translation level of Escherichia coli RNA polymerase enzyme that was irradiated at 72 Hz and magnetic flux density of 0.07 to 1.1mT (EMF strength) for different periods between 5 and 60 min. It was observed that translation rate increased at the magnetic flux density 0.07 mT. The decrease in the translation rate was also recorded at the high values of EMF strength/power. This was attributed to the instability of RNA in *in vitro* conditions.

Another study [180] showed that the effects of LF EMF at 50 Hz frequency 30 μT on the reproduction behaviors and the protein synthesis of E. coli and Saccharomyces

cerevisiae cells were obtained. EMF was generated with the Helmholtz coils and EMF parameters (50 Hz and 30 μT). There parameters were specifically selected as human beings are exposed to this type of exposures in their daily lives. According to the results of the study, the applied LF EMF decreased the total protein amount of the bacteria and yeast cells and also reduced the reproduction speed.

In study [181] the researchers showed that the enzymatic activity of ornithine decarboxylase (ODC) enzyme was increased when it was exposed to EMF. It was suggested that there is a connection between EMF exposures and cancer risk as it is known that this particular enzyme is active especially in fast growing cells and can induce a tumor's growth.

Another enzyme, whose interaction with the applied EMF was also examined, is the acetylcholinesterase. When the acetylcholinesterase activity was examined in rat bone marrow cells, which were exposed to a strong 1.4 T static magnetic field for 30 min (at the temperature of 37° C), a decrease in the enzymatic activities of cells after 2 h of exposures was observed. At 27 ℃, an increase in the enzymatic activity was detected after 3.5 h of exposures with the same static magnetic field [182].

3.3.2 Effects of ultraviolet (UV) light radiation

Ultraviolet B (UVB) irradiation has been studied as a source for the initiation of lipid peroxidation, and, in fact, a UVB-dependent generation of hydroxyl radicals and lipid

peroxides has been demonstrated in human keratinocytes and fibroblast cultures [183]. Ultraviolet (UV) is known to be able to induce the secretion of matrix degrading enzymes known as matrix metalloproteinases (MMPs) by various cells including keratinocytes, fibroblasts and inflammatory cells, thereby causing excessive collagenous connective tissue breakdown, and also known to decrease the level of collagen synthesis [184,185].

3.3.3 Effects of infrared light radiation

A study showed that with 808 nm infrared light radiation induced a dose-dependent alteration in microglial polarization and resultant microglial induced neurite growth. The infrared radiation of photobiomodulation (PBM) has been found to improve recovery after tissue damage known to be associated with significant neuroinflammation, such as spinal cord injury and traumatic brain injury [186].

In Vivo near-infrared mediated tumor destruction by photothermal effect of carbon nanotubes has been reported that near-infrared of photothermal effect of carbon nanotubes may potentially serve as an effective photothermal agent and pave the way to future cancer therapeutics [187].

It has been investigated that photobiomodulation effects of 1072 nm infrared light on the natural immune response involved in anti-bacterial and wound healing processes. It concluded that 1072 nm infrared light had a photobiomodulation effect which resulted

in an enhanced biological immune response to the bacterial infection by Methicillin-resistant *Staphylococcus aureus* (MRSA) and also increased the expression of Vascular endothelial growth factor (VEGF) to a significant level [188].

Clinical studies have demonstrated beneficial outcomes for low-level laser therapy (LLLT) using near-infrared (NIR) wavelengths. The result showed that Low-level exposure to 980 nm near-infrared laser light can accelerate wound healing in vitro without measurable temperature increases. However, these results also demonstrate the need for appropriate supervision of laser therapy sessions to prevent overexposure to NIR laser light that may inhibit cell growth rates observed in response to lower intensity laser exposure [189].

3.3.4 Effects of visible light radiation

Visible light irradiation of biological systems can be considered in terms of the wavelength, intensity and exposure duration. In the natural environment, light intensity fluctuates and, when in excess, can cause cellular damage. Photosynthetic organisms developed different mechanisms to cope with this fluctuation and to protect themselves from the effects of high UV and visible light, including the regulation of enzymatic activity [190,191].

Light has medical applications in two general categories: high intensity and low intensity light. Each category has therapeutic applications that are very different in

their concepts and applications. High intensity light therapy usually uses a different type of laser beam as its source of light. Due to its concentrated form of light, it is a very powerful and precise tool. These types of lasers are used to remove small tumors as a surgery tool, to apply heat to tumors to shrink them or as diagnostics tool in cancer. For instance, one application of laser in cancer therapy is known as laser therapy. This method utilizes high intensity laser light to shrink or destroy tumors due to the high energy transferred into and absorbed by a tumor. The major benefit of laser therapy is the fact that it causes less bleeding and damage to surrounding tissues [192,193].

Low intensity light (laser or LED) therapy is widely believed as a benign treatment modality. Even though this method is not considered to impose any severe side effects, it is still at its early experimental stages [194,195]. To firmly confirm that low intensity light exposure does not induce substantial side-effects, a number of research studies are being dedicated to this cause. For instance, [196] thoroughly investigates any possible DNA or protein damage in B14 cells after low intensity laser irradiation of near infrared range (810nm). This paper could not establish any cytotoxic or genotoxic effect as result of the exposures. The authors also showed that low level light exposures do not lead to direct damage in DNA.

Several recent studies concluded that biological signaling processes correspond to electrical properties of radiation such as frequency (Hz), intensity of exposure or exposure power (mW), duration (s), and amplitude modulations [197-199]. Effectiveness

of this treatment approach highly depends on their proposed energy transferred (measured by duration and intensity of exposure) and the wavelength of light irradiation. Any changes in these two crucial variables (energy transferred and wavelength) mitigate the therapeutic effect predicted by different research study. For instance, in [200–202], the authors found that the optimum therapeutic effect for bio-modulation is observed at the wavelengths between 630nm and 640nm. Any variation to the wavelengths or total transferred energy other than their specifically predicted parameters reverses the effect or results in a negative outcome [203,204].

Studies have shown that low intensity (less than 100 mW/cm2 range) laser or light therapy is confirmed to have positive effect in pain reduction [205,206], promotion of wound healing [207], tissue growth and post-surgical healing [208].

In wound healing applications, the investigations demonstrated that fibroblast activity could be regulated using light at low fluence/intensity. Using a variety of LED light sources with varying fluence and other parameters, pro-collagen synthesis could be up-regulated in human skin fibroblast culture. This was also found to correlate with the significant clinical changes in human skin [209,210].

The stimulatory effects of low energy lasers irradiation on cell activation have been demonstrated *in vitro* in a variety of cell lines. It was found that low level lasers stimulates the release of transforming growth factor (TGF) and platelet-derived growth

factor (PDGF) from cultured fibroblasts [211]. It's reported a 50% faster healing of wounds treated with a LED array with 3 wavelengths combined into a single unit (670 nm, 720 nm, 880 nm) [212].

3.3.5 Effects of electromagnetic radiation on bacteria and cell growth

A experimental study of Staphylococcus aureus both in Mueller-Hinton broth (MHB) and on Mueller-Hinton agar (MHA) exposed to (1) a low-frequency magnetic field (MF) 20 Hz, 5 mT; (2) a low-frequency MF combined with an additional alternating electric field (MF þ EF) 20 Hz, 5 mT, 470 mV/cm; (3) a sinusoidal alternating electric field (EF AC) 20 Hz, 470 mV/cm; and (4) a direct current electric field (EF DC) 588 mV/cm, the results showed that No significant difference between samples and controls was detected on MHA. However, in MHB each of the four fields applied showed a significant growth reduction of planktonically grown *Staphylococcus aureus* in the presence of gentamicin between 32% and 91% within 24 h of the experiment. The best results were obtained by a direct current EF, decreasing colony-forming units (CFU)/ml more than 91% [213].

Several *in vitro* studies have shown that high-energetic extracorporeal shock waves had a bactericidal effect on planktonic micro-organisms, such as Staphylococcus aureus, Streptococcus epidermidis, Pseudomonas aeruginosa and the MRSA 27065 strain [214,215].

Effects on the treatment of muscle and articular injuries have been reported with the use of radiofrequency radiation. Radiofrequency has been used for aesthetic purposes and some authors have suggested a thermal action in deep tissues, promoting collagen denaturalisation and neocollagenogenesis [216].

Electromagnetic radiation energy without breaking molecular bonds can cause the molecular dipoles to vibrate, inducing mechanical resonance of system. Bacterial effects of extremely high frequency EMR might be explained by EMR effects on charged particles containing structures and molecular chains [217].

Studies investigating the effects of magnetic fields on microorganisms showed that the growth could be inhibited depending on the field strength (power/intensity) and frequency. Some studies observed a decrease in colony forming units of Escherichia coli, Leclercia adecarboxylata and Staphylococcus aureus at 50 Hz, 0.5 mT LF EMF [218]. Strasak et al. [219] applied 5 – 21 mT ELF EMF to E. coli for 0 – 24 h and observed a decrease in bacteria cultures viability. A decrease in growth rate of E. coli subjected to 50 Hz, 2 mT for 6 h and static magnetic fields were also shown to be able to inhibit growth of bacteria [220].

3.3.6 Effects of visible light radiation on bacteria and cells growth

Sunlight is known to play an important role in determining the microbial quality of waste stabilization ponds (WSP) effluents and is a key factor affecting the fate of

pathogens in polluted waters [221]. Sunlight damage to inactive bacteria in pond systems has been described by previous researchers as involving three mechanisms [222]:

- direct damage by UVB wavelengths (280-320 nm) to DNA,
- indirect endogenous damage caused mainly by UVB wavelengths, and
- indirect exogenous damage involving UVB, UVA (320-400 nm) and visible wavelengths of up to 550 nm.

The use of light for environmental and food surface decontamination has generated much interest over many years. Ultraviolet (UV) light applications, although not largely utilized, have been demonstrated for decontamination of equipment in bakeries, and cheese and meat plants. However, despite the efficacy of this technology, due to the safety issues associated with UV light, its ability to degrade plastics and its limited transmissibility through various materials, overall applications have been limited [223].

Visible light radiation, however, has provided a more recent alternative, specifically the visible light wavelength of 405 nm, which has displayed extensive bactericidal properties without the detrimental effects associated with UV light. The inactivation mechanism of 405 nm light is accredited to the excitation of intracellular photosensitive porphyrin molecules, which results in the production of reactive oxygen species, inducing oxidative damage and consequently cell death [224].

A recent study [225] showed that both P. gingivalis and F. nucleatum bacteria are more susceptible *in vitro* to violet/blue light radiation (wavelengths 400–495 nm) than the streptococci bacterium. Although not as bactericidal as UV light, short-wave visible light in the blue wavelength range has been demonstrated to induce bactericidal effects in exposed bacteria, and has a number of potential advantages including improved safety due to the lower photon energy, and reduced photodegradation of materials [226,227].

3.3.7 Therapeutic applications of electromagnetic radiation

Electromagnetic radiation has been successfully used in various therapeutic applications. For example, pulsed electromagnetic field (PEMF) therapy has been used successfully in the management of postsurgical pain and edema, the treatment of chronic wounds, and in facilitating vasodilatation and angiogenesis [228]. Low-intensity ultrasound has been used to speed normal fracture healing and manage delayed unions [229].

In another study, the possibility of low intensity PEMFs to kill breast cancer cells were investigated [230]. It appears that PEMF-based anticancer strategies may represent a new therapeutic approach to treat breast cancer without affecting normal tissues in a manner that is non-invasive and can be potentially combined with the existing anti-cancer treatments.

The effects of low level laser phototherapy (visible light) on hand and forearm fractures were investigated, and the results showed that the phototherapy is effective for human bone healing and pain relief [231].

A study of the effects of light emitting diode (LED) phototherapy on bone defects grafted with MTA, bone morphogenetic proteins and guided bone regeneration was showed that infrared LED light irradiation improves the deposition of CHA in healing bone grafted [232].

CHAPTER 4

METHODOLOGY

4.1 Resonant Recognition Model (RRM)

The Resonant Recognition Model (RRM) was employed in this project to:

- design a bioactive peptide that can emulate the biological activity of a native anti-microbial protein Azurocidin;
- determine an activation frequency/wavelength of the visible light radiation that can modulate the biological activity of Collagenase enzyme that plays a key role in would healing process.

In Chapter 4 the concepts of the RRM approach and its particular applications are presented in details.

4.1.1 Proteins, DNA and RRM

Proteins are “the work horses” of biological systems at the cellular level. They are responsible for various biological activities including enzymatic analysis, transport and storage, immune protection, intracellular communication and many other tasks. Proteins are large, complex biological molecules, consisting of one or more long chains of amino acid residues that play many critical roles in our body. The primary structure

of a protein is made up of hundreds or thousands of smaller units called amino acids, which are attached to one another in long chains. It refers to the linear sequence of amino acids in the polypeptide chain. There are 20 different types of amino acids that can be combined to make a protein. The sequence of amino acids is unique to each protein, and defines the structure and function of the protein. Thus, proteins differ from one another primarily in their sequence of amino acids, which usually results in folding of the protein into a specific three dimensional structure that determines its activity. Proteins perform a vast array of functions within living organisms, including catalyzing metabolic reactions, replicating DNA, responding to stimuli, and transporting molecules from one location to another. Like other biological macromolecules such as polysaccharides and nucleic acids, proteins are essential parts of organisms and participate in virtually every process within cells.

The protein’s molecular structures are connected with its biological functions. Its structure and function is determined by its linear information contained in the amino acid sequence. The more understanding the structure of proteins, the more benefit we will have to aid in identification of the proteins interactions and function. It used to be that the structure of proteins could only be determined using X-ray crystallography, fluorescence spectroscopy and NMR spectroscopy. Now, through bioinformatics tools, there are computer programs that can predict and model the structure of proteins. As mentioned above, the information contained in the amino acid sequence determines the protein's chemical properties, chain conformation, protein’s function and its specificity.

Although both function and structure of a large number of proteins are becoming known throughout projects like Human Genome Project and are available through a number of data bases [233], the crucial problem of understanding how the biological function is "written" within the protein sequence still remains [234]. Once this understanding has been gained it should be possible to design peptides and even proteins *de novo* with the chosen biological function and thus to produce new and more efficient drugs and other biotechnological products [234-237].

With the rapid accumulation of databases of proteins' primary structures, there is an urgent need for theoretical approaches that are capable of analysing protein structure/function relationships. As described in the previous section, many attempts have been developed to predict the tertiary structure and biological function of protein from its sequence but only with limited success. These approaches have inherent limitations, i.e. they do not provide sufficient knowledge about the physical process for proteins folding and interacting. They also lack the informational, structural and physicochemical parameters crucial to the selectivity of protein interactions, which can be used for *de novo* design of peptide or protein analogous with the desired biological activity.

The physico-mathematical approach, applied in this project, is called the Resonant Recognition Model (RRM) [236,237]. The RRM, developed by I. Cosic [236], is based on the representation of the protein primary structure as a numerical series by assigning to

each amino acid a physical parameter value relevant to the protein's biological activity. A number of amino acid indices have been found to correlate in some way with the biological activity of the whole protein [238]. Previous investigations [237,238,241] have shown that the best correlation can be achieved with parameters, which are related to the energy of delocalised electrons of each amino acid. These findings can be explained by the fact that the electrons delocalised from the particular amino acid have the strongest impact on the electronic distribution of the whole protein. In previous studies [239], the energy of delocalised electrons (calculated as the electron-ion interaction pseudopotential, EIIP) of each amino acid residue was employed in the RRM approach. The resulting numerical series then represented the distribution of the free electrons' energies along the protein. This numerical series was then converted into a discrete Fourier spectrum, which carried the same information content about the arrangement of amino acids in the sequence as the original numerical sequence [242,243].

4.1.2 Definition of Common Frequency Characteristics

The RRM is a physicomathematical model. It interprets the protein's sequence linear information using signal analysis methods. It comprises two stages. The first involves the transformation of the amino acid sequence into a numerical sequence. Each amino acid is represented by the value of the electron-ion interaction potential (EIIP) [239], which describes the average energy states of all valence electrons in particular amino acid. The EIIP values for each amino acid were calculated using the pseudopotentials general model [239,241]:

$$\langle k + q \,|w|\, k \rangle \quad = \quad 0.25\ Z \sin(\pi\ 1.04Z)/(2\pi) \qquad (4.1)$$

where q is a change of momentum k of the delocalised electron in the interaction with potential w , while

$$Z = (\sum Zi) / N \qquad (4.2)$$

where Zi is the number of valence electrons of the i -th component of each amino acid and N is the total number of atoms in the amino acid. The EIIP values for 20 amino acids, as well as for five nucleotides (the whole procedure can be applied to the DNA and RNA), are shown in Table 4.1. A unique number can thus represent each amino acid or nucleotide, irrespective of its position in a sequence. Numerical series obtained in this way are then analyzed by digital signal analysis methods in order to extract information pertinent to the biological function. The original numerical sequence is transformed to the frequency domain using the discrete Fourier transform (DFT). As the average distance between amino acid residues in a polypeptide chain is about 3.8 Å, it can be assumed that the points in the numerical sequence derived are equidistant [236]. For further numerical analysis, the distance between points in these numerical sequences is set at an arbitrary value d=1. Then, the maximum frequency in the spectrum is $F=1/2\ d=0.5$. The total number of points in the sequence influences the resolution of the spectrum only. Thus, for N-point sequence the resolution in the spectrum is equal to $1/N$. The n-th point in the spectral function corresponds to the frequency f = n/N [235,236]. In order to extract common spectral characteristics of sequences having the same or similar biological function, the following cross-spectral

function was used:

$$Sn = XnYn^* \qquad n = 1,2,...,N/2 \qquad (4.3)$$

where *Xn* are the DFT coefficients of the series *x(m)* and *Yn** are complex conjugate DFT coefficients of the series *y(m)*. Peak frequencies in the amplitude cross-spectral function define common frequency components of the two sequences analyzed [235,236]. The whole procedure: **protein sequence → numerical series → amplitude spectra → cross-spectra** is shown in Fig. 4.1a. Fig 4.1b presents: (i) sequences of α and β human hemoglobins; (ii) graphical representation of the corresponding numerical sequences obtained by replacing every amino acid with its EIIP value; (iii) spectra of both α and β human hemoglobins; (iv) cross-spectral function of the spectra presented in (iii). The prominent peaks denote common frequency components. The abscissa represents RRM frequencies, and the ordinate is the normalized intensity.

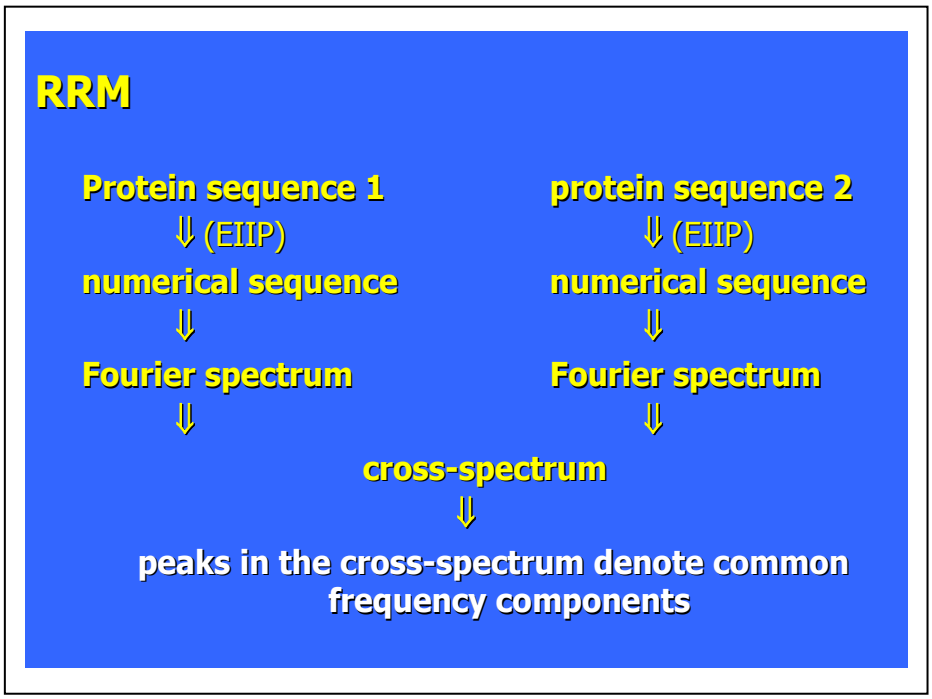

Figure 4.1a The Resonant Recognition Model (RRM) procedure

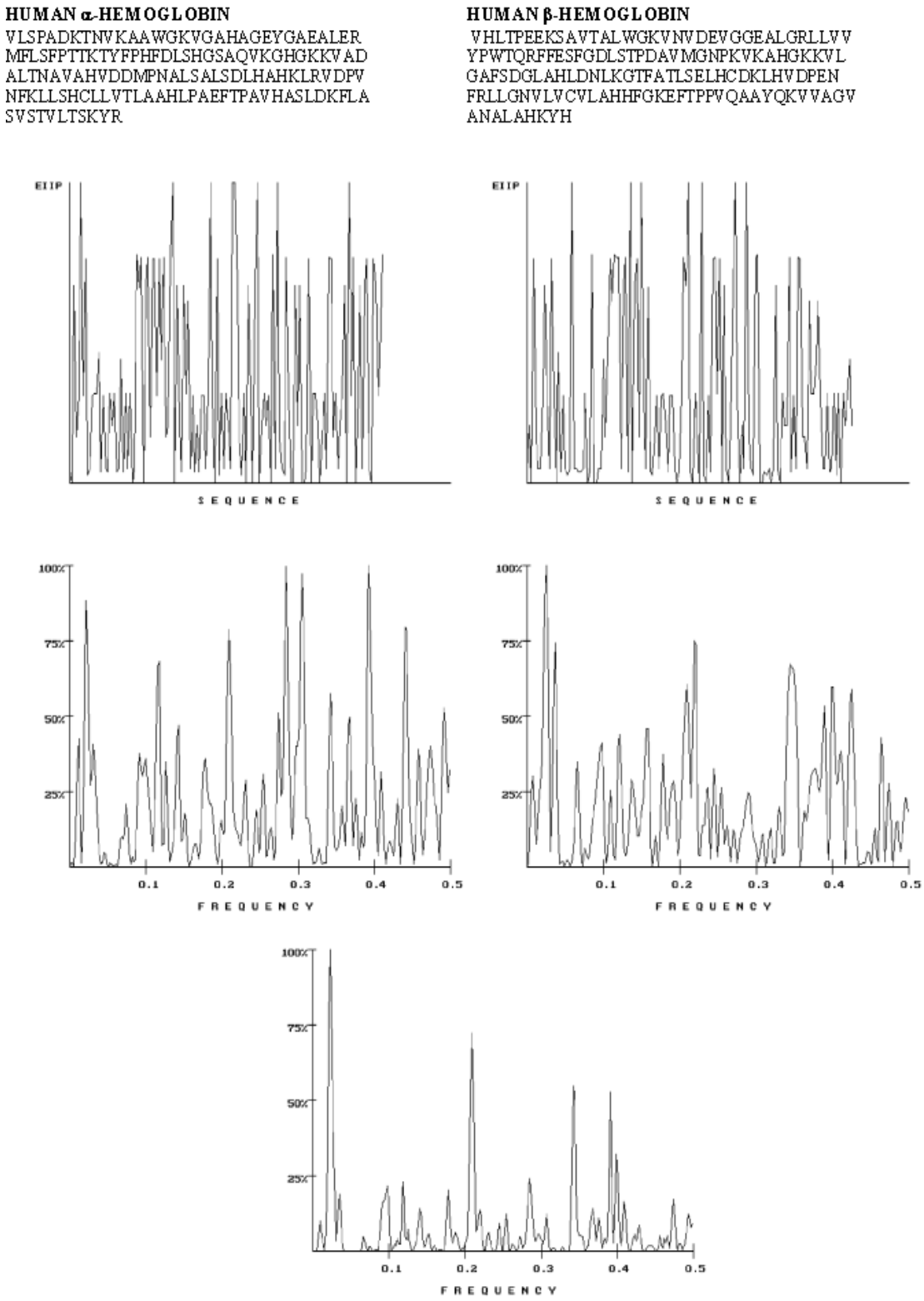

Figure 4.1b Graphical presentation of the RRM procedure [6]

Nucleotide	Nucleotide	EIIP
A	A	0.1260
G	G	0.8606
T	T	0.1335
C	C	0.1340
Amino Acid	**Amino Acid**	**EIIP**
Leu	L	0.0000
Ile	I	0.0000
Asn	N	0.0036
Gly	G	0.0050
Val	V	0.0057
Glu	E	0.0058
Pro	P	0.0198
His	H	0.0242
Lys	K	0.0371
Ala	A	0.0373
Tyr	Y	0.0516
Trp	W	0.0548
Gln	Q	0.0761
Met	M	0.0823
Ser	S	0.0829
Cys	C	0.0829
Thr	T	0.0941
Phe	F	0.0946
Arg	R	0.0959
Asp	D	0.1263

Table 4.1 The Electron-Ion Interaction Potential (EIIP) Values for Nucleotides and Amino Acids [6]

To determine the common frequency components for a group of protein sequences, the absolute values of multiple cross-spectral function coefficients *M* have been calculated as follows:

$$|Mn| = |X1n| \cdot |X2n| \ ... |XMn| \qquad n = 1, 2,....,N/2 \qquad (4.4)$$

Peak frequencies in such a multiple cross-spectral function denote common frequency components for all sequences analyzed. Signal-to-noise ratio (S/N) for each peak is defined as a measure of similarity between sequences analyzed [235,236]. S/N is calculated as the ratio between signal intensity at the particular peak frequency and the mean value over the whole spectrum.

The extensive experience gained from previous research suggests that an S/N ratio of at least 20 [234,240] can be considered significant. The multiple cross-spectral function for a large group of sequences with the same biological function has been named "consensus spectrum". The presence of a peak frequency with a significant S/N ratio in a consensus spectrum implies that all of the analyzed sequences within the group have one frequency component in common [235,236]. This frequency is related to the biological function provided the following **RRM criteria** are met:

A: One peak only exists for a group of protein sequences sharing the same biological function

B: No significant peak exists for biologically unrelated protein sequences

C: Peak frequencies are different for different biological functions.

In previous studies, the above criteria have been tested with over 1000 proteins from 25 functional groups [234-236,240]. The regulatory DNA sequences were analyzed in the same way. The following fundamental conclusion was drawn from these studies:

each specific biological function of protein or regulatory DNA sequence is characterised by a single frequency (Figure 4.2).

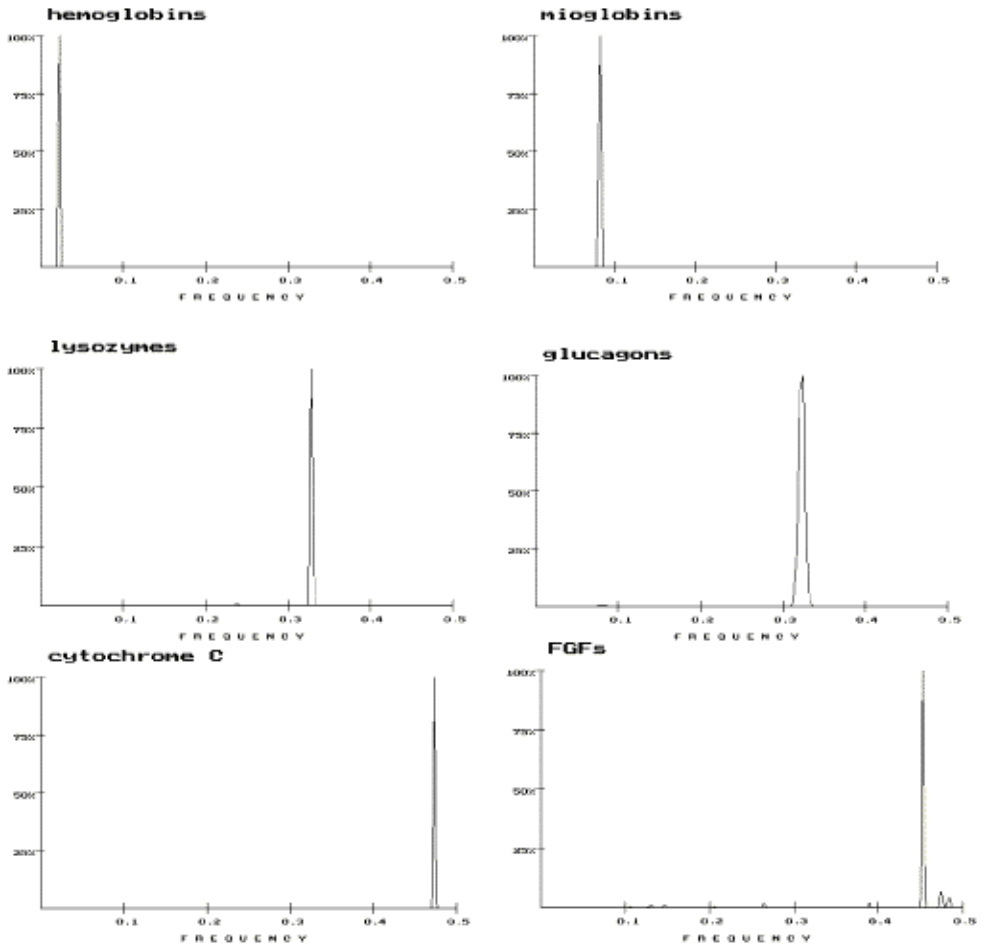

Figure 4.2. presents multiple cross-spectral functions of six different functional groups of proteins. Each specific biological function of protein sequence is characterized by a single frequency. The abscissa represents RRM frequencies, and the ordinate is the normalized intensity.

The RRM also provides a method to identify the individual amino acids that contribute mostly to a protein's specific biological function. Since the characteristic frequency correlates with the biological function, the positions of the amino acids that are most affected by the change of amplitude at the frequencies and consequently to the corresponding biological function. The inverse Fourier transform is used in this determining process. This "hot spots" identification method has been applied already to a number of examples. The previous studies with interleukin 2, SV40 enhancer, Ha-ras p21 oncogene product, glucagons, Cytochrome C, haemoglobins, myoglobins and lysozymes all have documented evidence that such predicted amino acids are found to be spatially clustered in the protein tertiary structure and to be positioned in and around the protein active site in some of those examples [234-236].

4.1.3 Signal-Noise Ratio Normalization

The frequency characteristic for an observed biological function is defined as the prominent peak frequency in the multiple cross-spectral function of the family of proteins having this function in common. This prominent peak denotes a common frequency component for all the protein sequences analyzed. Any common frequency component can be considered as a characteristic of the observed function providing certain criteria are satisfied [236]. To quantify those criteria it is important initially to define the index, which will be a measure of the level of commonality for any frequency component in the cross-spectral function. However, this definition of S/N is sensitive to the protein signal length and the number of sequences that computed in the

multiple cross-spectral function. Thus, it is not quite suitable for the development of the general criteria for a variety of protein families. There was a need to define S/N as a general comparable index that could be consistent and universally applied to the system under examination. This normalized S/N index has to be independent of the sequence length and the number of sequences analyzed. This index should measure the confidence of determining the characteristic frequency of a biological function. After an empirical and statistical testing, a new normalized S/N ratio (NSN) has been introduced to avoid the problem discussed above [237].

All these results show, the RRM represents a whole new view to protein activity, in particular protein-protein and protein-DNA interactions. The underlying hypothesis of this model is that certain periodicities in the distribution of energy of delocalised electrons along the protein molecule are critical parameters for protein biological function. This model allows extract the linear information contained in amino acid sequence and also provides a physical explanation of macromolecule's interaction processes. With a characteristic frequency identified by the RRM, it is possible then to design peptides of different length having desired periodicities in their distribution of energies of delocalised electrons along their sequence [235,236]. Thus, the RRM can identify signals that characterize protein biological functions. Applications of the RRM are mostly in the area of biotechnology, drug design and pharmacology. The particular RRM applications will be explored in the following sections.

4.1.4 Interaction of electromagnetic fields with molecules and cells: RRM activation frequency

Experimental investigations of the action of electromagnetic field (EMF) at the molecular level have shown mainly resonance effects, and these are in a very wide frequency range - from low to super-high. In recent years other new mechanisms of resonance absorption of EMF in biological media have been discovered [244,245]. For instance, conformational vibrations of protein molecules consist of the formation of folds, twisting or compression of protein polypeptide chains. Conformational vibrations of protein molecule lead to the displacement of electric charges on their surface and thus, EMF of the particular frequency can interact with these vibrations [244,245]. This mechanism might underlie the resonance absorption effects due to the action of audio frequency EMF on protein solutions. Another type of the resonance absorption is in the radiofrequency (RF) spectrum, the so-called "piezoelectric resonance", was observed in some biopolymers. It was hypothesised that piezoelectric resonance is attributed to the interaction of an elastic wave produced by the EMF with defects and non-homogeneities on the surface and in the interior of the substance [244,245]. Thus, if the effects observed in biopolymers are piezoelectric in nature then biological structures must contain regions consisting of many macromolecules with the piezoelectric properties.

In general, the studies of interactions of EMF with biological media have been

separated by frequency – where some research concerns with extremely low frequency (ELF) effects and others with RF exposures. Much of the research on the effects of weak EMF on organisms was concentrated on possible interactions with cell membranes [153,246-250]. It was proposed that cell membranes could act as non-linear resonators strongly amplified signals within a narrow range of frequencies. Interactions between EMF and bio-systems have been intensively studies for over a century and a quantitative understanding of many interaction mechanisms exists: effects arise from nerve excitations, electronically induced forces, the dielectric breakdown of cell membranes and other processes that directly involve electric fields [153,246-250].

Each biological process involves a number of interactions between proteins and their targets (other proteins, DNA regulatory segments or small molecules). Each of these processes involves an energy transfer between the interacting molecules. These interactions are highly selective, and this selectivity is defined within the protein primary structure. However, the physical nature of these interactions is not yet well understood. The most acceptable existing model, the so-called key-and-lock model that incorporates a selectivity of interactions, is based on a spatial complementarity between the interacting molecules. With knowledge of more 3-D structures of proteins and their complexes with ligands it can be observed that the spatial complementarity is not selective enough to be considered as a sole parameter able to describe the nature of protein interactions occurred in living systems.

On the other hand, there is much evidence that biological processes can be induced or modulated by induction of light of particular characteristic frequencies [251-253]. This is caused directly by the light-induced changes of energy states of macromolecules and in particular of proteins. The function of some proteins is directly connected with the absorption of visible light of defined wavelengths as in the case of rhodopsins. The strong light absorption is due to the presence of a colour prosthetic group bound to the protein, while the frequency selectivity of this absorption is defined by the amino acid sequence of the protein per se. In addition, there is evidence that light of a defined frequency can induce or enhance some biological processes, which are normally controlled by proteins only (i.e. cell growth and proliferation [253,254]).

All these frequency selective effects of light on biological processes of protein activation imply that protein activation involves energies of the same order and nature as the electromagnetic irradiation of light. Protein interactions can be considered as resonant energy transfer between the interacting molecules. This energy can be transferred through oscillations of a physical field, possibly electromagnetic in nature [234,255]. Since there is evidence that proteins have certain conducting or semi-conducting properties, a charge, moving through the protein backbone and passing different energy stages caused by different amino acid side groups, can produce sufficient conditions for a specific electromagnetic radiation or absorption. The frequency range of this field depends on a charge velocity estimated to be 7.87 x 105 m/s and on the distance between amino acids in a protein molecule, which is

3.8 Å. The frequency range obtained for protein interactions is 1013 to 1015 Hz. This estimated range includes IR, visible and UV light. These computational predictions were confirmed by comparison of:

a) Absorption characteristics of light absorbing proteins and their characteristic frequencies,

b) Frequency selective light effects on cell growth and characteristic frequencies of growth factors [253,255].

All these results lead to the conclusion that the specificity of protein interactions is based on the resonant electromagnetic energy transfer at the frequency specific for each interaction observed. Taking into account all these and other possible resonant effects taking place in the human body and different other leaving systems, it becomes possible for such effects of low-intensity EM radiation to occur if the energy goes through the resonant path [234,240,256]. Given the existence of these resonant effects, we consider here the possible interactions of the weak EM radiation and its influence on living systems.

To grasp the meaning of the RRM characteristic frequency it is important, at first, to understand what is meant by the biological function of proteins. As was pointed out above, each biological process is driven by proteins that selectively interact with other proteins, DNA regulatory segment or small molecules. These interactive processes that

involve energy transfer between the interacting molecules are highly selective. How is this selectivity achieved? In the RRM it is postulated that the selectivity is defined within the amino acid sequence. It has been shown that proteins and their targets share the same characteristic frequency [234,240,256] but of opposite phase [257-260] for each pair of interacting macromolecules. Thus, we conceptualise that RRM characteristic frequencies represent proteins general functions as well as a mutual recognition between a particular protein and its target (receptor, ligand, etc). As this recognition arises from the matching of periodicities within the distribution of energies of free electrons along the interacting proteins, it can be regarded as the resonant recognition. The RRM model assumes that characteristic frequencies are responsible for the resonant recognition between macromolecules at a distance. Thus, these frequencies have to represent oscillations of some physical field which can propagate through water dipoles. One possibility is that this field is electromagnetic in nature [234,240,256].

There is evidence that proteins and DNA have certain conducting properties [263-265]. If so, then charges would be moving through the backbone of the macromolecule and passing through different energy stages caused by the different side groups of various amino acids or nucleotides. This process provides sufficient conditions for the emission of electromagnetic waves. Their frequency range depends on the charge velocity, which in turn depends on the nature of charge movement (superconductive, conductive, soliton transfer, etc.) and on the energy of the field that causes charge transfer. The nature of this physical process is still unknown; however, some models of

charge transfer through the backbone of macromolecules have been accepted [266-268]. To simplify the calculations we assumed the electron transfer is attributed to the difference of the free Electron Ion Interaction Potentials (EIIP) at the N and C terminals of the protein molecule. According to the theory of pseudo-potentials [262] this potential difference is:

$$W = W(\mathrm{COOH}) - W(\mathrm{NH2}) = 0.13\,Ry$$

This energy difference allows for a maximum velocity of the electrons of:

$$V_{\max} = \sqrt{2eW/m}$$

where e is the electron charge, and m is electron mass. Therefore

$$V < 7.87 \cdot 10^5 \ \mathrm{m/sec}$$

As an inherent assumption is that amino acids in the protein sequence are equidistant at: $d = 3.8$ A

Then, the maximum frequency that could be emitted during the electron transfer is $F_{\max} < V/2d$; or $F_{\max} < 10^{15}$ Hz ; while the corresponding wavelength is $L_{\min} > 330$ nm.

The minimum frequency that could be emitted depends on the total length of the protein $F_{\min} = 2F_{\max} / N$, where *N* is the total number of amino acids in the protein. For example with proteins of 200 amino acids in length, the minimum frequency is $F_{\min} < 10^{13}$ Hz and the corresponding wavelength is $L_{\max} < 30\,000$ nm. The range from 30,000nm to 300nm is very wide, starting from the very *low infrared* through *the visible to the ultraviolet regions* [234,240].

To prove the possibility that macromolecular interactions are based on the resonant energy transfer between interacting molecules, we compared our computational predictions with the number of published experimental results. This assumption has been studied in a number of examples that include:

- Laser light growth promotion of cells using the particular frequencies of light and producing the similar effect as it would be with the presence of growth factor proteins [253-255].
- Chymotrypsin activation which was achieved by radiation of the laser light of 850-860nm only [269,270].
- Activation of highly homologous plant photoreceptors which although being very homologous absorb different wavelengths of light [251,261].
- Proteins activated by light (eg rhodopsins, flavodoxins etc.) These proteins absorb light through the prosthetic group but frequency selectivity of this absorption and consequent activation is defined by the protein sequence [271,272].

All these results lead to the conclusion that specificity of protein interactions is based on resonant electromagnetic energy transfer at the frequency specific for each observed interaction. The numerical frequencies obtained similarly by the RRM for various other groups of visible light-absorbing proteins are compared with their corresponding characteristic absorption frequencies in Table 4.2 and this linear correlation is shown in Figure 4.1.3. A result of considerable significance is that the scaling factor between these two sets of data is almost constant about the value of $K = 200$ [234,240]. Thus, a

strong linear correlation would seem to exist between the numerical characteristic frequencies defined by the RRM and the experimentally determined frequencies corresponding to the electromagnetic radiation absorption of such proteins. From this correlation it can be observed that the full range of wavelengths, which can be related to RRM characteristic frequencies, is over 400 nm.

protein	nm	rrm	cm-1	K
cyt c	415	0.473	24096.39	196
blue	430	0.475	23255.81	204
green	540	0.355	18518.52	191
red	570	0.346	17543.86	197
hem.	14770	0.02	677.0481	295
purple	860	0.281	11627.91	241
flavodoxin	470	0.379	21276.6	178
igf	400	0.492	25000	196
fgf	441.6	0.453	22644.93	200
insulin	552	0.344	18115.94	189
growth f.	633	0.293	15797.79	185
	650	0.293	15384.62	190
pdgf	830	0.242	12048.19	200
chymotr.	851	0.236	11750.88	200
calculative	400	0.5	25000	200

Table 4.2 The RRM frequencies and characteristic absorption frequencies of different visible light-absorbing protein groups and their scaling factor, K [234,240]

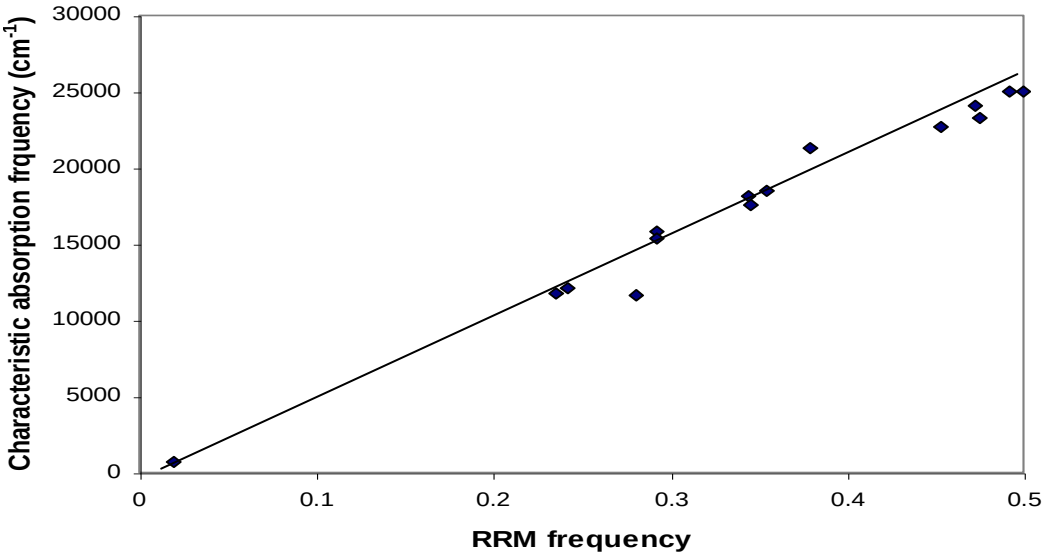

Figure 4.3. Linear correlation between RRM frequencies and corresponding absorption frequencies of different visible light-absorbing protein groups [234,240]

This finding is in complete accord with the frequency range previously associated to the RRM spectra and calculated from the charge velocities through the protein backbone. It can be now inferred from both correlations that approximate wavelengths in real frequency space can be calculated from the RRM characteristic frequencies for each biologically related group of sequences. Furthermore, these calculations can be used to predict the wavelength of visible and near-infrared irradiation which may produce a biological effect [234,240]. As described above, the selectivity achieved within the intermolecular protein interactions is still not completely understood.

There are some indications that these interactions involve a certain resonant energy transfer but the physics and frequency range of this transfer is not yet identified. In a

recent work, oscillations of OH groups found on proteins and water molecules were proposed as an interaction medium for the transfer of vibrational energy from one protein to another [22,244,245]. However, in the case of vibrations in the condensed phase, resonant energy transfer is limited with the time scale of vibrational relaxation [22,244,245]. On the other hand, electronic excitations as the basis of transfer between macromolecules are more rapid. Thus, the vibrational energy transfer is an unlikely mechanism for the resonant energy transfer between the interacting macro-molecules proteins, RNA or DNA [245].

In the RRM, it was hypothesized that the transfer between the interacting molecules presents an electromagnetic resonant energy rather than vibrational transfer. This possibility is based on the following findings within the RRM model [234,240]:

• The RRM frequencies are characteristic periodicities in the free electron energies along the protein or DNA molecule.

• There is a possibility of the resonant energy transfer between proteins and their DNA and protein targets, which could be relevant for protein functional specificity.

• This energy could be electromagnetic in nature. The frequency range is proposed to be from infra-red up to ultra-violet (10^{13} to 10^{15} Hz).

• This energy transfer should be resonant as the frequencies in its spectrum are critical for biological function (selectivity of macromolecular interactions).

• To further investigate the proposed resonant energy transfer between

macromolecules it is necessary to investigate the following aspects:

- Time scale of the proposed interaction
- Influence of water as a medium for electromagnetic radiation
- Chemical energy supplied to the activated molecule and its sufficiency to produce proposed EM radiation.

Time scale of the proposed interaction could be roughly estimated by taking into account the proposed velocity of charge along the protein backbone and the linear length of the protein. For an average protein of 200 amino acids the length of the backbone would be about 800Å. The velocity of the charge is estimated to be of the order of value of 10^6 m/s which gives an estimated time for the reaction to be of the order of value of 10^{-13}s. For shorter proteins this time would be shorter (order of $2x10^{-14}$s for proteins of 20 amino acids) and for longer proteins would be longer (up to $4x10^{-13}$s for proteins of 1000 amino acids). This time scale is of an order of value shorter than the proposed time needed for vibrational resonant energy transfer through the water dipoles [234,240,266-268]. The vibrational relaxation time scale is of the order of a few picoseconds (10^{-12} s) [266-268] while the time scale proposed for resonant energy transfer through electromagnetic coupling is proposed here to be of the order of value of 10^{-13} s. Although the speed of selective recognition between large linear macromolecules is not experimentally measured, there is some indication that this process, which precedes the chemical bonding, is quite quick and could be in the proposed time scale [234,240].

All these protein interactions occur in an aqueous environment and thus, it is important to investigate the water absorption characteristics for the particular frequencies relevant to a particular biological function. This is based on the assumption that photons constitute the carrier of energy from one protein to another. The depth of water required to absorb 50% of the radiation was then calculated for each of the different RRM frequencies that correspond to proteins of different biological function. The 50% point was chosen as it notionally marks the point where the probability of the emitted photon is more likely to have been absorbed by water than by another protein. Assuming that the RRM mechanism expresses its energy interchange in terms of infra-red photons, the absorption properties of water should not impede the RRM mechanism for most proteins at distances that are biologically significant. However, a group of proteins have been identified where the IR absorption properties of water may play a role, limiting the impost of biological order by this proposed mechanism to distances less than 10μm. [266-268]. In addition, the percentage of EM absorption in the water of 1μm thickness, chosen at a reasonably far distance to encompass any biomolecular interaction, is presented in Table 2. It can be observed that the majority of biological functions (except Cytochrome C) are performed at frequencies which do not have high absorbances in water. Thus, it could be concluded that water does not represent a big obstacle for EM radiation in the proposed range to be transferred from one to the other interacting molecule [266-268]. Further investigation was aimed to find out the energetics of the proposed mechanism. The energy contained in a single photon at

the RRM frequency was calculated using the relationship. Then the number of photons required to produce 2*ATP was calculated. Assuming that <50% absorption of the quanta by water in the boundaries calculated above, this would leave greater than 1*ATP worth of energy for a target protein for the resonance mechanism to proceed. It is assumed, that this energy is sufficient to activate the protein to perform its function [234,240].

4.1.5. Applications of the RRM

Once the characteristic frequency for a particular protein function/interaction is identified, it is possible then to utilize the RRM to predict the amino acids in the sequence predominantly contributed to this frequency and consequently to the observed function. Also it becomes possible to predict protein active sites using the CWT and design peptide analogous having only the desired periodicities and thus, the desired bioactivity [257-261].

The RRM can be used to predict:

1. "Hot spots" in terms of the RRM and 3-D protein structures
2. Protein active and/or binding site(s) using the Continuous Wavelet Transform (CWT)
3. Activation frequency for modulation of protein activity by applied electromagnetic radiation
4. Design bioactive peptides

Of particular importance to this PhD project the RRM applications 3) and 4).

The conducted previous studies revealed that biological activity of L-Lactate Dehydrogenase (LDH) enzyme can be modulated by the exposures of visible light radiation in the range of 550-850 nm and infrared light in the range of 1140 - 1200 nm that was predicted computationally by the RRM approach [20-22].

In other recent studies the RRM was employed to determine the frequency/wavelength of the applied electromagnetic radiation (far infrared light radiation in a range of 3500-6400nm) that can affect biological activity of oncogene proteins. The experimental evaluation conducted on different cancer and normal cells showed that the predicted wavelengths of far infrared light induce cytotoxic effects on studied cancer cells and produce no effect on normal cells [273,274].

4.2 Bioactive peptide design

Small molecular weight peptides have been recently applied in developing cancer therapeutics, mostly for their ability to easily penetrate cellular membranes and to interfere with enzymatic functions or protein-protein interactions within cells [275]. In the development of such therapies the focus is on small peptides with strong tumoricidal activity and low toxicity. This therapy aims at obtaining high therapeutic indices on cancer cells and to minimize undesirable side effects on normal cells [276]. It is generally recognized that the relationship between the structure and biological function of a protein and its ability to bind to a specific ligand, can be enunciated in terms of a multistage process which involves specific biorecognition, chemical binding and energy transfer. The Resonant Recognition Model (RRM) [234,240] is one attempt to identify the selectivity of protein interactions within an amino acid sequence.

The RRM represents a new view to protein activity, in particular protein-protein and protein-DNA interactions. The underlying hypothesis of this model is based on the finding that there is a significant correlation between spectra of the numerical presentation of amino acids and their biological activity. It has been found through extensive research that proteins with the same biological function have a common frequency in their numerical spectra. This frequency was found then to be a characteristic feature for protein biological function and interaction.

It is possible to determine the RRM characteristic frequency from analysis of the power spectra of proteins. In addition, from the analysis of their phase spectra we can identify the corresponding phase for a particular frequency. On the basis of determined RRM characteristic frequencies and phases for a particular group of protein sequences, we can design amino acid sequences (short peptides) having those specific characteristics related to a protein's biological function. It is expected that the designed peptide will exhibit the desired biological activity.

The strategy for design of such defined peptides is presented below*:*

1. The RRM characteristic frequency is determined from the multiple cross-spectral function for a group of protein sequences that share a common biological function (interaction).
2. The phases are calculated for the characteristic frequency or frequencies of a particular protein, which is selected as a parent for an agonist/antagonist.
3. The minimal length of the designed peptide is defined by the appropriate frequency resolution. An Inverse Fourier Transformation (IFT) is used to calculate a numerical sequence of different lengths, which exhibits the same prominent characteristic frequency as a parent protein.
4. To determine the amino acids that correspond to each element of the new numerical sequence defined above, the tabulated Electron Ion Interaction Potential (EIIP) parameter values are used. The resulting new amino acid sequence represents the anticipated designed peptide [234,241].

In previous studies the RRM approach was applied to structure-function analysis of basic fibroblast growth factor (bFGF) [277]. Property-pattern characteristics for biological activity and receptor recognition for a group of FGF-related proteins were defined and then used to aid the design of a set of peptides which can act as bFGF antagonists. Molecular modelling techniques were then employed to identify the peptide within this set with the greatest conformational similarity to the putative receptor domain of bFGF. The 16 mer peptide, which exhibits no sequence homology to bFGF, antagonised the stimulatory effect of bFGF on fibroblast thymidine incorporation and cell proliferation, but exerted no effect itself in these in vitro bioassays [277].

The RRM was also successfully applied for the analysis of HIV envelope proteins. The interaction between HIV virus envelope proteins and CD4 cell surface antigen has a central role in the process of virus entry into the host cell. Thus, blocking the interaction between the envelope glycoproteins and CD4 surface antigen, known to be the HIV receptor, should inhibit infection [278]. For this purpose, six peptides, each of 20 amino acids in length, were designed using the RRM methodology. To validate the RRM computational predictions, the activities of the designed peptides were evaluated experimentally. These investigations were performed initially by evaluating the reactivity and cross-reactivity of all designed peptides with their corresponding antibodies [278]. The results obtained showed significant cross-reactivity to the polyclonal antibodies raised against peptides that share at least one characteristic

frequency and phase at this frequency. The results provided an experimental confirmation of the concept that RRM frequency characteristics present important parameters associated with bio-molecular recognition and in particular, the antibody-antigen recognition.

More recently, the RRM analysis was used to find the characteristic frequency and the "hot spot" amino acids of Protoporphyrinogen oxidase (PpOI) proteins, and predicted the location of the proteins' active site(s) [279]. In another study, the RRM computational approach was applied to the analysis of oncogene and proto-oncogene proteins. The results obtained showed that the RRM is capable of identifying the differences between the oncogenic and proto-oncogenic proteins with the possibility of identifying the "cancer-causing" features within their protein primary structure. In addition, the rational design of bioactive peptide analogues displaying oncogenic or proto-oncogenic-like activity [242].

The RRM approach was also employed for structure-function analysis of anti-tumor cytokine, interleukin-12 (IL-12) and the design of a short therapeutic IL-12 analogue peptide having interleukin-like activity, with toxic anti-tumor effect which was experimentally validated on B16F0 mouse melanoma cell culture. The experimental results clearly indicated that the tested de-novo designed peptide analogue produced a toxic effect on the B16F0 melanoma mouse cancer cells. Importantly, it was found that its anti-tumor activity is dose and time dependent [237].

In the study [280] the authors applied the RRM approach to the structure-function analysis of selected myxoma virus (MV) proteins aiming to design a single short linear bioactive peptide that mimics MV protein activity. MV is a rabbit-specific poxvirus pathogen of the Leporipoxvirus genus. It was shown previously that MV is capable of targeting and destroying tumors, while causing no significant disease or collateral tissue infection in an immunocompetent host.

The *de novo* designed peptide RRM-MV was assessed for its biological effects in mammalian tumor and normal cell lines. The efficacy of RRM-MV peptide as a candidate for cancer therapy was experimentally validated *in vitro* on tumor and on normal cell lines/primary cultures. The cellular cytotoxicity of this bioactive peptide on cancer and normal cell lines was qualitatively confirmed by the fluorescent apoptosis/necrosis assay with CLSM, in addition to the quantitative evaluation of cellular cytotoxicity by LDH assay, and cellular viability by the Prestoblue reagent. Cellular viability of peptide treated cancer cells was compared to cellular viability of peptide treated normal cells. The cytotoxic effects of the bioactive peptide RRM-MV by LDH assay were obvious and significant on the mouse melanoma cells (B16F0) and on the human squamous cell carcinoma (COLO 16), when compared with the effect of the negative control RRM-C on these cell lines and with the non-treated cultures incubated under similar conditions. Normal cell lines were not significantly affected by the RRM-MV treatment which resulted in negligible damage to normal skin cells, to macrophages and to CHO cells, revealing that this bioactive peptide analogue

(RRM-MV) has a selective cytotoxic effect on cancer cells only.

In this PhD project, the RRM approach was employed to design a short bioactive peptide that can emulate the biological activity of the native anti-microbial protein Azurocidin. The computational design of the peptide analogue and experimental evaluation of its anti-microbial properties are presented in the Chapter 5.

4.3 Model systems under investigation

As was presented earlier, this PhD study aims at developing a novel methodology for wound healing promotion via:

(1) Experimental evaluation of visible light exposures on biological activity of Collagenase enzyme which plays a significant role in wound repair process; and

(2) Experimental evaluation of anti-microbial properties of the synthetic computationally designed Azurocidin peptide analogue on selected Gram-positive and Gram-negative bacteria. Hence, it is important to describe the selected model systems in great details.

Collagenase enzyme

Collagenase is a highly specific proteinase and is the only enzyme that can specifically cleave the triple helix of the fibrillar collagens. It is described in 2.1.11 in this thesis.

There is considerable rational for using Collagenase in wounds for the purpose of enhancing or accelerating reepithelization. Clinical trials of collagenase reported rapid cleansing and enhanced removal of necrotic debris. In this study, a computationally determined specific frequency of electromagnetic radiation is experimentally assessed in order to confirm that we can modulate collagenase enzymatic activity using EMR with a specific frequency, and thus to promote a wound healing process.

Azurocidin anti-microbial protein

Azurocidin is an Azurophil granule antibiotic protein, with monocyte chemotactic and antibacterial activity. It is described in 2.2.10 in this thesis. Azurocidin exerts its antimicrobial activity by directly disrupting the microbial cell membrane, based on the combination of cationicity, amphipathicity and hydrophobicity appear to be unique to this antimicrobial peptides. Wound infection is one of the key factors addressed in wound healing. In this study, a computationally designed synthetic Azurocidin peptide analogue is assessed experimentally in order to find a new antimicrobial reagent which can exhibit an antimicrobial activity and thus, promote wound healing process.

4.4 Materials and Methods

In this section, various materials and instruments utilized for characterization/evaluation of Collagenase enzymatic activity upon exposures to visible light radiation; and investigation of anti-microbial activity of synthetic Azurocidin peptide analogue are described. The experimental parameters for each technique are presented below. Please note, the specific experimental assays and procedures are presented in Chapter 5 (Results and Discussion).

4.4.1 Visible light irradiation of Collagenase enzyme

●Collagen Type I

Collagen Type I was purchased from Sigma-Aldrich Australia, Prod. No. C-9879. Chemical Formula: C2H5NOC5H9NOC5H10NO2

●Collagenase

Collagenase was purchased from Sigma- Aldrich Australia and used as received.

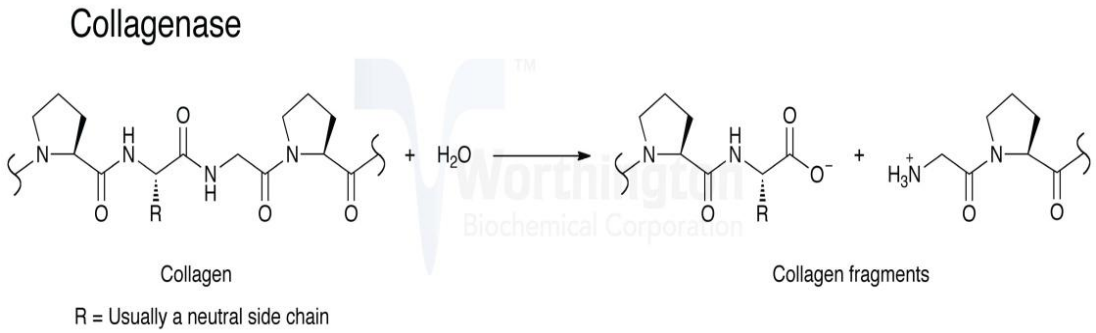

Figure 4.4. Mechanism of collagenolysis.
www.worthington-biochem.com/cls/default.html

Collagenase is a protease with specificity for the X-Gly bond in the sequence Pro-X-Gly-Pro, where X is most frequently a neutral amino acid. Such sequences are often found in collagen, but only rarely in other proteins. Collagenases split collagen in its native triple-helical conformation at a specific site yielding fragments, TC A and TC B, representing 3/4 and 1/4 lengths of the tropocollagen molecule. http://www.advancedbiomatrix.com/wp-content/uploads/2012/03/DFU_Collagenase_5030.pdf

●Equipment

In this study, as a source of visible light radiation a Monochromators SPEX 270M (Princeton Instruments, Trenton, NJ, USA) 1200 g/mm grating, focal length 270 mm, resolution 0.1 nm at 500 nm, dispersion 3.1 nm/mm, lamp Olympus 68v5A TP1 (35W), range 400 – 890 nm, RS232 connection with HP 34001A, controlled by LabView 6.1 (National Instruments) was employed.

A monochromator is an optical device that transmits a mechanically selectable narrow band of wavelengths of light or other radiation chosen from a wider range of wavelengths available at the input. Monochromators are used in many optical measuring instruments and in other applications where tunable monochromatic light is wanted. Sometimes the monochromatic light is directed at a sample and the reflected or transmitted light is measured. Sometimes white light is directed at a sample and the monochromator is used to analyze the reflected or transmitted light.

The monochromator works by reflection of the wavelengths that obey Bragg's Law for

the particular d spacings of the monochromator. For a silicon crystal (which is cubic with a unit cell size equal to 5.4309 Å), the largest *d* spacing is 3.136 Å. Application of the Bragg equation ($\lambda = 2\ d \sin\theta$) shows that for Cu $^{K\alpha}1$, the diffraction condition will be satisfied for $2\theta = 28.442°$, while for Cu $^{K\alpha}2$, it will be satisfied for $2\theta = 28.514°$, giving a difference in Bragg angle of only 0.072 °. Hence only monochromator crystals with a narrow band pass, e.g. silicon, will be able to separate the $K^{\alpha}1$ and $K^{\alpha}2$ wavelengths from a laboratory copper X-ray source. By contrast, pyrolytic graphite monochromators with their wide band pass will pass both K^{α} wavelengths, but not K^{β} for which the Bragg angle is considerably different. http://pd.chem.ucl.ac.uk/pdnn/inst1/monoc.htm

In this study, the optical apparatus required to produce the monochromatic light suitable for irradiation is shown in Figure 4.5. The distance from the slit and an experimental sample was 50 mm. During the measurements, all other light's sources in the laboratory were switched off.

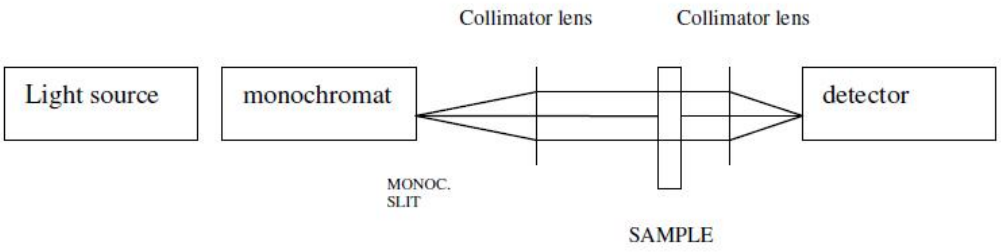

Figure 4.5. Laboratorial equipment. Source of light is a tungsten lamp beam directed to Monochromator SPEX 270. Beam was collimated and focused by lens (f=50 mm) [281]

In this study, to measure the changes in enzyme kinetics upon visible light exposures, a spectrophotometer (Ocean Optics, USA) was employed. A spectrophotometer is a photometer that can measure intensity as a function of the light source wavelength. Important features of spectrophotometers are spectral bandwidth and linear range of absorption or reflectance measurement.

For measurement of absorbance of the analysed Collagenase enzyme solutions, we used Ocean Optics USB2000 spectrometer. The Spectrometer USB2000 has following characteristic: CCD detector with 2048 pixels; USB-2 connection with Pentium IV (Windows XP); controlled with OOIBase32 software. The software was set to automatically monitor and save the absorption coefficient at 570nm every 10sec. This spectrometer was connected with the light source USB-ISS-UV/VIS (Ocean Optics, Inc. FL, USA) of range 190nm-870nm (Figure 4.6).

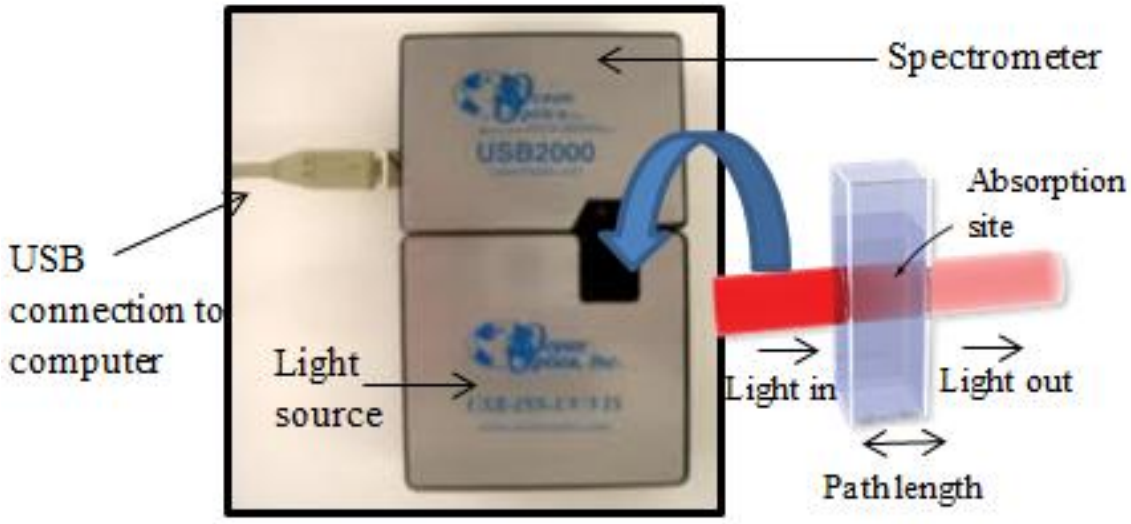

Figure 4.6. Typical setup of a Spectrometer with the light source and USB connections. A demonstration of a cuvette with experimental solution showing the absorption site and the location of cuvette placement for measuring absorption coefficients is also shown.

Absorption spectrophotometer measures the absorption of light by a sample as a function of wavelength. Sometimes the result is expressed as percent transmission and sometimes it is expressed as the inverse logarithm of the transmission. The Beer–Lambert law relates the absorption of light to the concentration of the light-absorbing material, the optical path length, and an intrinsic property of the material called molar absorptivity. According to this relation, the decrease in intensity is exponential in concentration and path length. The decrease is linear in these quantities when the inverse logarithm of transmission is used. The old nomenclature for this value was optical density (OD), current nomenclature is absorbance units (AU). One AU is a tenfold reduction in light intensity. Six AU is a millionfold reduction.

4.4.2 Evaluation of anti-microbial activity of synthetic Azurocidin peptide analogue

●Bacterial strains

In this study, Gram-positive bacterial strains used for experimentation were *Staphylococcus aureus* ATCC 25923, and *S. aureus*344 (ampicillin resistant strain). We have also used Gram-negative bacterium *E. coli* ATCC 25922. The bacterial isolates were obtained from the Microbiology Laboratory, Department of Biotechnology & Environmental Biology, School of Applied Sciences, RMIT University.

●Reagents

Mueller-Hinton Agar (MHA) and Mueller-Hinton Broth (MHB) were purchased from ThermoFisherScientific, Australia.

The *de novo* designed bioactive Azu-RRM and control Azc-RRM peptides were commercially synthesized to 95% purity by GL Biochem, China.

●Equipment

Biophotometer

Use of a spectrophotometer for measurement of the optical density of a bacterial culture at 600 nm (OD600) and monitoring bacterial growth has always been a central technique applied in microbiology. Three common applications where bacterial OD600 is used are as follows:

(a) Determination and standardization of the optimal time to induce a culture during bacterial protein expression protocols,

(b) Determination and standardization of the inoculum concentration for minimum inhibitory concentration (MIC) experiments, and

(c) Determination of the optimal time at which to harvest and prepare competent cells.

In this study, measurement of initial bacterial cell density is important for monitoring the experiment and evaluating the anti-microbial activity of the synthetic Aza-RRM peptide.

To determinate the initial bacterial inoculum concentration, the optical density (OD600) of bacterial suspensions in broth cultures was measured by Eppendorf Biophotometer (Figure 4.7) (Eppendorf, USA).

Figure 4.7. Eppendorf Biophotometer
http://scientiis.com/laboratorium/catalog/popup_image.php?pID=14677&osCsid=47b7467c0338da8b1132d6f0529e5ad6

McFarland standards

McFarland standards are used as a reference to adjust the turbidity of bacterial suspensions, so that a number of bacteria will be within a given range to standardize microbial testing.

McFarland Standard No.	0.5	1	2	3	4
1.0% Barium chloride (ml)	0.05	0.1	0.2	0.3	0.4
1.0% Sulfuric acid (ml)	9.95	9.9	9.8	9.7	9.6
Approx. cell density (1X10^8 CFU/mL)	1.5	3.0	6.0	9.0	12.0
% Transmittance*	74.3	55.6	35.6	26.4	21.5
Absorbance*	0.08 to 0.1	0.257	0.451	0.582	0.669

Table 4.3 McFarland Nephelometer Standards at wavelength of 600nm
http://site.iugaza.edu.ps/yabdelal/files/05.14.01.pdf

Micro-plate spectrophotometer

Multi-welled microtitre plates provide a convenient means of handling 'large block' multifactorial experiments with microbial cultures. Microplate Readers have been designed to detect microbial growth in each well, by transmitted light measurements. They are widely used in research, drug discovery, bioassay validation, quality control and manufacturing processes in the pharmaceutical and biotechnological industry and academic organizations. The most common microplate format used in academic research laboratories or clinical diagnostic laboratories is 96-well (8 by 12 matrix) with a typical reaction volume between 100 and 200 µL per well. Optional microcomputer control is employed to facilitate scanning of plates and data handling.

Cell suspensions are turbid: they absorb or scatter some of the light letting the rest of it pass through. The higher the cell concentration is, the higher the turbidity. Spectrophotometers are electrical appliances that can measure intensity of light very accurately. The culture is placed in a transparent cuvette, the cuvette is placed in the machine, and the optical density can be measured immediately.

Multiskan Ascent Reader

To quantify studying the growth of gram-negative and gram-positive bacteria in the 96-well plate, the microplate reader Thermo Multiskan Ascent Reader (Figure 4.8) from Thermo Electron Co. was used. The Multiskan Ascent Reader was connected with Dell Computer (Running Ascent Software). The software was set to automatically

monitor and save the absorption coefficient at wavelength of 600nm.

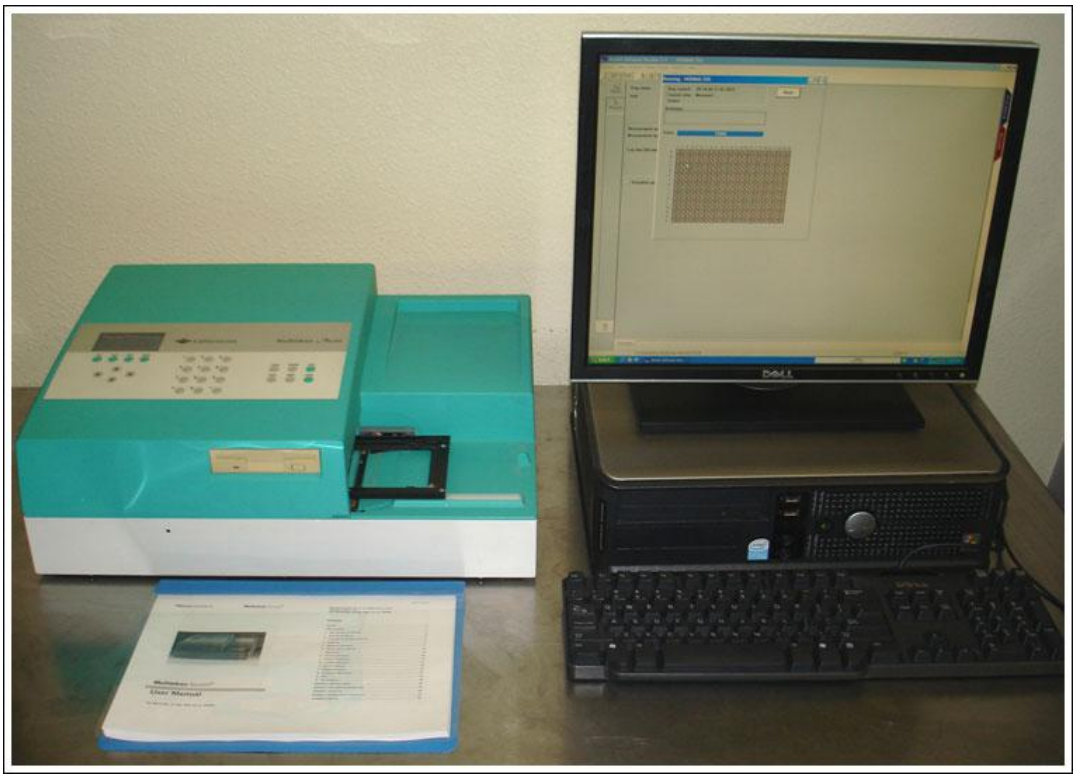

Figure 4.8. Multiskan Ascent 96/384 Plate Reader

http://www.labx.com/v2/adsearch/detail3.cfm?adnumb=513997#.U7YKOKiSxjY

Viable cell counts

The plate counting is used to estimate a number of cells present based on their ability to give rise to colonies under specific conditions of nutrient medium, temperature and time. In microbiology, colony-forming unit (CFU) is used to determine the number of viable bacterial cells in a sample per ml. Viable bacterial cell is defined as the ability of a cell to multiply via binary fission under the controlled conditions. In contrast, in a microscopic evaluation, all cells, dead and living are counted. In CFU analysis/assessment, the results are reported as CFU/mL (colony-forming units per

milliliter) for liquids.

In general, the initial concentration of bacteria is too great, and the colonies will grow into each other and the plate will be uncountable. To insure a countable plate, a series of dilutions should be performed for CFU assessment. Procedure of a series of dilutions is shown in Figure 4.9.

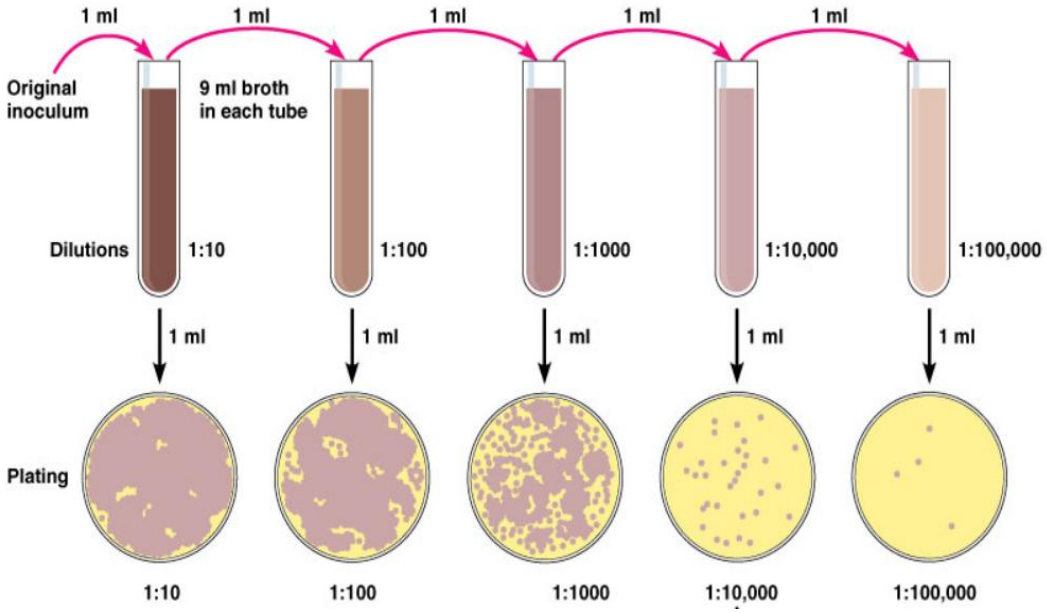

Figure 4.9. Calculation: Number of colonies on plate x reciprocal of dilution of sample = number of bacteria/ml

http://classes.midlandstech.com/carterp/Courses/bio225/chap06/Microbial%20Growth%20ss5.htm

CHAPTER 5

Results and Discussion

As presented in earlier Chapters, this PhD project aims at *developing an evidence-based methodology for wound healing promotion* and thus, is focused in two directions:

Study 5.1 - Evaluation of light radiation at the molecular and cellular levels for improvement of wound repair process

5.1.1 - Visible light irradiation of Collagenase enzyme

5.1.2 – Visible light irradiation of selected Gram-positive and Gram-negative bacteria

5.1.3 – Infrared light irradiation of selected Gram-positive and Gram-negative bacteria

Study 5.2 - Evaluation of anti-microbial properties of a novel *de novo* designed synthetic peptide on selected Gram-positive and Gram-negative bacteria.

Both Study 5.1 and Study 5.2 include the computational and experimental components. The results of the conducted studies are presented in Chapter 5 in great details.

Study 5.1 - Evaluation of light radiation at the molecular and cellular levels for improvement of wound repair process

5.1.1 - Visible light irradiation of Collagenase enzyme

5.1.1.1 Overview

Debridement is the process of removing necrotic burden or contaminated tissue from a wound bed until surrounding healthy tissue is exposed. Enzymatic debridement helps to remove non-viable tissue which can otherwise delay wound healing and lead to infection [36]. Collagenase enzyme is known to be able to promote cellular responses to injury and wound healing *in vivo*. Collagenase shows more selectively on denatured collagen in devitalized tissue. This selectivity is beneficial as it keeps the vital tissue and growth factors crucial to wound healing intact. There are studies showing that applied electromagnetic radiation (EMR) in the visible light range can modulate protein and cellular activity. By increasing Collagenase activity via light irradiation, a wound repair process can be enhanced.

Study 1.1 presents an experimental evaluation of the effects of applied visible light exposures on enzymatic activity of Collagenase. The RRM approach was employed for the computational analysis of 28 Collagenase primary sequences; and the activation frequency/wavelength range was determined to be within 450–460 nm. To evaluate the effects of light exposure in this range, the Collagenase enzyme solutions were irradiated by monochromatic light of 400 to 500 nm. The obtained results reveal that

Collagenase activity can be modulated at the particular wavelengths of **450nm, 456nm, and 460nm**, which are within the activation wavelength range defined computationally.

5.1.1.2 Introduction and problem definition

Debridement is an essential treatment process used in wound bed preparation as part of wound healing procedure. Since devitalized tissue can obstruct healing of a wound, debridement offers a comprehensive approach to removing barriers to healing and creating a wound environment for healing promotion and thus, reducing risk of local infection [36]. There are a number of methods currently used for debridement of wounds. These include surgical, chemical, enzymatic, mechanical and biological techniques [13,283]. Although enzymatic debridement is a time consuming process, it is still a primary technique for wound debridement in certain cases when the surgery or conservative sharp wound debridement are not feasible due to bleeding disorders or other complication [13]. Of particular interest to this study are the enzymatic debridement method and the possibility of accelerating/promoting this process aiming at its enhanced clinical practice in wound management.

There is evidence that applied EMR in the visible light range can modulate protein and cellular activity [284,285]. Reported studies show that endochondral bone formation can be regulated by exogenously applied biophysical stimuli that include EMR. Some studies revealed that exposures to pulsed electromagnetic fields (PEMF) enhance

chondrogenic differentiation and the synthesis of cartilage extracellular matrix proteins. Studies focused on investigating the effects of visible light on cell proliferation and their metabolisms were reported [286].

In [21,282], it was shown show that activity of L-Lactate Dehydrogenase enzyme can be affected by external light of particular wavelengths, computed by the Resonant Recognition Model [21,282]. The RRM theory states that an external EMR at a particular frequency would produce resonant effects on protein biological activity [240,282]. The resonant absorption and resonant interactions have been proposed as an explanation for the marked sensitivity of living systems to EMR [245]. Each biological process involves a number of interactions between proteins and their targets, which are based on energy transfer between the interacting molecules. The RRM is designed for analysis of protein (DNA) interactions and their interaction with EMR [21,240,282]. Collagenase enzyme was irradiated here by visible light in the wavelength range of 400-500 nm defined computationally by the RRM.

5.1.1.3. Materials and Methods

The RRM is a physico-mathematical approach based on digital signal processing [240]. The RRM concepts are presented in details in Chapter 4.

The application of the RRM involves two stages of calculation. The first is the transformation of the amino acid sequence into a numerical sequence. Each amino acid is represented by its Electron-Ion Interaction Potential (EIIP) value which describes the

average energy states of all valence electrons in a given amino acid [240]. A unique number can thus represent each amino acid or nucleotide, irrespective of its position in a sequence. Then the numerical series obtained are analyzed by digital signal analysis methods, Fourier and Wavelet transforms, in order to extract information pertinent to the biological function. A multiple cross-spectral function is defined and calculated to obtain the common frequency components from the spectra of a group of proteins. Peak frequencies in such a multiple cross-spectral function denote common frequency components for all sequences analyzed [243].

As shown in the RRM previous studies, all protein sequences with a common biological function have a common frequency component in the free energy distribution of electrons along the protein backbone. This characteristic frequency was shown to be related to protein biological function [21,240,282]. It was postulated that RRM frequencies characterize not only a general function but also a recognition/interaction between the particular proteins and their target at a distance. Thus, protein interactions can be viewed as a resonant energy transfer between the interacting molecules. This energy can be transferred through oscillations of a physical field, possibly electromagnetic in nature [240].

Since there is evidence that proteins have certain conducting or semi-conducting properties, a charge moving through the protein backbone and passing different energy stages caused by different amino acid side groups can produce sufficient conditions for

a specific electromagnetic radiation or absorption [240]. A strong linear correlation exists between the predicted and experimentally determined frequencies corresponding to the absorption of electromagnetic radiation of such proteins [240]. It is inferred that approximate wavelengths in real frequency space can be calculated from the RRM characteristic frequencies for each biologically related group of sequences. These calculations can be used to predict the wavelength of the light irradiation, which might affect the biological activity of exposed proteins [20]. A linear correlation between the absorption spectra of proteins and their RRM spectra with a regression coefficient of K=201 was established. Using RRM postulates, a computationally identified characteristic frequency for a protein functional group can be used to calculate the wavelength of applied irradiation, λ, defined as $\lambda=201/f_{RRM}$, which could activate this protein sequence and modify its bioactivity [240,282]. In this study, the above relationship was utilized to calculate the frequencies/wavelengths light that can modulate the bioactivity of the selected enzyme and investigate/evaluate their activation experimentally.

Computational analysis of selected Collagenase enzymes using the RRM

Here the RRM was used to compute the common characteristic frequency of 28 vertebrate collagenase proteins that corresponds to their common biological activity. Collagenase primary protein sequences were collected from the NCBI protein database ((http://www.ncbi.nlm.nih.gov/protein). A multiple cross-spectral analysis was performed resulting in one prominent RRM characteristic frequency identified at

f=0.4385 (Figure 5.1.1). This frequency is related to the biological activity of the analyzed Collagenase proteins.

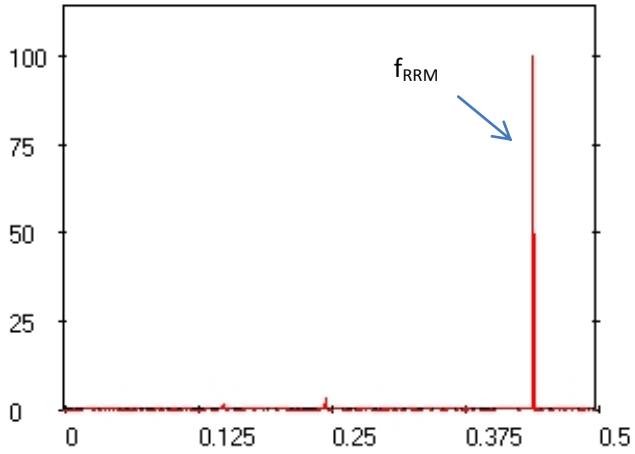

Figure 5.1.1 Multiple cross spectral function of 28 vertebrate collagenase sequences. The x axis represents the relative RRM frequency. The y axis represents the normalized intensity.

This RRM frequency $\mathbf{f_{RRM}=0.4385}$ is used to calculate the wavelength of external irradiation, λ, which can activate Collagenase protein and modify its bioactivity, $\lambda=201/f_{RRM}$. Thus, the wavelength of the EMR required for Collagenase enzyme activation will be at or near **456 nm**. For the experimental validation of this computational prediction, the irradiating range was set between 400 – 500 nm.

Experimental study of visible light irradiation of Collagenase enzyme

In these experiments, the selected Collagenase enzyme solutions were irradiated by visible light (400-500nm). Changes in its activity upon radiation were evaluated and compared with control samples.

Equipment: As a source of visible light radiation we used Monochromators SPEX 270M: (Princeton Instruments, Trenton, NJ, USA) 1200 g/mm grating, focal length 270 mm, resolution 0.1 nm at 500 nm, dispersion 3.1 nm/mm, range 400 – 890 nm, RS232 connection with HP 34001A, controlled by LabView 6.1 (National Instruments). For measurement of absorbance of the analyzed enzyme solutions we used Ocean Optics USB2000 spectrometer coupled with USBISS-UV/VIS, (Ocean Optics, FL, USA) range 190 – 870 nm, USB-2 connection with Pentium IV (Windows XP). Software automatically monitors and saves the absorption coefficient at 570 nm wavelength every 10 sec.

Enzymatic Assay: Experimental solutions were prepared according to the standard enzymatic assay of collagenase from Sigma-Aldrich. The experiments were divided into two groups: (i) Group 1 (sham-exposure), collagenase sample not exposed to applied irradiation. This sample was used as a control for evaluating effects of irradiation on exposed vs. non-exposed samples; and (ii) Group 2, collagenase samples irradiated with light of different wavelengths (400—500nm, with 5nm steps) for 600 sec. All experiments were performed at 37 ℃.

The assay was chosen to satisfy following criteria:

1. Time needed for catalyzing of 90% of the substrate should not be longer than 10 min.

2. Buffer does not include any substance that absorbs in visible/IR range and does not absorb at 570nm.

In accordance to the above mentioned prerequisites, the SIGMA Aldrich assay (c7521) was chosen.

PRINCIPLE: Collagen + $H_2O \xrightarrow{Collagenase}$ Peptides

CONDITIONS: T = 37 °C, pH= 7.4, A570nm, Light path=1cm

REAGENTS:

Chemicals: TES free acis, Calcium Chloride with Dihydrate, Collagen Type 1, Collagenase were all obtained from Sigma.

A. 50 mM TES Buffer with 0.36 mM Calcium Chloride, pH 7.4 at 37 °C

(Prepare 1000 ml in deionized water using TES Free Acid, Sigma Prod. No. T-1375, and Calcium Chloride, Dihydrate, Sigma Prod. No. C-3881. Adjust the pH to 7.4 at 37 °C with 1 M NaOH.)

B. Collagen Type I (Use Collagen, Type I, Sigma Prod. No. C-9879.)

C. Collagenase Enzyme Solution ((Immediately before use, prepare a solution containing 0.1 mg/ml Collagenase, Sigma Prod. No. C-0130, in Buffer A.)

Experimental protocol:

1. The cuvette, filled with the collagenase solution, was irradiated with light of a particular wavelength in a range of 400-500 nm for 600 sec or incubated for 600 sec for the control enzyme sample.

2. The irradiated (or control non-irradiated/sham-exposed samples) were added to the already prepared enzymatic substrate solution of Collagen Type I (pH 7.4).

3. The optical density of digested Collagen solution was measured at 570 nm

(according to Sigma assay) for each selected irradiating wavelengths (400 - 500nm, with a step of 5 nm) using the spectrophotometer. The same experimental procedure was used for control samples.

Method:

Continuous Spectrophotometric Rate Determination: This method is widely used for qualitative analysis in chemistry, biochemistry and clinical applications. In this method, the course of a reaction is followed by monitoring how much light the assay solution absorbs by measuring the intensity of light as a beam of light passes through sample solution. This method is established on the fundamental principle that a compound either absorbs or transmits light over a certain range of wavelength.

Measurement of Collagenase Enzyme Activity:

The activity of the Collagenase enzyme is measured by determining the rate of substrate utilization during the collagen-collagenase reaction. The temperature was controlled during Collagenase irradiation as well as during the activity measurement procedure. Experiments were performed at the temperature of 37 °C.

With the aim at eliminating the effects of all possible artifacts (pH, temperature, and concentrations), the measurements were repeated three (3) times for each irradiating wavelength to evaluate changes in collagenase absorbance (changes in activity of collagenase solutions) before and after the light exposures.

Experimental Results:

To validate the predicted activation wavelength, obtained within the computational analysis, the experiments were conducted according to the experimental protocol outlined above with the results presented in Fig.5.1.2 and Fig. 5.1.3.

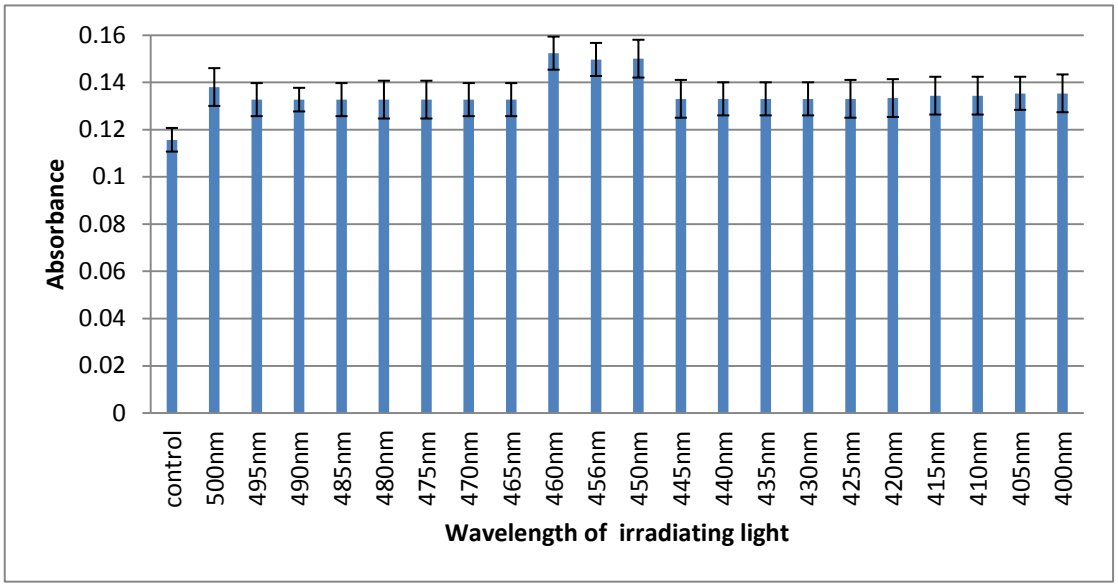

Figure 5.1.2 The effects of irradiating light on absorbance of Collagen

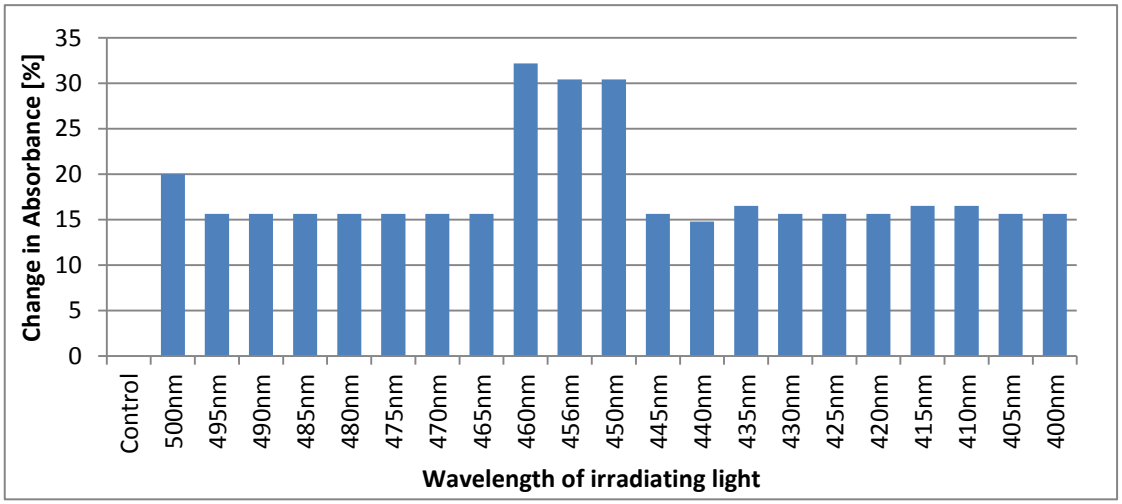

Figure 5.1.3 Relative change in Collagen absorbance upon light irradiation, %.

Figure 5.1.2 shows that the selected light irradiation affected the enzymatic activity of Collagenase that resulted in the increase in Collagen's absorbance. A significant effect (compared to the control sample) is seen at the wavelengths of **450, 456, and 460nm**. Figure 5.1.3 presents relative changes in absorbance of Collagen. As can be seen from Figure 5.1.3, the increase of 30-32% in Collagen's absorbance is achieved at these particular wavelengths. The maximum change in absorbance of digested Collagen is recorded at the wavelengths which are in the range predicted computationally by the RRM.

An increase of 20% in Collagen's absorbance can be observed at 500nm, and even smaller increases of 15-16% are seen at all other wavelengths (Figure 5.1.3). Clearly, these findings support the hypothesis that protein activity of Collagenase can be modulated by external light of the particular wavelengths predicted by the RRM approach. Modulated activity of irradiated Collagenase induced changes in this biochemical reaction via affecting the absorbance of Collagen. Interestingly, the results show that light exposures (400-500nm) affect the absorbance of digested collagen at different degrees, thus suggesting that these *modulating effects are frequency-dependent*.

Final remarks:

The results presented reinforce the previously developed linear relationship between the calculated RRM frequencies and wavelengths of light radiation. With this correlation in mind, it is now possible to calculate wavelengths of light irradiation which will affect different biological processes. These findings suggest that EMR can be used as a non-invasive treatment to promote enzymatic debridement and thus assist wound healing. The possibility to computationally calculate the RRM frequencies, followed by the use of IR and visible light to produce the desired biological mutations and alterations in proteins will benefit the development of new biomaterials, and advanced technologies.

5.1.2 Visible Light Irradiation of selected Gram-positive and Gram-negative bacteria

Overview:

There are several theoretical and experimental studies published that evaluated the effects of visible light and infrared light exposures on bacterial growth [287,288,290,291]. This study was aimed at investigating the phototoxic effects of visible and far infrared light on the selected bacterial strains. In this comprehensive experimental study, the biological effects induced by a LED-based exposure system on the selected gram-positive and gram-negative bacteria were evaluated using quantitative analyses. The LED-based exposure device was designed and developed to emit light at the selected wavelengths of **466nm, 585nm, 626nm (visible light)** and at the selected **far infrared wavelengths of 3400nm, 3600nm, 3800nm, 3900nm, 4100nm, 4300nm**.

LED-based exposure system

The experimental setup and the exposure system were designed in a way to avoid any cross talk between different LEDs. To make sure that there are no heating effects on irradiated cells (from the heat generated by the LEDs), a heat-shielding gel (Inventables, USA) was used between the wells in order to prevent heat dissipation and absorption produced by other LEDs irradiating at the selected wavelengths [273,274]. The gel was placed around the wells in the 96-well plate from outside and between the gaps. For a minimum dispersion, the device was designed to have the narrowest possible

irradiation angle and the gap between the device and an exposed sample was set at less than 1mm. For the consistency of the experimental exposure and power irradiated at each particular wavelength, all LEDs used in the experiments had the irradiation angle of less than 40^0 (for minimum power dissipation from the energy source). More importantly, any cross-talk between the neighboring LEDs and the effect of two frequencies on the same well was eliminated by having the empty wells around each well that were used for running the experiments.

Figure 5.1.4. The custom-build LED-based exposure device was designed and developed to emit light at the selected wavelengths.

In this study, the selected bacterial cells were exposed and sham-exposed (control) using the custom-build LED-based exposure device. Its design and construction are

presented in details in [273,274]. The main characteristics of the exposure systems are given below:

1. Adaptor of 12v and 1A current has been fed into circuitry.

2. The selected irradiating wavelengths: 3400nm, 3600nm, 3800nm, 3900nm, 4100nm, 4300nm, 466nm, 585nm, 626nm, 810nm, 850nm and 950nm.

3. To have these selected LEDs to operate in their optimal region, the input signal of 250mA, 2 kHz and 50% duty cycle has been fed into the system.

4. To have the minimum dispersion, the device was designed to have the narrowest possible irradiation angle and the gap between the device and an exposed sample was set at less than 1mm.

5. All the LEDs used had the irradiation angle of less than 40o for minimum power dissipation from the energy source.

6. The system was designed in a way to avoid any cross talk between different the LEDs. To make sure that there are no heating effects on irradiated cells, a heat-shield material was used between the wells in order to prevent heat dissipation and absorption produced by LEDs irradiating at the selected wavelengths.

7. The intensity of each frequency was constant (between 15 µW to 30 µW) and was not changed during the experiments. The relevance conversion factor between radiant intensity and luminous intensity can be calculated as follows:

K (λ) = Iv (Luminous Intensity)/ Ie (Radiant Intensity)

–In the experimental set up, the intensity of the exposure was kept constant for a better

comparison factor. All experiments were conducted three times in triplicates for the accuracy of the results. Three visible light wavelengths: 466nm, 585nm and 626nm were selected for the experimental evaluation of irradiation exposures. Six frequencies were selected for the experimental evaluation of far infrared exposures: 3400nm, 3600nm, 3800nm, 3900nm, 4100nm, and 4300nm.

Bacterial strains, inoculums preparation, and bacteria irradiation

The selected Gram-positive bacterial strains, used in this experimentation, were *Staphylococcus aureus* ATCC 25923, and *Staphylococcus aureus* 344 (Ampicillin resistant strain). The selected Gram-negative bacterium used in this study was *E. coli* ATCC 25922. The bacterial isolates were obtained from the Microbiology Laboratory, Department of Biotechnology & Environmental Biology, School of Applied Sciences, RMIT University.

The following exposure regimes were applied in this experimental study:

(1) – 30 min of exposure and no post-exposure incubation

(2) – 30 min of exposure followed by 1.5 hr of post-exposure incubation

Regimes (1) and (2) were used to irradiated all three bacteria (*S. aureus* ATCC 25923, *S. aureus* 344 (ampicillin resistant strain) and *E. coli* ATCC 25922)

(3) – 1.5 hr of exposure and no post-exposure incubation

(4) – 1.5 hr of exposure followed by 1.5 hr of post-exposure incubation

Regimes (3) and (4) were used to irradiate two Gram-positive bacteria (*S. aureus*

ATCC 25923 and *S. aureus* 344 (ampicillin resistant strain).

(5) – 2 hr of exposure and no post-exposure incubation

(6) – 2 hr of exposure followed by 1.5 hr of post-exposure incubation

Regimes (5) and (6) were used to irradiate one bacterium (Gram-negative *E. coli* ATCC 25922)

To assess the phototoxic effects of visible light and far infrared light radiation on gram-positive and gram-negative bacteria, a well isolated colony of either *S. aureus* ATCC 25923, *S. aureus* 344 (ampicillin resistant strain) or *E. coli* ATCC 25922 from the fresh MHA plate was inoculated into 2ml of Mueller-Hinton Broth (MHB) tube (to ensure a proper viability), and incubated at 37^0 C overnight. In order to attain the desired initial concentration of bacteria for the experiment, the initial concentration for inoculation was adjusted to 0.5 McFarland's turbidity standard[293] while the density of the bacterial suspensions in following procedure were measured via optical density reading by Eppendorf BioPhotometer (to determine an approximate concentration of bacteria which is used as a basis for the experiment initial inoculation). Then, immediately after the optical density (OD_{600}) of the bacterial suspension in MHB was adjusted, all bacteria, including gram-positive and gram-negative cells, were seeded in designated wells in 96-well plates.

<u>The experiments were divided into two groups:</u>

(i) Group 1 – control (sham-exposure/no irradiation): the bacterial samples were not

exposed by applied irradiation. These samples were used as a control group for evaluating effects of irradiation on exposed *vs*. non-exposed samples; and

(ii) Group 2 – irradiated bacteria: bacterial samples were irradiated with light of different wavelengths (***visible light*: 466nm, 585nm, and 626nm**; and ***far IR light*: 3400nm, 3600nm, 3800nm, 3900nm, 4100nm, and 4300nm**).

Different exposure regimes (presented above) were utilized. Irradiation of bacterial cells was conducted at room temperature. In the exposure regimes (2), (4) and (6), immediately after exposures the bacterial cells were then placed inside the incubator for 1.5 hr at the temperature of 37°C. After incubation, the changes induced by light exposures in studied bacterial cells were evaluated by the OD reading and CFU techniques. All experiments were treated in triplicate in the same plate. Each combination of different exposure and incubation times was repeated three times in order to find the statistically significant results and reveal any specific effect on bacterial cell viability.

Visible light LED radiation experimental results

Cell viability assessment was performed on each type of bacteria in suspension, which were exposed to different wavelengths of light radiation under the above stated conditions. In particular, effects of applied exposures to visible light at the wavelengths **466nm, 585nm**, and **626nm** were evaluated and expressed by optical density (OD) of bacteria in suspension and by live cell count of colony forming units (CFU). The experimental findings are is shown and discussed below.

Exposure regime (1) – 30 min of exposure with no post-exposure incubation

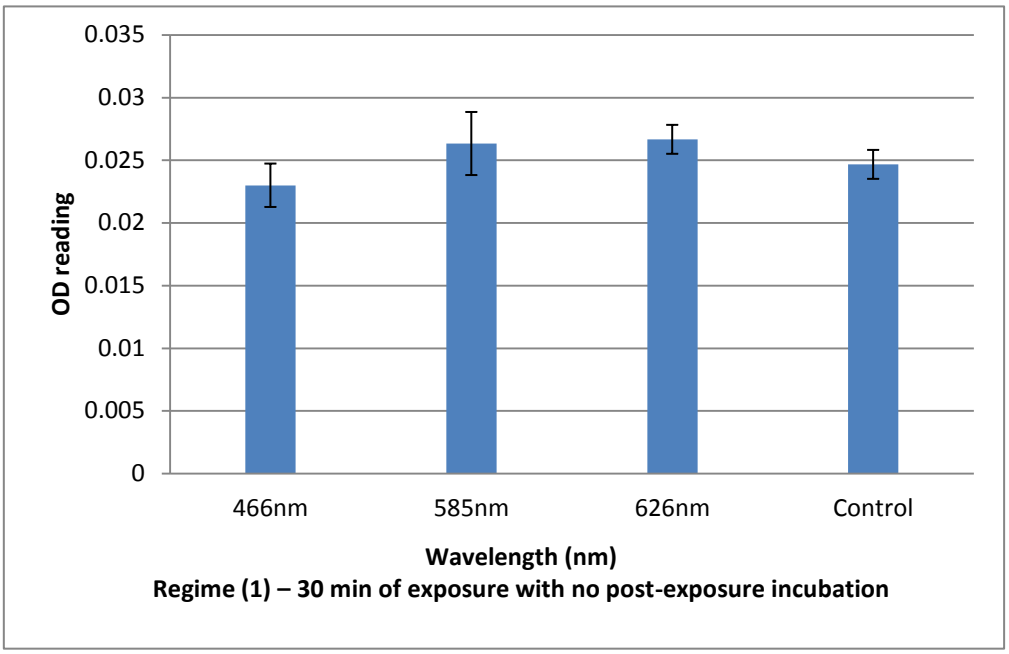

Figure 5.1.5 OD reading for *S. aureus* ATCC25923 irradiated with visible light.

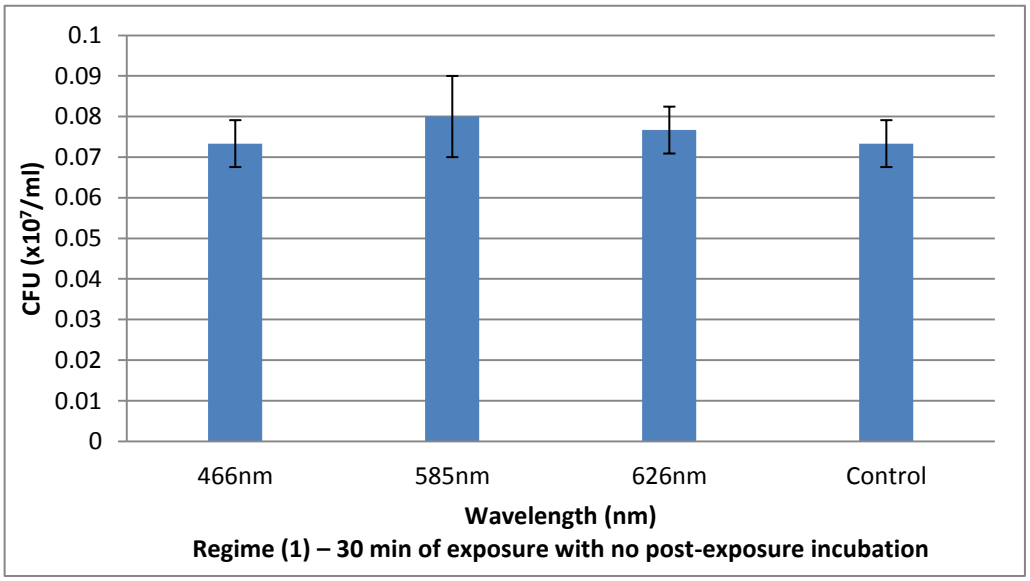

Figure 5.1.6 CFU for *S. aureus* ATCC 25923 irradiated with visible light.

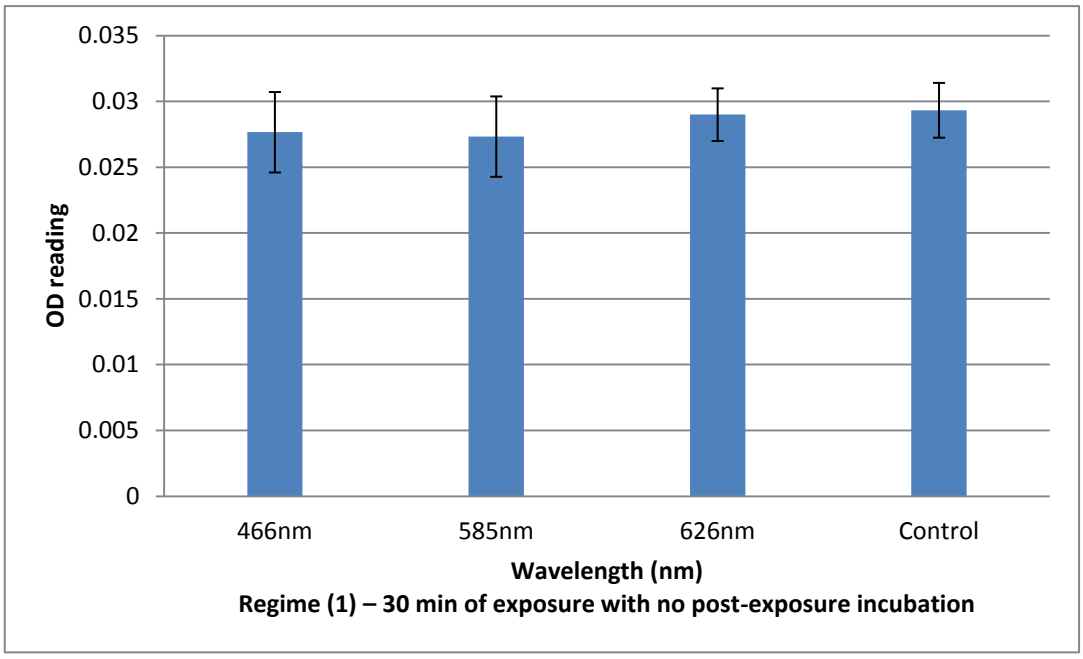

Figure 5.1.7 OD reading for *S. aureus* 344 (Ampicillin resistant strain) irradiated with visible light.

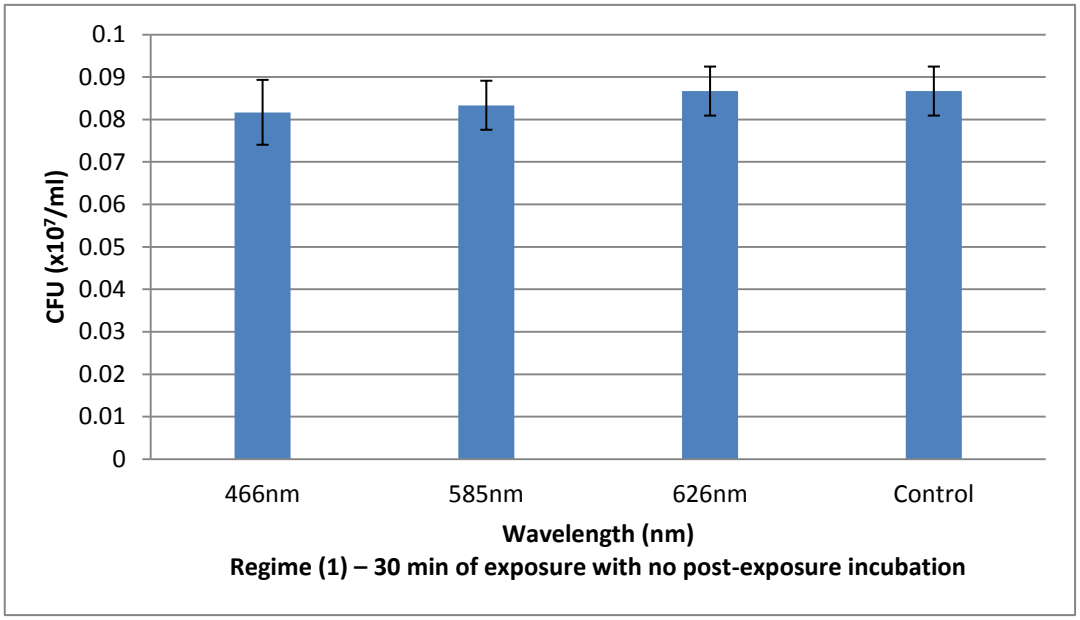

Figure 5.1.8 CFU for *S. aureus* 344(Ampicillin resistant strain) irradiated with visible light.

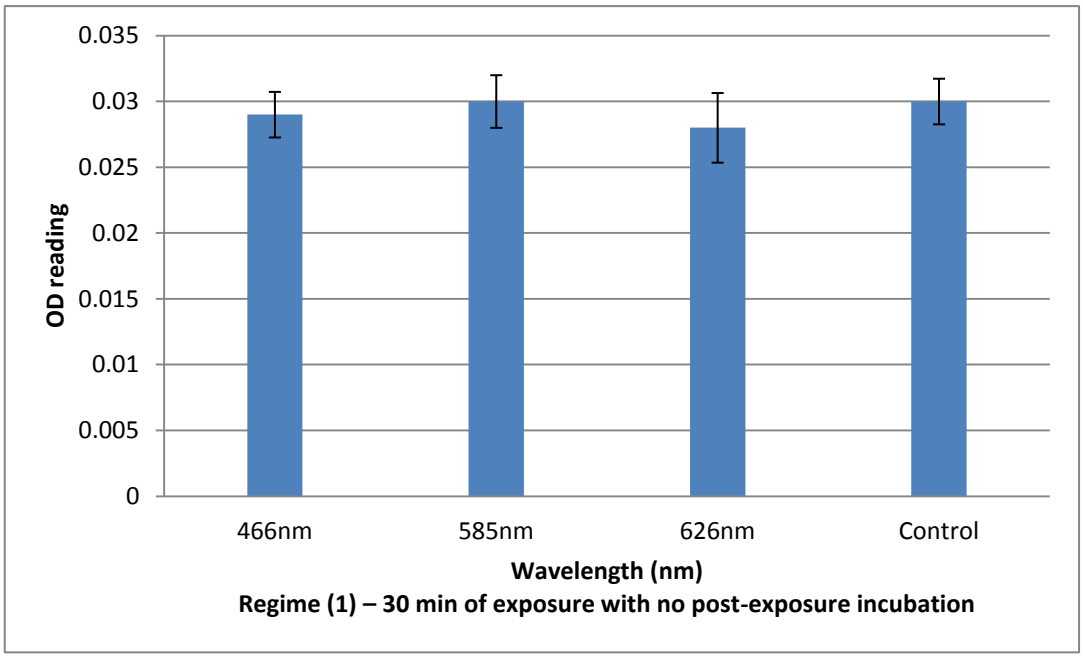

Figure 5.1.9 OD reading for *E. coli* ATCC 25922 irradiated with visible light.

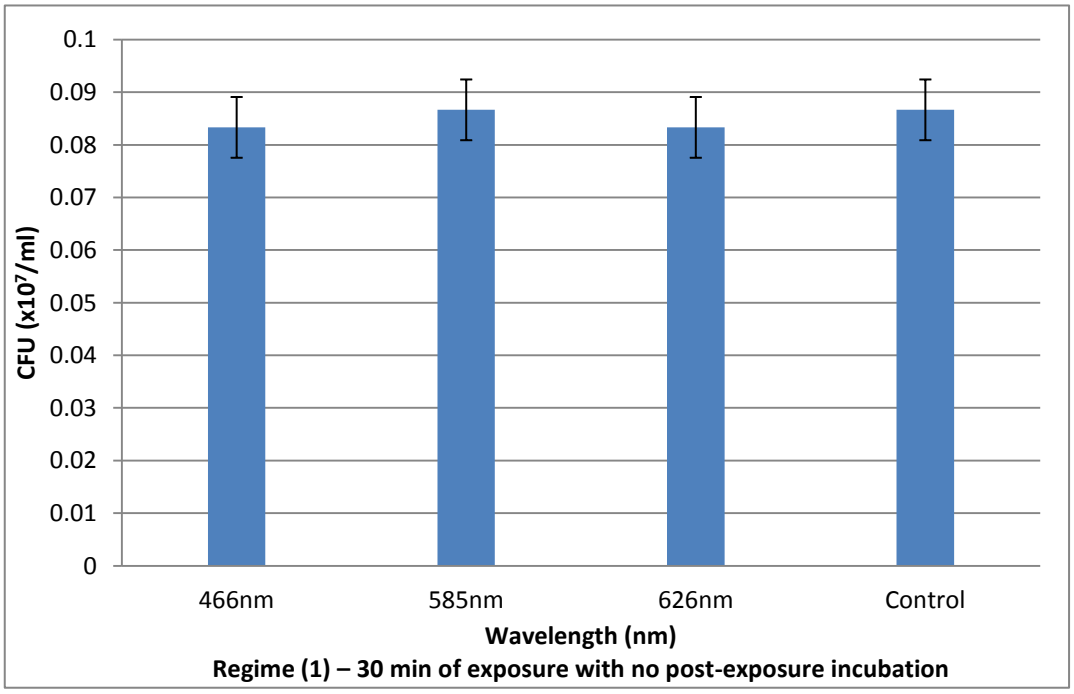

Figure 5.1.10 CFU for *E. coli* ATCC 25922 irradiated with visible light.

Exposure regime (2) – 30 min of exposure followed by 1.5 hr of post-exposure incubation

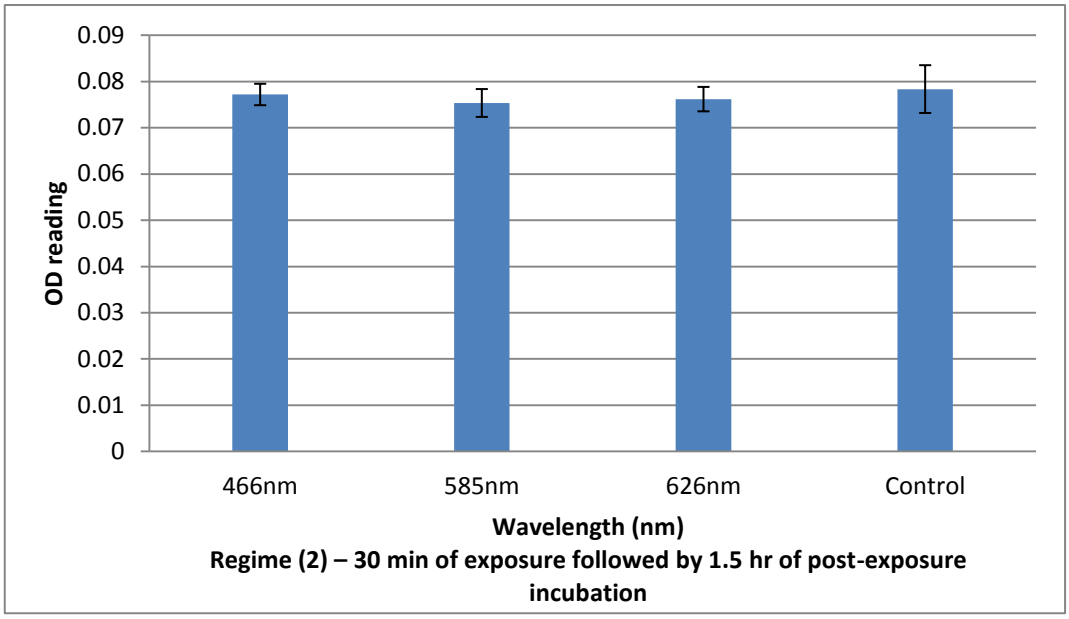

Figure 5.1.11 OD reading for *S. aureus* ATCC 25923 irradiated with visible light

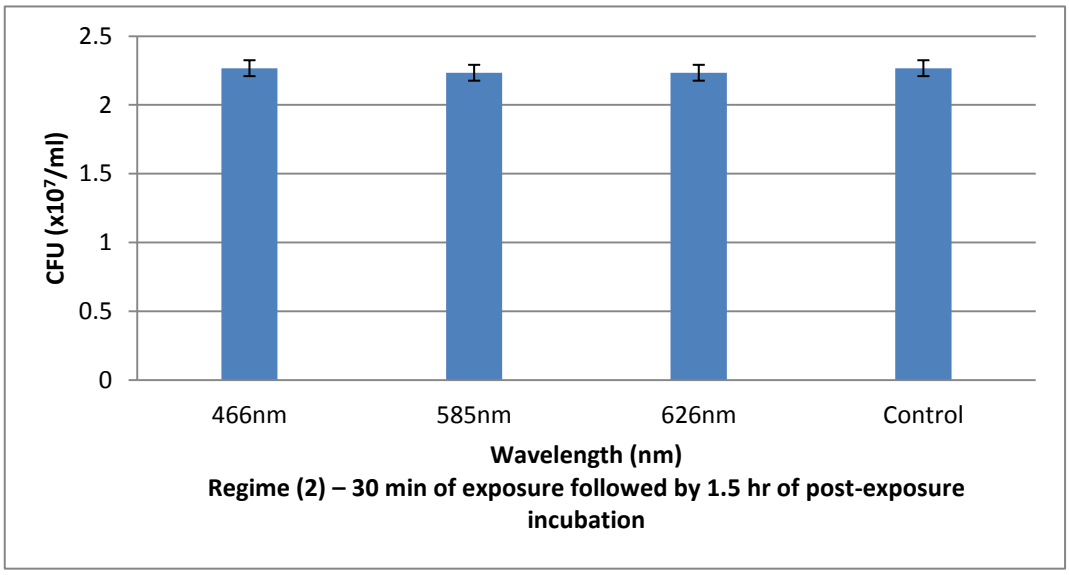

Figure 5.1.12 CFU for *S. aureus* ATCC 25923 irradiated with visible light.

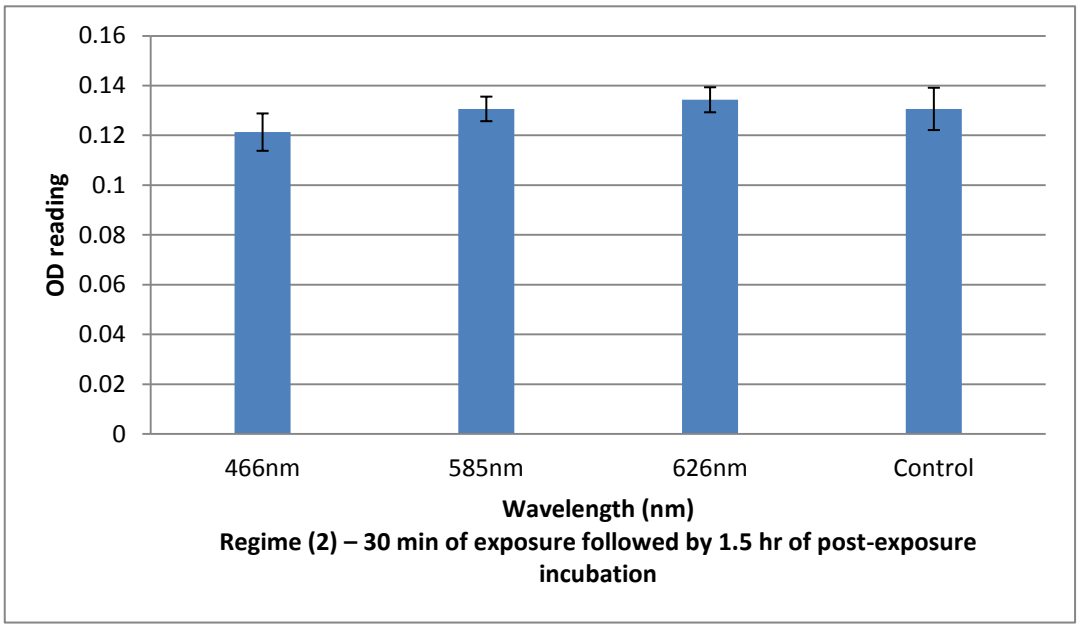

Figure 5.1.13 OD reading for *S. aureus* 344 (Ampicillin resistant strain) irradiated with visible light

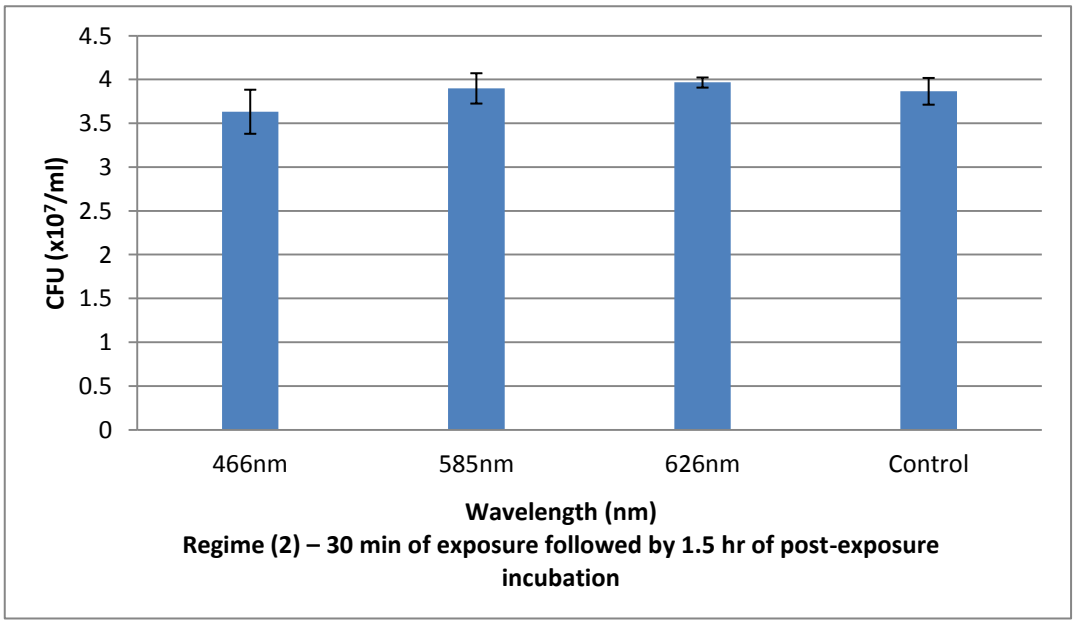

Figure 5.1.14 CFU for *S. aureus* 344 (Ampicillin resistant strain) irradiated with visible light

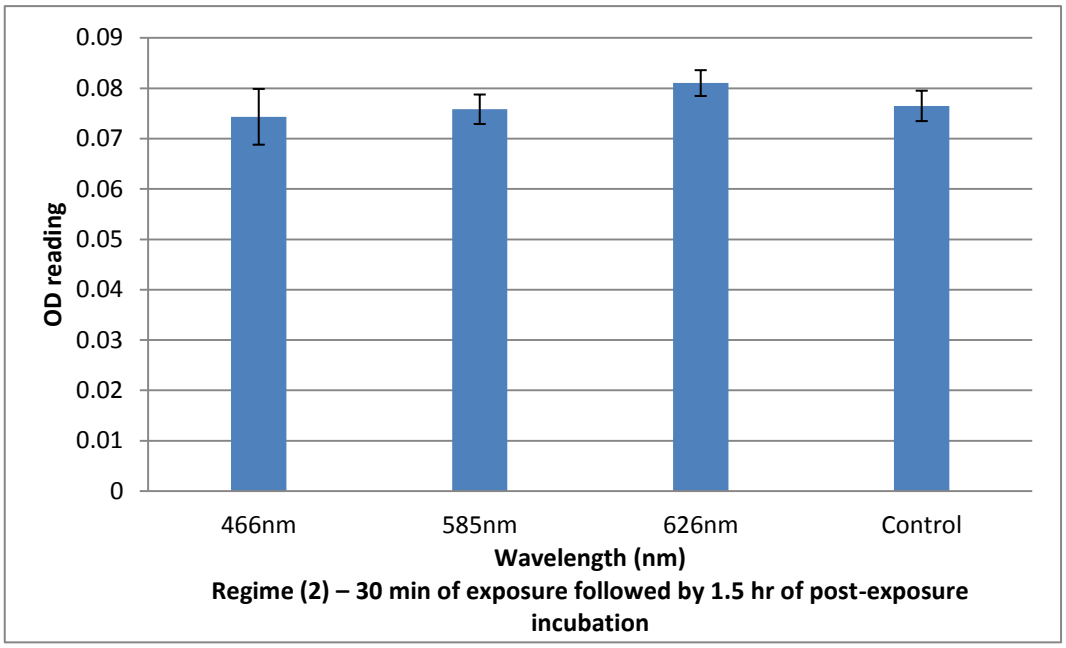

Figure 5.1.15 OD reading for *E. coli* ATCC 25922 irradiated with visible light

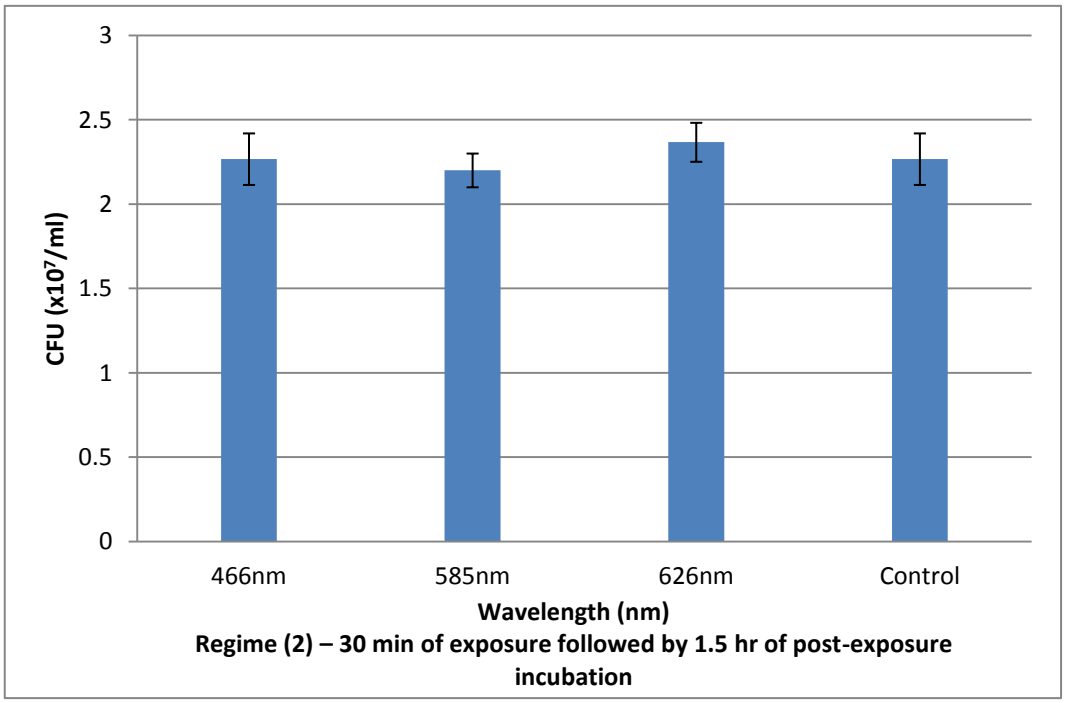

Figure 5.1.16 CFU for *E. coli* ATCC 25922 irradiated with visible light.

Exposure regime (3) – 1.5 hr of exposure and no post-exposure incubation

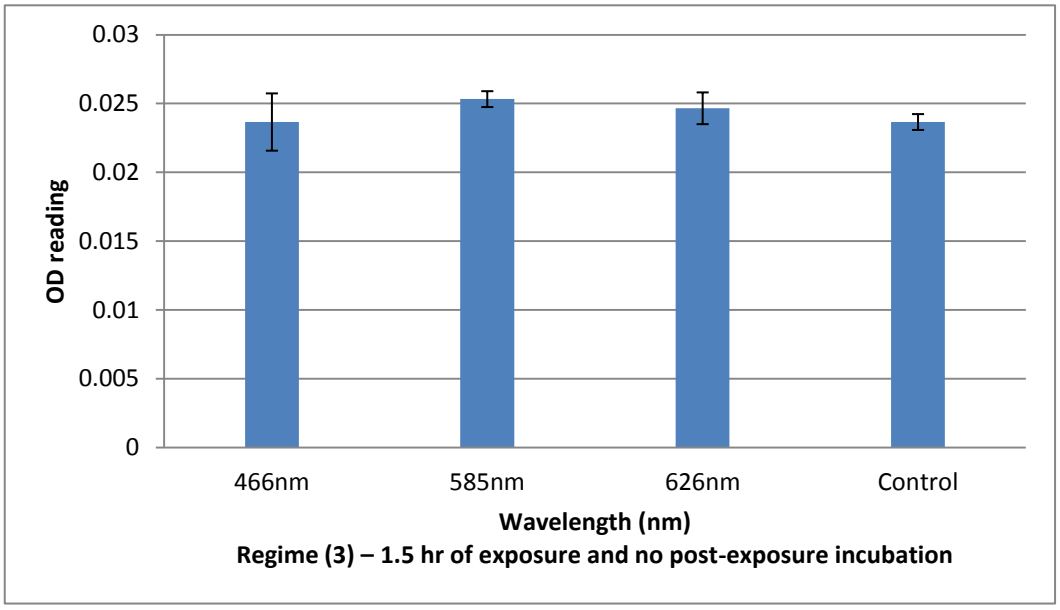

Figure 5.1.17 OD reading for *S. aureus* ATCC 25923 irradiated with visible light

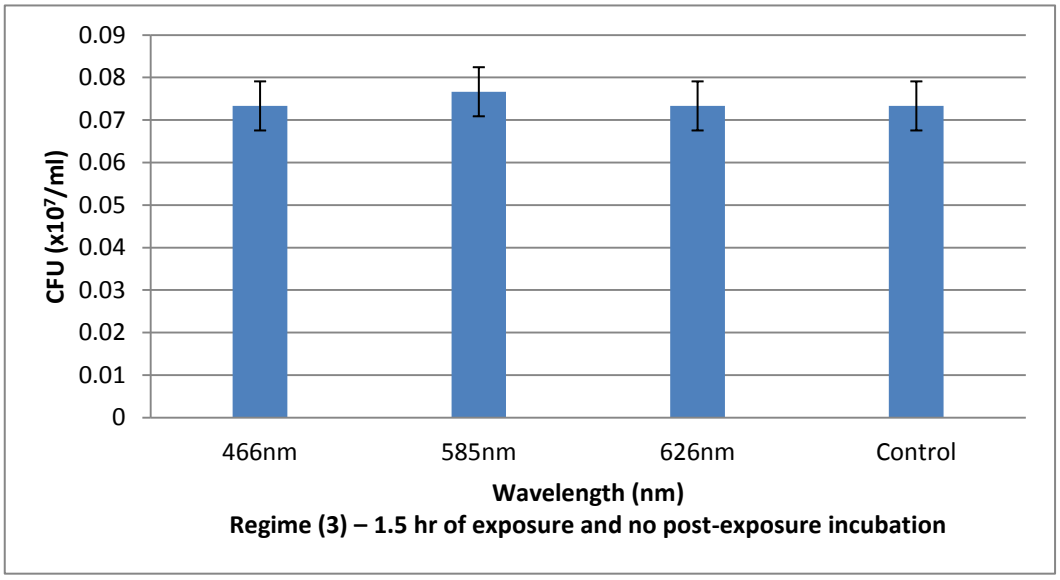

Figure 5.1.18 CFU for *S. aureus* ATCC 25923 irradiated with visible light

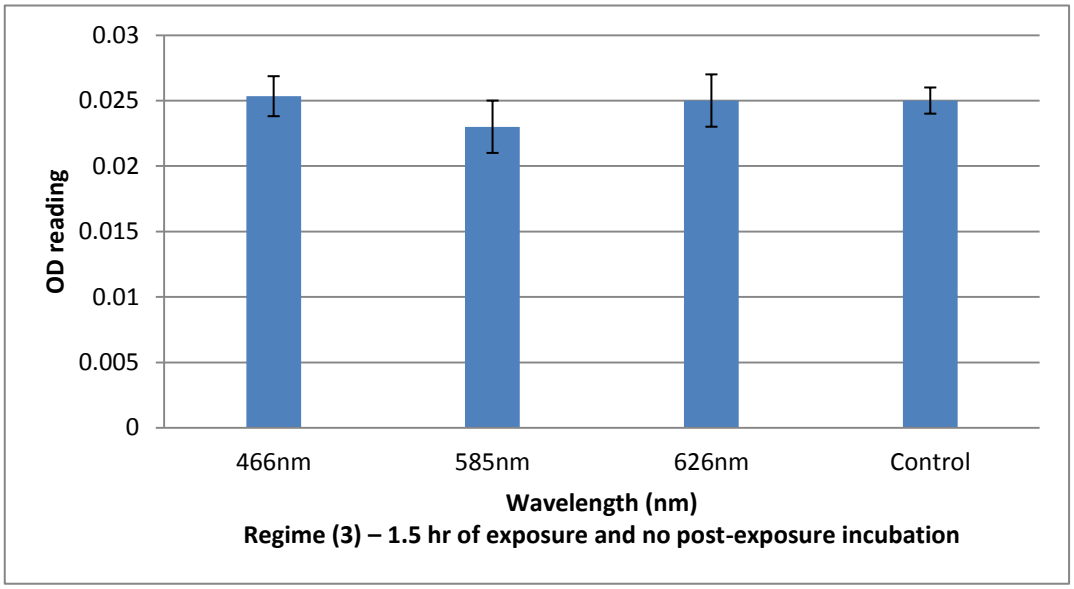

Figure 5.1.19 OD reading for *S. aureus* 344 (Ampicillin resistant strain) irradiated with visible light.

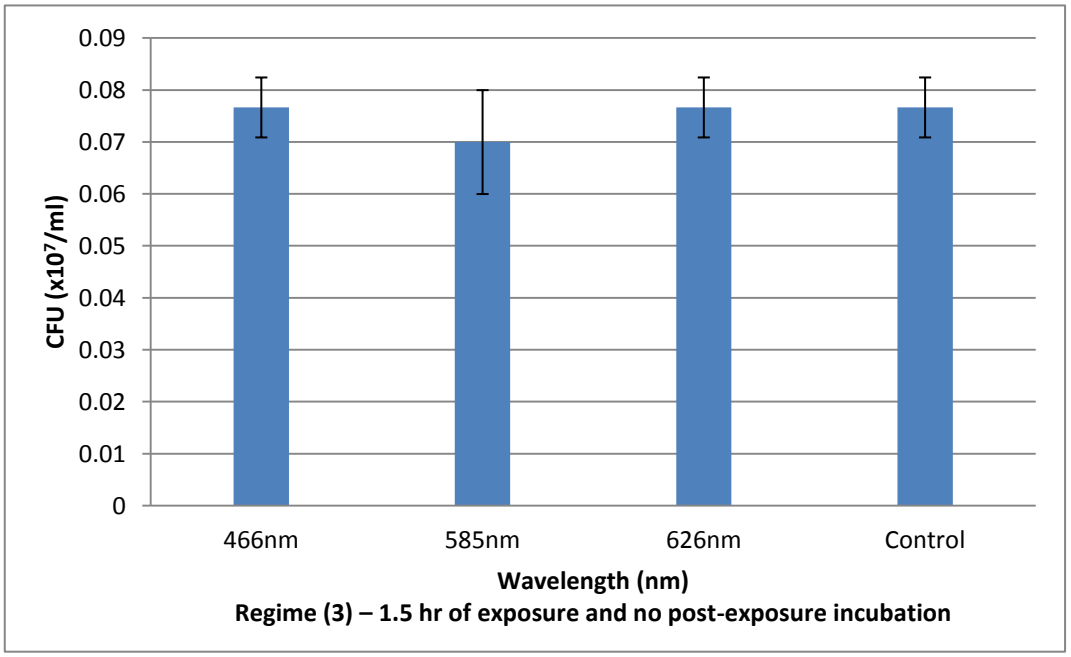

Figure 5.1.20 CFU for *S. aureus* 344 (Ampicillin resistant strain) irradiated with visible light

Exposure regime (4) – 1.5 hr of exposure followed by 1.5 hr of post-exposure incubation

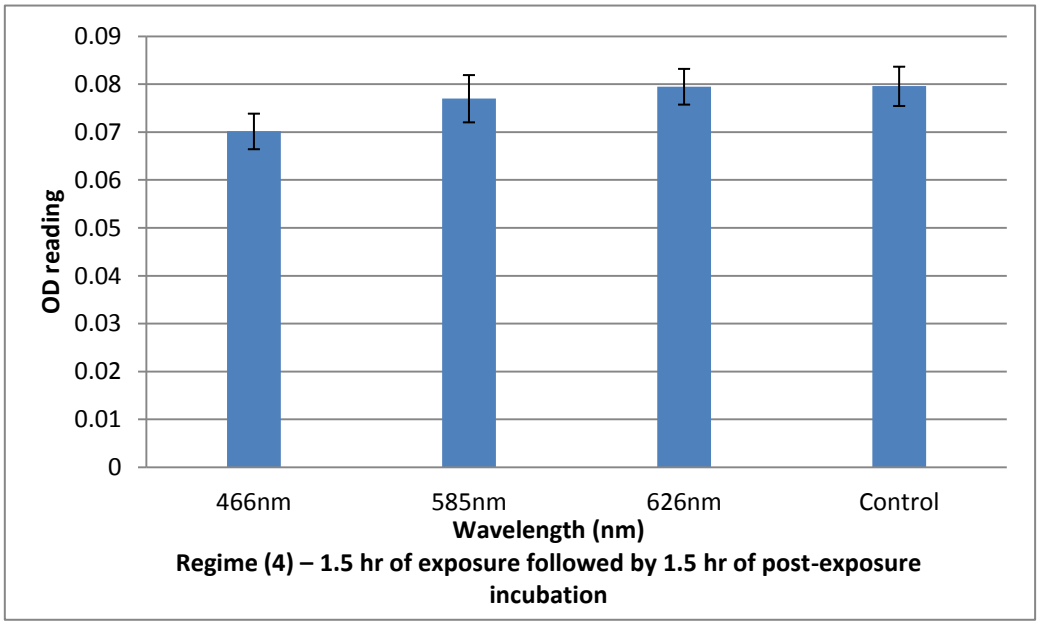

Figure 5.1.21 OD reading for *S. aureus* ATCC 25923 irradiated with visible light.

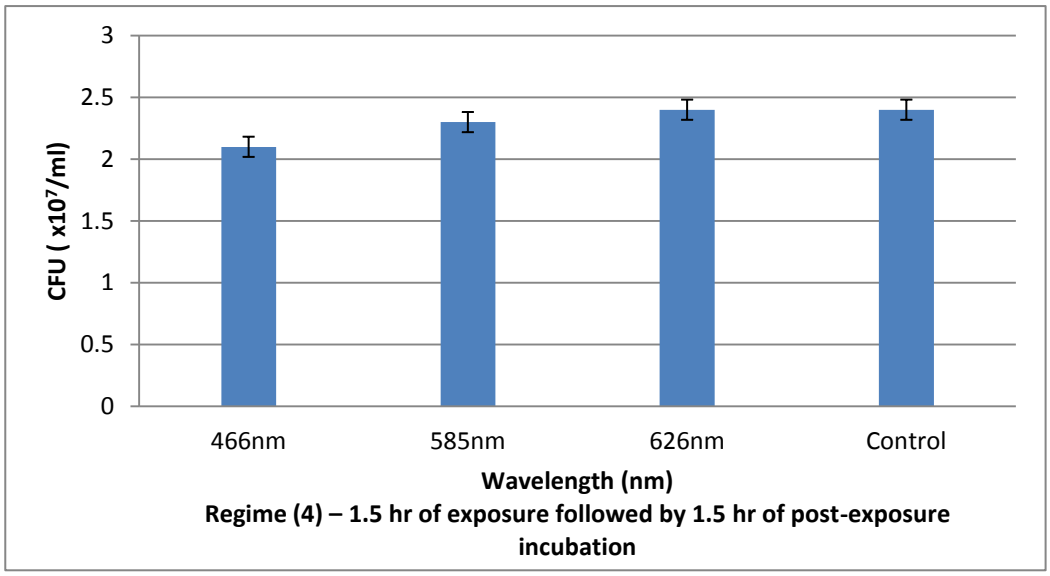

Figure 5.1.22 CFU for *S. aureus* ATCC 25923 irradiated with visible light

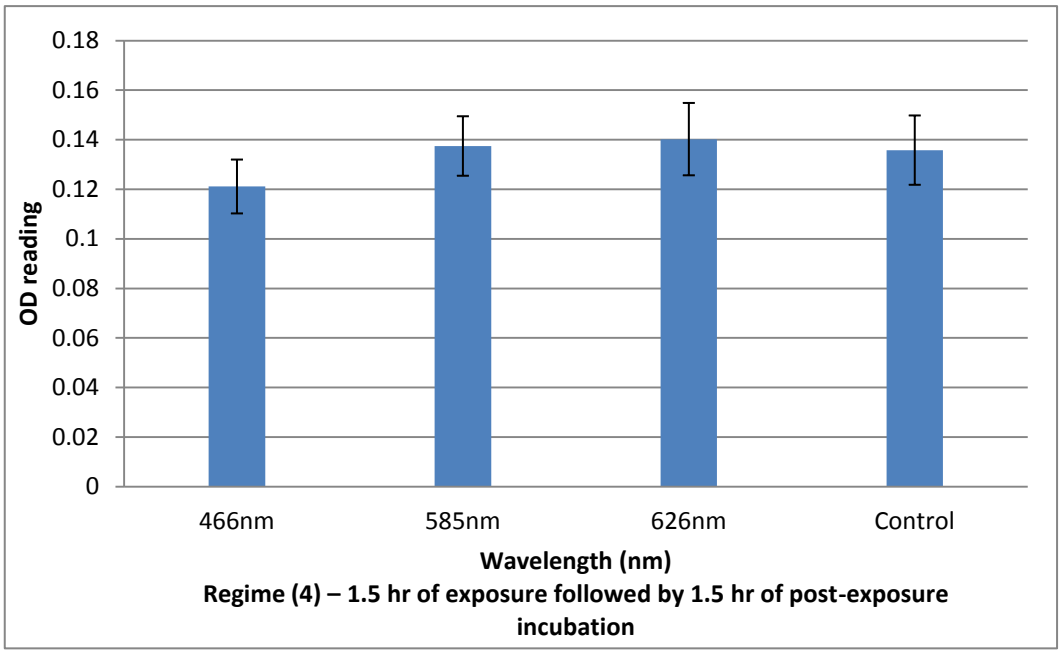

Figure 5.1.23 OD reading for *S. aureus* 344 (Ampicillin resistant strain) irradiated with visible light.

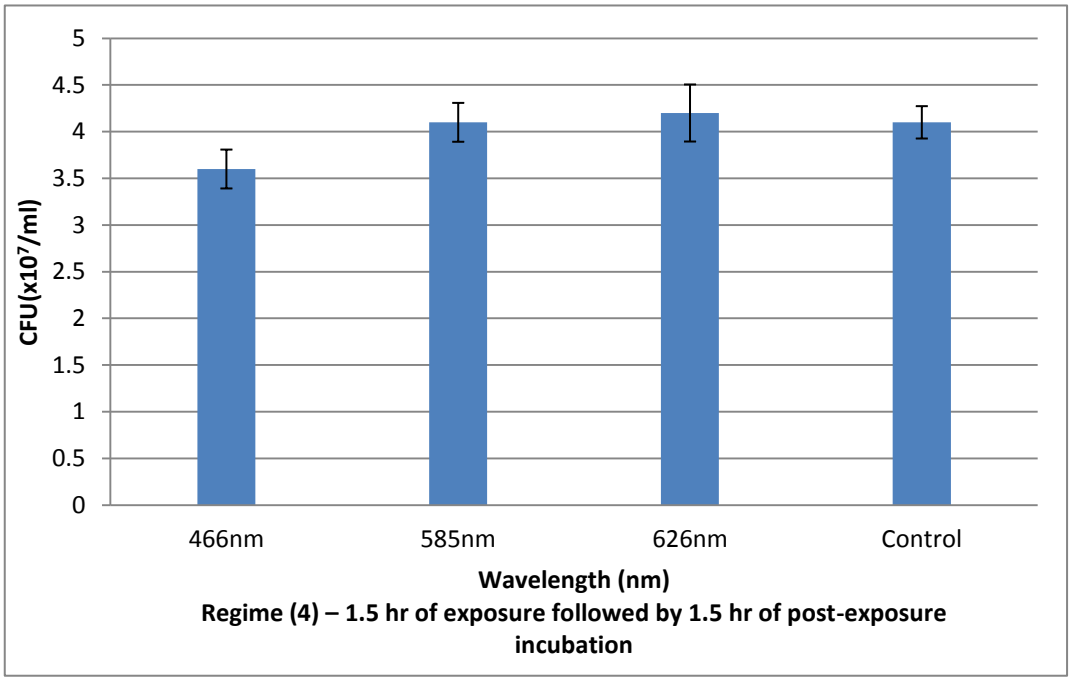

Figure 5.1.24 CFU for *S. aureus* 344 (Ampicillin resistant strain) irradiated with visible light

Exposure regime (5) – 2 hr of exposure and no post-exposure incubation

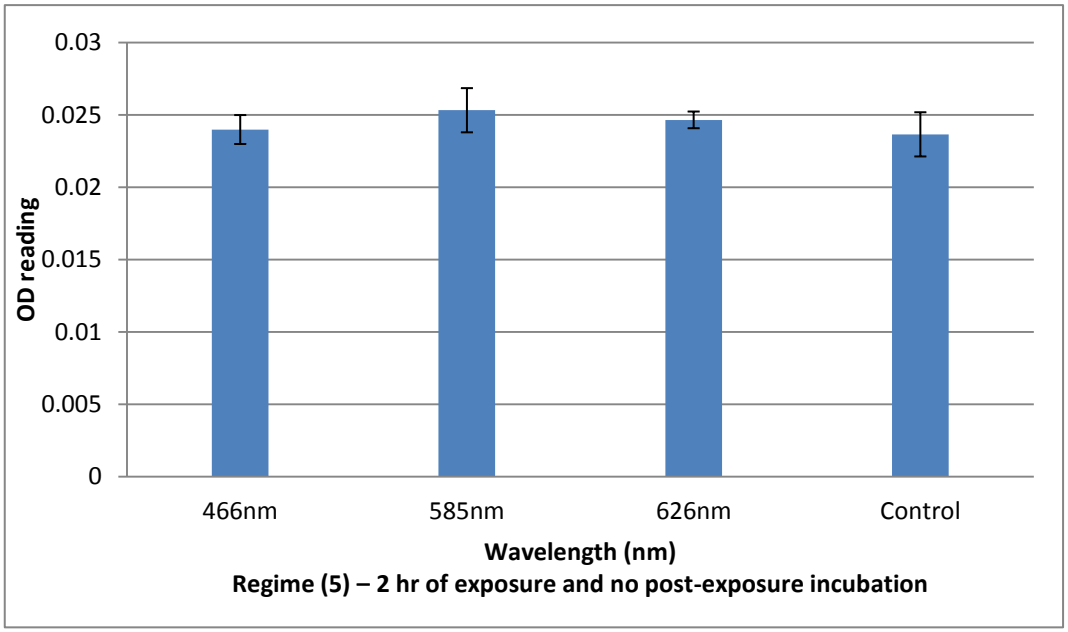

Figure 5.1.25 OD reading for *E. coli* ATCC 25922 irradiated with visible light

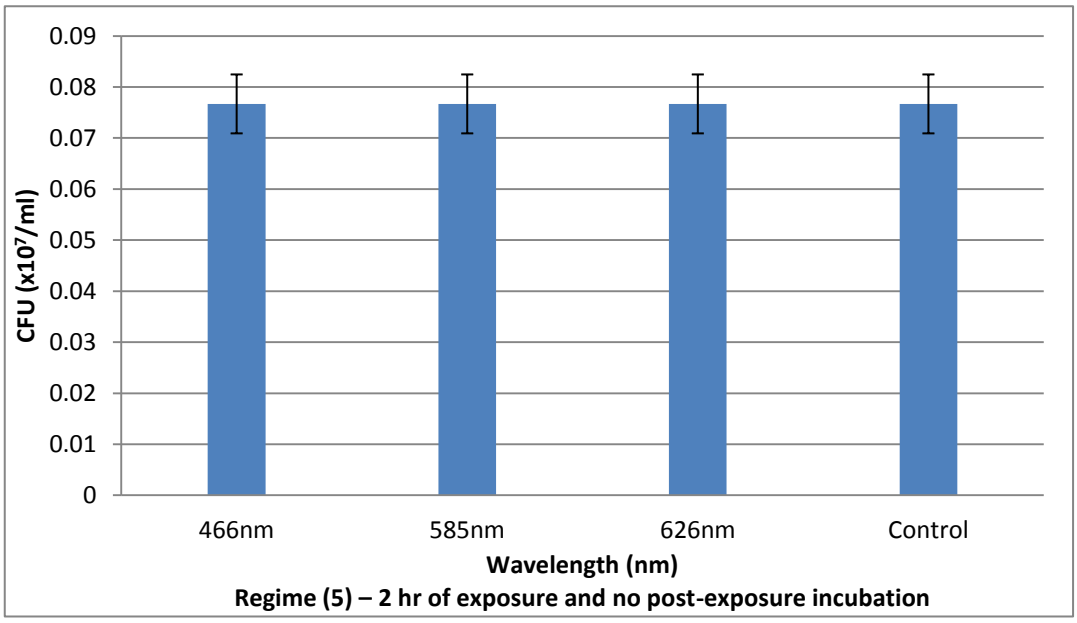

Figure 5.1.26 CFU for *E. coli* ATCC 25922 irradiated with visible light

Exposure regime (6) – 2 hr of exposure followed by 1.5 hr of post-exposure incubation

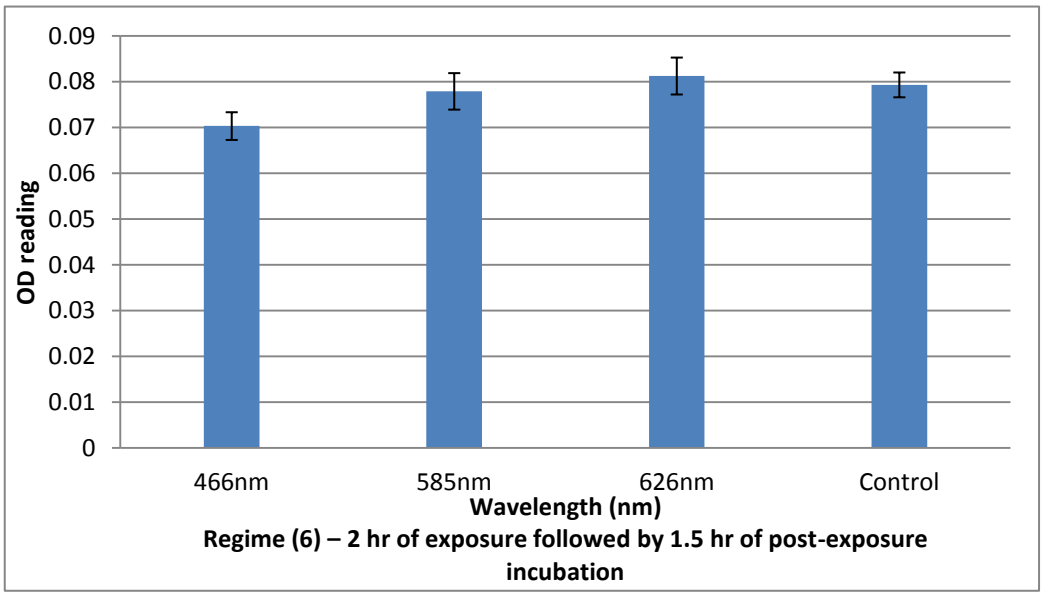

Figure 5.1.27 OD reading for *E. coli* ATCC 25922 irradiated with visible light

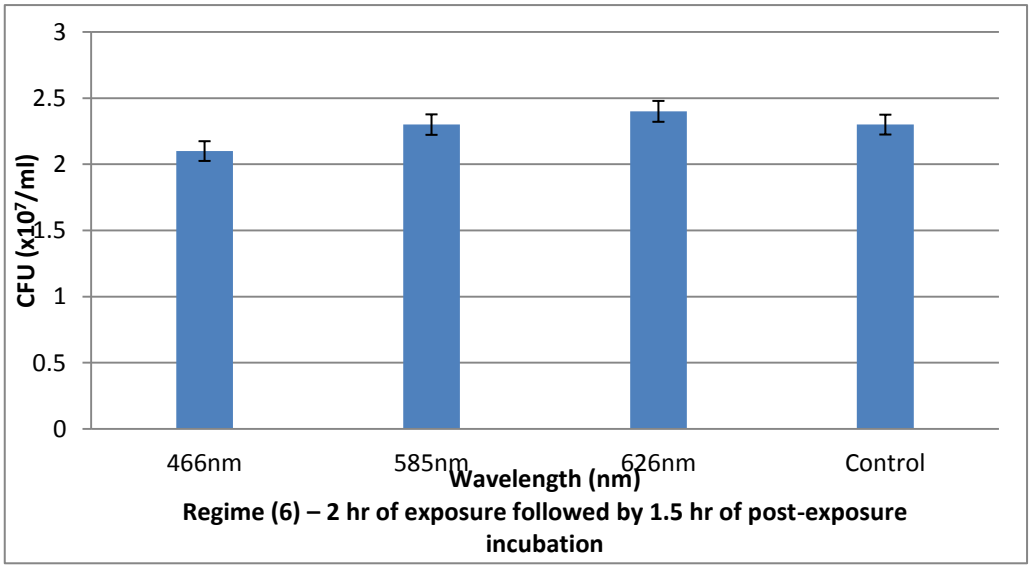

Figure 5.1.28 CFU for *E.coli* ATCC 25922 irradiated with visible light.

Discussion

The obtained results show that the exposures of Gram-positive bacteria *S. aureus* ATCC 25923 and *S. aureus* 344 (ampicillin resistant strain) to blue light LED (466nm) produce inhibitory effects on their population growth that in turn leads to an inactivation of pathogens present. From Figure 5.1.21 to Figure 5.1.24, it can be observed that both Gram-positive bacteria *S. aureus* ATCC 25923 and *S. aureus* 344 (ampicillin resistant strain) irradiated for 1.5 hr and subjected to post-exposure incubated for 1.5 hrs at 37^0C, ware affected the most (compared to the non irradiated control) by blue light exposures at 466nm. There is significant difference in OD reading/CFU data (Figures 5.1.21-5.1.24) between the control group and irradiated samples ($p=6 \times 10^{-6} <0.01$) exposed at the wavelengths of 466nm. The same result was observed with Gram-negative bacteria *E.coli* ATCC25922 irradiated by blue light (466nm). As seen from Figure 5.1.27 to Figure 5.1.28, there is a significant difference ($p=5x10^{-7}<0.01$) in OD reading/CFU data between the control groups and bacterial cultures irradiated by blue light LED (466nm) for 2 hours and post-exposure incubated for another 1.5hrs at 37°C. Clearly, at the appropriate exposure duration, this exposure reduces the bacterial growth. These findings are in accordance with the published research [287,288].

On the other hand, it can be also seen in (Figures 5.1.21-5.1.24 and Figure 5.1.27 to Figure 5.1.28) that there is no significant difference between samples irradiated by light exposures at 585 nm (yellow light) and 626nm (red light) and control groups.

Thus, it can be concluded that only light at wavelength 466nm induced changes on *S. aureus* ATCC 25923 and *S. aureus* 344 (ampicillin resistant strain) and suppress their growth.

The experimental results also showed (from Figure 5.1.5 to Figure 5.1.16) that there are no significant effects induced by light exposures on Gram-positive bacterium *S. aureus* ATCC 25923, *S. aureus* 344 (ampicillin resistant strain) and Gram-negative bacterium *E. coli* ATCC 25922 , which were irradiated for 30 minutes. Clearly, the results demonstrate no significant difference between irradiated bacteria and control groups (Figures 5.1.5-5.1.16 respectively). Similar results were obtained for Gram-negative bacteria *Ecoli.* The findings reveal that there is no significant difference in *Ecoli* bacteria growth between the irradiated samples and the non irradiated control (Figures 5.1.9-5.1.10, 5.1.15-5.1.16 and 5.1.25-5.1.26).

In summary, the experimental results of visible light exposures on the studied bacterial cultures revealed the following:

- Light exposures by **regime (1)** – *30 min of exposure with no post-exposure incubation,* **regime (3)** – *1.5 hr of exposure with no post-exposure incubation,* and **regime (5)** – *2 hr of exposure and no post-exposure incubation* (Figures 5.1.5-5.1.10, 5.1.17-5.1.20 and 5.1.25-5.1.26) induce no changes on the growth rate of Gram-positive and Gram-negative bacteria irradiated for 30 min, 1.5hr and 2hr with no post-exposure incubation respectively.

- Light exposure with **regime (2)** - *30 min of exposure followed by 1.5 hr of post-exposure incubation* (Figures 5.1.11-5.1.16) produced no significant effects on the studied bacteria. There is no statistically significant change between the irradiated bacterial cultures and control groups. However, by comparing the results of exposures of **regimes (1), (3) and (5)** and **regime (2)**, we can observe that all values of OD reading and CFU are higher for regime (2) than for regimes (1), (3) and (5). This is interesting, as it shows that 1.5 hr of post-exposure incubation affects slightly the bacterial growth.
- The results of visible light exposures with **regime (4)** – *1.5hr of exposure followed by 1.5 hr of post-exposure incubation* and **regime (6)** – *2 hr of exposure followed by 1.5 hr of post-exposure incubation* (Figures 5.1.21-5.1.24 and 5.1.27-5.1.28) showed the significant inactivation/change in bacterial growth rate between the Gram-positive and Gram-negative bacteria irradiated by blue light (wavelength 466nm) and control samples.
- The results also revealed that inactivation of Gram-positive bacteria S. aureus ATCC25923 and S. aureus 344 (ampicillin resistant strain) appeared to occur at a faster rate, within 30-60 min of experimentation compared to 60-90 min for the Gram-negative bacterium *E.coli*. Thus, Gram-positive bacteria are shown to be more responsive to visible light treatment than Gram-negative bacteria. This finding is similar to the results reported in other research studies [227,289].

5.1.3 Infrared Light Irradiation of Selected Gram-positive and Gram-negative Bacteria

In this experimental sub-study, the anti-microbial effects of infrared (IR) light irradiation were evaluated on *S. aureus* ATCC 25923 and *E. coli* ATCC 25922 bacteria. Four different regimes of exposures were tested. The effects of different far IR wavelengths were examined.

The following exposure regimes were applied:

(1) – 30 min of exposure and no post-exposure incubation

(2) – 30 min of exposure followed by 1.5 hr of post-exposure incubation

(3) – 1.5 hr of exposure and no post-exposure incubation

(4) – 1.5 hr of exposure followed by 1.5 hr of post-exposure incubation

IR LED irradiation experimental results

Cell viability assessment was performed on each type of bacteria in suspension, which were exposed to different wavelengths of far IR light radiation under the above stated conditions. In particular, effects of applied exposures at the wavelengths **3400nm, 3600nm, 3800nm, 3900nm, 4100nm, and 4300nm** were evaluated and expressed by optical density (OD reading) of bacteria in suspension (Figures 5.1.29-5.1.43) and live cell count (CFU) data is shown in (Figures 5.1.30-5.1.44).

Exposure regime (1) – 30 min of exposure with no post-exposure incubation

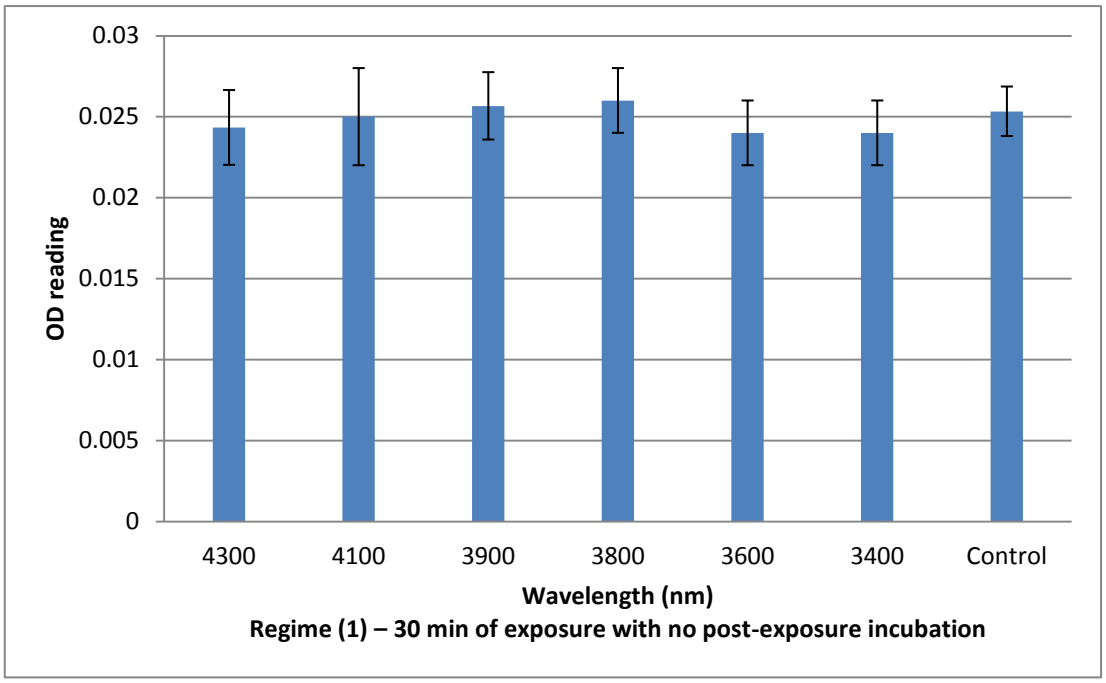

Figure 5.1.29 OD reading for *S. aureus* ATCC 25923

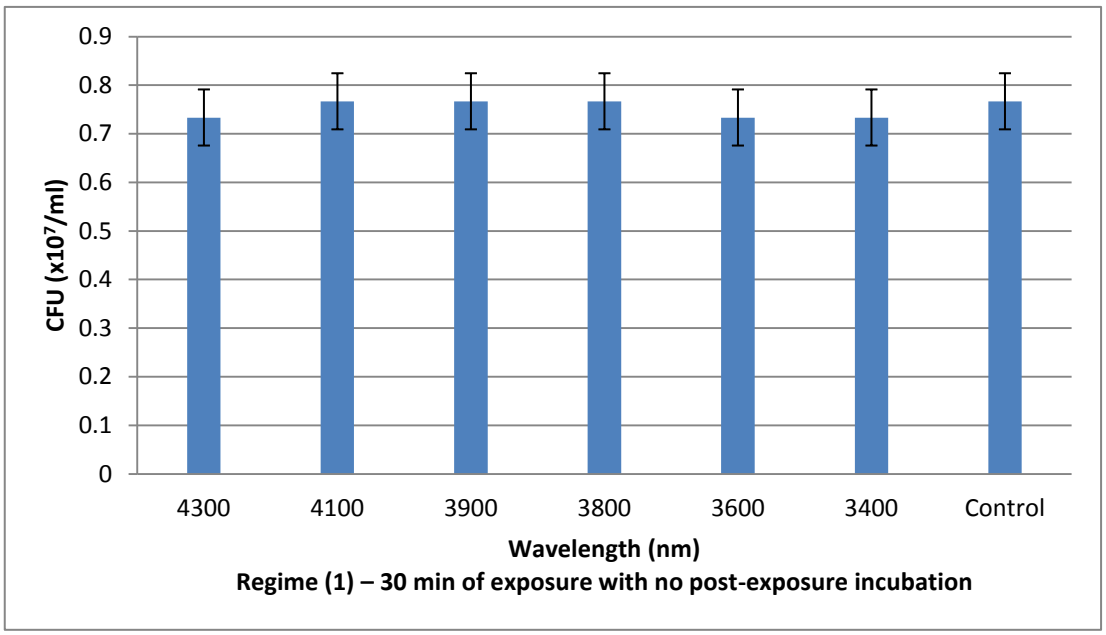

Figure 5.1.30 CFU for *S. aureus* ATCC 25923

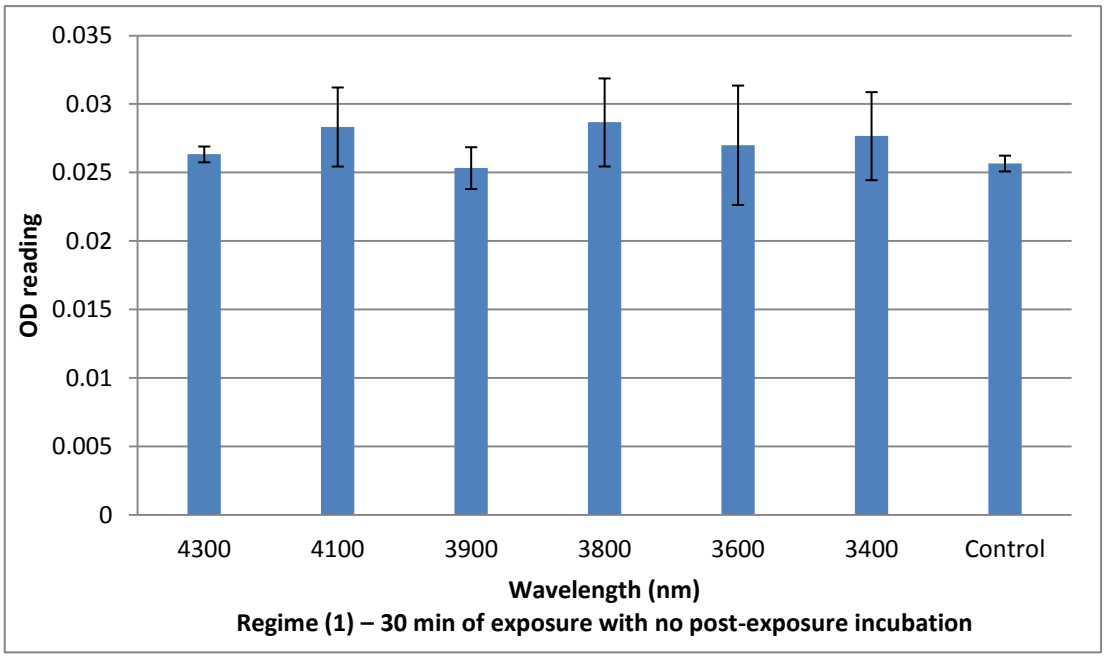

Figure 5.1.31 OD reading for *E. coli* ATCC 25922

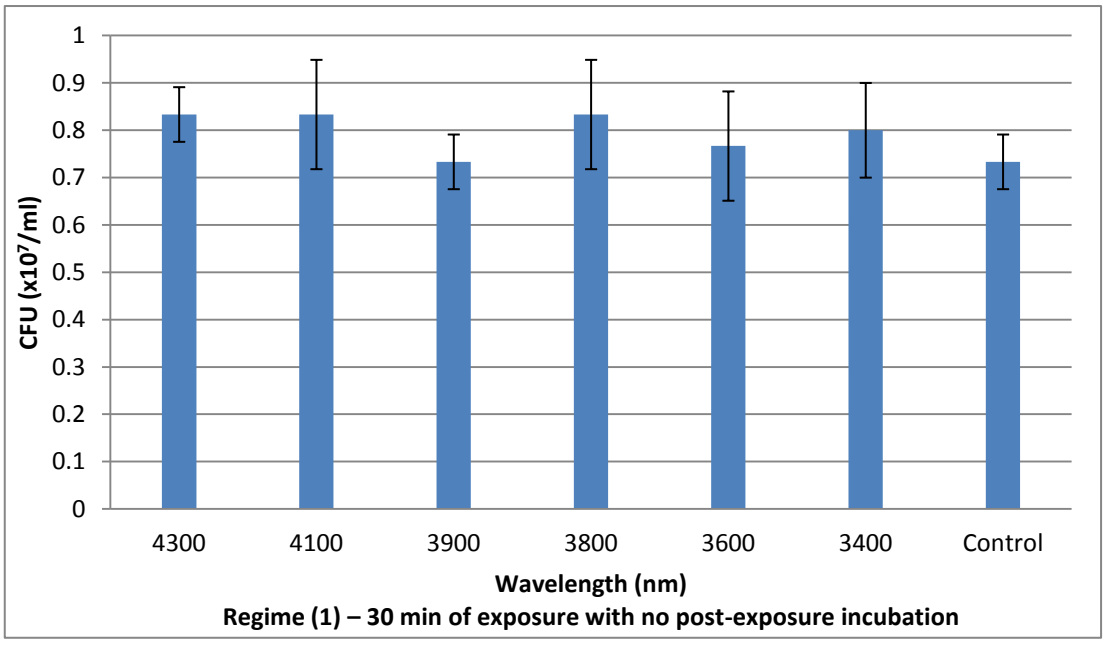

Figure 5.1.32 CFU for *E. coli* ATCC 25922

Exposure regime (2) – 30 min of exposure followed by 1.5 hr of post-exposure incubation

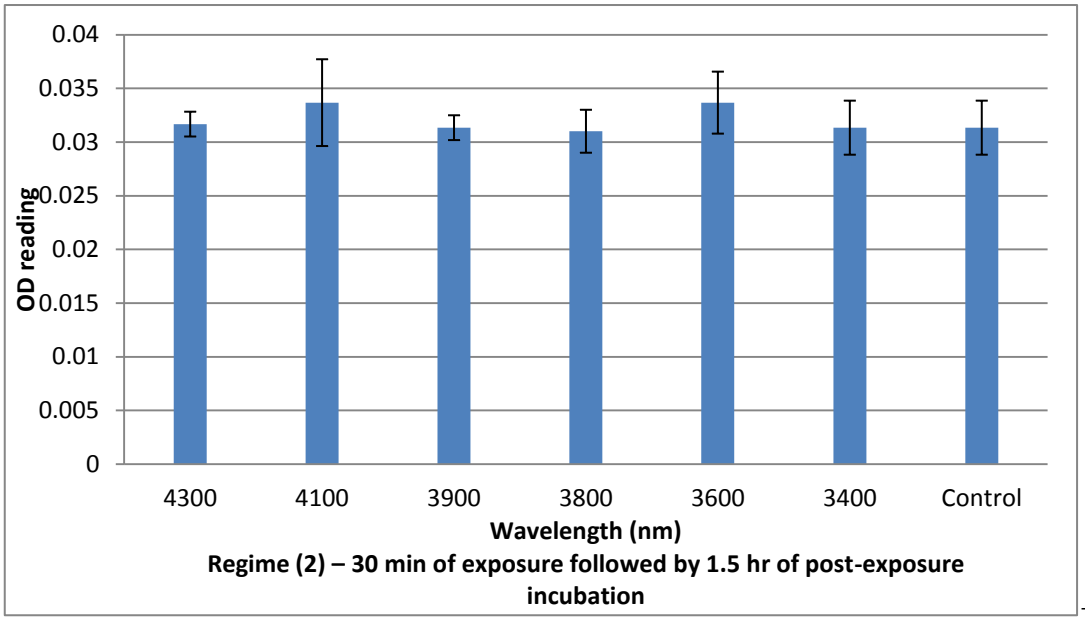

Figure 5.1.33 OD reading for *S. aureus* ATCC 25923

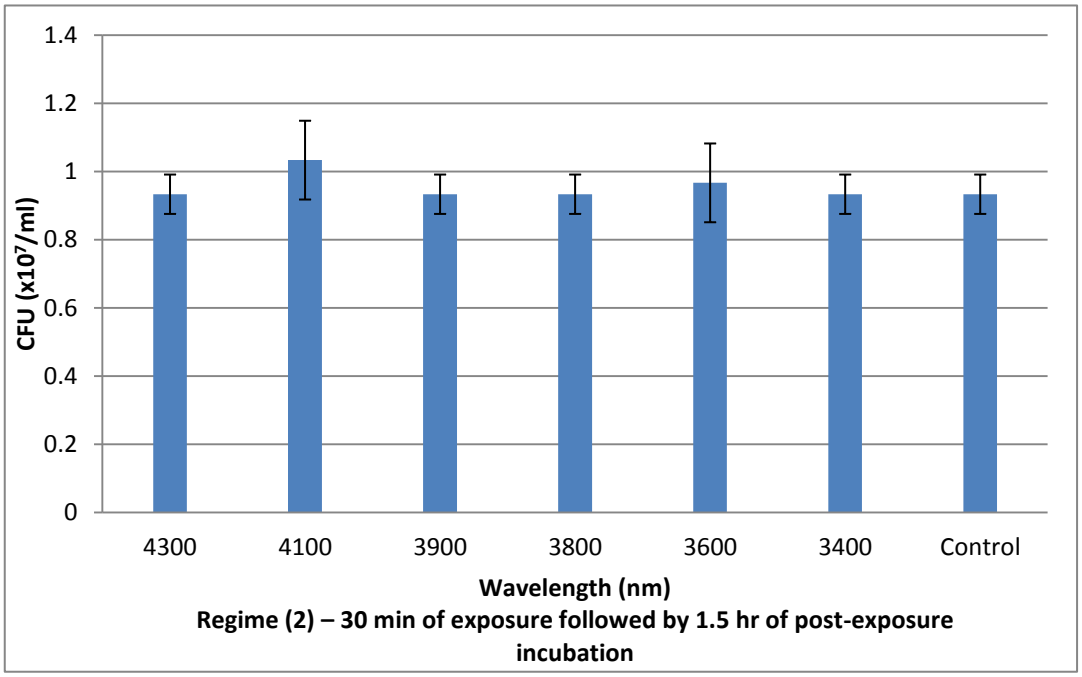

Figure 5.1.34 CFU for *S. aureus* ATCC 25923

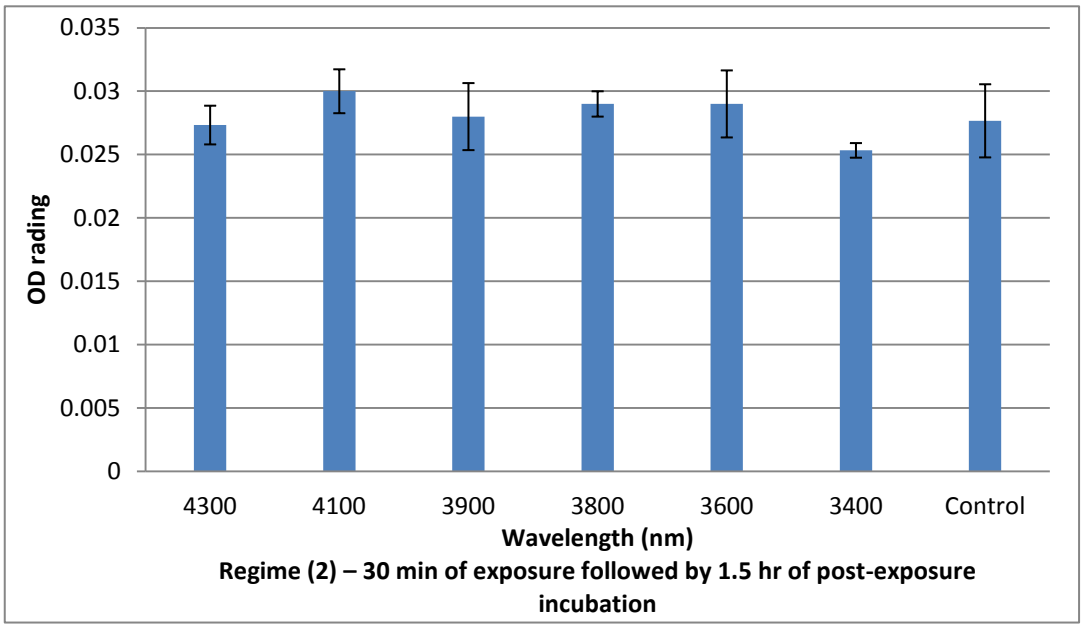

Figure 5.1.35 OD reading for *E. coli* ATCC 25922

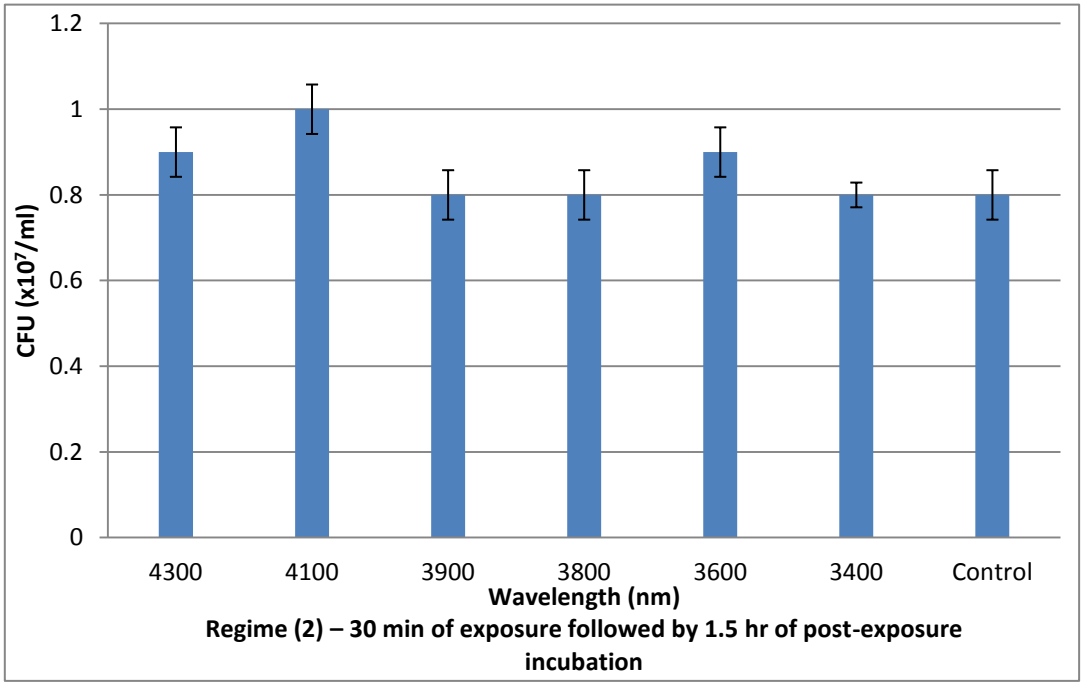

Figure 5.1.36 CFU for E. coli ATCC 25922

Exposure regime (3) – 1.5 hr of exposure and no post-exposure incubation

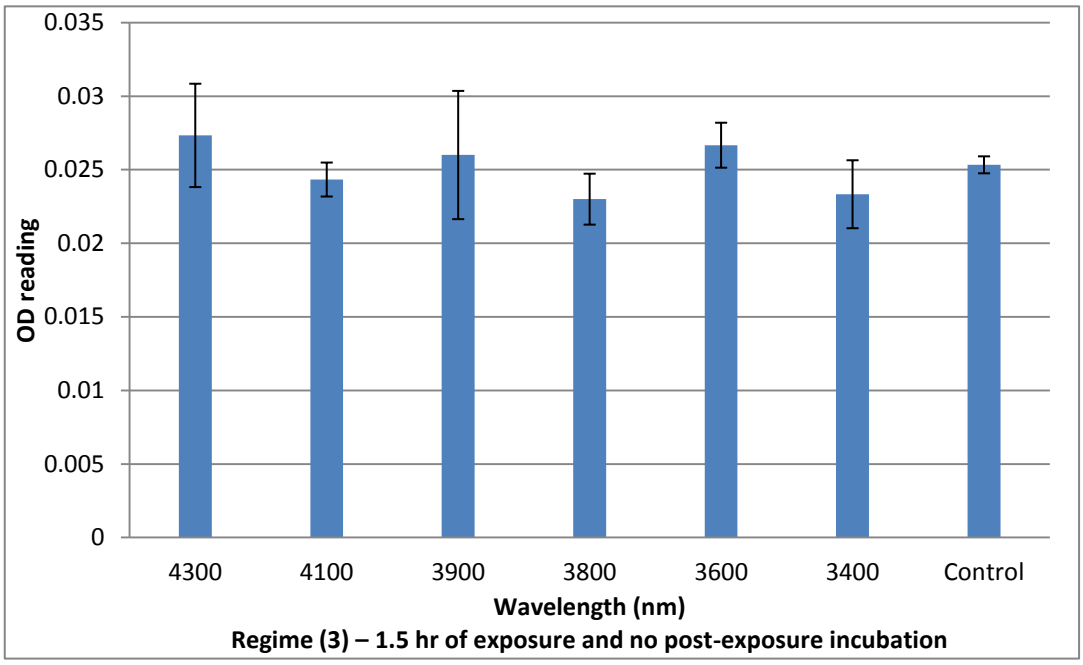

Figure 5.1.37 OD reading for *S. aureus* ATCC 25923

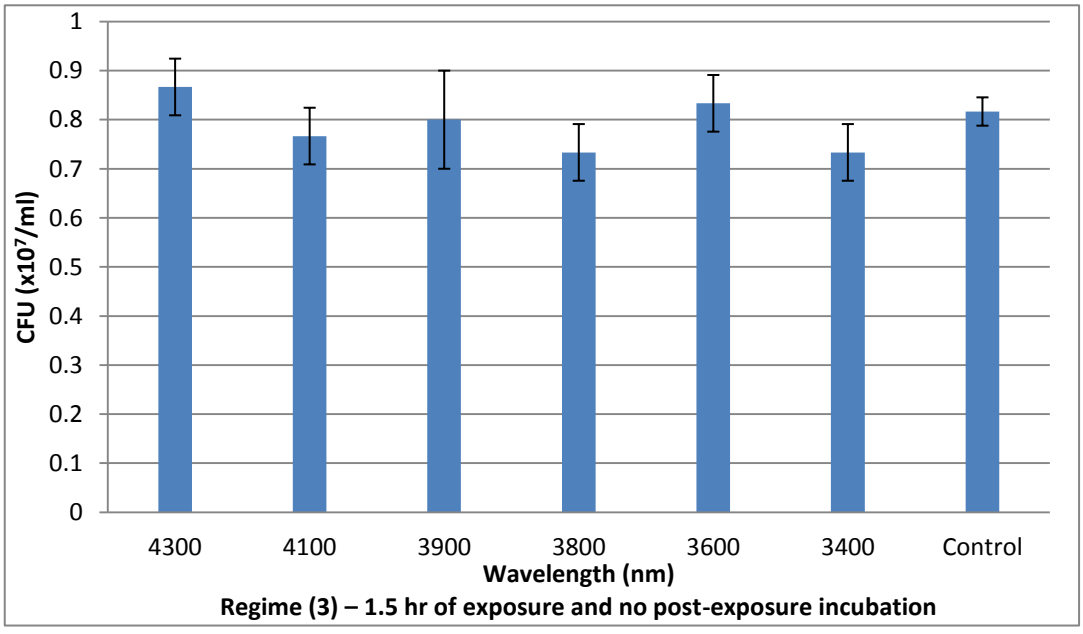

Figure 5.1.38 CFU for *S. aureus* ATCC 25923

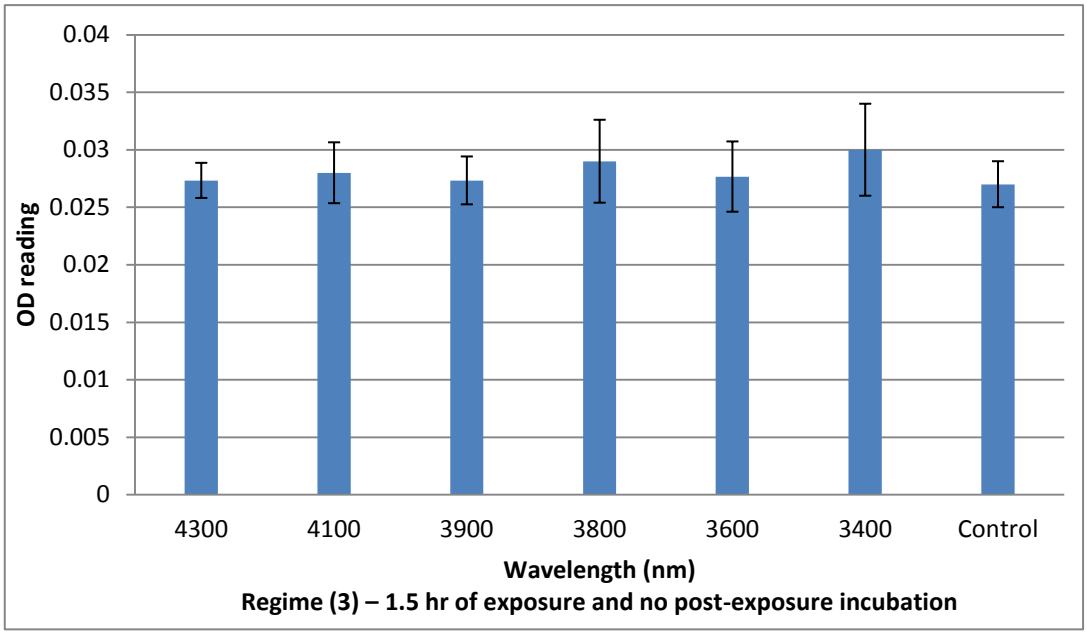

Figure 5.1.39 OD reading for *E. coli* ATCC 25922

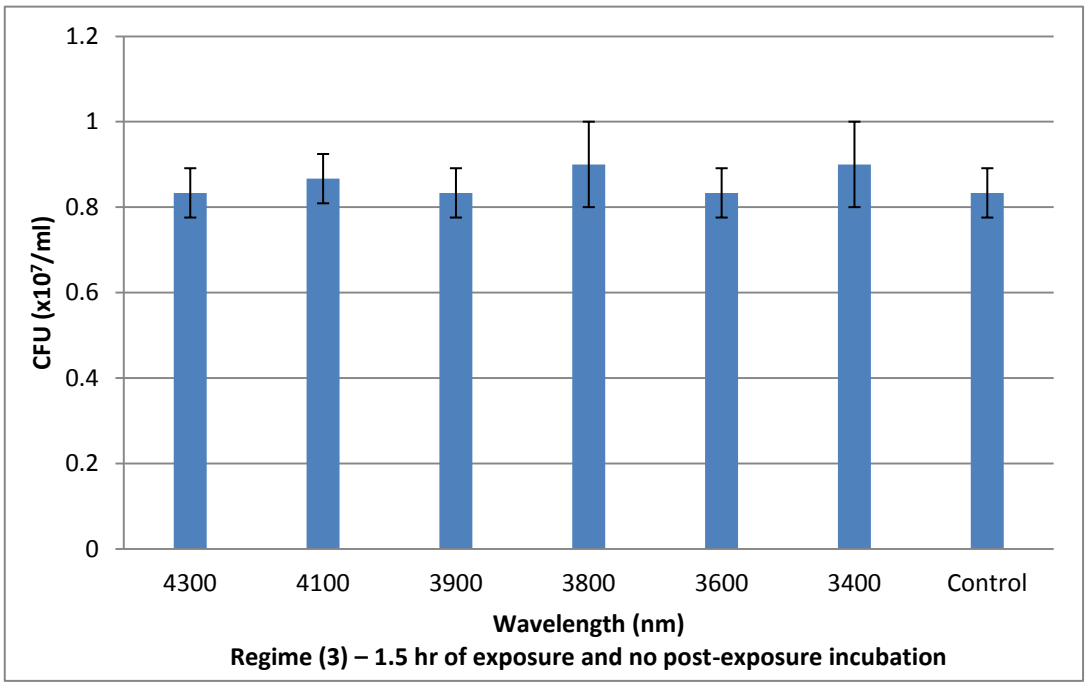

Figure 5.1.40 CFU for *E. coli* ATCC 25922

Exposure regime (4) – 1.5 hr of exposure followed by 1.5 hr of post-exposure incubation

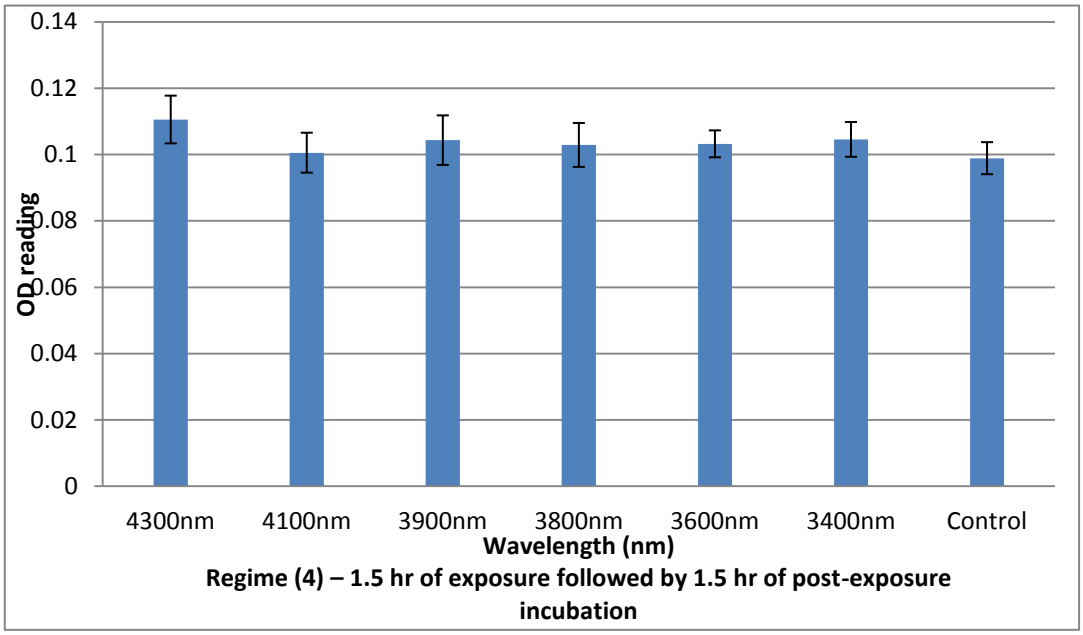

Figure 5.1.41 OD reading for *S. aureus* ATCC 25923

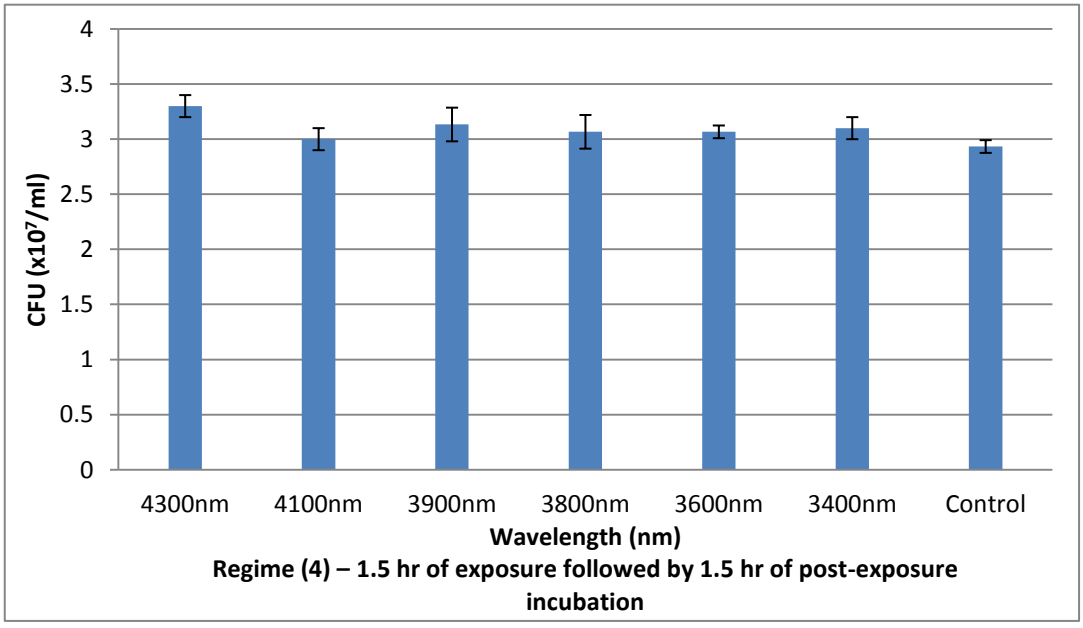

Figure 5.1.42 CFU for *S. aureus* ATCC 25923

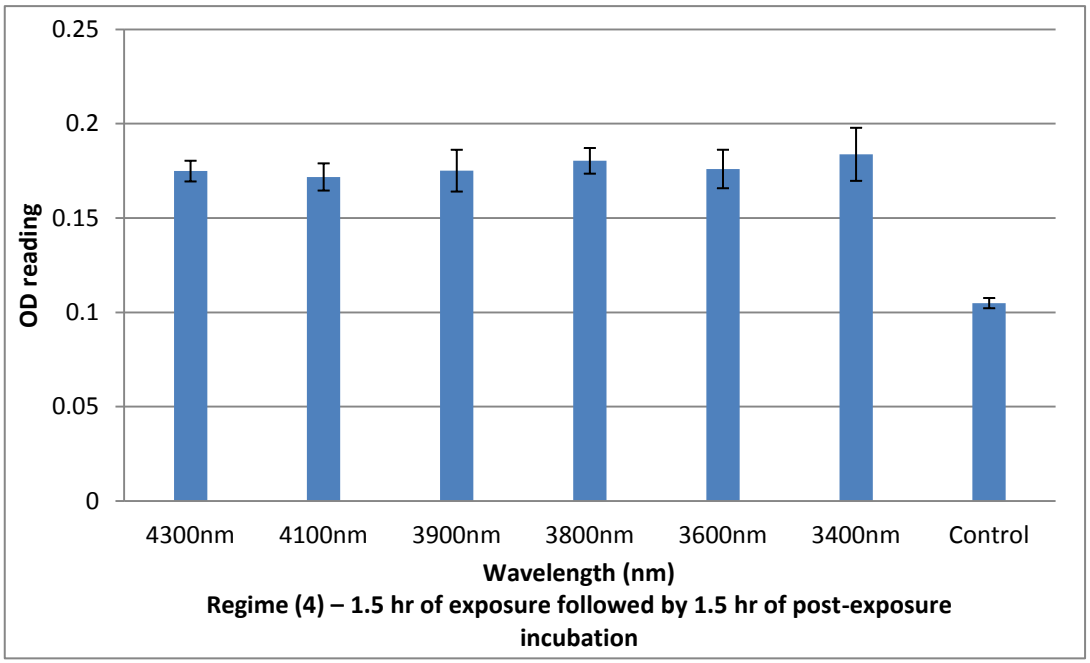

Figure 5.1.43 OD reading for *E. coli* ATCC 25922

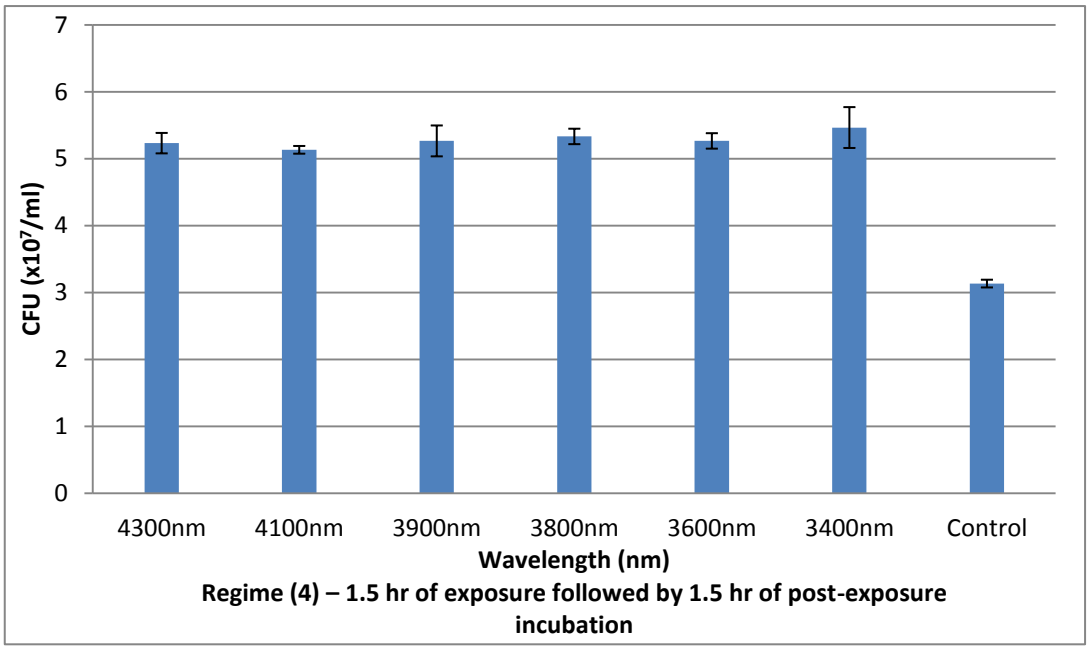

Figure 5.1.44 CFU for *E. coli* ATCC 25922

Discussion

The findings show that IR irradiation at the wavelength of 4300nm can accelerate *S. aureus* ATCC 25923 bacteria proliferation (Figure 5.1.41 and Figure 5.1.42). IR light at 4300 nm induces the changes in the bacterial growth, when these bacteria are irradiated for 1.5 hrs and post-exposure incubated for 1.5 hr. There is a significant difference in OD reading and CFU values between the irradiated bacteria and control group ($p<0.01$). There is no significant difference between bacteria exposed at all other far IR light wavelengths and control samples. The results also reveal that IR light exposures, in general, promote *E. coli* bacterial growth.

The findings are summarized below:

- For *S. aureus* ATCC 25923, findings obtained for **Regime (1)** – *30 min of exposure with no post-exposure incubation* and **regime (3)** – *1.5hr of exposure with no post-exposure incubation* (Figures 5.1.29-5.1.30 and Figures 5.1.37-5.1.38) showed that there are no significant changes in the bacterial growth rate when compared to the control groups. However, irradiation by **regime (1)** - *30 min of exposure and no post-exposure incubation* **–** slightly increases the bacterial growth of *E. coli* at the wavelengths 3400nm, 3800nm and 4100nm (Figures 5.1.31-5.1.32).

- The results for irradiation of *S. aureus* ATCC 25923 **by Regime (2)** - *30 min of exposure followed by 1.5 hr of post-exposure incubation* (Figure 5.1.33-5.1.34)

showed that there is no statistically significant change between the irradiated bacterial cultures and control groups. However, all values of OD reading and CFU induced by **regime (2)** exposures are slightly higher than the results obtained for **regime (1) and regime (3).** This is interesting, as the results suggest that 1.5 hr of post-exposure incubation is an important factor in promotion of bacterial growth.

- For Gram-negative *E. coli* bacteria, irradiation by **regime (2)** – *30 min of exposure followed by 1.5 hr of post-exposure incubation* – the results reveal the increase in bacterial growth by IR light at the wavelengths of 3600nm, 3800nm, 4100nm and 4300nm. Irradiation by **regime (3)** – 1.*5 hr of exposure and no post-exposure incubation* – increased bacterial growth by exposures at 3400nm and 3800nm.

- Irradiation of *S. aureus* ATCC 25923 by IR light in **regime (4)** – 1.*5 hr of exposure followed by 1.5 hr of post-exposure incubation* – induced a slight increase in bacterial growth at 4300nm (Figure 5.1.41-5.1.42).

- In contrast, irradiation of *E.coli* by regime (4) induced a very significant increase in bacterial growth. This significant proliferation rate is observed at all studied wavelengths of far IR light. There is a significant difference between all radiated bacterial cultures and control groups ($p<0.01$).

It is important to note, the results demonstrate that the Gram-negative bacterium *E.coli* appeared to be more susceptible to the applied IR exposures than the Gram-positive bacteria *S. aureus* ATCC25923 (Figures 5.1.41-5.1.42 and Figure 5.1.43-5.1.44). Trushin [290] And Tsai [291] reported that the irradiation with visible red and infrared light can accelerate the rate of division and growth of *E.coli*. Hence, the findings of this experimental evaluation are in agreement with the results of other studies.

5.2 Computational design of Azurocidin peptide analogue: a novel agent with anti-microbial activity

Antimicrobial peptides (AMPs) are small (6 to 100 amino acids) amphipathic molecules of variable length, sequence, and structure with bioactivity against a wide range of microorganisms including bacteria, protozoa, yeast, fungi, viruses and even tumor cells. AMPs represent a new family of antibiotics that have stimulated research and clinical interest as new therapeutic options for treatment of infections caused by multidrug-resistant bacteria. This sub-study was aimed at designing a novel short bioactive peptide analogue that can emulate the biological activity of a native antimicrobial Azurocidin protein. The antimicrobial activity of the *de novo* designed Azurocidin peptide analogue was then evaluated *in vitro* on the selected Gram-positive and Gram-negative bacteria. Hence, this sub-study has two arms: computational and experimental *in vitro*.

5.2.1 Computational analysis of Azurocidin proteins using the RRM approach

The concepts of the RRM approach were presented in great details in Chapter 4 of this thesis. Azu-RRM peptide analogue was designed using the following strategy for the defined peptide design:

1) The RRM characteristic frequency is determined from the multiple cross-spectral functions for a group of protein sequences that share a common biological function.

2) The phases are calculated for the characteristic frequency or frequencies of a

particular protein, which is selected as a parent for an agonist/antagonist.

3) The minimal length of the designed peptide is defined by the appropriate frequency resolution. An Inverse Fourier Transformation (IFT) is used to calculate a numerical sequence of different lengths, which exhibits the same prominent characteristic frequency as a parent protein.

4) To determine the amino acids that correspond to each element of the new numerical sequence defined above, the tabulated Electron Ion Interaction Potential (EIIP) parameter values are used. The resulting new amino acid sequence represents the anticipated designed peptide. The de novo designed peptide has no homology to the original protein sequence but is expected to exhibit the same biological function as an original/parent protein.

Peptide design procedure (graphical presentation)

Peptide/frequency	f1	f2	φ1	φ2
A	*	*	-	-
B	*		-	
C		*		-
D	*	*	+	+
E	*		+	
F		*		+

According to the RRM design procedure (shown above), on the basis of two frequencies and two phases determined within the computational analysis, it is possible to design six different peptide analogues for one parent protein.

To utilize the RRM to design a novel bioactive peptide analogue, eight Azurocidin protein sequences were collected from the National Center for Biotechnology Information (NCBI) protein database (http://www.ncbi.nlm.nih.gov/protein). The RRM was used to compute the RRM characteristic frequency of the collected Azurocidin protein sequences.

A multiple cross-spectral analysis was performed resulting in two prominent RRM characteristic frequencies identified at **f_1=0.1133** (prominent peak) and **f_2=0.0293** (less significant peak) shown in Figure 5.2.1. These frequencies are related to the biological activity of the analysed native Azu peptides. According to the RRM concepts, the prominent peak(s) characterizes the common biological activity of the analyzed Azu peptides. Less prominent peaks observed in Fig 5.2.1. indicate that these selected Azu peptides can be involved in a different biological process (interact with other proteins or small molecules).

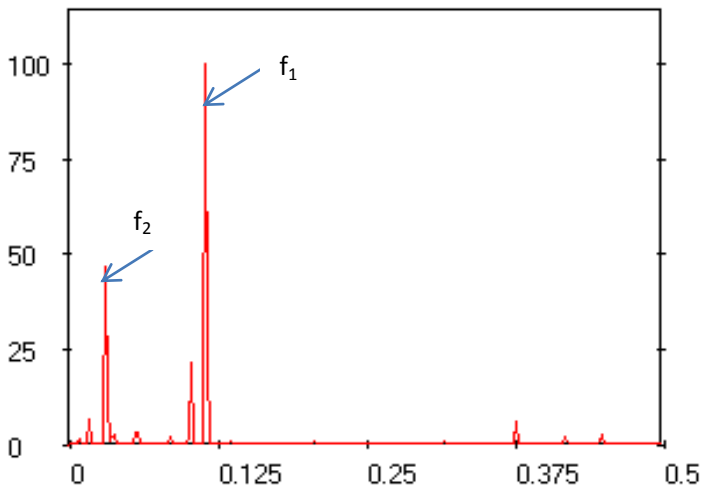

Figure 5.2.1. Multiple cross-spectral function of eight Azurocidin protein sequences. The abscissa represents RRM frequencies, and the ordinate - relative signal intensities.

When the common RRM was determined for all eight Azurocidin sequences, we then selected the particular sequence Azurocidin (179302 gb AAB59353.1 Homo sapiens) as a parent protein to design the synthetic peptide analogue that can mimic its anti-microbial activity.

Selected original native Azurocidin amino acid sequence

MTRLTVLALLAGLLASSRAGSSPLLDIVGGRKARPRQFPFLASIQNQGRH
FCGGALIHARFVMTAASCFQSQNPGVSTVVLGAYDLRRRERQSRQTFSI
SMSENGYDPQQNLNDLMLLQLDREANLTSSVTILPLPLQNATVEAGTRCQ
VAGWGSQRSGGRLSRFPRFVNVTVTPEDQCRPNNVCTGVLTRRGGICNGD
GGTPLVCEGLAHGVASFSLGPCGRGPDFFTRVALFRDWIDGVLNNPGPGPA

Then the phases were calculated at two frequencies **f_1=0.1133** (prominent peak) and **f_2=0.0293** (less significant peak). On the basis of the determined characteristic frequencies and phases **f_1=0.1133 and φ_1=-1.880;** and **f_2=0.0293** and **φ2=-1.624,** the short novel peptide analogue was designed, **Azu-RRM** (LPAQQQWAKAQRDDDRQWQCRDDTWAHHAWQWYPI).

ProtParam (http://au.expasy.org/tools/protparam.html) was used as a tool to compute physical and chemical parameters of the synthetic Azu-RRM peptide analogue. This computationally designed peptide (35 amino acids) is 4.4358 kDa; theoretical pI: 6.00; estimated half-life in mammalian reticulocytes: 5.5 h; and instability index: 16.84 which classifies the protein as stable. This peptide was further evaluated experimentally.

The control peptide **Azc-RRM** was also designed (**with no active frequency**)

Azc-RRM: (GKMDDRQHLEACDDRWPL)

Peptide length 18 amino acids, Molecular weight: 2283.4. The instability index (II) is computed to be 34.11. This classifies the protein as stable (used as control in experimental evaluation).

5.2.2 Evaluation of antimicrobial properties of the synthetic computationally designed Azurocidin peptide on growth of Gram-negative and Gram-positive bacteria

In this experimental study a number of experiments were conducted to evaluate dose- and time-response of the selected bacteria to synthetic peptides treatment. These experiments are described below, with the findings being presented and discussed.

5.2.2.1 Evaluation of antimicrobial activity of synthetic Azu-RRM and Azc-RRM analogues *vs.* native Azurocidin (Azu) against the Gram positve bacterium *Staphylococcus aureus* (ATCC25923)

The computationally designed peptides Azu-RRM (bioactive analogue) and Azc-RRM (control) were commercially synthesized to 95% purity by GL Biochem (China). The native human neutrophil Azurocidin (Azu) protein was purchased from Sigma-Aldrich Pty Ltd, Australia. The gram-positive bacterium *Staphylococcus aureus* ATCC 25923 was used here to assess the antimicrobial effects of the studied Azu-RRM, Azc-RRM peptide analogue and native Azu. Mueller-Hinton Agar (MHA) and Mueller-Hinton Broth (MHB) were obtained from ThermoFisher Scientific, Australia.

To assess the antimicrobial activity of Azu-RRM and the native Azu peptide, a well isolated *S. aureus* colony from a fresh MHA plate was inoculated into 2ml of MHB and incubated at 37^0 C overnight. Then, in order to attain the desired initial concentration of bacteria for the experiment, the initial concentration

for inoculation was adjusted to 0.5 McFarland's turbidity standard [293] while the density of the bacterial suspensions in following procedure were measured via optical density reading by Eppendorf BioPhotometer to determine an approximate concentration of bacteria which is used as a basis for the experiment starting inoculation.

To examine the antimicrobial activity of Azu-RRM, Azc-RRM and native Azu peptide at different concentrations, the assay was conducted in a 96-well microtitre-plate as explained below:

1. First, 100µl of MHB were added to each well from column 1 to column 12 in all rows of A, B, C, F, G, and H
2. Then, 100µl of Azu or Azu-RRM, Azc-RRM working solution with an initial dose of 0.6 µM for Azu, Azu-RRM, Azc-RRM were added to the first well in rows A, B and C. Serial dilutions of the peptides were then created in wells (2-10).
3. In the next step, all wells of rows F, G, and H were used for halving the concentration of the peptide in each consecutive well.
4. The extra 100µl solution in the last column well of rows F, G, and H was discarded.
5. 100µl of bacterial suspension was added to all wells in column 1 to 10.
6. Negative growth controls of sterile MHB (100µl) were added in all wells in column 11. And 100µl of bacterial suspensions were added to wells in column 12 as full positive growth controls.

7. The seeded plate was then incubated at 37 ℃ overnight.

The antimicrobial experiments were repeated three times. The growth of *S. aureus* ATCC 25923 was measured with the microplate reader Thermo Multiskan Ascent Reader. The software was set to automatically monitor and save the absorption coefficient at wavelength of 600nm. The average of the three times OD_{600} reading was taken for the data analysis.

The anti-microbial effects of the designed synthetic Azu-RRM peptide analogue and native Azurocidin (Azu) were evaluated against bacterial growth of *S. aureus* as shown in Figures 5.2.2, 5.2.3. Different concentrations of native and synthetic peptides have been used in order to find the optimal concentrations that can induce the maximum suppressing effects on bacterial growth. For Azu-RRM, Azc-RRM and Azu, we started from a concentration of $3x10^{-1}$ μM, then reduced it in half until it reached $5x10^{-6}$ μM.

The negative control is added all with MHB solution. The positive control is added all with bacterial suspensions (without the peptide).

Figure 5.2.2 demonstrates the effects of the native Azu protein on the bacterial growth of *S. aureus*. The results show that the anti-microbial activity of Azu is noticeably strong at the concentrations ranging from $3x10^{-1}$ μM to $5x10^{-3}$ μM when compared to the positive control ($p<0.01$). However, the anti-microbial effects of Azu are significantly reduced at the lower concentrations in a range of $2.5x10^{-3}$ μM - $5x10^{-6}$ μM.

As can be seen from Fig. 5.2.2, no significant effects are observed when compared to the positive control.

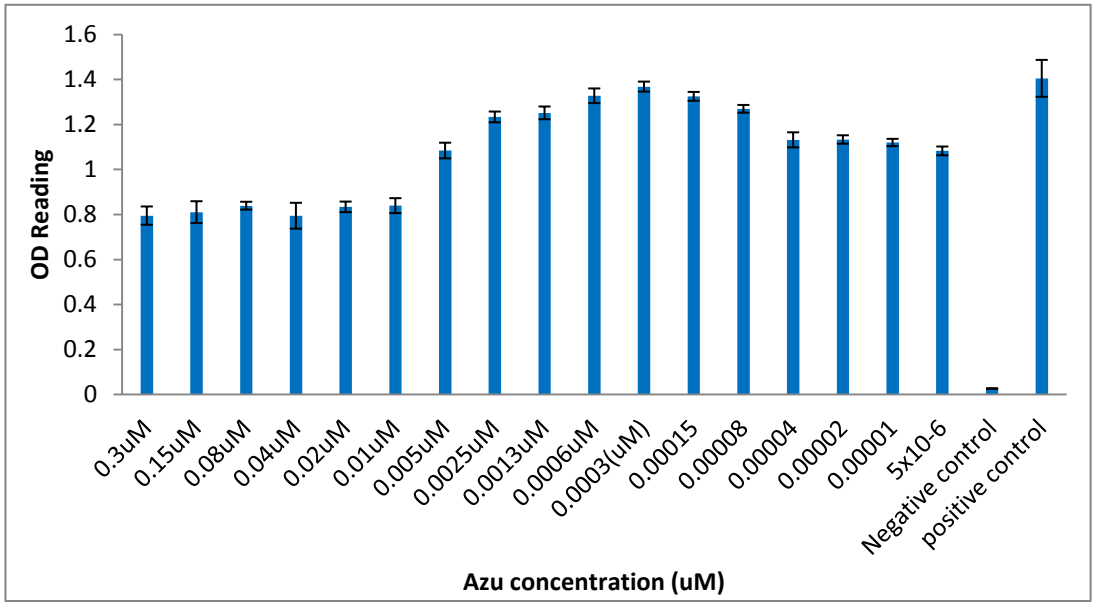

Figure 5.2.2. Effect of native Azurocidin on the growth of Gram-positive bacteria *S. aureus*.

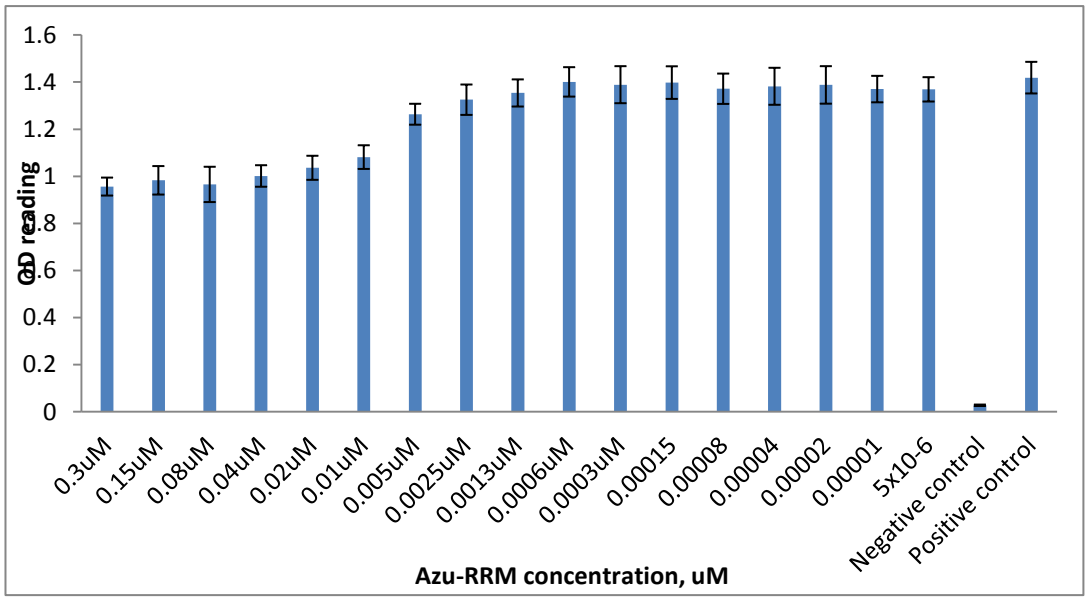

Figure 5.2.3. Effect of bioactive peptide analogue Azu-RRM on the bacterial growth of *S. aureus.*

Figure 5.2.3 demonstrates the effects of the synthetic peptide analogue Azu-RRM on the bacterial growth of *S. aureus*. As it can be observed from Figure 5.2.2, Azu-RRM at the concentrations range of 0.3 μM to $5x10^{-3}$ μM shows a significant anti-microbial activity against Gram-positive bacteria *S. aureus.* However, the anti-microbial effects of Azu-RRM are reduced at the lower concentrations: ranging from $5x10^{-3}$ μM to $5x10^{-6}$ μM, at which no significant effects can be seen, when compared to the positive control ($p<0.01$).

The experimental results reveal that the *in vitro* inhibitory effect of the synthetic Azu-RRM peptide analogue on *Staphylococcus aureus* is comparable to the inhibitory effect of the native Azurocidin against this pathogenic bacterium (Figure 5.2.4).

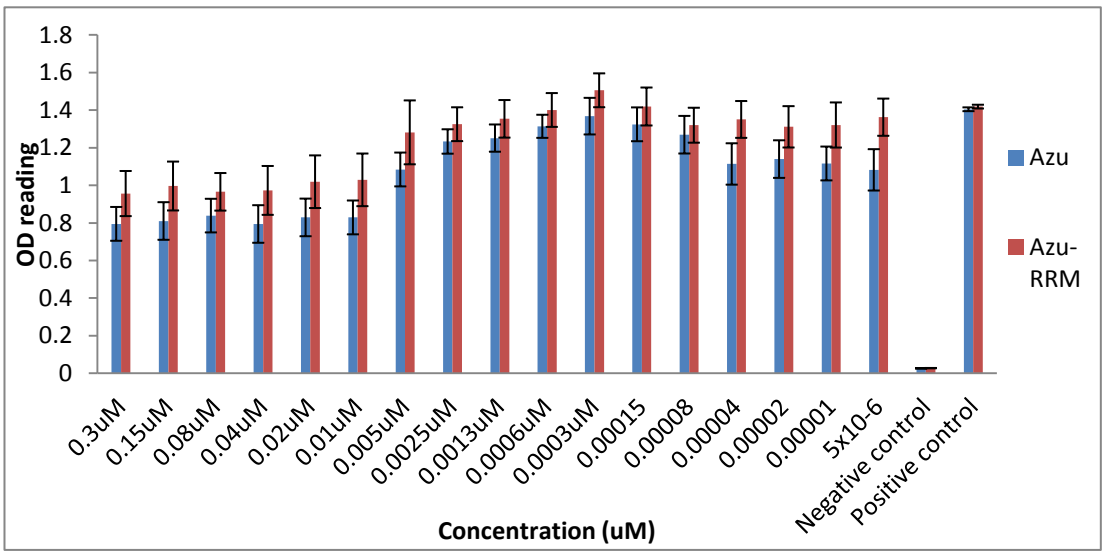

Figure 5.2.4. *Staphylococcus aureus* ATCC25923 treated with Azu-RRM and native Azu.

The findings show that dose-dependent activity of the synthetic Azu-RRM was comparable to that of the native Azurocidin. The designed Azu-RRM peptide analogue exhibited a potent activity against the bacteria. The peptide's treatments at the particular concentrations lead to the reduced bacterial growth.

The results showed that the survival level of bacterial cells treated by Azu-RRM and native Azu at the concentrations range of 0.3 μM - 0.005 μM was significantly lower ($p<0.05$) when compared to the positive control. The statistical analysis was performed using the Microsoft Office 2003 Excel and MATLAB software. The statistical significance of the differences between the Azu-RRM and native Azu treatments of bacteria and the positive control group were analysed by one-way ANOVA. These findings reveal that the computationally designed Azu-RRM exhibits the inhibitory activity (similarly to the native antimicrobial protein Azu) against pathogenic bacteria.

The results of experimental evaluation of anti-microbial activities of the synthetic Azu-RRM (bioactive), Azc-RRM (control) peptides and the native Azurocidin (Azu) against *S. aureus* (ATCC25923) are shown in Figure 5.2.5. The obtained results demonstrate that the designed native control peptide analogue Azc-RRM does not exhibited any potent activity against the studied bacteria.

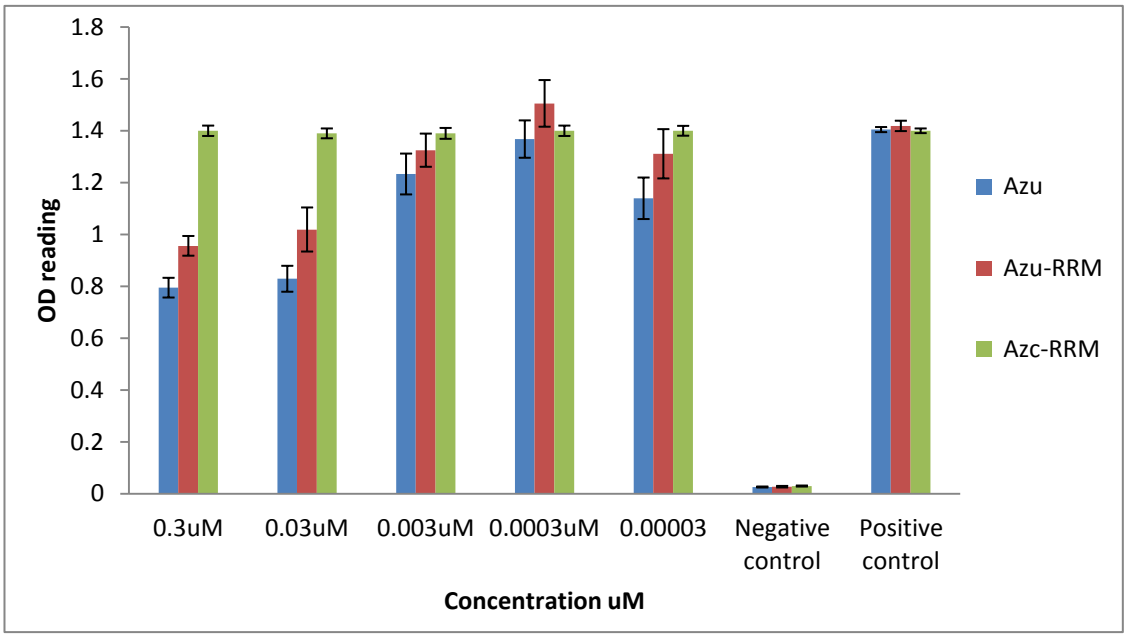

Figure 5.2.5. Comparison of the effects on *Staphylococcus aureus* ATCC25923 treated with Azu-RRM (bioactive), Azc-RRM (control) and native Azurocidin (Azu).

Final Remarks:

In this sub-study, the efficacy of the synthetic Azu-RRM peptide analogue was experimentally evaluated *in vitro* on the gram positive bacterium *S. aureus*, with its bioactivity being compared with the activity of the native Azu peptide. The results show that the anti-microbial effects, induced by Azu-RRM treatment on the bacterium *S. aureus*, are comparable to the effects of the native Azu in the concentrations range of 0.3 µM to 0.005 µM. It was previously reported by Watorek [29] that Azu induces significant anti-microbial effects (the most effective dosage) at concentrations range of 10^{-5}-10^{-6} M that corroborate our current experimental findings. The results obtained reveal that both, native and synthetic peptides, induce growth suppressing effects on *S. aureus*. Treatments at the particular concentrations

can significantly affect the bacterial growth. Moreover, the results showed that their activities against *S. aureus* are rather bacteriostatic than bactericidal.

5.2.2.2 Time- and dose-dependency of anti-microbial effects of synthetic Azu-RRM and Azc-RRM peptides: evaluation study on Gram-positive and Gram-negative bacteria

Materials

Gram-positive bacterial strains used in this sub-study were *S. aureus* ATCC 25923, and *S. aureus*344 (Ampicillin resistant strain). The Gram-negative bacterium, used in this study, was *E. coli* ATCC 25922. The bacterial isolates were obtained from the Microbiology Laboratory, School of Applied Sciences. The bacterial isolates were cultures in Mueller-Hinton Agar (MHA) and Mueller-Hinton Broth (MHB) (ThermoFisherScientific, Australia). The optical density (OD600) of bacterial suspensions in broth cultures was measured by Eppendorf OD600 reader (Biophotometer). Ascent software for Multiskan Ascent Reader for OD600 was from Thermo Electron Co. The *de novo* designed peptide Azu-RRM was commercially synthesized to 95% purity by GL Biochem, China.

Antimicrobial Assay

To assess the anti-microbial activities of the synthetic peptides Azu-RRM and Azc-RRM, well isolated colonies of *Staphylococcus aureus* ATCC25923; *Staphylococcus aureus* 344; and *E. coli* ATCC25922 from a fresh MHA plate were inoculated into 2ml of MHB (to ensure a proper viability), and incubated at 37^0C overnight.

In order to attain the desired initial concentration of bacteria for the experiments, the starting concentration for inoculation was adjusted to 0.5 McFarland's turbidity standard [293] while the density of the bacterial suspensions in following procedure were measured via optical density reading by Eppendorf BioPhotometer to determine an approximate concentration of bacteria which is used as a basis for the experiment starting inoculation.

To examine the antimicrobial activity of Azu-RRM (bioactive) and Azc-RRM (control) peptides at different concentrations and incubation times, the assay was conducted in a 96-well microlitre-plate as presented below:

1. Firstly, 100µl of MHB were added to each well from column 1 to column 12 in all rows of A, B, C, F, G, and H.
2. Then, 100µl of Azu-RRM working solution with an initial dose of 1000 µM was added to the first well in rows A, B and C. Serial dilutions of the peptides were then created in wells (2-10).
3. In the next steps, all wells of rows F, G, and H were used for halving the concentration of the peptide in each consecutive well. Then the extra 100µl solution in each well from the last column of rows F, G, and H were discarded. This was followed by adding 100µl of the bacterial suspension to all wells in column 1 to 10. Negative growth controls of sterile MHB (100µl) were added in all wells in column 11. And 100µl of bacterial suspensions were added to wells in column 12 as full

growth positive controls.

4. Then the seeded plates were incubated at 37 ℃ for 8 hours and overnight.

Antibiotics susceptibility testing

In order to measure the activity of Azu-RRM against the studied bacterium, Multiskan Ascent Reader for OD_{600} reading was carried out with Ascent software. The antimicrobial activity was assessed by measuring the optical density of the seeded plates, which were, as previously indicated, incubated at 37^0 C for 8 hours and overnight. The experiments were performed in triplicates with three repeats for each experiment. The average of the three times OD_{600} reading was taken for the data analysis.

Viable cell counts

The colony-forming unit (CFU) count is an estimate of viable bacterial numbers. Unlike direct optical density counts, where all bacterial cells, dead and living, are counted, CFU estimates viable cells only. This method is employed here to assess the effects induced by the synthetic peptide treatment on the selected Gram-negative and Gram-positive bacteria.

1. Firstly, 10ul samples of bacterial suspensions were collected from wells with 8h incubation, treated with Azu-RRM at the concentration of 2 uM and 4 uM, and positive control after OD_{600} reading. Secondly, the collected samples were diluted to final concentrations of 10^{-2}, 10^{-4}, 10^{-5}, 10^{-6}, and 10^{-7} uM.

2. Then, 100 ul from the last 3 dilutions (10^{-5}, 10^{-6}, and 10^{-7}) were spread as lawn culture on MHA plates and incubated overnight at 37^{0} C. The next day, the data of CFU was conducted according to the standard methods of surface plate dilution and cell counting in a similar way to Roszak [292].

Data analysis

The statistical analysis was performed using the Microsoft Office 2003 Excel and MATLAB software. The statistical significance of the differences between the Azu-RRM treatments of bacteria and the positive control group were analyzed by one-way ANOVA.

Results

The anti-microbial effects of Azu-RRM and Azc-RRM peptide analogues on the growth of Gram-positive *S. aureus* ATCC25923, *S. aureus* 344 (ampicillin resistant strain) and Gram-negative *E. coli* bacteria are shown in Figures 5.2.6-5.2.14.

Different concentrations of Azu-RRM at 8h and overnight incubations were used in order to determine the optimal treatment concentrations and time that can induce the maximum suppressing effects on bacterial growth.

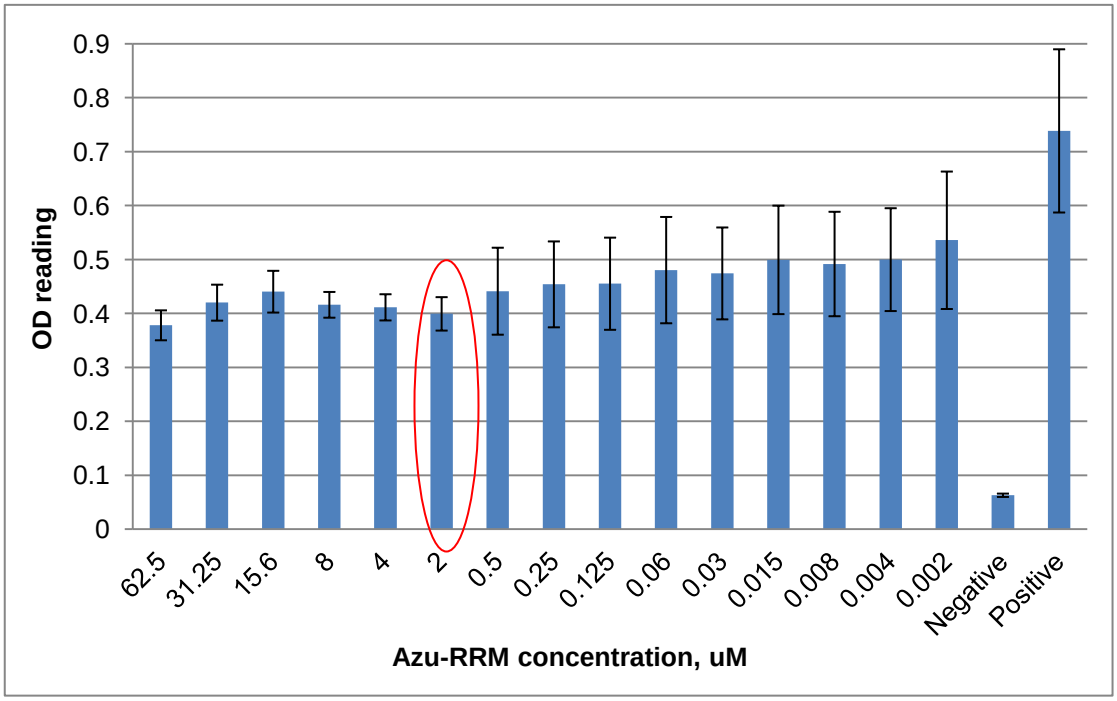

Figure 5.2.6. Effects of Azu-RRM (bioactive) peptide analogue on the growth of *S. aureus* ATCC 25923 at 8 hours incubation

Figure 5.2.6 demonstrates the effects of different concentrations of Azu-RRM peptide analogue on *S. aureus* ATCC25923 at 8 hour incubation. Its antimicrobial activity is noticeably most effective at the concentration of **2µM**, when compared to the positive control ($p<0.01$). At this concentration the synthetic peptide Azu-RRM treatment of *S. aureus* induces a relative change of 48% in absorbance (OD reading) as can be seen from Fig. 5.2.6.

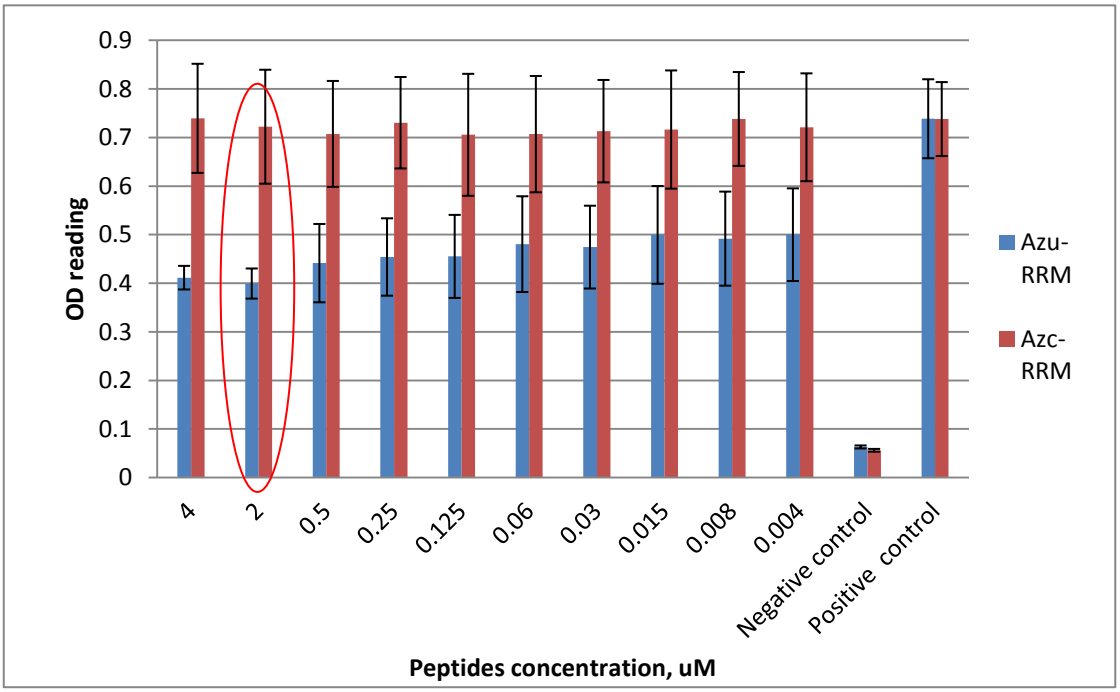

Figure 5.2.7. Effects of Azu-RRM (bioactive) and Azc-RRM (control) peptides on the growth of *S. aureus* ATCC 25923 at 8 hours incubation

The obtained results clearly show that the designed synthetic control peptide Azc-RRM does not exhibit any potent activity against the studied *S. aureus* bacteria, when compared with the anti-microbial effects induced on bacterial growth by treatment with the designed bioactive peptide Azu-RRM.

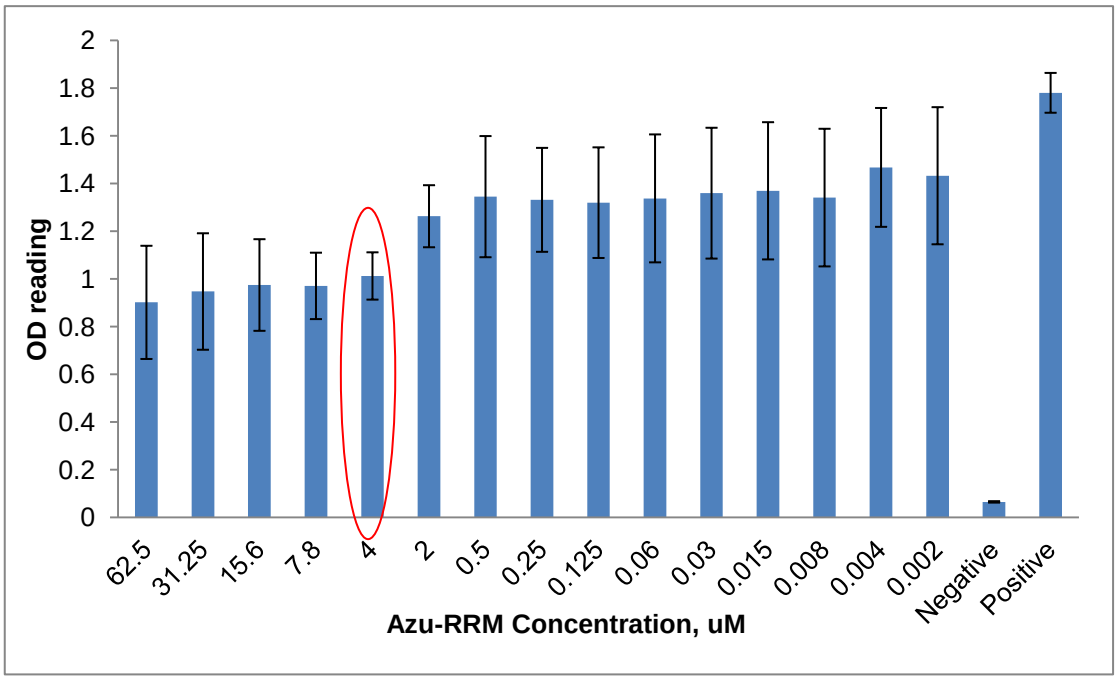

Figure 5.2.8. Effects of Azu-RRM on the growth of *S. aureus* ATCC 25923 at overnight incubation

Figure 5.2.8 demonstrates the effects of different concentrations of Azu-RRM peptide on Gram-positive *S. aureus* ATCC25923 bacteria at overnight incubation. Its antimicrobial activity is significant at the concentration of **4μM**, when compared to the positive control ($p<0.01$). A change of 40% in absorbance (OD reading) in bacterial growth can be seen with the synthetic peptide treatment at the concentration of 4μM.

The above experimental results (Figure 5.2.6, 5.2.8) reveal that the *in vitro* inhibitory effects of the synthetic Azu-RRM peptide analogue on bacterial growth of *S. aureus* ATCC25923 are *time- and dose-dependent*. The noticeably strong antimicrobial

activity of Azu-RRM is demonstrated at the concentration of 2uM and 8hours incubation, and at the concentration of 4uM and overnight incubation.

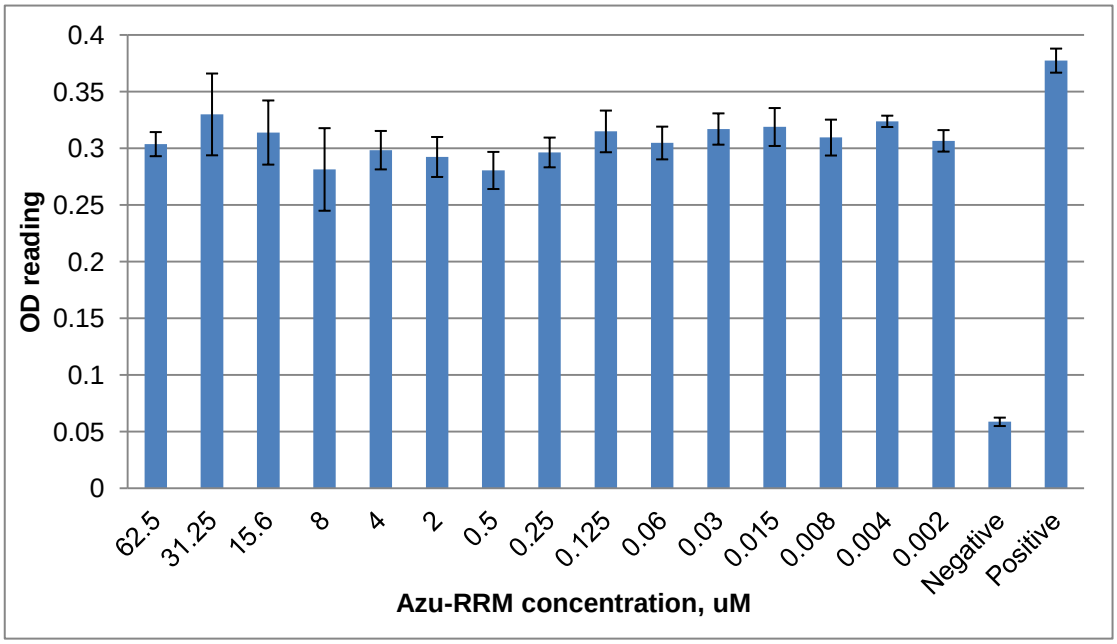

Figure 5.2.9. Effects of Azu-RRM on the growth of Gram-negative *E. coli* ATCC25922 bacterium at 8 hours incubation

Figure 5.2.9 demonstrates the effects of different concentrations of the bioactive Azu-RRM peptide on Gram-negative *E.coli* ATCC25922 bacteria at 8 hours incubation. Its anti-microbial activity is noticeably strong at the concentration of **0.5µM**, when compared to the positive control ($p<0.01$). A change of 26% in absorbance (OD reading) can be seen at 0.5 µM concentration of the synthetic peptide treatment.

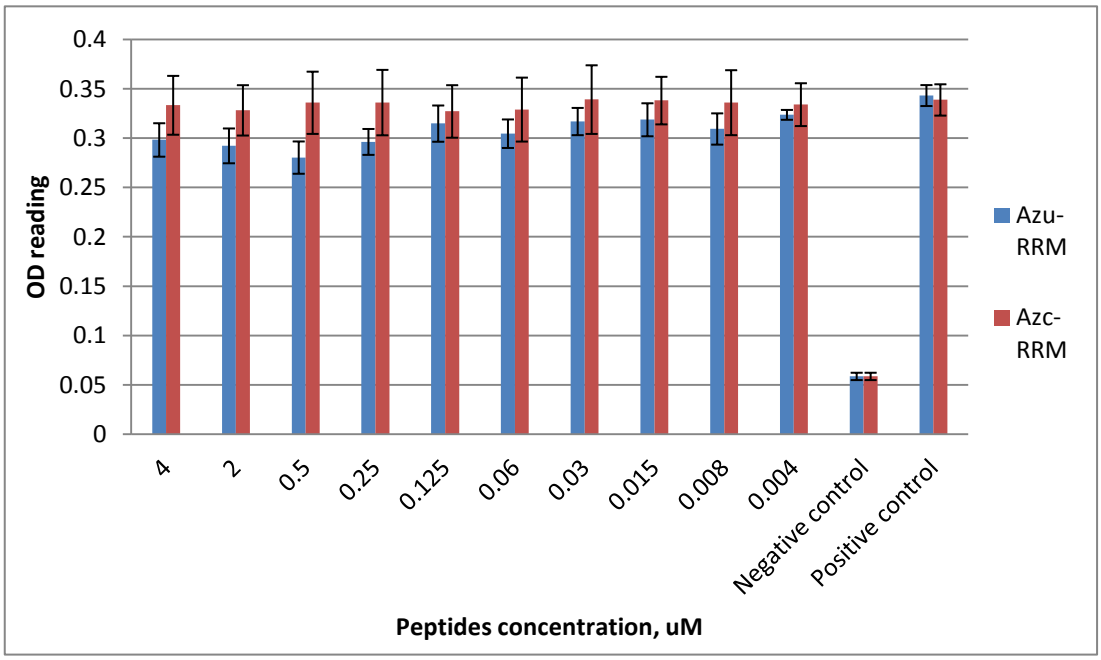

Figure 5.2.10. Effects of Azu-RRM (bioactive) and Azc-RRM (control) peptides on the growth of Gram-negative *E.coli* ATCC 25922 at 8 hours incubation

Figure 5.2.10 shows that treatment with the designed Azc-RRM control peptide analogue does not exhibit any potent anti-microbial activity against *E.coli* bacteria when compared to the anti-microbial activity of designed synthetic Azu-RRM peptide analogue.

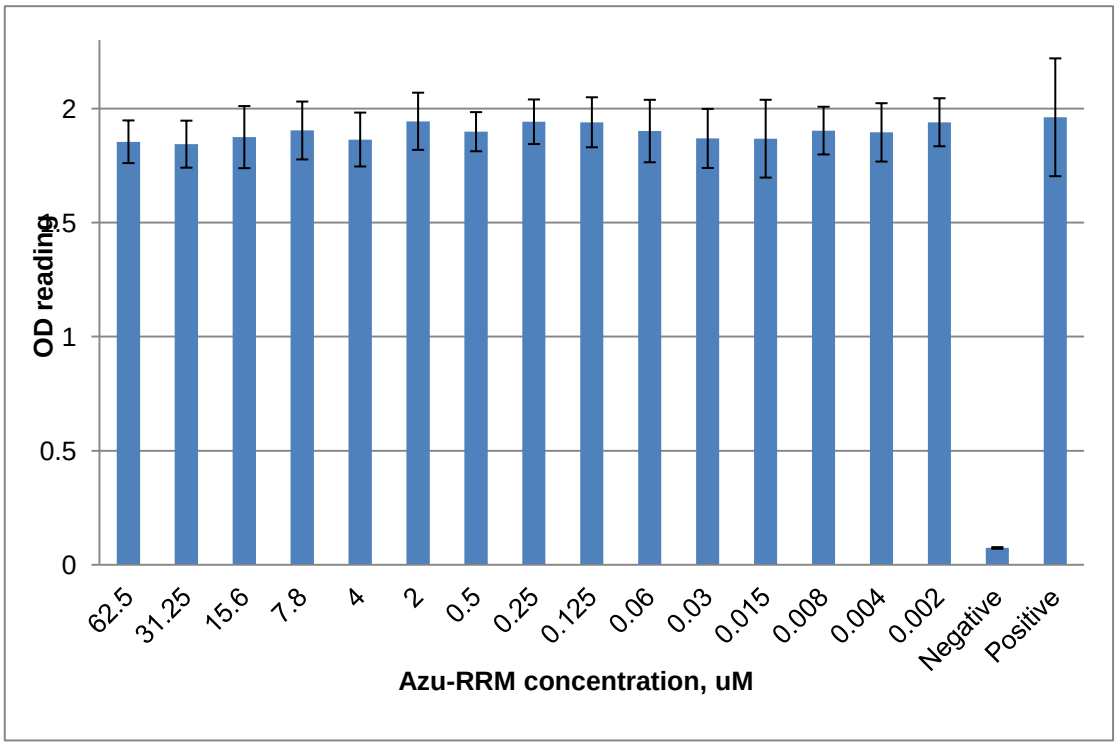

Figure 5.2.11. Effects of bioactive Azu-RRM peptide on the growth of Gram-negative *E. coli* ATCC25922 bacterium at overnight incubation

As can be observed from Figure 5.2.11, there are no noticeable effects of the synthetic Azu-RRM peptide analogue treatment on Gram-negative *E. coli* ATCC25922 at overnight incubation.

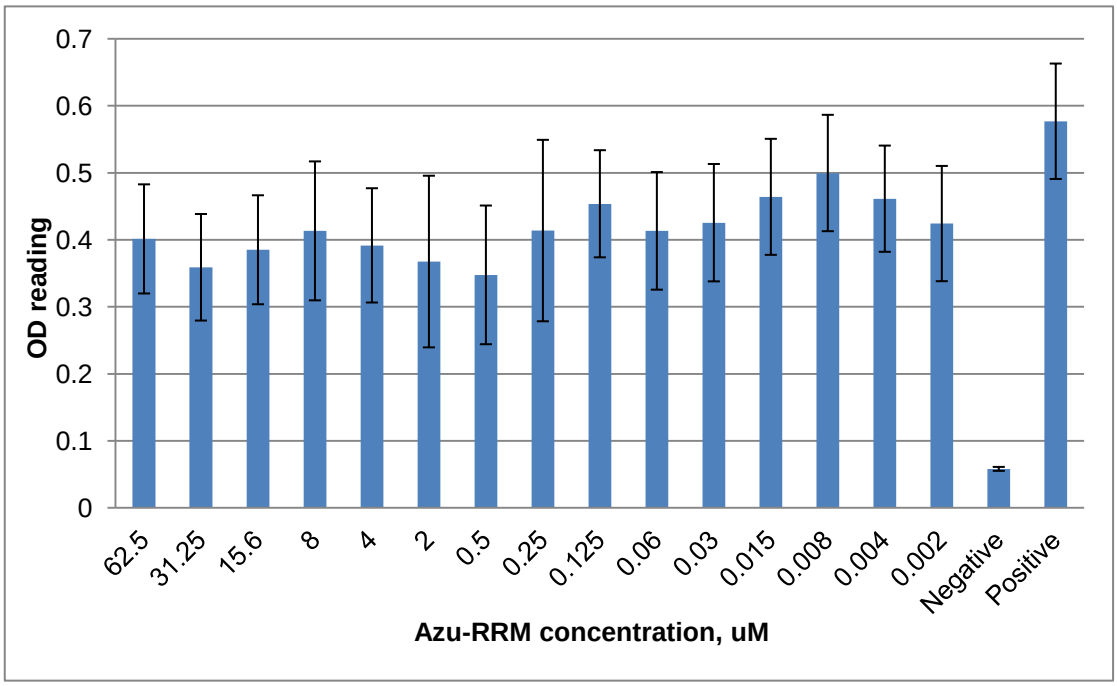

Figure 5.2.12. Effects of Azu-RRM on the growth of *S. aureus* 344 (ampicillin resistant bacterium) at 8 hours incubation

Figure 5.2.12 demonstrates the effects of different concentrations of bioactive Az-RRM peptide on Gram-positive *S. aureus* 344 (ampicillin resistant strain) at 8 hour incubation. Its anti-microbial activity is noticeably strong at the concentration of 0.5 μM, when compared to the positive control ($p<0.01$). The significant anti-microbial effect is observed at this concentration, which leads to a change of 40% in absorbance OD reading.

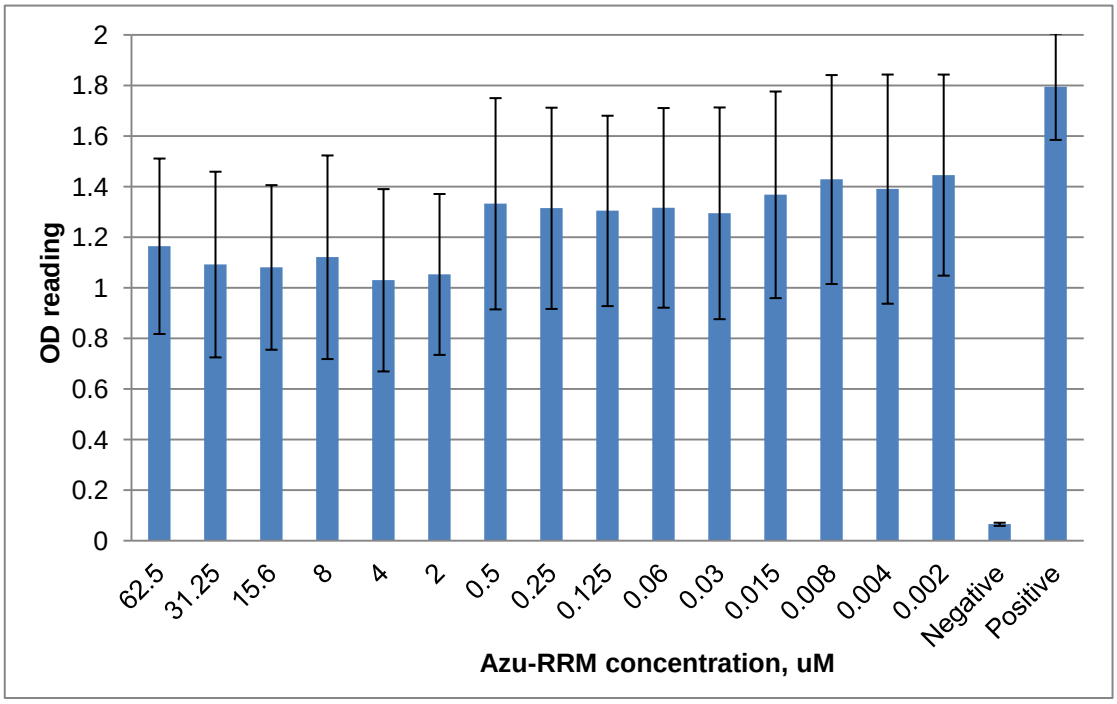

Figure 5.2.13. Effects of Azu-RRM on the growth of *S. aureus* 344 (ampicillin resistant bacterium) at overnight incubation

Figure 5.2.13 demonstrates the effects of different concentrations of the bioactive Azu-RRM peptide on Gram-positive *S. aureus* 344 (ampicillin resistant strain) at the overnight incubation. Its anti-microbial activity is noticeably most effective at the concentration of 2 μM when compared to the positive control ($p<0.01$). A change of 44% in absorbance (OD reading) can be seen at this concentration of the synthetic peptide treatment.

In essence, the results shown in Figures 5.2.6-5.2.13 indicate that the synthetic computationally designed Azu-RRM peptide analogue has a broad range of antimicrobial activity against the studied Gram-positive and Gram-negative bacteria at the particular concentrations and incubation times. It should be noted, that the studied Gram-positive bacteria are well susceptible to the Azu-RRM treatment at the concentrations ranging from 62.5 μM to 0.5 μm at 8 hours incubation. It can be also noted that Gram-negative bacteria *E. coli* 25922 are susceptible (the effects vary depending on Azu-RRM concentration) to Azu-RRM treatment at the concentrations of 62.5 μM - 2 μM at 8 hours incubation; with the maximum suppressing effect achieved at 0.5 μM (Figure 5.2.9). However, there are no noticeable effects of Azu-RRM treatment on Gram-negative *Ecoli* 25922 bacteria at overnight incubation (Figure 5.2.11).

Viable cell counts: Azu-RRM treatment at 8 hours incubation

The viable cell count (CFU) results from plates inoculated with the 10^{-6} bacterial suspension dilutions are shown in Figure 5.2.14. The viable count of bacterial cultures (Figure 5.2.14) shows that both Gram-positive bacteria *S. aureus* ATCC 25923 and *S. aureus* 344 ampicillin resistant strain are more susceptible to Azu-RRM treatment than the Gram-negative bacterium *E. coli* 25922 at 8 hours incubation.

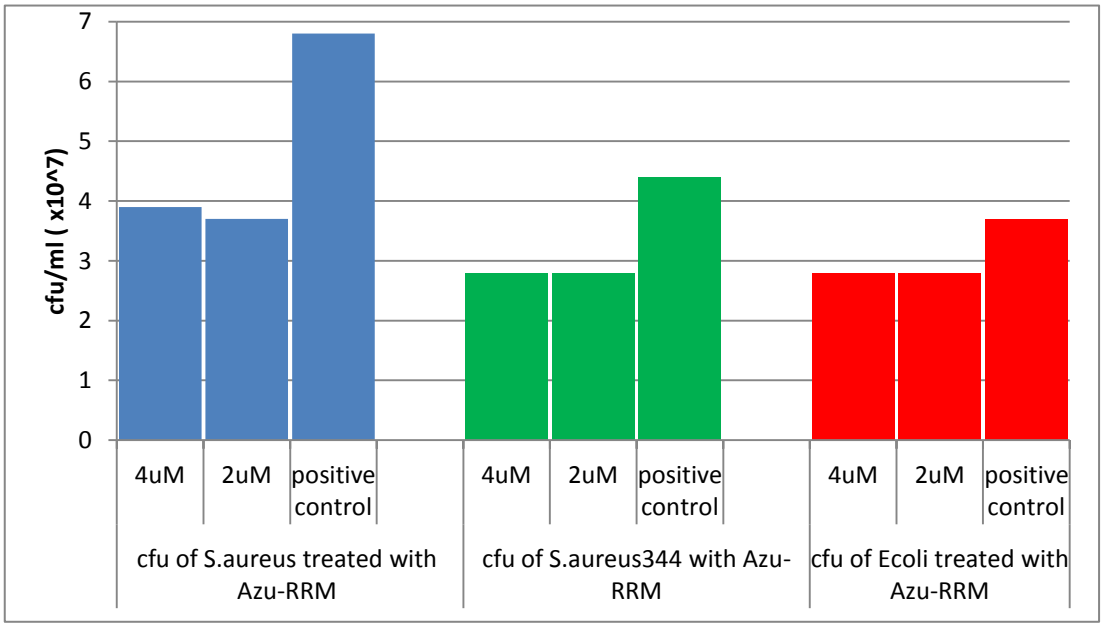

Figure 5.2.14. Viable cell counts (CFU) of *S.aureus* ATCC25923, *S. aureus* 344 and *E. coli* ATCC25922 cultures following treatment with Azu-RRM at 8h incubation

It also can be seen that:

(i) there is a significant reduction of 44% in viable cell counts of *S. aureus* ATCC25923 induced by Azu-RRM treatment at the concentrations of **2 µM and 4 µM**, when compared to CFU of positive control at 8h incubation;

(ii) a reduction of 36% in viable cell counts of *S.aureus* 344 induced by Azu-RRM treatment at the concentrations of 2 µM and 4 µM, when compared to CFU of the non treated control at 8h incubation; and

(iii) a reduction of 25% in viable cell counts of *Ecoli* ATCC25922 induced by Azu-RRM treatment at the concentrations of 2 µM and 4 µM, when compared to CFU of the non treated control at 8h incubation.

The findings reveal that the growth rates of these three selected bacterial species were significantly affected by Azu-RRM treatment at the concentrations in a range of 62.5 µM to 0.5 µM at 8h incubation, when compared to the non-treated positive control. The statistical analysis of the experimental data shows that the survival rates of bacterial cultures of *S. aureus* ATCC 25923, *S. aureus*344 and *E. coli* 25922 treated with Azu-RRM (62.5µM-0.5µM) at 37^0C, 8 hour incubation were significantly lower ($p<0.01$), when compared to the non-treated cultures (positive control). Hence, these findings allow summarizing that the computationally designed Azu-RRM peptide analogue exhibits an inhibitory activity against the studied pathogenic bacteria.

Discussion

Wound infection could prolong the time of wound healing, obstruct the effective treatment and increase patient morbidity. Currently, the rising antibiotics resistance is a major problem to limit the use of traditional antibiotics. Hence, there is a growing need to develop new antimicrobial drugs as therapeutic agents to overcome this problem. Antimicrobial peptides (AMP) from different organisms can serve as the natural defense molecules to combat these pathogenic microorganisms. Azurocidin is an Azurophil granule antibiotic protein that possesses some features whick make it unique among other neutrophil granule proteins. As one of the defense key players of the immune system, it has attracted much interest from medical scientists. Azurocidin is described in details in Chapter 2.2.10.

In this study, the RRM approach was used to design computationally Azurocidin synthetic peptide analogue (Azu-RRM) having native Azurocidin-like anti-microbial activity. The experimental results clearly showed that the anti-microbial activity of Azu-RRM is very comparable to the activity of the native Azurocidin (Figure 5.2.2-5.2.4). The RRM approach has been previously utilized in computational analysis of oncogene and proto-oncogene proteins and the results showed that the RRM is capable of to identify the differences between oncogenic and proto-oncogenic proteins with the possibility of identifying the ‘‘cancer-causing’’ features within their protein primary structure [242].

The activity of anti-microbial peptides is diverse. Due to their high effectiveness against the disease causing organisms, Gram-positive and Gram-negative bacteria, viruses, fungi and protozoa are susceptible to anti-microbial peptide’ treatments at their very low concentration (in micro-molar concentration or below) [29,139]. The findings of this experimental evaluation are in accord with the results reported in other studies.

Chapter 6

Conclusion

Based on the findings presented and discussed in Chapter 5, the following conclusive remarks are made:

1. The results of electromagnetic radiation (visible light) of the computationally determined frequency reinforce the previously developed linear relationship between the calculated RRM frequencies and wavelengths of light radiation. With this correlation in mind, it is now possible to calculate wavelengths of light irradiation which will affect different biological processes. To evaluate the effects of visible light exposures, Collagenase enzyme solutions were irradiated by monochromatic light of 400 to 500 nm. The obtained results reveal that Collagenase activity can be modulated at the particular wavelengths of **450nm, 456nm, and 460nm,** which are within the activation wavelength range defined computationally. These findings suggest that *EMR can be used as a non-invasive treatment to promote enzymatic debridement and thus, assist wound healing.*

2. In the experimental *in vitro* study evaluating the antimicrobial activity of the synthetic computationally design peptide analogue Azu-RRM, its efficacy was compared with the native Azurocidin (Azu) proteins against the Gram-positive

bacterium *S. aureus* ATCC25923. The results showed that the antimicrobial activity of Azu-RRM was **strong and comparable** to the activity of the native Azu in the concentration range of **0.3µM to 0.005µM**. It was previously reported by Watorek [29] that Azu induces significant anti-microbial effects (the most effective dosage) at the concentrations range of 10^{-5}-10^{-6}(M). These results are in accord with the experimental findings of this PhD project. The results obtained reveal that both native and synthetic peptides induce suppressing effects on *Staphylococcus aureus*, their treatments at the particular concentrations do affect significantly the bacterial growth of *S. aureus*.

3. In the experimental evaluation (Chapter 5), the efficacy of the synthetic Azu-RRM peptide analogue, as a candidate for anti-infection therapy, was studied on Gram-positive bacteria (*S.aureus* ATCC 25923, and *S.aureus*344) and the Gram-negative bacterium (*E. coli* 25922). According to our results, the activity of Azu-RRM peptide against Gram-positive bacterium (*S. aureus* ATCC 25923, *S. aureus* 344) and Gram-negative bacterium (*Ecoli* ATCC 25922) is **dose-dependent**. It is important to note, that at 8 hours incubation the most significant antimicrobial, supressing effects of Azu-RRM against *S.aureus* ATCC25922 was recorded at the concentration of 2 µM. While for the penicillin resistant strain *S. aureus*344, the killing effect is most noticeable at the concentration of 0.5 µM. For *E. coli* ATCC 25922 bacterium, the most significant effect of Azu-RRM treatment is observed at the concentration of 0.5 µM.

4. Furthermore, the results also showed that the effects of Azu-RRM peptide against Gram-positive and Gram-negative bacteria are **time-dependent**, when compared to the same concentration treatment of Azu-RRM (0.5 μM, 2 μM and 4 μM) on these bacteria at 8 hours and overnight incubations. Interestingly, the test results of Gram-negative bacterium *E.coli* ATCC25922 treatment by Azu-RRM at 8 hours incubation clearly demonstrate the antimicrobial effects. In contrary, the Azu-RRM treatment at overnight incubation induces no effects on the bacterial growth of *E.coli* ATCC25922.

5. The results also showed that the **activity of Azu-RRM against the Gram-positive bacterial strains is stronger than against Gram-negative bacterium**. The antimicrobial activity data from the live cells count revealed that Azu-RRM activity against the studied bacteria was rather **bacteria-static than bacteria-cidal** as the viable cell count (CFU) results showed that there were still live bacterial cells that survived the peptide treatment.

6. As was shown through the experimental evaluation, the RRM is capable of identifying the key amino acids in the native Azurocine peptide sequence, which predominantly contributes to its characteristic frequency and thus, to the desired function, and design of the *de novo* peptide analogue. Since this *de novo* peptide carries the common characteristic of Azurocidin, specifically in terms of its antimicrobial activity, the peptide analogue will exhibit the same biological activity

as the native Azurocidin. The experimental findings corroborate our previous results of using the RRM approach to *de novo* design of different peptide analogues [237,242,243,280]. The novel Azu-RRM peptide analogue emulates the activity of the native anti-microbial Protein Azu and presents itself as **a potent therapeutic agent** against the studies bacteria. It can be successfully used to treat infections caused by these particular pathogens and thus, promote wound healing process.

Chapter 7

Future work

This research project was focused on *improvement of wound bed preparation* and *development of a novel anti-infection treatment for wound healing promotion*. Within the study two hypotheses have been tested:

1. *Electromagnetic radiation of the computationally determined frequency can modulate the enzymatic activity and thus, promote a wound healing process.*
2. *The computationally designed synthetic peptide can exhibit an antimicrobial activity and thus, promote wound healing process.*

Upon completion of the project, the above hypotheses and identified research questions have been successfully addressed through the conducted computational and experimental studies. However, there are still some experiments can be performed to continue with this particular research topic:

1. Firstly, it will be interesting to study the synergetic effects of the combined treatment (visible light and synthetic peptide analogue Azu-RRM) on selected bacterial cultures.

2. Secondly, it will be also impotant to investigate the synergetic effects of the

combined treatment (synthetic peptide analogue Azu-RRM and traditional antibiotics, i.e. penicillin, ampicillin) on selected bacterial cultures.

3. Third, to study and evaluate the effects of the synthetic peptide analogue RRM-Azu on infected tissue cultures.

4. Fnally, to study the effects of the synthetic peptide analogue Azu-RRM on experimental animals (treatment of acute wounds).

References

[1] S. K. Kurd, O.J. Hoffstad, W.B. Bilker and D.J. Margolis, "Evaluation of the use of prognostic information for the care of individuals with venous leg ulcers or diabetic neuropathic foot ulcers". *Wound Repair Regen.* 2009, 17(3):318-325

[2] J. Firth, E.A. Nelson, C. Hale, J.Hill and P. Helliwell, "A review of design and reporting issues in self-reported prevalence studies of leg ulceration". *J Clin Epidemiol*. 2010, 63(8):907-913

[3] P. Kirby. "Quality of life, exudate management and the Biatain foam dressing range". *Br. J Nurs*. 2008, 17(15):S32-7

[4] http://www.woundcrc.com

[5] L.J. Cowan, J.K. Stechmiller, P. Phillips, Q. Yang, G. Schultz. "Chronic wounds, biofilms and use of medicinal Larvae". *Ulcers*. 2013

[6] T.N. Demidova-Rice, E.V. Salomatina, A.N. Yaroslavsky, I.M. Herman, M.R. Hamblin. "Low-level light stimulates excisional wound healing in mice". *Lasers Surg Med*. 2007, 39(9):706-15

[7] P.M. Carrinho, A.C. Renno, P. Koeke, A.C. Salate, N.A. Parizotto, B.C. Vidal. "Comparative study using 685-nm and 830-nm lasers in the tissue repair of tenotomized tendons in the mouse". *Photomed Laser Surg*. 2006, 24(6):754

[8] F.S. Oliveira, C.E. Pinfildi, N.A. Parizoto, R.E. Liebano, P.S. Bossini, E.B. Garcia and L.M. Ferreira, "Effect of low level laser therapy (830 nm) with different therapy regimes on the process of tissue repair in partial lesion calcaneous tendon". Lasers Surg Med. 2009, 41(4):271-6

[9] L.M. Plavnik, M.E. De Crosa, A.I. Malberti, "Effect of low-power radiation (helium/neon) upon submandibulary glands". *J. Clin Laser Med Surg*. 2003, 21(4):219-25

[10] A. Gosain, LA. DiPietro, "Aging and wound healing".World J Surg 2004, 28:321-326

[11] S. Guo and L.A. DiPietro, "Factors Affecting Wound Healing" J Dent Res. 2010, 89(3): 219-229

[12] G.S. Schultz, G. Ladwig and A. Wysocki, "Extracellular matrix: Review of its roles in acute and chronic wounds", World Wide Wounds 2005, Vol 13

[13] L. Shi and D. Carson, "Collagenase Santyl Ointment: A Selective Agent for Wound Debridement", J Wound Ostomy Continence Nurs. 2009, VOL 36(6S):S12-S16,

[14] K. Ousey and C. McIntosh, "Understanding wound bed preparation and wound debridement" Wound Care, 2010, s22-s28,

[15] J. Panuncialman and V. Falanga,"The Science of Wound Bed Preparation", Surgical Clinics of North America. 2009, Volume 89(3):611-626

[16] J. Ramundo and M. Gray, "Enzymatic Wound Debridement", J Wound Ostomy Continence Nurs. 2008, VOL 35(3): 273-280

[17] C. Critchley and A. W. Russell, "Photoinhibition of photosynthesis in vivo: The

role of protein turnover in photosystem II" PHYSIOLOGIA PLANTARUM 1994, 92: 188-196
[18] M.M Rossa, M.C de Oliveira1, O.K Okamoto and P. Colepicolo, "Effect of visible light on superoxide dismutase (SOD) activity in the red alga Gracilariopsis tenuifrons (Gracilariales, Rhodophyta)" Journal of Applied Phycology 2002, 14:151–157
[19] Y.J. Suzuki and G.D. Ford, "Redox Regulation of Signal Transduction in Cardiac and Smooth Muscle" J Mol Cell Cardiol 1999, 31:345–353
[20] E. Pirogova, I. Cosic, J. Fang and V. Vojisavljevic, "Use of infrared and visible light radiation as modulator of protein activity" Estonian Journal of Engineering, 2008, 14(2):107–123
[21] V. Vojisavljevic; E. Pirogova and I. Cosic. "The effect of electromagnetic radiation (550 - 850 nm) on l-Lactate dehydrogenase kinetics Int". J. Radiat. Biol., 2007, Vol. 83(4):221 – 230
[22] V. Vojisavljevic, E. Pirogova and I. Cosic, "Investigation of the Mechanisms of Electromagnetic Field Interaction with Proteins" Proceedings of the 2005 IEEE, Engineering in Medicine and Biology 27th Annual Conference Shanghai, China, September 1-4, 2005
[23] N. Petrosillo, A. Capone, S. Di Bella, and F. Taglietti,"Management of antibiotic resistance in the intensive care unit setting", Expert Review of Anti-Infective Therapy 2010, Vol 8(3): 289-302
[24] R.E.W. Hancock and G. Diamond, "The role of cationic antimicrobial peptides in innate host defences", TRENDS IN MICROBIOLOGY 2000, Vol 8(9):402-410
[25] A. Peschel, "How do bacteria resist human antimicrobial peptides", Trends in Microbiology 2002, Vol 10(4):179-186
[26] D. Campanelli, P.A. Detmers and J.E. Gabay, "Azurocidin and homologus serine protease from neutrophils", J Clin. Invest. 1990, 85: 904-915
[27] R.P. Almeida, A. Vanet and J.E. Gabay,"Azurocidin, a natural antibiotic from human neutrophils: expression, antimicrobial activity, and secretion", Protein Expression and Purification, 1996, 7:355-366
[28] D. McCabe, T. Cukierman and J.E. Gabay, "Basic residues in Azurocidin/HBP contribute to both heparin binding and antimicrobial activity", The J. of Bbiological Chemistry, 2002, 227(30): 27477-27488
[29] W. Watorek, "Azuorcidin-inactive serine proteinase homolog acting as a multifunctional inflammatory mediator", Acta Biochimica Polonica, 2003, 50(3):743-752
[30] S.V. Witko, P. Rieu, L.B. Descamps, P. Lesavre and M.L. Halbwachs, "Neutrophils: molecules, functions and pathophysiological aspects", Lab Invest 2000, 80(5): 617–53
[31] C. Nathan, "Neutrophils and immunity: challenges and opportunities", Nature Reviews Immunology 2006, Vol 6(3):173-182
[32] S.W. Edwards, "Biochemistry and physiology of the neutrophil". Cambridge University Press. p.6, 1994
[33] D.T. Nguyen, D.P. Orgill and G.F. Murphy, "The Pathophysiologic Basis for

Wound Healing and Cutaneous Regeneration". Biomaterials For Treating Skin Loss Woodhead Publishing & CRC Press, Cambridge/Boca Raton, p. 25-57, 2009
[34] H. Rasche,"Haemostasis and thrombosis: an overview". European Heart Journal Supplements 2001, 3(Q): Q3–Q7
[35] A. Tatsioni, E. Balk, T. O'Donnell and J. Lau, "Usual Care in the Management of Chronic Wounds: A Review of the Recent Literature". J Am Coll Surg. 2007, Vol 205(4):617-624
[36] V. Falanga, "Wound Bed Preparation and the Role of Enzymes: A Case for Multiple Actions of Therapeutic Agents". WOUNDS-A COMPENDIUM OF CLINICAL RESEARCH AND PRACTICE 2002, Vol14(2): 47-57
[37] C.-Ki Min, U.M.E. Wikesjo and C.-K. Kim,"Wound healing/regeneration using recombinant human growth/differentiation factor-5 in an injectable poly-lactideco-glycolide-acid composite carrier and a one-wall intra-bony defect model in dogs", J Clin Periodontol 2011, 38: 261–268
[38] K. Ousey, and C. McIntosh,"Understanding wound bed preparation and wound debridement", British Journal of Community Nursing 2010, Vol15(3): S22-S28
[39] S. Enoch, J.E. Grey and K.G. Harding,"ABC of wound healing: Recent advances and emerging treatments". BMJ. 2006, 332(7547): 962–965
[40] G.D. Boon, "An Overview of Hemostasis". Toxicologic Pathology 1993, 21(2): 170-79
[41] A.K. Deodhar and R.E. Rana, "Surgical physiology of wound healing: a review". Journal of Postgraduate Medicine 1997, 43(2):52–56
[42] M.M. Santoro and G. Gaudino, "Cellular and molecular facets of keratinocyte reepithelization during wound healing". Experimental Cell Research 2005, 304(1): 274–28
[43] B. Hinz, "Masters and servants of the force: the role of matrix adhesions in myofibroblast force perception and transmission". European Journal of Cell Biology 2006, 85(3–4):175–181
[44] G. Song, D.T. Nguyen, G. Pietramaggiori, S. Scherer, B. Chen, Q. Zhan, R. Ogawa, and I.V. Yannas,"Use of the parabiotic model in studies of cutaneous wound healing to define the participation of circulating cells". Wound Repair and Regeneration 2010, 18(4): 426-432
[45] A. Desmouli ère, C. Chaponnier and G. Gabbiani, "Tissue repair, contraction, and the myofibroblast". Wound Repair and Regeneration 2005, 13(1):7–12
[46] V. Falanga, "The chronic wound: Impaired healing and solutions in the context of wound bed preparation". Blood Cells, Molecules, and Diseases 2004, 32(1): 88–94
[47] M. Flanagan, "Assessment Criteria". Nursing Times: 1994, 90(35): 76 – 86,
[48] Flanagan, M., "A practical framework for wound assessment 2: methods". British Journal of Nursing: 1997, 6(6): 8 - 11
[49] S. Enoch and K. Harding, "Wound bed preparation: The science behind the removal of barriers to healing". Wounds 2003, Vol 15(7): 213-229
[50] S.Y. Proskryakov, A.G. Konoplyannikov and V.L.Gabai, "Necrosis: a specific form of programmed cell death?" Exp. Cell Res. 2003, Vol 283 (1):1–16
[51] M. Laato, J. Niinikoski and C. Lundberg, "Inflammatory reaction in blood flow

and experimental wounds inoculated with Staphylococcus aureus". Eur Surg Res 1998, Vol 20:33
[52] D.L. Steed, D. Donohoe, M.W. Webster and L. Lindsley, "Effect of extensive debridement and treatment on the healing of diabetic foot ulcers". J Am Coll Surg 1996, Vol183:61-64
[53] H. Zacur and R.S. Krisner, "Debridement: Rational and therapeutic options". Wounds 2002, Vol 14(suppl E):2E-7E
[54] A.F. Falabella, "Debridement and wound bed preparation". Dermatologic Therapy, 2006, Vol19:317–325
[55] L. Rosenberg, O. Lapid, A. Ogdanov-Berezovsky, "Safety and efficacy of a proteolytic enzyme for enzymatic burn debridement: a preliminary report". Burns 2004, 30:843–50
[56] L. Koller, P. Bukovcan, M. Orsag, R. Kvanteni and I. Graffinger, "Enzymatic necrolysis of acute deep burns—report of preliminary results with 22 patients". Acta Chirurg Plast 2008, 50:109–14, 2008
[57] A.J. Singer, S.A. McClain, B.R. Taira, J. Rooney, N. Steinhauff and L. Rosenberg, "Rapid and selective enzymatic debridement of porcine comb-burns with bromelain derived Debrase®: acute phase preservation of non-injured tissue and zone of stasis". J Burn Care Res 2010, 31:304 – 309
[58] C. Kirshen, K. Woo, E.A. Ayella and R.G. SIbbald, "Debridement: a vital component of wound bed preparation". Adv Skin Wound Care 2006, 19(9):506–517
[59] A.J. Singer, B.R. Taira, R. Anderson, S.A. McClain and L. Rosenberg, "The Effects of Rapid Enzymatic Debridement of Deep Partial-Thickness Burns With Debrase® on Wound Reepithelialization in Swine". J Burn Care Res 2010, 31:795–802
[60] J.Q. Del Rosso, "Application of Protease Technology in Dermatology". J Clin Aesthet Dermatol 2013, 6(6):14–22
[61] R. Pullen, R. Popp, P. Volkers and I. Fusgen,"Prospective randomized double-blind study of the wound-debriding effects of collagenase and fibrinolysin/deoxyribonuclease in pressure ulcers". Age and Ageing 2002, 31:126-130
[62] J.R. Mekkes, J.E. Zeegelaar, W. Westerhof, "Quantitative and objective evaluation of wound debriding properties of collagenase and fibrinolysin/desoxyribonuclease in a necrotic ulcer animal model". Arch Dermatol Res 1998, 290:152–157
[63] B.S. Karagol, N. Okumus, A. Dursun, N. Karadag and A. Zencıroglu, "Early and Successful Enzymatıc Debridement Via Collagenase Application to Pinna in a Preterm Neonate". Pediatric Dermatology 2011, Vol 28(5): 600–601
[64] M.I. Altman, L. Goldstein, S. Horowitz. "Collagenase: An adjunct to healing trophic ulcerations in the diabtic patient". J Am Pod Assoc 1978, 68:11-15
[65] G.A. Di Lullo, S.M. Sweeney, J. Körkkö, L. Ala-Kokko and J.D. San Antonio, "Mapping the Ligand-binding Sites and Disease-associated Mutations on the Most Abundant Protein in the Human, Type I Collagen". J. Biol. Chem. 2002, 277(6): 4223–4231
[66] P. Szpak, "Fish bone chemistry and ultrastructure: implications for taphonomy and stable isotope analysis". Journal of Archaeological Science 2011,

38(12):3358–3372
[67] http://www.fastbleep.com/biology-notes/40/116/1174
[68] J. Mylyharju and k.I. Kivirkko,“Collagens, modifying enzymes and their mutations in humans”. Flies and worms. 2004, 20(1): 33-43
[69] U. Eckhard, E. Schonauer, D. Nuss and H. Brandstetter, “Structure of collagenase G reveals a chew-and-digest mechanism of bacterial collagenolysis”. Nature Structural and Molecular Biology 2011, Vol 18(10):1109-1115
[70] J. Li, P. Brick, M.C. O'Hare, T. Skarzynski, V.A. Curry, I.M. Clark, H.F. Bigg, B.L .Hazleman, T.E. Cawston and D.M. Blow, “Structure of full-length porcine synovial collagenase reveals a C-terminal domain containing a calcium-linked, four-bladed P-propeller”. Structure, 1995, 3(6):541-549
[71] H. Vijaykumar, S. A. Pai, V. Pandey and P. Kamble, “Comparative study of collagenase and papain-urea based preparations in the management of chronic nonhealing limb ulcers”. Indian Journal of Science and Technology, 2011, Vol 4(9):1096-1110
[72] M.D. Sternlicht and Z.Werb, “How Matrixmetalloproteinase Regulate Cell Behavior. Annu. Rev. Cell Dev. Biol. 2001, 17:463–516
[73] S. Iyer, R. Visse, H. Nagase and K. R. Acharya, “Crystal Structure of an Active Form of Human MMP-1”. J. Mol. Biol. 2006, 362:78–88
[74] V. Memtsas, A. Zarros and S. Theocharis, “Matrix met7ll oproteinases in the pathophysiology and progression of gynecological malignancies: could their inhibition be an effective therapeutic approach?” Expert Opin. Ther. Targets 2009, Vol 13(9):1105-1120
[75] T. Hirose, C. Patterson, T. Pourmotabbed, C.L. Mainaridi and K.A. Hasty, “Structure-function relationship of human neutrophil collagenase: Identification of regions responsible for substrate specificity and general proteinase activity”. Proc. Natl. Acad. Sci.Vol 1993, 90:2569-2573
[76] M.F. Paige, A.C. Lin, M.C. Goh, “Real-time enzymatic biodegradation of collagen "brills monitored by atomic force microscopy”. International Biodeterioration & Biodegradation 2002, 50:1–10
[77] I. Herman “Stimulation of human keratinocyte migration and proliferation in vitro: insights into the cellular responses to injury and wound healing”. Wounds 1996, 8(2):33-41
[78] J.W. Swanson, A.J. Watt, N.B. Vedder,“Skin graft loss resulting from collagenase clostridium histolyticum treatment of Dupuytren contracture: Case report and review of the literature”. Journal of Hand Surgery 2013, Vol 38(3):548-551
[79]http://www.betterhealth.vic.gov.au/bhcv2/bhcarticles.nsf/pages/Infections_bacterial_and_viral
[80] http://www.metapathogen.com
[81] W.B. Whitman, D.C. Coleman, W.J. Wiebe,“Prokaryotes: the unseen majority”. Proceedings of the National Academy of Sciences of the United States of America 1998, 95(12):6578–83
[82] R. Austrian, “The Gram stain and the etiology of lobar pneumonia, an historical note”. Bacteriol. Rev. 1960, 24(3):261–265

[83] http://www.microrao.com/micronotes/pg/Gram%20stain.pdf
[84] http://www.dermnetnz.org/bacterial/staphylococci.html
[85]http://www.foodstandards.gov.au/publications/Documents/Staphylococcus%20aureus.pdf
[86] https://microbewiki.kenyon.edu/index.php/Staphylococcus
[87] C. Griffiths, T.L. Lamagni, N.S. Crowcroft, G. Duckworth, C. Rooney, "Trends in MRSA in England and Wales: analysis of morbidity and mortality data for 1993-2002". Health Stat Q. 2004, 21:15-22
[88] R.M. Klevens, M.A. Morrison and J. Nadle, "Invasive methicillin-resistant Staphylococcus aureus infections in the United States". JAMA. 2007, 298:1763-1771
[89] L. Furchtgott, N.S. Wingreen and K.C. Huang, "Mechanisms for maintaining cell shape in rod-shaped Gram-negative bacteria". Mol. Microbiol. 2011, 81(2):340-53
[90] M.P. Doyle, and J.L. Schoeni, "Survival and growth characteristics of Escherichia coli associated with hemorrhagic colitis". Appl. Environ. Micrbiol. 1984, 48(4):855-856
[91] R.L. Vogt and L. Dippold,"Escherichia coli O157:H7 outbreak associated with consumption of ground beef, June–July 2002". Public Health Rep 2005, 120(2):174–178
[92] http://www.cdc.gov/ecoli/general/
[93] H. Karch, P. Tarr, M. Bielaszewska, "Enterohaemorrhagic Escherichia coli in human medicine". Int J Med Microbiol 2005, 295(6–7): 405–418
[94] M.-L. Ackers, P.M. Griffin and L. Slutsker, "An Outbreak of Escherichia coli O157:H7 Infections Associated with Leaf Lettuce Consumption". J Infect Dis. 1998, Vol 177(6):1588-1593
[95] F. Wang, Q. Yang, J.A. Kase, J. Meng, L.M. Clotilde, A. Lin and B. Ge, "Current Trends in Detecting Non-O157 Shiga Toxin–Producing Escherichia coli in Food". FOODBORNE PATHOGENS AND DISEASE, 2013, Vol 10(8):1-13
[96] D.A. Tadesse, S. Zhao, E. Tong, S. Ayers, A. Singh, M.J. Bartholomew, and P.F. McDermott, "Antimicrobial Drug Resistance in Escherichia coli from Humans and Food Animals, United States, 1950–2002". Emerging Infectious Diseases 2012, Vol 18(5):741-749
[97] L. Colobatiu, O. Oniga, S. Dan Daniel and M. Mihaiu, "An Analysis of E. Coli Isolations for Antimicrobial Resistance Genes". Journal of Food Safety 2014, 1-6
[98] http://www.healthline.com/health/e-coli-infection#Causes3
[99] http://www.medterms.com/script/main/art.asp?articlekey=8121
[100] J.J. Rahal Jr.and M.S. Simberkoff, "Bactericidal and Bacteriostatic Action of Chloramphenicol Against Meningeal Pathogens". Antimicrob. Agents Chemother. 1979, Vol1 6(1):13-18
[101] W.M. Scheld and M.A. Sande, "Bactericidal versus Bacteriostatic Antibiotic Therapy of Experimental Pneumococcal Meningitis in Rabbits". J Clin Invest. 1983, 71(3): 411–419
[102] P. Periti, F. Tonelli, and E. Mini, "Selecting antibacterial agents for the control of surgical infection". J. Chemother. 1998, 10:83–90
[103] L.J. Eron, "Targeting lurking pathogens in acute traumatic and chronic wounds".

J. Emerg. Med. 1999, 17:189–195
[104] G. McDonnell and A.D. Russell. “Antiseptics and disinfectants: Activity, action and resistance”. Clinical Microbiology Reviews 1999, 12(1):147-79
[105] F.C. Tenover, J.M.Hughes, “The challenges of emerging infectious diseases: Development and spread of multiply-resistant bacteria pathogens”. JAMA 1996, 275:300–4
[106] R.E.W. Hancock, and R. Lehrer, “Cationic peptides: a new source of antibiotics. Trends Biotechnol”. 1998, 16:82–88
[107] D.A. Goldman and W.C.Huskins, “Control of nosocomial antimicrobial-resistant bacteria: a strategic priority for hospitals worldwide”. Clin Infect Dis 1997, 24(Suppl.1):S139–45
[108] ML. Cohen, “Antimicrobial resistance: prognosis for public health”. Trends Microbiol 1994, 2:422–425
[109] N.S. Crowcroft and M. Catchpole, “Mortality from methicillin resistant Staphylococcus aureus in England and Wales: analysis of death certificates”. BMJ 2002, 325:1390–1391
[110] G. Godebo, G. Kibru and H. Tassew, “Multidrug-resistant bacterial isolates in infected wounds at Jimma University Specialized Hospital, Ethiopia”. Ann Clin Microbiol Antimicrob 2013, 12:17
[111] J. Fernebro, “Fighting bacterial infections—Future treatment options”. Drug Resistance Updates 2011, 14:125–139
[112] G. Wang, X. Li, Z. Wang, “APD2: the updated antimicrobial peptide database and its application in peptide design”. Nucleic Acids Res 2009, 37:933-937
[113] S.A. Baltzer and M.H. Brown, “Antimicrobial peptides: promising alternatives to conventional antibiotics”. J Mol Microbiol Biotechnol 2011, 20(4):228-235
[114] P. Bala, J. Kumar and N. Kumar, “Therapeutic Perspective View of Antimicrobial Peptides”. Int J Pharm Bio Sci 2014, 5(2): (B)261-264
[115] F. Garcia, E. Villegas, GP Espino-Solis, A. Rodriguez, J.F. Paniagua-Solis, G. Sandoval-Lopez, L.D. Possani, G. Corzo,“Antimicrobial peptides from arachnid venoms and their microbicidal activity in the presence of commercial antibiotics”. J Antibiot Tokyo 2013, 66(1):3-10
[116] L.T. Nguyen, E.F. Haney, H.J.Vogel, “The expanding scope of antimicrobial peptide structures and their modes of action”. Trends Biotechnol 2011, 29:464-72
[117] K. Splith and I. Neundorf, “Antimicrobial peptide with cell penetrating peptide properties and vice versa”. Eur Biophys J, 2011, 40:387–397
[118] M.R. Yeaman and N.Y. Yount,“Mechanisms of antimicrobial peptide action and resistance”. Pharmacol Rev 2003, 55: 27–55
[119] M. Harris, H.M. Mora-Montes, N.A. Gow and P.J. Coote,“Loss of mannosylphosphate from Candida albicans cell wall proteins results in enhanced resistance to the inhibitory effect of a cationic antimicrobial peptide via reduced peptide binding to the cell surface”. Microbiology 2009, 155:1058–1070
[120] Y. Lai and R.L. Gallo, “AMPed up immunity: how antimicrobial peptides have multiple roles in immune defense”. Trends Immunol 2009, 30:131–141
[121] M.R. Yeaman and N.Y. Yount,“Mechanisms of antimicrobial peptide action and

resistance". Pharmacol Rev 2003, 55:27–55
[122] M. Harris, N.A. Gow and P.J. Coote,"Loss of mannosylphosphate from Candida albicans cell wall proteins results in enhanced resistance to the inhibitory effect of a cationic antimicrobial peptide via reduced peptide binding to the cell surface". Microbiology 2009, 155:1058–1070
[123] J.J. Oppenheim, and D. Yang,"Alarmins: chemotactic activators of immune responses". Curr Opin Immunol 2005, 17:359–365
[124] D.M.E. Bowdish, D.J. Davidson, and R.E.W. Hancock, "A re-evaluation of the role of host defense peptides in mammalian immunity". Curr Protein Pept Sci 2005, 6:35–51
[125] W.M. Nauseef, "How human neutrophils kill and degrade microbes: an integrated view". Immunol Rev 2007, 219:88-102
[126] V. Brinkmann, "Neutrophil extracellular traps kill bacteria". Science 2004, 303:1532-1535
[127] D.E. Jenne, "Structure of the azurocidin, proteinase 3 and neutrophil elastase genes. Implications for inflammation and vasculitis". Am J Respir Crit Care Med. 1994, 150: S147–54
[128] L.F. Iversen, J.S. Kastrup, I.K. Larsen, H.J. Flodgaard and P.B. Rasmussen, "Structure and function of the N-linked glycans of HBP0CAP370azurocidin: Crystal structure determination and biological characterization of nonglycosylated HBP". Protein Science 1999, 8:2019–2026
[129] M. Olczak and W. Waztorek, "Structural analysis of N-glycans from human neutrophil azurocidin". Biochemical and Biophysical Research Communications 2002, 293:213–219
[130] O. Soehnlein and L. Lindbom, "Neutrophil-derived azurocidin alarms the immune system". J. Leukoc.Biol. 2009, 85:344–351
[131] H.A. Pereira, X. Ruan, P. Kumar, "Activation of microglia: a neuroinflammatory role for CAP37". Glia 2003, 41:64–72
[132] J. J. Oppenheim, and D. Yang, "Alarmins: chemotactic activators of immune responses". Curr. Opin. Immunol. 2005, 17,359–365
[133] R.I. Lehrer, A. Barton, K.A. Daher, S.S. Harwig, T. Ganz, M.E. Selsted, "Interaction of human defensins with Escherichia coli". Mechanism of bactericidal activity. J Clin Invest 1989, 84:553–561
[134] A. Belaaouaj, KS Kim, SD Shapiro, "Degradation of outer membrane protein A in Escherichia coli killing by neutrophil elastase". Science 2000, 289:1185–1188
[135] KA Brogden, "Antimicrobial peptides: pore formers or metabolic inhibitors in bacteria?" Nat Rev Microbiol 2005, 3:238–250
[136] A. W. Segal, M. Geisow, R. Garcia, A. Harper, and R. Miller, "The respiratory burst of phagocytic cells is associated with a rise in vacuolar pH". Nature (London) 1981, 290:406-409
[137] W.M. Shaffer, L.E. Martin and J.K. Spitznagel,"Late Intraphagosomal Hydrogen Ion Concentration Favors the In Vitro Antimicrobial Capacity of a 37-Kilodalton Cationic Granule Protein of Human Neutrophil Granulocytes". Infection and Immunity 1986, Vol 53(3):651-655

[138] R.P. Almeida, A. Vanet, V.W. Sarsat, “Azurocidin, a natural antibiotic from human neutrophils: expression, antimicrobial activity, and secretion”. Protein expression and purification 1996, 7:355-366
[139] H.A. Pereira, K. Wozniak and P.L. Fidel Jr, “Candidacidal activity of synthetic peptides based on the antimicrobial domain of the neutrophil-derived protein, CAP37”. Medical Mycology 2010, 48:263-272
[140] http://whatis.techtarget.com/definition/electromagnetic-field
[141] http://imagine.gsfc.nasa.gov/docs/dict_ei.html#em_spectrum
[142] http://csep10.phys.utk.edu/astr162/lect/light/spectrum.html
[143] http://lasp.colorado.edu/cassini/education/Electromagnetic%20Spectrum.htm
[144] http://andromeda.rutgers.edu/~rogerlal/115_F13/CHAPTER7LEC1.HTM
[145]
http://chemistry.tutorvista.com/inorganic-chemistry/electromagnetic-radiation.html
[146] http://www.ualberta.ca/~pogosyan/teaching/ASTRO_122/lect3/lecture3.html
[147] http://www.safespaceprotection.com/overview-electromagnetic-fields.aspx
[148] http://www.epa.gov/rpdweb00/understand/ionize_nonionize.html
[149] Cecie Starr, “Biology: Concepts and Applications”. Publisher: Thompson 2005
[150] http://science-edu.larc.nasa.gov/EDDOCS/Wavelengths_for_Colors.html
[151] http://www.manfredkaiser.com/health_effects_of_sunlight.html
[152] http://drpawluk.com/education/biomagnetic-fields/
[153] W. R. Adey, “Biological Effects of Electromagnetic Fields”. Journal of Cellular Biochemistry 1993, 51(4):410-416
[154] M.G. Yost and R.P. Liburdy,“Time-varying and static magnetic fields act in combination to alter calcium signal transduction in the lymphocyte”. FEBS 1992, Vol 296(2):117-122
[155] E. Lindstrom, E. Lundgren,“lntracellular Calcium Oscillations Induced in a T-cell Line by a Weak 50 Hz Magnetic Field”. J. of Cellular Physiology 1993, 156:395-398
[156] R.H.W. Funk, T. Monsees and N. Ozkucur, “Electromagnetic effects – From cell biology to medicine”. Progress in Histochemistry and Cytochemistry 2009, 43:177–264
[157] L.S. Taylor and A.Y. Cheung, “The physical basis of electromagnetic interactions with biological systems”. Proceedings of a workshop held at the university of Maryland, College Park, Maryland, 1977, 15-17
[158] M.C. Ziskin, “Millimeter Waves: Acoustic and Electromagnetic”. Bioelectromagnetics 2013, 34(1):3–14
[159] S. Banik, S. Bandyopadhyay and S. Gangul,“Bioeffects of microwave—a brief review”. Bioresource Technology 2003, 87:155–159
[160] S. Yalcin and G. Erdem, “Biological effects of electromagnetic fields”. African Journal of Biotechnology 2012, Vol 11(17):3933-3941
[161] http://users.rcn.com/jkimball.ma.ultranet/BiologyPages/C/CellMembranes.html
[162] http://biology.tutorvista.com/animal-and-plant-cells/plasma-membrane.html

[163] R.H.W. Funk, T. Monsees and N. Ozkucur, “Electromagnetic effects – From cell biology to medicine”. Progress in Histochemistry and Cytochemistry 2009, 43:177–264
[164] Z. Somosy, T. Kubasova, G. Ecsedi and G.J. Koteles, “Radiationinduced changes of negative charges on the cell surface of primary human fibroblasts”. International Journal of Radiation Biology 1986, Vol49:969–978
[165] M.C. Nievergelt-Edido, C. Michel and W. Schmahl, “Histochemical investigations on lectin binding in normal and irradiated mouse embryos”. Radiation Environmental Biophysics 1993, 32:119–128
[166] L.L. Traikov, M.S. Markov, M.A. Kuzmanova and S.P. Ivanov, “Use of lectins as indicators for magnetic field action on erythrocytes”. Reviews on Environmental Health 1994, 10:243–246
[167] B. Condaminet, G. Redziniak, M. Monsigny and C. Kieda, “Ultraviolet rays induced expression of lectins on the surface of a squamous carcinoma keratinocyte cell line”. Experimental Cell Research 1997, 232:216–224
[168] S. Paradisi, G. Donelli, M.S. Santini, E. Straface and W. Malori, “A 50-Hz magnetic field induces structural and biophysical changes in membranes”. Bioelectromagnetics 1993, 14:247–255
[169] C. Andrew and L. Bassett, “Beneficial Effects of Electromagnetic Fields”. Journal of Cellular Biochemistry 1993, 51:387-393
[170] E. Lindstrom, K. Hansson M. Lundgren and E. Lundgren “lntracellular Calcium Oscillations Induced in a T-cell Line by a Weak 50 Hz Magnetic Field”. Journal of Cellular Physiology 1993, 156:395-398
[171] M.G. Yost and R.P. Liburdy, “Time-varying and static magnetic fields act in combination to alter calcium signal transduction in the lymphocyte”. FEBS 1992, Volume 296(2):117-122
[172] R. Cadossi, G. Torelli and C. Franceschi, “Lymphocytes and 1ow-frequency electromagnetic fields”. FASEB J. 1992, 6: 2667-2674
[173] J. Teissie and T.Y. Tsong, “Electric field induced transient pores in phospholipid bilayer vesicles”. Biochemistry, 1981, 20:1548-1554
[174] E.H. Serpersu and T.Y. Tsong, “Stimulation of a ouabain-sensitive rubidium ion uptake in human erythrocytes with an external electric field”. J. Membrane Biol. 1983, 74:191-202
[175] E.H. Serpersu and T.Y. Tsong, “Activation of electrogenic rubidium transport of (sodium, potassium)-atpase by an electric field”. J.Biol.Chem. 1984, 259:7155-7162
[176] G. Nindl, J.A. Swez, J.M. Miller and W.X. Balcavage, “Growth stage dependent effects of electromagnetic fields on DNA synthesis of Jurkat cells”. FEBS Letters 1997, 414:501-506
[177] H. Lai and N.P. Singh, “Magnetic-field-induced DNA strand breaks in brain cells of the rat”. Environmental Health Perspectives. 2004, 112(6):687-694
[178] V. Romano-Spica,N. Mucci, C.L. Ursini, A. Ianni and N.K. Bhat, “Ets1 Oncogene Induction by ELF-Modulated 50MHz Radiofrequency Electromagnetic Field”. Bioelectromagnetics 2000, 21:8-18

[179] E.M. Goodman, B. Greenebaum and M.T. Marron, “Altered protein synthesis in a cell-free system exposed to a sinusoidal magnetic field”. Biochimica et Biophysica A cta, 1993, 1202:107-112
[180] O. Erol, S. Oldacay and E. Erdem, “The reproduction behaviours of Escherichia coli and Saccharomyces cerevisiae strains at electromagnetic fields”. J. Assoc. Turk. Microbiol. 2003, 33:191-196
[181] C.V. Byus, S.E. Pieper and W.R. Adey, “The effects of low-energy 60-Hz environmental electromagnetic fields upon the growth-related enzyme ornithine decarboxylase”. Carcinogenesis 1987, Vol 8(10):1385-1389
[182] S. Stegemann, K.I. Airman, H. Miihlensiepen and L.E. Feinendegen, “Influence of a stationary magnetic field on acetylcholinesterase in murine bone marrow cells”. Radiat Environ Biophys 1993, 32:65-72
[183] P. Brenneisen, J. Wenk, H. Sies and K. Scharffetter-Kochanek, “Central Role of Ferrous/Ferric Iron in the Ultraviolet B Irradiation-mediated Signaling Pathway Leading to Increased Interstitial Collagenase (Matrix-degrading Metalloprotease (MMP)-1) and Stromelysin-1 (MMP-3) mRNA Levels in Cultured Human Dermal Fibroblasts”. The Journal of Biological Chemistry 1998, Vol 273(9):5279-5287
[184] G.J. Fisher, S. Kang and J.J. Voorhees, “Pathophysiology of Premature Skin Aging Induced by Ultraviolet Light”. N Engl J Med 1997, 1337:1419-1428
[185] K.J. Johnston, J.G. Clark and J. Uitto, “Ultraviolet radiation-induced connective tissue changes in the skin of hairless mice”. The journal of investigative dermatology 1984, 82:587-590
[186] R.E. von Leden, S.J. Cooney, T.M. Ferrara, J.J. Anders and K.R. Byrnes, “808 nm Wavelength Light Induces a Dose-Dependent Alteration in Microglial Polarization and Resultant Microglial Induced Neurite Growth”. Lasers in Surgery and Medicine 2013, 45:253–263
[187] H. K. Moon, S.H. Lee and H. C. Choi,“In Vivo Near-Infrared Mediated Tumor Destruction by Photothermal Effect of Carbon Nanotubes”. ACS Nano 2009, Vol 3 (11):3707–3713
[188] S. Y. C. Lee, I-W. Seong, J.-S. Kim, K-A. Cheon, S. H. Gu, H. H. Kim and Ki Ho Park, “Enhancement of cutaneous immune response to bacterial infection after low-level light therapy with 1072 nm infrared light: A preliminary study”. Journal of Photochemistry and Photobiology B: Biology 2011, 105:175–182
[189] M.D. Skopin and S.C. Molitor, “Effects of near-infrared laser exposure in a cellular model of wound healing”. Photodermatology, Photoimmunology & Photomedicine 2009, 25:75–80
[190] F. Hollosy, “Effects of ultraviolet radiation on plant cells”. Micron 2002, 33:179-197
[191] D.P. Hader, H.D. Kumar, R.C. Smith and R.C. Worres, “Effects of solar UV radiation on aquatic ecosystems and interactions with climate change”. Photochem. Photobiol. Sci. 2007, 6:267–285
[192] T.J. Dougherty, D. Boyle and A. Mittleman, “Photoradiation Therapy for the Treatment of Malignant Tumors”. CANCER RESEARCH 1978, 38:2628-2635

[193] J.E. Kennedy, “High-intensity focused ultrasound in the treatment of solid tumours”. Nature Reviews Cancer 2005, 5:321-327
[194] A. Fonseca, “Low-level infrared laser effect on plasmid dna,” Lasers in Medical Science, 2011.
[195] C.F. Oliveira, F.G. Basso, R.I. Dos Reis, V.S. Bagnato, C.A. De Souza Costa, “In vitro transdentinal effect of low-level laser therapy,” Laser Physics, 2013, Vol23(3): 288–297
[196] J.Kujawa, I.B.Zavodnik, A. Lapshina, M. Labieniec, M. Bryszewska, “Cell survival, dna, and protein damage in b14 cells under low-intensity near-infrared (810 nm) laser irradiation,” Photomedicine and Laser Surgery, 2004, Vol 22(6): 504–508
[197] A. Vazquez, “Neural and hemodynamic responses elicited by forelimb- and photo-stimulation in channelrhodopsin-2 mice: Insights into the hemodynamic point spread function,” Oxford Journals, 2013.
[198] K. Dittmann, C. Mayer, B. Fehrenbacher, R. Kehlbach, H.P. Rodemann, “Radiation-induced epidermal growth factor receptor nuclear import is linked to activation of dna-dependent protein kinase,” Journal of Biological Chemistry, 2005, Vol280:31182–31189
[199] J. Kujawa, “Effect of low-intensity (3.75-25 j/cm2) nearinfrared (810nm) laser radiation on red blood cell atpase activities and membrane structure,” Journal of Clin Laser Med Surg, 2004, vol. 22, no. 2, pp. 111–117
[200] H. Frohlich, “The extraordinary dielectric properties of biological materials and the action of enzymes,” Proceeding of National Academy of Science USA, 1975, vol. 72, no. 11, p. 4211-4215
[201] R. Sroka, M. Schaffer, C. Fuchs, E. Dühmke, R. Baumgartner, “Effects on the mitosis of normal and tumor cells induced by light treatment of different wavelenghts,” Lasers Surgery Medicine, 1999, vol. 25, no. 3, p. 263-271
[202] X.Y. Zhang, Al-Watban, F., “Comparison of the effects of laser therapy on wound healing using different laser wavelengths,” Laser Therapy, 1996, vol. 8, no. 2, p. 127-135
[203] W. Posten, D.A. Wrone, J.S. Dover, S. Silapunt, M. Alam, “Low-level laser therapy for wound healing: Mechanism and efficacy,” Dermatology Surgery, 2005, vol. 31, pp. 334–340
[204] D. Hawkins, N. Houreld, H. Abrahamse, “Low level laser therapy (lllt) as an effective therapeutic modality for delayed wound healing,” New York Academy of Science, 2005, vol. 1056, pp. 486–493
[205] T. Ohno,“Pain suppressive effect of low power laser irradiation. a quantitative analysis of substance p in the rat spinal dorsal root ganglion,” Nihon Ika Daigaku Zasshi, 1997, vol. 64, no. 5, p. 395400
[206] K. Saber, N. Chiniforush, S. Shahabi,“The effect of low level laser therapy on pain reduction after third molar surgery,” Minerva Stomatol, 2012, vol. 61, no. 7-8, p. 319-322
[207] M. Miloro, L.E. Halkias, S. Mallery, S. Travers, R.G. Rashid, “Low-level laser effect on neural regeneration in gore-tex tubes,” Oral Surg Oral Med Oral Pathol Oral Radiol Endod, 2002, vol. 93, pp. 27–34

[208] R. Neira, J. Arroyave, H. Ramirez, F. Sequeda, M.I. Gutierrez, "Fat liquefaction: Effect of low-level laser energy on adipose tissue," Plast Reconstr Surg, 2002, vol. 110, no. 3, p. 912922 - 923925
[209] R. P.Abergel, R. F. Lyons, J. C. Castel, R. M. Dwyer and J.Uitto, "Biostimulation of wound healing by lasers: experimental approaches in animal models and in fibroblast cultures". Dermatol. Surg. Oncof. 1987, 13:127-133
[210] T.S. Lam, R. P. Abergel, J. C. Castel, C. A. Meker, R. M.Dwyer and J. Uitto, "Laser stimulation of collagen synthesis in human skin fibroblast culture". Lasers Life Sci. 1986, 1:61-77
[211] W. Yu, J.O. Naim, R.J. Lanzafame, "The effect of laser irradiation on the release of bFGF from 3T3 fibroblasts". Photochem Photobiol 1994, 59:167-170
[212] H.T. Whelan, R.L. Smits Jr, EV Buchman, "Effect of NASA light-emitting diode irradiation on wound healing". Clin Laser Med Surg 2001, 9:105-114
[213] F.D. Matl, A.Obermeier, J. Zlotnyk, W.Friess, A.Stemberger and R.Burgkart, "AugmentationofAntibiotic Activity by Low-Frequency Electric and Electromagnetic Fields Examining Staphylococcus aureus in BrothMedia". Bioelectromagnetics 2011, 32:367-377
[214] C. Von Eiff, J. Overbeck, G. Haupt, G. Peters and H.U. Spiegel, "Bactericidal effect of extracorporeal shock waves on Staphylococcus aureus". J Med Microbiol 2000, 49:709–712
[215] L. Gerdesmeyer, C. Von Eiff, P. Diehl and H. Gollwitzer,"Antibacterial effects of extracorporeal shock waves". Ultrasound Med Biol 2005, 31:115–119
[216] P. F. Meyer, O.A. Ronzio and Mario Bernardo-Filho, "Cellular and molecular effects of electromagnetic radiation and sonic waves". South African Journal of Science 2013, Vol 109(7/8):1-4
[217] H.Torgomyan, K.Hovnanyan and A.Trchounian, "*Escherichia coli* Growth Changes by the Mediated Effects After Low-Intensity Electromagnetic Irradiation of Extremely High Frequencies". Cell Biochem Biophys 2013, 65:445–454
[218] A. Inhan-Garip, B. Aksu, Z. Akan, D. Akakin, A. N. Ozaydin and T. San, "Effect of extremely low frequency electromagnetic fields on growth rate and morphology of bacteria". International Journal of Radiation Biology 2011, 87(12):1155–1161
[219] L. Strasak, V. Vetter and J. Smarda, "The effect of low-frequency electromagnetic fields on living organisms". Sbornik Lekarsky 1998, 99(4):455–464
[220] A.G. El-Sayed, H.S. Magda, Y.T. Eman and H.I. Mona, "Stimulation and control of E.coli by using an extremely low frequency magnetic field". Romanian Journal of Biophysics 2006, 16(4):283–296
[221] T.P. Curtis, D.D. Mara, S.A. Silva, "Influence of Ph, oxygen, and humic substances on ability of sunlight to damage fecalcoliforms in waste stabilization pond water". Appl. Environ. Microbiol. 1992, 58:1335-1343
[222] R.J. Davies-Colley, A.M. Donnison and D.J. Speed, "Towards a mechanistic understanding of pond disinfection". Water Sci. Technol. 2000, 42:149-158
[223] T. Koutchma, "UV light for Processing foods". The Journal of the International Ozone Association 2008, 10:24-29

[224] T. Dai, G. Asheesh, G.P. Tegos and M.R. Hamblin, “Blue light rescues mice from potentially fatal Pseudomonas aeruginosa infection: efficacy, safety and mechanism of action”. Antimicrob. Agents Chemother. 2012, 57:1238–1245
[225] O. Feuerstein, N. Persman and E.I. Weiss, “Phototoxic effect of visible light on Porphyromonas gingivalis and Fusobacterium nucleatum: an in vitro study”. Photochem Photobiol 2004, 80:412–415
[226] E.R. Blatchley III, and M. M. Peel,“Disinfection by ultraviolet irradiation”. In Disinfection, Sterilisation and Preservation, 4th Edition. (Edited by S. S. Block), pp. 823–851. Lea & Febiger, Philadelphia (1991)
[227] M.R. Hamblin and T. Hasan, “Photodynamic therapy: A new antimicrobial approach to infectious disease?” Photochem. Photobiol. Sci. 2004, 3:436–450
[228] B. Strauch, C. Herman, R. Dabb, L.J. Ignarro and A.A. Pilla, “Evidence-Based Use of Pulsed Electromagnetic Field Therapy in Clinical Plastic Surgery”. Aesthetic Surgery Journal 2009, 29(2):135-143
[229] F.R. Nelson, C.T. Brighton, M. Bolander and J. Seelig, “Use of physical forces in bone healing”. The Journal of the American Academy of Orthopaedic Surgeons 2003, 11(5):344-354
[230] S. Crocetti, C. Beyer, Alfredo Franco-Obregon, “Low Intensity and Frequency Pulsed Electromagnetic Fields Selectively Impair Breast Cancer Cell Viability”. PLOS ONE 2013, Volume 8(9):1-13
[231] D.C. Wen, Y.L.Hung and T.L.Ping, “The effects of phototherapy of an 808nm diode laser on bone fracture”. J. Phys. Ther. Sci. 2012, 24:695-697
[232] L.B. Antonio Pinheiro, G.P. Luiz Soares, Artur Felipe S. Barbosa and Landulfo Silveira Júnior, “Effects of LED phototherapy on bone defects grafted with MTA, bone morphogenetic proteins and guided bone regeneration: a Raman spectroscopic study”. Lasers Med Sci 2012, 27:903–916
[233] http://www.genome.gov
[234] I. Cosic, “Macromolecular Bioactivity: Is It Resonant Interaction Between Macromolecules?-Theory and Applications”. IEEE TRANSACTIONS BME 1994, Vol. 41(12):1101-1114
[235] I. Cosic, Q. Fang, E. Pirogova, “Modification of the RRM model using wavelet transform and Ionisation constant to predict protein active sites”, IEEE EMBS, 21, 1999, Vol.2, 1215-1217
[236] I. Cosic, E. Pirogova, "Usage of Ionization constant of amino acids for protein signal analysis within the RRM - Application to Oncogene", IEEE-EMBS Asia-Pacific Conference on Biomedical Engineering, 2000, 413-414
[237] E. Pirogova, T. Istivan, E. Gan and I. Cosic, “Advances in Methods for Therapeutic Peptide Discovery, Design and Development”. Current Pharmaceutical Biotechnology, 2011, 12(6): 1117-1127
[238] S. Kawashima and M. Kanehisa, “Aaindex: amino acid index database”. Nucleic Acid Res., 2000, 28, 374
[239] I. Cosic, E. Pirogova, “Applications of Ionization Constant of Amino Acids for Protein Signal Analysis Within the Resonant Recognition Model”, Proceedings of 20th

Annual International Conference of the IEEE Engineering in Medicine and Biology Society, Hong Kong, October 1998, Vol.20, No.2, 1072-1075.
[240] I. Cosic, "The resonant recognition model of macromolecular bioactivity", BioMethods (Birkhauser, Basel) Vol. 8. 1997
[241] I. Veljkovic and M. Slavic,"General model of pseudopotentials", Phys. Rev. Lett. 1972, 29:105–108
[242] I. Cosic and E. Pirogova, "Bioactive peptide design using the Resonant Recognition Model".Nonlinear Biomedical Physics 2007, 1:7
[243] E. Pirogova, T. Istivan, E. Gan, P. Coloe and I. Cosic, "Computationally designed Interleukin-like peptide as a candidate for cancer treatment". IFMBE Proceedings 25/IV, 2009, 1973–1976
[244] H. Frolich, "Further evidence for coherent excitations in biological systems". Phys. Lett, 1985, 110A, 480-481
[245] H. Frohlich, "Coherent excitation in active biological systems". In: Modern Bioelectro-chemistry, F. Gutmann, & H. Keyzer, eds., New York: Plenum, 1986, pp. 241-261
[246] T. Karu, "Photobiological fundamentals of low-power laser therapy". IEEE Journal of Quantum Electronics, 1978, QE-23, pp. 1703-1717
[247] T. Karu, "Primary and Secondary Mechanisms of Actions of Visible to Near-IR Radiation on Cells". J. Photochem. Photobiol, Biol, 1999, 49, pp. 1-17
[248] S. Kiontke, "Natural Radiation and its effects on biological systems". Naturheilpraxis mit Naturmedizin, Pflaum Verlag, 2000
[249] E.J. Lerner,–ed., "Biological effects of electro-magnetic fields". IEEE Spectrum. 1984
[250] F.M. Uckun, T. Kurosaki, J. Jin, X. Jun, M. Takata, J. Bolen, R. Luben, "Exposure of B-lineage lymphoid cells to low energy electromagnetic fields stimulations Lyn kinase". J. Biological Chemistry, 1995, 270(46):1-5
[251] M. Ahma, A.R. Cashmore, "HY4 Gene of A. Thaliana Encodes a Protein with Characteristics of Blue-light Photoreceptor". Nature, 1993, 366:162-166
[252] H.F. Blum, "Carcinogenesis by Ultraviolet Light". New Jersey, Princeton University Press Princeton, 1959
[253] I. Cosic, V. Vojisavljević, M. Pavlovic, "The Relationship of the Resonant Recognition Model to effects of Low-intensity Light on Cell Growth". Int. J. Radiat. Biology, 1989, 56:179-191
[254] O. Holian, R.D. Astumian, R.C. Lee, H.M. Reyes, B.M. Attar and R.J. Walter, "Protein kinase C activity is altered in HL60 cells exposed to 60 Hz AC electric fields". Bioelectromagnetics, 1996, 17:504-509
[255] I. Cosic, M. Pavlovic, V. Vojisavljević, "Prediction of hot spots in Il-2 cased on information spectrum characterictics of growth regaling factors". Biochemie, 1989, Vol.71:333-342
[256] I. Cosic, "Virtual Spectroscopy for Fun and Profit". Biotechnology, 1995, 13:236-238

[257] I. Cosic, A. N. Hodder, M. Aguilar, M.T.W. Hearn, “Resonant Recognition Model and Protein Topography: Model Studies with Myoglobin”. Hemoglobin and Lysozyme, Eur. J. Biochem, 1991, 198:113-119
[258] I. Cosic, M.T.W. Hearn, “Hot spot amino acid distribution in Ha-ras oncogene product p21: relationship to Guanine Binding Site”. J. of Molecular Recognition, 1991, Vol.4, pp. 57-62
[259] I. Cosic, M.T.W. Hearn, “Studies on protein-DNA interactions using the resonant recognition model. Application to repressors and transforming proteins”. Eur. J. Biochem., 1992, 205, pp. 613-619
[260] I. Cosic, A.E. Drummond, “Underwood J.R., Hearn M.T.W., “A new approach to growth factor analogous design: modelling of FGF analogous”. Molecular and Cellular Biochemistry, 1993, 130:1-9
[261] I. Cosic, S. Birch, “Photoreceptors Having Similar Structure but Different Absorptions Can be Distinguished using the Resonant Recognition Model”. Proc. IEEE EMBS, 1994, 16:265-266
[262] V. Veljković, M. Slavić, “General Model of Pseudopotentials”. Physical Review Letters, 1972, 29:105-108
[263] I.V. Bodnar, Y. V. Rud, “Novel I–III–VI2 semiconductor–native protein structures and their photosensitivities”. Semicond. Sci. Technol, 2002, 17:1044-1047
[264] C.M. Niemeyer, “Self-assembled nanostructures based on DNA: towards the development on nanotechnology”. Biopolymers, 2000, 4:609-620
[265] P. Ciblis, I. Cosic, “IR Absorption of Water and RRM Frequencies”. Medical & Biological Eng. And Comp, 1999, 37(1):306-307
[266] I. Cosic, P. Ciblis, “Investigations of Water as a Media for Bioactive Energy Transfer between Interacting Proteins using the RRM”. Medical & Biological Engineering and Computing, 1999, 37(2):608-609
[267] P. Ciblis, I. Cosic, “The Possibility of Soliton?, Exciton transfer in Proteins”. Journal of Theoretical Biology, 1997, 184:331-338
[268] G. Biscar, “Photon Enzyme Activation”. Bull. Math. Biology, 1976, 38:29-38
[269] I. Cosic, “Correlation between Predicted and Measured Characteristic Frequency of Chymotrypsin Activation”. Proc. IEEE EMBS, 1993, 15:1541-1542
[270] A. Raven, “Do Plant Photoreceptors Act at the Membrane Level? J. A. Philosophical Transactions of the Royal Society of London. Series B, Biological Sciences, 1983, Vol. 303(116):403-417
[271] V. Bianchi, R. Eliasson, M. Fontecave, E. Mulliez, D.M. Hoover, R.G. Matthews, P. Reichard,“Flavodoxin is required for the activation of the anaerobic ribonucleotide reductase”. Biochem. Biophys. Res. Comm., 1993, 197(2):792-7
[272] I. Cosic, “The Resonant Recognition Model of Bio-molecular Interactions: possibility of electro-magnetic resonance”. Polish Journal of Medical Physics and Engineering, 2001, vol. 7(1):73-87
[273] P. Peidaee, N. Almansour, R. Shukla and E. Pirogova,“In vitro evaluation of visible, near and far infrared light radiation on cancer and normal cells”. MD-Medical Data 2013, 5(1):7-13

[274] P. Peidaee, N. Almansour, R. Shukla, E. Pirogova,“The cytotoxic effects of low intensity visible and infrared light on human breast cancer (MCF7) cells”. Computational and Structural Biotechnology Journal 2013, 6(7):a14
[275] Y.J. Park, L.C. Chang, J.F. Liang, C. Moon, C.P. Chung, V.C. Yang,“Nontoxic membrane translocation peptide from protamine, low molecular weight protamine (LMWP), for enhanced intracellular protein delivery: in vitro and in vivo study”. FASEB J., 2005, 19:1555–1557
[276] M.M. Schmidt and K.D. Wittrup, “A modeling analysis of the effects of molecular size and binding affinity on tumor targeting”. Mol. Cancer Ther., 2009, 8: 2861-2871
[277] I. Cosic, A.E. Drummond, J.R. Underwood, M.T.W. Hearn,“In vitro inhibition of the actions of basic FGF by a novel 16 amino acid peptide”. Mol. Cell. Biochem., 1994, 130:1-9
[278] V. Krsmanovic, J.M. Biquard, I. Cosic, A. Achour and M.T.W. Hearn, “Investigation into the cross-reactivity of rabbit antibodies raised against nonhomologous pairs of synthetic peptides derived from HIV-1 gp120 proteins”. J. Peptide Res. 1998, 52(5):410-412
[279] M. Sauren, E. Pirogova and I. Cosic, “RRM analysis of protoporphyrinogen oxidase”. Australas Phys Eng Sci Med. 2004, 27(4):174-179
[280] T.S. Istivan, E. Pirogova, E. Gan, N.M. Almansour, P.J. Coloe, I. Cosic, “Biological Effects of a De Novo Designed Myxoma Virus Peptide Analogue: Evaluation of Cytotoxicity on Tumor Cells”. PLoS ONE 2011, Vol. 6(9):1-10
[281] Z. Huang, Y. Lin, X. Xiang, D. Wang and T. Lian, “In situ probe of photocarrier dynamics in water-splitting hematite (α-Fe2O3) electrodes”. Energy and Environmental Science 2012, 5(10):8923-8926
[282] V. Vojisavljevic, E. Pirogova and I. Cosic, “Review of studies on modulating enzyme activity by low intensity electromagnetic radiation”, Proc. 32nd Annual Intl. Conf. IEEE EMBS, 2010, 835-838
[283] J. Ramundo, M. Gray, “Enzymatic Wound Debridement”, Journal of Wound Ostomy Continence Nurs. 2008, Vol 35(3): 273-280
[284] M. Blank, L. Soo, “Optimal frequencies for magnetic acceleration of cutochrome oxidase and NaK-ATPase reactions”, Bioelectrochemistry and Bioenergetics, 2001, Vol. 53, No. 2, 171-174
[285] J. Kujawa, L. Zavodnik and I. Zavodnik, “Low-Intensity Near-Infrared Laser Radiation-Induced Changes of Acetylcholinesterase Activity of Human Erythrocytes”, Journal of Clinical Laser Medicine Surgery, 2003, Vol.21, No. 6, 351–355
[286] T.I. Karu, L.V. Pyatibrat and G.S. Kalendo, “Photobiological modulation of cell attachment via cytochrome c oxidaze”, Photochem.l and Photobiol.l Science, 2004, Vol 3(2): 211-216
[287] R.S. McDonald, S. Gupta and M.H. Grant, “405 nm Light exposure of osteoblasts and inactivation of bacterial isolates from arthroplasty patients: potential for new disinfection applications?” European cells and materials 2013, Vol25:204-214

[288] T. Dai, A. Gupta and M. R. Hamblin, “Blue light for infectious diseases: Propionibacterium acnes, Helicobacter pylori, and beyond?” Drug Resistance Updates 2012, 15:223-236
[289] M. Maclean, S. J. MacGregor, J. G. Anderson and Gerry Woolsey, “Inactivation of Bacteria Pathogens following Exposure to Light from a 405-Nanometer Light-Emitting Diode Array”. APPLIED AND ENVIRONMENTAL MICROBIOLOGY, 2009, 1932–1937
[290] M.V. Trushin, “Culture-to-culture physical interactions causes the alteration in red and infrared light stimulation of Escherichia coli growth rate”. J Microbiol Immunol Infect 2003, 36:149-152
[291] S.R. Tsai, T.C. Huang, H.F. Juan and S.C. Lee, “The effect of narrow bandwidth infrared radiation on the growth of Escherichia coli”. Appl. Phys. Lett. 2011, 99, 163704
[292] C. Roszak, “Metabolic activity of bacterial cells enumerated by direct viable count”. Applied and environmental microbiology. 1987, 2889-2983
[293] W.H Hancock.,Agar and broth dilution methods to determine the minimal inhibitory concentration (MIC) of antimicrobial substances”. Nature Protocols; 2008, Vol 3(2):163-175

PUBLICATIONS FROM THIS RESEARCH

Published papers (1 journal paper and 2 peer-reviewed conference proceedings):

1) Jie Hu, Taghrid S.Istivan, Elena Pirogova. "Experimental Evaluation of Antimicrobial Effects of the synthetic peptide on pathogenic bacteria" *MD-Medical Data* 6(1): 011-016; 2014

2) J. Hu, P. Peidaee, E. Elshagmani, T. Istivan and E. Pirogova. "The Effects of Synthetic Azurocidin Peptide Analogue on Staphylococcus Aureus Bacterium" *13th IEEE International Conference on BioInformatics and BioEngineering*, November 10-13, Chania, Greece, 2013 (978-1-4799-3163-7/13)

3) J. Hu, V. Vojisavljevic, E. Pirogova. "The Effects of Visible Light Radiation (400–500 nm) on enzymatic activity of Collagenase", *33rd Progress In Electromagnetics Research Symposium PIERS*, Taipei, 392-396, 25-28 March, 2013

In preparation:

1 journal paper

Appendix I

Primary amino acid sequences of collagenase used in thesis:

PRT>P1;

ATFFLLSWTHCWSLPLPYGDDDDDDLSEEDLEFAEHYLKSYYHPVTLAGILKKSTVTSTV
DRLREMQSFFGLDVTGKLDDPTLDIMRKPRCGVPDVGVYNVFPRTLKWSQTNLTYRIVNY
TPDISHSEVEKAFRKAFKVWSDVTPLNFTRIHDGTADIMISFGTKEHGDFYPFDGPSGLL
AHAFPPGPNLGGDAHFDDDETWTSSSKGYNLFIVAAHELGHSLGLDHSKDPGALMFPIYT
YTGKSHFMLPDDDVQGIQSLYGPGDEDPNPKHPKTPEKCDPALSLDAITSLRGETMIFKD
RFFWRLHPQQVEPELFLTKSFWPELPNHVDAAYEHPSRDLMFIFRGRKFWALNGYDIMEG
YPRKISDLGFPKEVKRLSAAVHFEDTGKTLFFSGNHVWSYDDANQTMDKDYPRLIEEEFP
GIGDKVDAVYEKNGYIYFFNGPIQFEYSIWSNRIVRVMPTNSLLWC

PRT>P2;

MLSGLWSSILALLGVFLQSVGEFRAETQEQDVEIVQKYLKNYYNSDKRNSGLVVEILKQF
FGLKVTGKPDAETLVMKQSTCGVPDVGEYVLTPGNPRWENTHLTYRIENYTPDLVSPLTF
TKVSEGQADIMISFVRGDHRDKYPFDGPGGNLAHASQPGPGIGGDAHFDEYERWTKNFQD
YNLYRVAAHELGHSLGLSHSTDIGALMYPTYLRGDVQLSQDDIDGPSGNPVQPRGPQTPQ
VCDSKLTFDAITTVRGELMFFKMRTNRFYPEVELGLQAAYEMADRDEVRFFKGNKYWAVS
GQDVLYGYPKDIHSSFGFPTGVAHECWSYDEYKQSMDTGYADEFPGDAVFQKFFHGTRQY
QFDLKTKRILTLQKANSWFNCRKN

PRT>P3;

MHSFPPLLLLLFWGVVSHSFPATLETQEQDVDLVQKYLEKYYNLKNDGRQVEKRRNSGPV
VEKLKQMQEFFGLKVTGKPDAETLKVMKQPRCGVPDVAQFVLTEGNPRWEQTHLTYRIEN
YTPDLPRADVDHAIEKAFQLWSNVTPLTFTKVSEGQADIMISFVRGDHRDNSPFDGPGGN
LAHAFQPGPGIGGDAHFDEDERWTNNFREYNLHRVAAHELGHSLGLSHSTDIGALMYPSY
TFSGDVQLAQDDIDGIQAIYGRSQNPVQPIGPQTPKACDSKLTFDAITTIRGEVMFFKDR
FYMRTNPFYPEVELNFISVFWPQLPNGLEAAYEFADRDEVRFFKGNKYWAVQGQNVLHGY
PKDIYSSFGFPRTVKHIDAALSEENTGKTYFFVANKYWRYDEYKRSMDPGYPKMIAHDFP
GIGHKVDAVFMKDGFFYFFHGTRQYKFDPKTKRILTLQKANSWFNCRKN

PRT>P4;

MRTVCALLGLLAAVHCMPVSQETMEEQRFAQSYLKNFFNLTEEAGPAVRRGFSQVTSKLI
EMQTFFGLQITGTLDAETLAMMKKPRCGVSDSRVARFSTFGNNLKWEKNSLTYRITNYTP
DMSKEEVDESIEKALQVWARVTPLRFTKIYSSTADIMVSFGQRAHGDYYPFDGPDGTLAH
AFAPAPGIGGDAHFDDDETFTFRSNTGYVLFMVAAHEFGHSLGLSHSDDPGALMYPIYSY
RNPETFVLPRDDVRGIQSLYGPNLDPAQPEPTAPPTPDACDSTMVLDAVATLRGEMFFFK
DSFFWRVHPQSYTPQQTFITNFWPDAPLSVDAAYENQQSDRIFLFKGRQVWAFRGYDLVQ
GYPQAISSFGLPKRIEKVDAALYDAQSGKTLFFVGRNYYSYDEAKGTMDAGFPKAVDQKF
SGMSGRVTAALQYRGFAYLYSGPYMFEYSLRTGQLLRLLRNSYFLPCTSY

PRT>P5;

MQSLLCLLLLCAASSRAFPAASDPDSEESDIQRAEAYLKRFYGLDTEKKHFTRKNGSPFS

EKLREMQEFFGLEVTGRLDSETLEVMEKPRCGVSDVARYSITPGNPVWKHTEITYRILNY
TPDMAKADVDAAIQRALNVWADVTPLTFTRLYEGTADIQISFAAGDHRDNSPFDGPDGLL
AHAFEPGRGIGGDAHFDEDERWTKGSERYNLFLMAAHEFGHSLGLSHSNDPGALMYPTYS
STDPDEFRLPQDDINGIQSLYGESKNPVQPTGPTTPSICDTKVIFDAVATLRGEMLFLKE
RFFWRRHAQYPEAELHFIKSFWPSLPSDIEAAYENPEQDEVLIFKGSKYWALNGYDIVQG
YPKNIHTLGFPTTVKKIDAAVYNEETGKTFFFVGNQYWSYDESTRTMDQGFPKETINDFP
GIGQKVHAVFQSNGFLYFFSGKYQFEFSMKSKRVMRVLRNNSWLGCQEA
PRT>6;
MFSLLLLLLLLCNTGSHGFPAATSETQEQDVEIVQKYLKNYYNLNSDGVPVEKKRNSGLV
VEKLKQMQQFFGLKVTGKPDAETLNVMKQPRCGVPDVAEFVLTPGNPRWENTHLTYRIEN
YTPDLSREDVDRAIEKAFQLWSNVSPLTFTKVSEGQADIMISFVRGDHRDNSPFDGPGGN
LAHAFQPGPGIGGDAHFDEDERWTKNFRDYNLYRVAAHELGHSLGLSHSTDIGALMYPNY
IYTGDVQLSQDDIDGIQAIYGPSENPVQPSGPQTPQVCDSKLTFDAITTLRGELMFFKDR
FYMRTNSFYPEVELNFISVFWPQVPNGLQAAYEIADRDEVRFFKGNKYWAVRGQDVLYGY
PKDIHRSFGFPSTVKNIDAAVFEEDTGKTYFFVAHECWRYDEYKQSMDTGYPKMIAEEFP
GIGNKVDAVFQKDGFLYFFHGTRQYQFDFKTKRILTLQKANSWFNCRKN
PRT>P7;
MPGLPLLLLLLWGVGSHGFPAASETQEQDVEMVQKYLENYYNLKDDWRKIPKQRGNGLAV
EKLKQMQEFFGLKVTGKPDAETLKMMKQPRCGVPDVAQFVLTPGNPRWEQTHLTYRIENY
TPDLSRADVDNAIEKAFQLWSNVTPLTFTKVSKGQADIMISFVRGDHRDNSPFDGPEGQL
AHAFQPGLGIGGDVHFDEDDRWTKDFRNYNLYRVAAHELGHSLGLSHSTDIGALMYPNYM
FSGDVQLAQDDIDGIQAIYGPSQNPSQPVGPQTPKVCDSKLTFDAITTIRGEIMFFKDRF
YMRANPYYSEVELNFISVFWPHLPNGLQAAYEVAHRDEILFFKGNKYWTVQGQNELPGYP
KDIHSSFGFPRSVNHIDAAVSEEDTGKTYFFVANKYWRYDEYKRSMDAGYPKMIEYDFPG
IGNKVDAVFKKDGFFYFFHGTRQYKFDPKTKRILTLQKANSWFNCRKN
PRT>P8;
MHSAILATFF LLSWTHCWSL PLPYGDDDDD DLSEEDLEFA EHYLKSYYHP VTLAGILKKS
TVTSTVDRLR EMQSFFGLDV TGKLDDPTLD IMRKPRCGVP DVGEYNVFPR TLKWSQTNLT
YRIVNYTPDI SHSEVEKAFR KAFKVWSDVT PLNFTRIHDG TADIMISFGT KEHGDFYPFD
GPSGLLAHAF PPGPNLGGDA HFDDDETWTS SSKGYNLFIV AAHELGHSLG LDHSKDPGAL
MFPIYTYTGK SHFMLPDDDV QGIQSLYGPG DEDPNPKHPK TPEKCDPALS LDAITSLRGE
TMIFKDRFFW RLHPQQVEPE LFLTKSFWPE LPNHVDAAYE HPSRDLMFIF RGRKFWALNG
YDIMEGYPRK ISDLGFPKEV KRLSAAVHFE DTGKTLFFSG NHVWSYDDAN QTMDKDYPRL
IEEEFPGIGD KVDAVYEKNG YIYFFNGPIQ FEYSIWSNRI VRVMPTNSLLWC
PRT>P9;
SSLSVLVLSLSFAYCLSAPVPQDEDSELTPGDLQLAEHYLNRLYSSSSNPVGMLRMKNVN
SIETKLKEMQSFFGLEVTGKLNEDTLDIMKQPRCGVPDVGQYNFFPRKLKWPRNNLTYRI
VNYTPDLSTSEVDRAIKKALKVWSDVTPLNFTRLRTGTADIMVSFGKKEHGDYYPFDGPD
GLLAHAFPPGEKLGGDTHFDDDEMFSTDNKGYNLFVVAAHEFGHALGLDHSRDPGSLMFP
VYTYTETSRFVLPDDDVQGIQVLYGPGNRDPHPKHPKTPEKCDPDLSIDAITELRGEKMI
FKDRFFWRVHPQMTDAELVLIKSFWPELPNKLDAAYEHPAKDLSYLFRGKKFWALNGYDI
VEDYPKKLHELGFPKTLKAIDAAVYNKDTGKTFFFTEDSYWSFDEEARTLDKGFPRLISE
DFPGIGEKVDAAYQRNGYLYFFNGALQFEYSIWSQRITRILKTNFVLMC
PRT>P10;

MFSLKTLPFLLLLHVQISKAFPVSSKEKNTKTVQDYLEKFYQLPSNQYQSTRKNGTNVIV
EKLKEMQRFFGLNVTGKPNEETLDMMKKPRCGVPDSGGFMLTPGNPKWERTNLTYRIRNY
TPQLSEAEVERAIKDAFELWSVASPLIFTRISQGEADINIAFYQRDHGDNSPFDGPNGIL
AHAFQPGQGIGGDAHFDAEETWTNTSANYNLFLVAAHEFGHSLGLAHSSDPGALMYPNYA
FRETSNYSLPQDDIDGIQAIYGLSSNPIQPTGPSTPKPCDPSLTFDAITTLRGEILFFKD
RYFWRRHPQLQRVEMNFISLFWPSLPTGIQAAYEDFDRDLIFLFKGNQYWALSGYDILQG
YPKDISNYGFPSSVQAIDAAVFYRSKTYFFVNDQFWRYDNQRQFMEPGYPKSISGAFPGI
ESKVDAVFQQEHFFHVFSGPRYYAFDLIAQRVTRVARGNKWLNCRYG
PRT>P11;
MHPRALAGFL FFSWTACWSL PLPSDGDSED LSEEDFQFAE SYLKSYYYPQ NPAGILKKSA
ASSVIDRLKE MQSFFGLEVT GRLDDNTLDI MKKPRCGVPD VGEYNVFPRT LKWSKMNLTY
RIVNYTPDLT HSEVEKAFRK AFKVWSDVTP LNFTRIHNGT ADIMISFGTK EHGDFYPFDG
PSGLLAHAFP PGPNYGGDAH FDDDETWTSS SKGYNLFLVA AHEFGHSLGL DHSKDPGALM
FPIYTYTGKS HFMLPDDDVQ GIQSLYGPGD EDPNSKHPKT PDKCDPSLSL DAITSLRGET
LIFKDRFFWR LHPQQVEAEL FLTKSFWPEL PNRIDAAYEH PSHDLIFIFR GRKFWALSGY
DILEDYPKKI SELGFPKDVK KISAALHFED SGKTLFFSEN QVWSYDDTNH VMDKGYPRFI
EEVFPGIGDK VDAVYQKNGY IYFFNGPIQF EYSIWSNRIV RVMPTNSLLW C
PRT>P12;
MFRLKTLPLL IFLHTQLANA FPVPEHLEEK NIKTAENYLR KFYNLPSNQF RSSRNATMVA
EKLKEMQRFF SLAETGKLDA ATMGIMEMPR CGVPDSGDFL LTPGSPKWTH TNLTYRIINH
TPQLSRAEVK TAIEKAFHVW SVASPLTFTE ILQGEADINI AFVSRDHGDN SPFDGPNGIL
AHAFQPGQGI GGDAHFDSEE TWTQDSKNYN LFLVAAHEFG HSLGLSHSTD PGALMYPNYA
YREPSTYSLP QDDINGIQTI YGPSDNPIQP TGPSTPKACD PHLRFDATTT LRGEIYFFKD
KYFWRRHPQL RTVDLNFISL FWPFLPNGLQ AAYEDFDRDL VFLFKGRQYW ALSGYDLQQG
YPRDISNYGF PRSVQAIDAA VSYNGKTYFF INNQCWRYDN QRRSMDPGYP KSIPSMFPGV
NCRVDAVFLQ DSFFLFFSGP QYFAFNFVSH RVTRVARSNL WLNCS
PRT>P13;
MLHLKTLPFL FFFHTQLATA LPVPPEHLEE KNMKTAENYL RKFYHLPSNQ FRSARNATMI
AEKLKEMQRF FGLPETGKPD AATIEIMEKP RCGVPDSGDF LLTPGSPKWT HTNLTYRIIN
HTPQMSKAEV KTEIEKAFKI WSVPSTLTFT ETLEGEADIN IAFVSRDHGD NSPFDGPNGI
LAHAFQPGRG IGGDAHFDSE ETWTQDSKNY NLFLVAAHEF GHSLGLSHST DPGALMYPNY
AYREPSTYSL PQDDINGIQT IYGPSDNPVQ PTGPSTPTAC DPHLRFDAAT TLRGEIYFFK
DKYFWRRHPQ LRTVDLNFIS LFWPFLPNGL QAAYEDFDRD LVFLFKGRQY WALSAYDLQQ
GYPRDISNYG FPRSVQAIDA AVSYNGKTYF FVNNQCWRYD NQRRSMDPGY PTSIASVFPG
INCRIDAVFQ QDSFFLFFSG PQYFAFNLVS RRVTRVARSN LWLNCP
PRT>P14;
MEALMARGAL TGPLRALCLL GCLLSHAAAA PSPIIKFPGD VAPKTDKELA VQYLNTFYGC
PKESCNLFVL KDTLKKMQKF FGLPQTGDLD QNTIETMRKP RCGNPDVANY NFFPRKPKWD
KNQITYRIIG YTPDLDPETV DDAFARAFQV WSDVTPLRFS RIHDGEADIM INFGRWEHGD
GYPFDGKDGL LAHAFAPGTG VGGDSHFDDD ELWTLGEGQV VRVKYGNADG EYCKFPFLFN
GKEYNSCTDT GRSDGFLWCS TTYNFEKDGK YGFCPHEALF TMGGNAEGQP CKFPFRFQGT
SYDSCTTEGR TDGYRWCGTT EDYDRDKKYG FCPETAMSTV GGNSEGAPCV FPFTFLGNKY
ESCTSAGRSD GKMWCATTAN YDDDRKWGFC PDQGYSLFLV AAHEFGHAMG LEHSQDPGAL
MAPIYTYTKN FRLSQDDIKG IQELYGASPD IDLGTGPTPT LGPVTPEICK QDIVFDGIAQ

IRGEIFFFKD RFIWRTVTPR DKPMGPLLVA TFWPELPEKI DAVYEAPQEE KAVFFAGNEY
WIYSASTLER GYPKPLTSLG LPPDVQRVDA AFNWSKNKKT YIFAGDKFWR YNEVKKKMDP
GFPKLIADAW NAIPDNLDAV VDLQGGGHSY FFKGAYYLKL ENQSLKSVKF GSIKSDWLGC

PRT>P15;
MSPWQPLLLA LLAFGCSSAC PYQRHATFVV FPKDLKTSNL TDTQLAEAYL YRYGYTRAAQ
MMGEKQSLRP ALLMLQKQLS LPQTGELDSQ TLKAIRTPRC GVPDVGRFQT FKGLKWDHHN
ITYWIQNYSE DLPRDMIDDA FARAFAVWGE VAPLTFTRVY GPEADIVIQF GVAEHGDGYP
FDGKDGLLAH AFPPGAGVQG DAHFDDDELW SLGKGVVIPT YYGNSNGAPC HFPFTFEGRS
YSACTTDGRN DGTPWCSTTA DYDKDGKFGF CPSERLYTEH GNGEGKPCVF PFIFEGRSYS
ACTTKGRSDG YRWCATTANY DQDKLYGFCP TRVDATVVGG NSAGELCVFP FVFLGKQYSS
CTSDGRRDGR LWCATTSNFD TDKKWGFCPD QGYSLFLVAA HEFGHALGLD HSSVPEALMY
PLYSYLEGFP LNKDDIDGIQ YLYGRGSKPD PRPPATTTTE PQPTAPPTMC PTIPPTAYPT
VGPTVGPTGA PSPGPTSSPS PGPTGAPSPG PTAAPTAGSS EASTESLSPA DNPCNVDVFD
AIAEIQGALH FFKDGWYWKF LNHRGSPLQG PFLTARTWPA LPATLDSAFE DPQTKRVFFF
SGRQMWVYTG KTVLGPRSLD KLGLGPEVTH VSGLLPRRPG KALLFSKGRV WRFDLKSQKV
DPQSVIRVDK EFSGVPWNSH DIFQYQDKAY FCHGKFFWRV SFQNEVNKVD PEVNQVDDVG
YVTYDLLQCP
PRT>P16;
MAPSSLSVFV LSLSFTYCLS APVSQDEDSE LTPGALQLAE HYLNRLYSSS SNPAGMLRMK
DVNSVETKLK EMQSFFGLEV TGKLNEDTLD IMKQPRCGVP DVGQYNFFPR KLKWPRNNLT
YRIVNYTPDL STSDVDRAIK KALKVWSDVT PLNFTRLRTG TADIMVAFGK KEHGDYYPFD
GPDGLLAHAF PPGEKIGGDT HFDDDEMFST DNKGYNLFVV AAHEFGHALG LDHSRDPGSL
MFPVYTYTET SRFVLPDDDV QGIQALYGSG NRDPHPKHPK TPEKCDPDLT IDAITELRGE
KMIFKDRFFW RVHPQMTDAE LVLIKSFWPE LPNKIDAAYE HPAKDLIYIF RGKKFWALNG
YDFVEDYPKK LHELGFPKTL KAIDAAVYNK AIGKTLFFAE DSYWSFDEEA RTMDKGFPRL
ISEDFPGIGE KVDAAYQRNG YIYFFNGALQ FEYSIWSKRI TRILKTNFVL MC
PRT>P17;
MEARLVWGVL VGPLRVLCVL CCLLGHAIAA PSPIIKFPGD VAPKTDKELA VQYLNTFYGC
PKESCNLFVL KDTLKKMQKF FGLPQTGDLD QNTIETMRKP RCGNPDVANY NFFPRKPKWD
KNQITYRIIG YTPDLDPETV DDAFARALKV WSDVTPLRFS RIHDGEADIM INFGRWEHGD
GYPFDGKDGL LAHAFAPGTG VGGDSHFDDD ELWTLGEGQV VRVKYGNADG EYCKFPFLFN
GREYSSCTDT GRSDGFLWCS TTYNFEKDGK YGFCPHEALF TMGGNADGQP CKFPFRFQGT
SYNSCTTEGR TDGYRWCGTT EDYDRDKKYG FCPETAMSTV GGNSEGAPCV FPFTFLGNKY
ESCTSAGRND GKVWCATTTN YDDDRKWGFC PDQGYSLFLV AAHEFGHAMG LEHSQDPGAL
MAPIYTYTKN FRLSHDDIKG IQELYGPSPD ADTDTGTGPT PTLGPVTPEI CKQDIVFDGI
AQIRGEIFFF KDRFIWRTVT PRDKPTGPLL VATFWPELPE KIDAVYEAPQ EEKAVFFAGN
EYWVYSASTL ERGYPKPLTS LGLPPDVQQV DAAFNWSKNK KTYIFAGDKF WRYNEVKKKM
DPGFPKLIAD SWNAIPDNLD AVVDLQGGGH SYFFKGAYYL KLENQSLKSV KFGSIKSDWL
GC
PRT>P18;
MHPGVLAAFL FLSWTHCRAL PLPSGGDEDD LSEEDLQFAE RYLRSYYHPT NLAGILKENA
ASSMTERLRE MQSFFGLEVT GKLDDNTLDV MKKPRCGVPD VGEYNVFPRT LKWSKMNLTY
RIVNYTPDMT HSEVEKAFKK AFKVWSDVTP LNFTRLHDGI ADIMISFGIK EHGDFYPFDG

PSGLLAHAFP PGPNYGGDAH FDDDETWTSS SKGYNLFLVA AHEFGHSLGL DHSKDPGALM
FPIYTYTGKS HFMLPDDDVQ GIQSLYGPGD EDPNPKHPKT PDKCDPSLSL DAITSLRGET
MIFKDRFFWR LHPQQVDAEL FLTKSFWPEL PNRIDAAYEH PSHDLIFIFR GRKFWALNGY
DILEGYPKKI SELGLPKEVK KISAAVHFED TGKTLLFSGN QVWRYDDTNH IMDKDYPRLI
EEDFPGIGDK VDAVYEKNGY IYFFNGPIQF EYSIWSNRIV RVMPANSILW C
PRT>P19;
MMPSVLSAAI FFLSLAFGLP VPVPHERDSD VTEQELRLAE KYLKTFYVAS DHAGIMTKKG
GNALASKLRE MQSFFDLEVT GKLDEDTLEV MKQPRCGVPD VGEYNVFPRS LKWPRFNLTY
RIENYTPDMT HAEVDRAIKK AFRVWSEVTP LNFTRLRSGT ADIMISFGTK EHGDFYPFDG
PNGLLAHAFP PGQRIGGDTH FDDDETFTSG SNGYNLFIVA AHEFGHALGL DHSRDPGSLM
YPVYSYTEPS RFLLPDDDVQ GIQSLYGPGN RDPNPKHPKT PEKCDPELSL DAITEMRGEK
LIFKDRFFWR QHPQMTDVEL VLIRNFWPEL PSKIDAAYEY PEKDLIYIFR GRKFWALNGY
DILADYPKKI QELGFPKSLR TIDAAVYNRA MGKTLFFTGE KYWSFDEEKQ TVEKGYPRFI
ADDFPGIGET VDAAYQRNGY IYFFSGSLQF EYSTWSNKVI RVLKTNSILW C
PRT>P20;
MLLAPLTLAL LALCRAAPLH SKPQAVITFP GELLSAPSDV ELAENYLLRF GYIQEAEVRR
SSKHVSLAKA LRRMQKQLGL EETGELDAST LEAMRAPRCG VPDVGGFLTF EGELKWDHMD
LTYRVMNYSP DLDRAVIDDA FRRAFKVWSD VTPLTFTQIY SGEADIMIMF GSQEHGDGYP
FDGKDGLLAH AFPPGSGIQG DAHFDDDEFW TLGTGLEVKT RYGNANGASC HFPFIFEGRS
YSRCITEGRT DGMLWCATTA SYDADKTYGF CPSELLYTNG GNSDGSPCVF PFIFDGASYD
TCTTDGRSDG YRWCATTANF DQDKKYGFCP NRDTAAIGGN SQGDPCVFPF TFLGQSYSAR
TSQGRQDGKL WCATTSNYDT DKKWGFCPDR GYSIFLVAAH EFGHSLGLDH SSVREALMYP
MYSYVQDFQL HEDDVQGIQY LYGRGSGPEP TPPAPLPTEE PQSIPTEAGS ASTTEEEEEE
TPEPTAEPSP VDPSRDACME KNFDAITEIN GELHFFKNGK YWTHSSFWKS GTQGAFSIAD
TWPGLPAVID AAFQDVLTKR VFFFAGRQFW VFSGKNAVGP RRIEKLGIGK EAGRITGALQ
RGRGKVLLFS GEHYWRLDVK VQTVDKGYPR DTDDVFTGVP LDARNVFLYQ DKYHFCRDSF
YWRMTPRYQV DRVGYIRYDL LQCPQH
PRT>P21;
MKTYYQFLTT SILIGLVFRA HSGPVAPSET DDHEFAKNYL KKLYNMEEDN TPSFGRKVNE
MSLKLGEMQE FFGLKVTGTL DAETMEMMKK PRCGVPDVAA LKARALTYKW TTNSLTYRIE
NYTPDMSVAE VDDSIQRALQ VWARVTPLKF KRIYSGIADI MISFVVGDHR DGSPFDGPNG
FLAHAFFPGV GIGGDAHFDD DETFSFRSTR GYNLFLVAAH EFGHSLGLEH SNVPGALMYP
TYSYTNPDTF VLPRDDVKRI QALYGSNRDK PVNPDKPEPT PPVNPDACDP NLALDAVTTL
RGEKLFFKNR FFWRIHPQLT ETDQYLIKFF WPELPDNIDA AFENPSTDLV YIIKGQKVWA
LSGYDVVQRL SLSSFGLPDT VKKIDAAVYD VDTEKALFFL GKSYYSYDVN GKVMDRGFPK
PVEQSFPGMT TKVTAAFQEN GNTYLFSGPD VFQYNSGRLV NVLKSNSFLR C
PRT>22;
MAPSSLSVFV LSLSFTYCLS APVSQDEDSE LTPGALQLAE HYLNRLYSSS SNPAGMLRMK
DVNSVETKLK EMQSFFGLEV TGKLNEDTLD IMKQPRCGVP DVGQYNFFPR KLKWPRNNLT
YRIVNYTPDL STSDVDRAIK KALKVWSDVT PLNFTRLRTG TADIMVAFGK KEHGDYYPFD
GPDGLLAHAF PPGEKIGGDT HFDDDEMFST DNKGYNLFVV AAHEFGHALG LDHSRDPGSL
MFPVYTYTET SRFVLPDDDV QGIQALYGSG NRDPHPKHPK TPEKCDPDLT IDAITELRGE
KMIFKDRFFW RVHPQMTDAE LVLIKSFWPE LPNKIDAAYE HPAKDLIYIF RGKKFWALNG
YDFVEDYPKK LHELGFPKTL KAIDAAVYNK AIGKTLFFAE DSYWSFDEEA RTMDKGFPRL

ISEDFPGIGE KVDAAYQRNG YIYFFNGALQ FEYSIWSKRI TRILKTNFVL MC
PRT>23;
MHPRVLAGFL FFSWTACWSL PLPSDGDSED LSEEDFQFAE SYLKSYYYPQ NPAGILKKTA
ASSVIDRLRE MQSFFGLEVT GRLDDNTLDI MKKPRCGVPD VGEYNVFPRT LKWSKMNLTY
RIVNYTPDLT HSEVEKAFRK AFKVWSDVTP LNFTRIHNGT ADIMISFGTK EHGDFYPFDG
PSGLLAHAFP PGPNYGGDAH FDDDETWTSS SKGYNLFLVA AHEFGHSLGL DHSKDPGALM
FPIYTYTGKS HFMLPDDDVQ GIQSLYGPGD EDPYSKHPKT PDKCDPSLSL DAITSLRGET
LIFKDRFFWR LHPQQVEAEL FLTKSFGPEL PNRIDAAYEH PSHDLIFIFR GRKFWALSGY
DILEDYPKKI SELGFPKHVK KISAALHFED SGKTLFFSEN QVWSYDDTNH VMDKDYPRLI
EEVFPGIGDK VDAVYQKNGY IYFFNGPIQF EYSIWSNRIV RVMTTNSLLW C
PRT>P24;
MELTAVVLLV IAAHALAKPI SSEEKDKVLF AEKYLRRYYG MPAGLQGKEK TSDVMYKKKI
QEMQEFFKLN VTGKLDDDTL ELMEMARCGV PDVAEYNHFP NDLKWKTTEV TFRILNYTPD
LRKADVDRAV RNGLNVWSSV TPLKFKKLYE GNADIMISFG AREHGDFNPF DGPDGLLAHA
YPPGNGIGGD THFDEDETWT KDFHEFNLFL VAAHEFGHAL GMAHSSDPGS LMYPVYSYGK
GYPLSEDDIK GIQSLYGENP NHRRIKPKPD APSKCDPELS FDAVTELRGE TIIFKDRFYW
RLHSQIPEPE QTLIKSTWPE IPNKVDAAYE NPEKDVVIIF SGIKMWALNG YNLVDGYPKY
IHKLGLPKTV RKIDAAVNIR DTGKTLLFVE EEYWSYDERT GTMDSGYPRS IEEDFPGIGD
EVDAAAYHFG YLYFYHEHIQ FEYSYNSRKV MRIMRANSIL NC
PRT>P25;
MKTCFRLCVFITLLFSGHSSPIAPPAGGDQDTLAENYLTRLYGLPKPAQNPSPSGGEKRS
SDVSLRLKEMQQFFKLKVSGKLDQETLEVMKKPRCGVPDIKAYSTFAGDYKWKKHQLTYR
IGNYTPDMSVAEVDDSISKALKVWADVTPLRFTRIYSGTADIMISFATGDHRDGYPFDGP
NGFLAHAFPPFEGIGGDAHFDDDETFSYRSPQYYNLFLVAAHEFGHSLGLEHSQDPGALM
YPTYVYRDVDRFVLPRDDVNGIQSLYGPNTDVNTDDSKPTPPVTPNTCDPNLVLDAVTML
RGEIMFFKNSFFWRSYPQSADVEQQLIKSFWPEAPDNIDAAFESVMQDKVFLIKGEKVWA
LYGYDMVQGYPKSLSMFRLPKNVRKIDAVLYKEDSNSILFFANNQVYSYNEGIRQMDKGF
PKPVEEVFPGMTGKVTAAFQYRGLNYLFSGSKMLEFGSNNRLFRVLNNNYFLPCK
PRT>P26;
MHPGVLAAFLFLSWTRCWSLPVPNDDDDDDDMSEEDFQLAERYLKSYYYPLNPAGILKKT
AANSVVDRLREMQSFFGLEVTGKLDDNTLDIMKKPRCGVPDVGEYNVFPRTLKWPKMNLT
YRIVNYTPDLTHSEVEKAFKKAFKVWSDVTPLNFTRLYNGTADIMISFGTKEHGDFYPFD
GPSGLLAHAFPPGPNYGGDAHFDDDETWTSSSKGYNLFLVAAHEFGHSLGLDHSKDPGAL
MFPIYTYTGKSHFVLPDDDVQGIQYLYGPGDEDPNPKHPKTPDKCDPSLSLDAITSLRGE
TMVFKDRFFWRLHPQLVDAELFLTKSFWPELPNRIDAAYEHPSKDLIFIFRGRKFWALNG
YDILEGYPQKISELGFPKDVKKISAAVHFEDTGKTLFFSGNQVWRYDDTNRMMDKDYPRL
IEEDFPGIGDKVDAVYEKNGYIYFFNGPIQFEYSIWSNRIVRVMPTNSLLWC
PRT>P27;
MHSAILATFFLLSWTHCWSLPLPYGDDDDDDLSEEDLEFAEHYLKSYYHPVTLAGILKKS
TSTVDRLREMQSFFGLDVTGKLDDPTLDIMRKPRCGVPDVGEYNVFPRTLKWSQTNLT
YRIVNYTPDISHSEVEKAFRKAFKVWSDVTPLNFTRIHDGTADIMISFGTKEHGDFYPFD
GPSGLLAHAFPPGPNLGGDAHFDDDETWTSSSKGYNLFIVAAHELGHSLGLDHSKDPGAL
MFPIYTYTGKSHFMLPDDDVQGIQSLYGPGDEDPNPKHPKTPEKCDPALSLDAITSLRGE
TMIFKDRFFWRLHPQQVEPELFLTKSFWPELPNHVDAAYEHPSRDLMFIFRGRKFWALNG

YDIMEGYPRKISDLGFPKEVKRLSAAVHFEDTGKTLFFSGNHVWSYDDANQTMDKDYPRL
IEEEFPGIGDKVDAVYEKNGYIYFFNGPIQFEYSIWSNRIVRVMPTNSLLWC
PRT>P28;
MHPGVLAAFLFLSWTHCRALPLPSGGDEDDLSEEDLQFAERYLRSYYHPTNLAGILKENA
ASSMTERLREMQSFFGLEVTGKLDDNTLDVMKKPRCGVPDVGEYNVFPRTLKWSKMNLTY
RIVNYTPDMTHSEVEKAFKKAFKVWSDVTPLNFTRLHDGIADIMISFGIKEHGDFYPFDG
PSGLLAHAFPPGPNYGGDAHFDDDETWTSSSKGYNLFLVAAHEFGHSLGLDHSKDPGALM
FPIYTYTGKSHFMLPDDDVQGIQSLYGPGDEDPNPKHPKTPDKCDPSLSLDAITSLRGET
MIFKDRFFWRLHPQQVDAELFLTKSFWPELPNRIDAAYEHPSHDLIFIFRGRKFWALNGY
DILEGYPKKISELGLPKEVKKISAAVHFEDTGKTLLFSGNQVWRYDDTNHIMDKDYPRLI
EEDFPGIGDKVDAVYEKNGYIYFFNGPIQFEYSIWSNRIVRVMPANSILWC

Appendix II

Primary amino acid sequences of Azurocidin used in thesis:

PRT>P1;

MTRLTVLALLAGLLASSRAGSSPLLDIVGGRKARPRQFPFLASIQNQGRHFCGGALIHARFVMTAASCFQS
QNPGVSTVVLGAYDLRRRERQSRQTFSISSMSENGYDPQQNLNDLMLLQLDREANLTSSVTILPLPLQNAT
VEAGTRCQVAGWGSQRSGGRLSRFPRFVNVTVTPEDQCRPNNVCTGVLTRRGGICNGDGGTPLVCEGLA
HGVASFSLGPCGRGPDFFTRVALFRDWIDGVLNNPGPGPA

PRT>P2;

MFKYAAVFVLAVATVSAATLKNPVSSENRQGRIAGGEVANPNQFPYHAALQTADGLTFCGAAIVNQRWV
ITAGSCAQGKATTDVLVIVGTNRVDALAVPRHTVDRIVIHPNFDVNVYANDVAVLRVLRPFIFSESIQPITLG
SDNVEAESNAVATGFGRTAISDSTPASYLRYVNVDVITNEECQEAFDDSYQERLHGNTVCTRSAEGSGICL
GDAGGPLVIDDTLVGVISWGIPCGMGMPDVYARVSAHRAWVLVHTMI

PRT>P3;

IVGGRRAQPQEFPFLASIQKQGRPFCAGALVHPRFVLTAASCFRGKNSGSASVVLGAYDLRQQEQSRQTFSI
RSISQNGYDPRQNLNDVLLLQLDREARLTPSVALVPLPPQNATVEAGTNCQVAGWGTQRLRRLFSRFPRVL
NVTVTSNPCLPRDMCIGVFSRRGRISQGDRGTPLVCNGLAQGVASFLRRRFRRSSGFFTRVALFRNWIDSVL
NNPP

PRT>P4;

MVVSKSVPKPKSHKPALKKKQALKFSICCSPGVIDEDIISPGILEKYLKEHIKVNKKLNNLGKDIHIERDKSTI
NITANIPFSKRYLKYLTKNSSKDTNFGIFSESLQSLKILTNYDSSTLRMRTRMMKKRADHFP

PRT>P5;

MTRLTVLALLAGLLVSSRAGSSPLADIVGGRKARPRQFPFLASIQNQGRHFCGGALIHPRFVMSAASCFRN
QNPGTVTVVLGAYDLRRRERRSRQMFSISSMSENRYDPQQNLNDLVLLQLDREANITSSVAILALPLQNAM
VEAGTRCQVAGWGTRRSGGRLSRFPRFVNVTVTPEDQCRPNNVCTGVLARRAGICNGDGGTPLICDGLGH
GVASFSMGPCGRGPDFFTRVSVFRDWIDGVLNGGPVPA

PRT>P6;

MGTMKTQRDSPSLGRWSLVLLLLGLVMPLAIVAQVLSYQEAVLRAIDGINQRSSDANLYRLLDLDPRPTM
DGDPDTPKPVSFTVKETVCPRTTQKSPEDCDFKEDGLVKRCVGTVILNQARDSFDISCDKDNRRSARLGNF
FRKVKEKIGGGLKKVGQKIKDFLGNLVPRTAS

PRT>P7;

MTALRLLAMLASLLATSRAGSAPLVDIVGGRKARPQELPFLASIQNQGRHFCGGALIHPNFVLTAASCFQS
RNTGIATVVLGAYDLRRRERSRQTFFIRSVSENGYDPQQNLNDVLLLQLDRQANLTSSVALVPLPEQNATV
EAGTGCQVAGWGTRRRRGRLSRVPRVLNVTVTPANQCRPNNVCTGVLTRRGGICQGDGGTPLVCNGLAH
GVASWSRGPCGRGTDFFARVALFRNWIDSVINQPA

PRT>P8;

MEKIVCLLLIALYGCSAAPAELEIRETPTLDNVTTVAIHLVANDGQFPFMVSIQQRFEPGQLGHTCGGTLISL
QHVLTAASCLYQTTSGSPVLINPQFYRVFGGHRSLGNNMNDPDRVRMIENFTIHPDFVGNNQHLNDIAIITL
DSPFVAGQYLQPLPLPEQDEQPSEQEGDCTICGWGKKTADTSLMQNSLTYAPKTVLNQTECIAEYYTKFNI

PTAMDENMVCAASTRSLTYGCPGDEGGPLVCNKRLAGVLFTSVRCGISTDPLLYTRVSPYANWAKGVVG
EPLSTSSSATFQPGVALVFMLAVKQFVATFSF